NOVA SCHOOL OF SCIENCE & TECHNOLOGY

DEPARTAMENT OF LIFE SCIENCES

STRATEGIES TO PREVENT THE TIMELY SUB-CELLULAR LOCALIZATION OF THE CAPSULE SYNTHETIC MACHINERY IN *STREPTOCOCCUS PNEUMONIAE*

JOANA BAPTISTA DA SILVA FIGUEIREDO

Master in Molecular Biology and Genetics

DOCTORATE IN MOLECULAR BIOSCIENCES
NOVA University Lisbon
November, 2021

NOVA SCHOOL OF SCIENCE & TECHNOLOGY

DEPARTAMENT OF LIFE SCIENCES

STRATEGIES TO PREVENT THE TIMELY SUB-CELLULAR LOCALIZATION OF THE CAPSULE SYNTHETIC MACHINERY IN *STREPTOCOCCUS PNEUMONIAE*

JOANA BAPTISTA DA SILVA FIGUEIREDO

Master in Molecular Biology and Genetics

Supervisor: Dr. Sérgio Joaquim Raposo Filipe,
Assistant Professor, FCT NOVA, NOVA University Lisbon

Co-Supervisor: Dr. Mariana Luísa Tomás Gomes de Pinho,
Associate Professor, ITQB NOVA, NOVA University Lisbon

Examination Committee:

Chair: Dr. Isabel Maria Godinho de Sá Nogueira,
Full Professor, FCT-NOVA, NOVA University Lisbon

Rapporteurs: Dr. Waldemar Vollmer,
Full Professor, Newcastle University
Dr. Christophe Grangeasse,
Director of research CNRS, University of Lyon

Adviser: Dr. Sérgio Joaquim Raposo Filipe,
Assistant Professor, FCT-NOVA, NOVA University Lisbon

Members: Dr. Madalena Maria Vilela Pimentel,
Associate Professor, Faculty of Pharmacy, University of Lisbon
Dr. Raquel de Sá Leão Domingues da Silva,
Principal Investigator, ITQB NOVA, NOVA University Lisbon
Dr. Isabel Maria Godinho de Sá Nogueira,
Full Professor, FCT-NOVA, NOVA University Lisbon

DOCTORATE IN MOLECULAR BIOSCIENCES

NOVA University Lisbon
November, 2021

Strategies to prevent the timely sub-cellular localization of the capsule synthetic machinery in *Streptococcus pneumoniae*

À minha família

ACKNOWLEDGEMENTS

Since I was little science has been a passion, so it was not surprising when I decided to pursue a career in research and do a PhD. Even though that was an individual decision, it would not be possible without the help, understanding, collaboration and strong support of several people. To all the people that accompanied me in this journey and encouraged me to achieve my goals I would like to express my gratitude and give my acknowledgments.

First, I would like to thank my supervisor Professor Sérgio Filipe for welcoming me in his laboratory in 2011 to do a master thesis, and afterwards for grooming me and encourage me to take a step forward and enroll in a PhD. Without his guidance and helpful discussions, I would not learn and evolve to be a better scientist as I did. His out of the box questions and attention to detail developed my critical thinking, so important in science. Thank you for trusting in my abilities, for helping me surpass the challenges I encountered on the way and for all the opportunities given.

I would also like to thank my co-supervisor Professor Mariana Pinho who continuously encouraged me to move further, even when my worked seemed stalled or when I faced challenging times. Most of all, thank you for offering me your extremely helpful ideas and suggestions and for being a driving force for the publication of my work.

I thank Professor Jaime Mota and Professor Mário Ramirez for accepting to be part of my thesis committee, your different perspective and insightful suggestions strengthened the progress of my work.

I express my gratitude to our collaborators Dr. Didier Cabanes and all the members of the Molecular Microbiology laboratory at the i3S institute for allowing me to work there and for receiving me so well. A special thanks to Francisco Mesquita who did all the injections in the zebrafish experiments and helped me always with a smile on his face.

To all the present and former members of my laboratory I am deeply thankful. Working in the Bacterial Cell Surfaces and Pathogenesis laboratory was both a privilege and a pleasure. Throughout the years of a PhD there are always ups and downs but having a great work environment always made me feel lucky. Maria João Catalão, Gonçalo, Rita, Mafalda, Denise, Jorge, Rúben, Sara Pinheiro, and Maria João Frias, thank you. I must start by thanking Maria João Catalão, who was and is, without a doubt my inspiration. Your resilience, confidence, competence, and strength make you a great leader and scientist, a model to follow. Thank you for being my mentor and my friend! Thank you for all the advice you gave me, for all the support in the lab and outside, for all the caring, for all the talks, for always being there when I needed, thank you, thank you, thank you!!! You taught me so much about science and about

life I could never thank you enough. Gonçalo, you were our "bobo da festa"! You always made me laugh even when it was the last thing I wanted to do. You helped me through tough times and made me see the bright side of things. Your joy was contagious and although you were grumpy sometimes (like the Muppets) it was part of your style which always made me laugh even more. If I had to pay in crepes all the favours you did, I think Haagen Daz would open a store just for you and you would finally gain a few pounds (and I am only counting the technology assists). Jokes aside thank you for being a great friend and for all that you have taught me (or tried, because I think I am still a leading zero as regards technology stuff). Rita, you were a great colleague, but specially a huge friend. It was you I resorted to complain about my problems and failed experiments, and you had always the power to show me the light at the end of the tunnel and that everything was going to work out. Thank you for always listening and for all the support. You were always there for me when I asked and even when I did not, always with kindness and compassion. I admire your courage to pursue a career in science, especially in a foreign (and so cold) country, and with your knowledge and competence I know you are going to be an incredibly successful scientist. Mafalda, although you were not in the lab when I started my PhD you were the one that patiently taught me how to do science and how to work with the peculiar bacteria *Streptococcus pneumoniae*. These teachings accompanied me through this journey, and I attempted to be the excellent teacher that you were to all the students that crossed my path. It was also a privilege to continue your work in a very interesting and exciting project. Sara Pinheiro, you were my lab partner in the last year of my PhD and heard me complaining about time and results, allowing me to express my frustration, typical of the last steps of a PhD. Thank you for listening and for giving me all the assistance I needed.

My sincere gratitude to Teresa Baptista da Silva, an outstanding competent technician, always kind and eager to help and do everything in her power to make our life easier.

I also thank my colleagues from the Bacterial Cell Biology laboratory: Ambre, Andreia Duarte, Andreia Tavares, Bruno, Helena, João, Mário, Moritz, Nathalie, Nils, Pedro Matos, Pedrinho, Raquel, Sara, Simon, and Trish. Bruno, thank you for all the help using eHooke, and, together with Sara for the great time I had doing the bioentrepreneurship course. I loved our project and the way we worked together, which helped a lot, since I was returning to work after Pedro was born and was not sleeping much. Helena, Raquel, and Trish for all the patient to answer my questions, wise discussions, and scientific advice. Pedrinho, thank you for all the small favours and for sometimes being a life (or in this case experiments) saver.

I want to thank all my friends and colleagues from the PhD program, other labs at ITQB (Cátia Bárria, Susana Barahona, Sara Ramalhete), and other labs at FCT (Joana Bugalhão, Inês Grilo, Raquel Portela, Bárbara Gonçalves).

I would also like to acknowledge the MolBioS PhD program, ITQB-NOVA and FCT-NOVA, both great institutes to work in, and Fundação para a Ciência e Tecnologia for funding my PhD scholarship.

Quero agradecer também aos meus amigos. À minha amiga de sempre, como uma irmã, Catarina, a melhor amiga que alguém poderia ter! Obrigada por me apoiares sempre, pela amizade, compreensão e pela tua contagiante alegria que nos faz acreditar que tudo ficará bem. À Sofia por me ouvires tantas vezes e me aconselhares, por me fazeres acreditar em mim e que os nossos sonhos podem ir mudando com o tempo e está tudo bem. E também ao Pedro por tantos momentos de diversão. À Joaninha que me aturou tantas vezes o mau feitio, que sempre teve paciência para mim e que sempre esteve ao meu lado, apesar da distância. Ao Rafael cuja coragem, força e resiliência eu admiro. Obrigada pelo teu carinho e amizade sincera, tenho muitas saudades tuas! Ao Francisco que sempre adorou as minhas piadas secas e que é o mais divertido do grupo. Obrigada por todas as palhaçadas e brincadeiras.

Por fim, e principalmente, quero agradecer à minha família. Aos meus pais que são sem dúvida os melhores do mundo. Eles são os meus ídolos, os meus exemplos de vida. Ambos trabalharam e lutaram muito, desde sempre, para se instruírem, para conseguirem ser alguém que realmente faça a diferença no mundo e para me darem o melhor futuro possível. São o exemplo de valores, bondade, generosidade, honestidade que fizeram de mim quem sou e que quero transmitir ao meu filho. Mãe, és a minha força. Espero conseguir ser para o Pedro o que foste e sempre serás para mim. Obrigada por me amares incondicionalmente, por acreditares sempre nas minhas capacidades, por me fazeres acreditar que todos os sonhos são possíveis e por me ajudares a superar todos os desafios com a certeza de que estarás sempre lá se eu cair. Pai, obrigada por me ensinares que vale a pena lutar por um mundo melhor, por me ensinares a seguir as minhas convicções e por me apoiares em todas as minhas decisões. Talvez um dia consiga chegar ao teu nível de organização e calma, mesmo quando estamos no meio de um furacão. À minha avó São que me educou e cuidou de mim (enquanto os meus pais trabalhavam), que me ensinou a ser briosa, a saber estar e me levou sempre às aulas de ballet. À minha Titi Lena que foi sempre uma lutadora mesmo com todos os desafios que enfrentou! Apesar de às vezes não o demonstrar como gostaria, gosto muito de ti! Obrigada por todo o apoio que sempre me deste e por seres a Dadá querida do Pedrinho. Aos meus tios e tias e todos os primos sempre presentes e que de várias formas me ajudaram até hoje. Só desejo que a pandemia seja ultrapassada para podermos retomar os nossos encontros de família normalmente. À minha mana mais velha Aida e aos meus sobrinhos que apesar de longe estão sempre presentes. Ao mimado Félix que dá muito amor. Aos meus sogros, amigos, que entraram na minha vida e para a minha família, dando-me sempre todo o apoio e carinho, e que são mais um pilar na minha vida. Por último, mas o mais importante,

ao Jorge, minha alma gémea, meu marido, amigo, que é o meu porto de abrigo, meu grande amor. Tenho um orgulho imenso em ti, no teu talento, mas principalmente na pessoa que és. Obrigada por me apoiares incondicionalmente e puxares por mim para que eu consiga realizar todos os meus/nossos sonhos e por me fazeres feliz infinitamente muito. Foi durante o PhD que nos casámos e que, três anos depois, me deste o filho mais lindo do mundo! E ao Pedrinho que, é a luz dos meus olhos, que me deu muitas noites sem dormir, mas que me mostrou um amor absoluto e me fez crescer para tentar ser melhor todos os dias.

"Se podes olhar, vê. Se podes ver, repara."

(Livro dos Conselhos e epígrafe de "Ensaio sobre a Cegueira" de José Saramago)

RESUMO

A capacidade de *Streptococcus pneumoniae* em causar doença está normalmente dependente da presença do polissacárido capsular, também denominado de cápsula, no exterior da superfície deste organismo bacteriano. Assim, o estudo do processo que regula e realiza a síntese deste polímero é fundamental para o desenvolvimento de novas estratégias que possam ser empregues no combate a este agente patogénico humano.

De forma a estudar como ocorre a coordenação da síntese da cápsula durante o ciclo celular bacteriano, tornou-se necessário o desenvolvimento de novas ferramentas que permitissem a localização de proteínas específicas em bactérias, durante o processo de divisão bacteriana. Para isso, construímos várias ferramentas que permitem a fusão de proteínas de interesse com proteínas fluorescentes em *S. pneumoniae*, que podem ser usadas noutras bactérias Gram-positivas. Através da manipulação da estrutura e da estabilidade do terminal 5' da molécula de mRNA, e consequentemente do acesso do ribossoma a esta molécula, foi possível garantir a expressão de proteínas fluorescentes de modo a obter um sinal de fluorescência intenso.

Em quase todos os serótipos de pneumococos, a regulação da síntese da cápsula está a cargo das proteínas Wzd e Wze, que co-localizam no septo bacteriano e que garantem a expressão da cápsula nesse local. Neste trabalho, observámos uma interação entre a proteína Wzg, a ligase que está envolvida na ligação da cápsula à parede bacteriana, e a proteína reguladora Wzd. Propusemos que o par Wzd/Wze garante que a bactéria está totalmente envolvida pela cápsula através do recrutamento da proteína Wzg para o septo. Um maior número das enzimas Wzg no septo poderá ajustar o ritmo de ligação da cápsula ao peptidoglicano com o ritmo a que o peptidoglicano é sintetizado. De acordo com este modelo, mutantes em que o gene *wzd* foi deletado, não apresentam cápsula no septo de divisão, mas mantêm a presença deste polímero na superfície lateral.

A ausência de cápsula no septo de divisão parece ser suficiente para tornar as bactérias suscetíveis à lise induzida por hidrolases de peptidoglicano e para diminuir a sua capacidade de causar doença no modelo de infeção de embrião de *Danio rerio* (peixe-zebra). Estes resultados indicam que ao impedir o completo envolvimento da bactéria pela cápsula, mesmo que de forma transiente ou num local específico, poderemos conseguir facilitar a eliminação de bactérias devido à exposição da parede bacteriana.

Uma vez que a presença do par Wzd/Wze é fundamental para que *S. pneumoniae* consiga causar doença num hospedeiro infetado, decidimos desenvolver um método que permitisse a identificação de compostos capazes de impedir esta interação do par Wzd/Wze

no septo de divisão. Para isso, construímos uma estirpe que produz as proteínas Wzd e o Wze ligadas a diferentes proteínas fluorescentes. Assumimos que caso a interação destas proteínas fosse inibida, os sinais de fluorescência associados à proteína Wzd e à proteína Wze, em vez de estarem co-localizados no septo de divisão, estariam espalhados, respetivamente, pela membrana celular e pelo citoplasma. A aplicação deste método foi bem-sucedida dado que a análise de um pequeno número de compostos testados permitiu a identificação de um candidato promissor.

Esta tese demonstrou que as bactérias de *S. pneumoniae* precisam de estar completamente envolvidas por uma cápsula de modo a assegurar a sua sobrevivência na presença de enzimas capazes de degradarem o seu peptidoglicano, ou na presença do sistema imunitário do hospedeiro, e permitiu a identificação de um método para a identificação de compostos que impedem o correto processo de síntese da cápsula.

Palavras-chave: *Streptococcus pneumoniae*, cápsula, virulência, complexo Wzd/Wze.

ABSTRACT

The ability of *Streptococcus pneumoniae* to cause disease is dependent on its ability to synthesize a capsular polysaccharide, also known as the capsule. The study of the regulation of the capsule synthesis is crucial for the development of new strategies to fight this human pathogen.

To study how capsule synthesis is regulated during the pneumococcal cell cycle, it was necessary to develop improved tools that permit the localization of proteins in dividing pneumococcal bacteria. We have therefore constructed several tools that allow the fusion of proteins of interest with fluorescent proteins in *S. pneumoniae* and that can be used in other Gram-positive bacteria. By manipulating the structure and stability of the 5′ end of the mRNA molecule, which influences its ability to be recognized by the ribosome, we ensured the expression of the fluorescent protein at levels that result in high fluorescent signals.

In most capsular pneumococci, regulation of capsule synthesis requires two proteins, Wzd and Wze, that co-localize at the division septum and guarantee the presence of capsule at this subcellular location. In this work, we detected an interaction between Wzg, the ligase that attaches capsule to the bacterial cell wall, and the regulatory Wzd protein. We propose that the Wzd/Wze pair ensures full encapsulation of bacteria by recruiting higher number of Wzg proteins to the septum, so that the pace of capsule attachment can match the rate of peptidoglycan synthesis. In accordance with this model, pneumococcal *wzd* null mutants lack capsule at the septum while still having this polysaccharide at their lateral wall.

Absence of capsule at the division septum is sufficient to increase encapsulated bacteria susceptibility to lysis induced by PGN hydrolases, as well as to decrease their survival in the zebrafish embryo infection model. These results indicate that impairing the encapsulation process, even if transiently or at localized subcellular sites, facilitates elimination of bacteria by exposing their cell wall.

As the presence of a functional Wzd/Wze pair is determinant to pneumococci ability to cause disease in the infected host, we developed a screening method for the identification of compounds that prevent Wzd/Wze interaction or their septal localization. This was achieved through the construction of a mutant pneumococcal strain that encodes Wzd and Wze fused to different fluorescent proteins. We assumed that if Wzd and Wze proteins do not interact, their fluorescent derivatives, which normally are co-localized at the division septum, will spread over the membrane and throughout the cytoplasm, respectively. This screening method was successful, as we identified one promising candidate from a small screen of a few compounds.

This thesis shows the importance of full encapsulation of pneumococcal cells for survival in the presence of peptidoglycan hydrolases and for evasion from the host immune system. It has also identified an innovative method to find compounds that interfere with the synthesis of pneumococcal capsule.

Keywords: *Streptococcus pneumoniae*, capsule polysaccharide, virulence, Wzd/Wze complex.

TABLE OF CONTENTS

LIST OF FIGURES

LIST OF TABLES

ABBREVIATIONS AND ACRONYMS

AU	Arbitrary Units
aa	Amino acids
Amp	Ampicillin
ATP	Adenosine triphosphate
bp	Base pairs
BTH	Bacterial Two-Hybrid
BY-kinase	Bacterial tyrosine kinase
CBD	Choline-binding domain
CBPs	Choline-binding proteins
CDC	Centers for disease control and prevention
CDCs	Cholesterol Dependent Cytolysins
cDNA	Complementary DNA
CFP	Cyan Fluorescent Protein
CM	Cytoplasmic Membrane
CPS	Capsular polysaccharide
CSP	Competence-stimulating peptide
DDT	Dichlorodiphenyltrichloroethane
DEAE	Diethylaminoethanol
DNA	Deoxyribonucleic acid
DNA-PPF	DNA Polymerase Processivity Factor
dpf	Days post-fertilization
EDTA	Ethylenediaminetetraacetic acid
Ery	Erythromycin
FucNAc	*N*-acetylfucosamine
FR	Fluorescence Ratio
Gal	Galactose
GalNAc	*N*-acetylgalactosamine
GFP	Green Fluorescent Protein
Glc	Glucose
Glc1-P	Glucose-1-Phosphate
GlcA	Glucuronic acid
GlcNAc	*N*-acetylglucosamine
Gro	Glycerol
GTP	Guanosine triphosphate
hpi	Hours post infection
IPTG	Isopropyl-β-D-1-thiogalactopyranoside
IC	Inhibitory Compound
IS	Insertion Sequence
Kan	Kanamycin
LA	Luria bertani broth Agar
LB	Luria Bertani broth
LCP	LytR,CspA,Psr
LTA	Lipoteichoic acid

ManNAc	*N*-acetylmannosamine
MurNAc	*N*-acetylmuramic acid
mRNA	Messenger RNA
NAM-amidase	*N*-acetylmuramyl-L-alanine amidase
NDP	Nucleotide diphosphate
NETs	Neutrophil Extracellular Traps
OD	Optical Density
ORF	Open Reading Frame
P	Phosphate
PCC	Pearson Correlation Coeficient
P-Cho	Phosphorylcholine
PCP	Polysaccharide Co-Polymerase
PCR	Polymerase Chain Reaction
PCV	Pneumococcal Conjugated Vaccine
PGN	Peptidoglycan
PHP	Polymerase and Histidinol Phosphatase
Ply	Pneumolysin
PMSF	Phenylmethylsulfonyl fluoride
PPV	Pneumococcal Polysaccharide Vaccine
PsaA	Pneumococcal surface adhesin A
PspC	Pneumococcal surface protein C
qPCR	Quantitative Polymerase Chain Reaction
Rha	Rhamnose
RNA	Ribonucleic acid
RS	Reporter strain
SDS	Sodium Dodecyl Sulphate
SDS-PAGE	Sodium Dodecyl Sulphate Polyacrylamide Gel Electrophoresis
SR-SIM	Super Resolution Structured Illumination Microscopy
TA	Teichoic Acids
Tet	Tetracycline
tRNA	Transfer RNA
TSA	Tryptic Soy Agar
TSB	Tryptic Soy Broth
UDP	Uridine diphosphate
Und-P	Undecaprenyl-phosphate
WHO	World Health Organization
WT	Wild type
WTA	Wall Teichoic Acids
X-gal	5-bromo-4-chloro-3-indolyl-β-D-galactopyranoside

Chapter 1

Introduction

1.1. General Introduction

Streptococcus pneumoniae, or pneumococcus, is a lancet-shaped facultative anaerobic coccus and a member of the Firmicutes phylum. This Gram-positive organism was first isolated in 1881 by George Sternberg (Sternberg, 1881) and Louis Pasteur (Pasteur, 1881) in two almost simultaneous and independent works. Both researchers recognized the presence of a capsule surrounding the diplococcal form of individuals that belonged to this microorganism. Further studies on the capsular polysaccharide (CPS) played a significant role in our understanding of biological processes, elucidating how capsular polysaccharides act (Dochez and Avery, 1917) or influence bacterial virulence (Avery and Dubos, 1931). Furthermore, in an experiment with CPS - conducted by Griffith in 1928 – it was suggested that bacteria are capable of naturally transferring genetic information (Griffith, 1928), which prompted the discovery that DNA is the material that encodes the genetic information of an organism (Avery, Macleod and Mccarty, 1944).

S. pneumoniae are highly adapted pathogen that can colonize the mucosal surfaces of the human upper respiratory tract. Colonization is generally asymptomatic and transmission occurs by aerosols that potentially result in the contamination of objects with mucosal secretions containing biofilm streptococci (Marks, Reddinger and Hakansson, 2014). Although carriage rates can differ based on where the samples are collected from, a rate of <10% has been observed in healthy adults (Yahiaoui et al., 2016). However, a different study demonstrates that carriage in healthy adults seems to be more dynamic than previously supposed since 20% of adults were intermittent carriers and 10% of adults were persistent carriers (with some examples of a serotype being carried for >6 months) (Almeida et al., 2021). These discrepancies seem to occur due to low colonization density in adults which some traditional culture detection methods could not uncover (Almeida et al., 2021). In children, this rate varies between 27% in European countries and 65% in some African countries (Abdullahi et al., 2012; Yahiaoui et al., 2016). In contrast, a recent study shows that pneumococcal carriage in Portugal is around 60% in children under the age of 6 years old (Félix et al., 2021). In addition, pneumococcal disease develops when this organism is able to disseminate to other sites of an infected human individual, such as the middle ear, lungs, bloodstream, or brain. This opportunistic pathogen is a leading cause of a wide spectrum of infections that include otitis

media, community acquired pneumonia, meningitis, and sepsis. The risk groups that are particularly vulnerable include the elderly, children and immunocompromised patients (Loughran, Orihuela and Tuomanen, 2019). As colonization precedes pneumococcal disease development, high rates of colonization in the human population result in extensive morbidity and mortality, which creates a global burden. *S. pneumoniae* is estimated to cause over a million deaths per year, worldwide; among those, half a million are children under 5 years old (Troeger et al. 2018; WHO 2012). Furthermore, *Streptococcus pneumoniae* is included in a list of 12 bacterial families, representing the greatest threats to human health, which were published in 2017 by the World Health Organization (WHO) (WHO, 2017). It is also important to highlight the economic burden associated with pneumococcal infections. For instance, the total healthcare costs related to community acquired pneumonia in Europe were estimated to be around 10 billion euros annually, a value that is much higher in the USA, estimated to be 17 billion euros annually (Gibson, Loddenkemper and Sibille, 2003; File et al., 2010).

Some particular traits facilitate the spread and persistence of pneumococcal bacteria in the human population, making pneumococcus a particularly difficult pathogen to fight. First, high carriage rates and asymptomatic colonization allows the pneumococcus to thrive and persist in the community (Loughran, Orihuela and Tuomanen, 2019). Secondly, this pathogen has the ability to undergo natural transformation, being able to remodel its genome by uptake and integrating exogenous DNA, either from other pneumococci or closely related streptococci (Mostowy et al., 2017; Sørensen et al., 2016). The pneumococcal transformation process is induced by the competence-stimulating peptide (CSP), released by growing pneumococcal bacteria, which concentration is dependent on cell density as in other bacterial processes dependent on quorum sensing mechanisms. The natural capacity to uptake DNA allows pneumococcal clinical isolates to maintain beneficial mutations and to gain additional functions by horizontal gene transfer, promoting an extensive serotype diversity and the resilience of pneumococcal populations (Weiser, 2010). As a result, pneumococcal bacteria are able to adapt and acquire a broad diversity of resistance mechanisms, either single antibiotic resistance or, more alarmingly, multidrug-resistance (Van Bambeke et al., 2007). Therefore, it is extremely important to understand the molecular basis of mechanisms used by pneumococci to adapt to challenges posed by their environment, which is expected to help in the discovery and development of new anti-infective agents.

One strategy that has been successfully used to fight *S. pneumoniae* infections is vaccination. All pneumococcal vaccines currently available on the market target the pneumococcal polysaccharide capsule. Pneumococcal polysaccharide vaccines (containing the capsular polysaccharide, PPV) and conjugated vaccines (containing capsular polysaccharides conjugated with a highly immunogenic protein, such as tetanus toxoid, diphtheria toxoid or a mutated diphtheria toxoid, PCV) have been produced (Pollard et al., 2009). However, both vaccines only conferred protection against the serotypes contained in these formulations. As there are more than 100 different pneumococcal serotypes, current vaccines can only target a small number of serotypes, particularly those that are frequently found in association with pneumococcal disease (Geno et al., 2015; Geno, Saad and Nahm, 2017; Ganaie et al., 2020). It should be highlighted that certain serotypes are more commonly associated with carriage whereas others are associated with disease (Brueggemann et al., 2003; Hanage et al., 2005).

There are additional limitations associated with the current pneumococcal vaccines. With an immature immune system, children under the age of 2 years present a poor immunological reaction to pure polysaccharide antigens. Thus, conjugated vaccines (PCV) which elicits T-cell help in a combined B- and T- cell response, that results in improved memory B- cell formation, are recommended to individuals of this age group (Pletz et al., 2008).

Despite the success observed in the reduction of the incidence of pneumococcal disease after the introduction of pneumococcal vaccines, there are several factors that undermine the effectiveness of vaccines. First, different pneumococcal serotypes are unevenly distributed according to the geographical region (Yahiaoui et al., 2018; Lee, Banks and Li, 1991). Second, the cost of PCVs is high, hindering its use in developing countries, where the death rate of children from invasive pneumococcal disease is highest (Chen et al., 2019). Finally, and more disturbing, is the current observation of increase rates of disease caused by pneumococcal serotypes not included in the current vaccines. This phenomenon can be explained by the occurrence of two different processes: pneumococcal serotype replacement and/or capsular switching. In the first case, a vacant niche, which can be created upon the introduction of vaccines, is occupied by the expansion of pre-existing nonvaccine serotypes. Serotype replacement seems to be occurring in several reported cases of pneumococcal carriage and in some types of pneumococcal disease (Eskola et al., 2001; Huang, 2005; Aguiar et al., 2010). Capsular switching appears via recombination of large DNA fragments and may include the transfer of a complete capsule locus or of particular chromosomal DNA

polymorphisms. Despite the likelihood that DNA recombination events have occurred throughout the history of pneumococcal evolution, it has been proposed that vaccine selective pressure and the widespread antibiotics use have probably increased its occurrence (Wyres et al., 2013; Andam and Hanage, 2015). In conclusion, as the use of PCVs is shifting the serotype distribution observed in pneumococcal isolates that are associated with carriage in the human population and pneumococcal disease, a constant surveillance and periodic changes of vaccine composition has been recommended (Andam and Hanage, 2015). Therefore, it is important to promote a timely study of how pneumococcal bacteria produce different capsular polysaccharides and the development of new ways capable of eliminating the shortcomings referred above. The later may include the discovery of new pneumococcal anti-infective agents, such as novel antibiotics, or the development of vaccines based on pneumococcal proteins that contribute to virulence and are common to all serotypes.

1.2. Capsular polysaccharide

1.2.1 Structure of the S. pneumoniae *capsular polysaccharide*

The major virulence factor of *S. pneumoniae* is the pneumococcal capsular polysaccharide as nonencapsulated pneumococcal bacteria are unable cause disease in the infected host (Avery and Dubos, 1931; Bender and Yother, 2001; Morona et al*.,* 2004). This capsule shield forms the outmost layer of the bacterial cell, with an approximately 200-400 nm thickness, and represents more than half of the pneumococcal volume (Sørensen et al*.,* 1988). Capsular polysaccharides are generally anionic due to the presence of uronic acid, phosphate, and pyruvate, but there are some exceptions which have no net charge (e.g., serotype 14) (Kamerling et al., 2000). In most cases, capsular polysaccharides are considered to be covalently attached to the cell wall peptidoglycan and to be composed of long chains of repeating oligomeric units (Sørensen et al*.,* 1990). Capsular polysaccharides are structurally different as they may vary in complexity: from linear polymers, constituted by one or two monosaccharides, to complex polysaccharides, that can contain up to eight different monosaccharides, with a branched structure that can include side chains in combination of particular modifications. The repeating units of pneumococcal capsular polysaccharides often have O-acetyl, and pyruvyl acetal substitutions, at various sites, with different substitution rates

(Calix et al., 2012; Geno et al., 2015). This heterogeneity among capsular polysaccharides - both structurally and antigenically - is originated by the diversity of sugars, the presence of different sugar linkages or of diverse side chains (Figure 1.1). To date there are more than 100 different serotypes reported in *S. pneumoniae* and the capsule is used as a classification system, assigning each isolate into a different serogroup (Geno et al., 2015; Geno, Saad and Nahm, 2017; Ganaie et al., 2020). The chemical structure of the repeat units have been determined in approximately 70% of the serotypes (Geno et al., 2015). For example, the capsular polysaccharide of the pneumococcal serotype 14 (one of the predominant serotypes in South American countries before implementation of vaccination programs (Hortal et al., 1997)) is composed of a tetrasaccharide repeating unit (Figure 1.1) containing D-glucose, N-acetyl-D-glucosamine, and D-galactose (Lindberg, Lonngren and Powell, 1977)

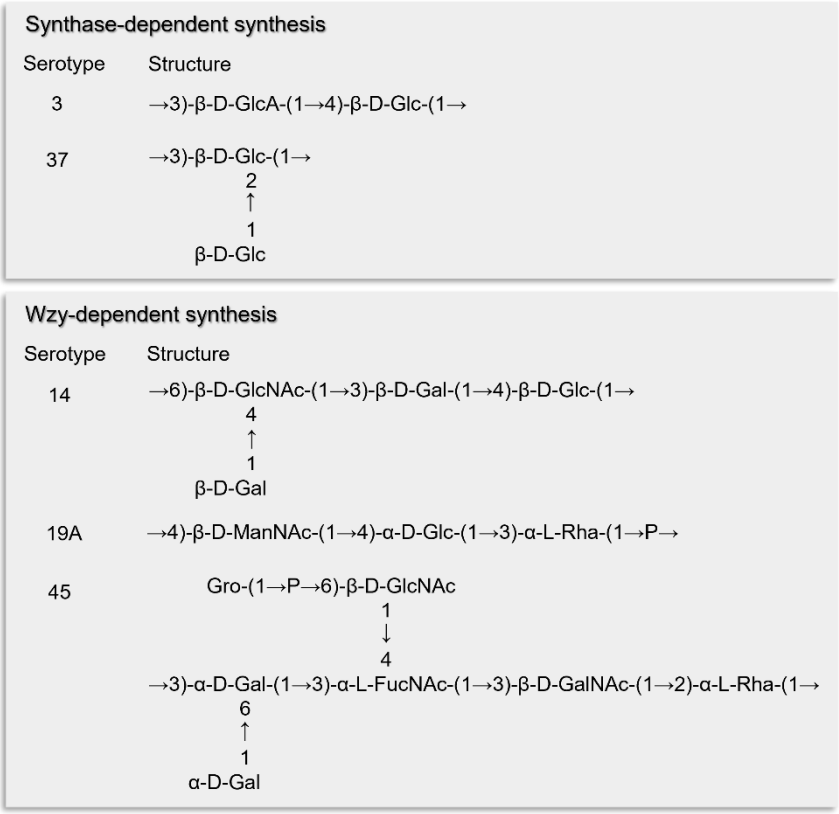

Figure 1.1: Capsular polysaccharide repeating units. Examples of the biochemical structure present in the repeating units of capsular polysaccharides either synthesized by the synthase-dependent mechanism or the Wzy-dependent mechanism, showing the vast diversity of structures between serotypes. FucNAc, *N*-acetylfucosamine; Gal, galactose; GalNAc, *N*-acetylgalactosamine; Glc, glucose; GlcNAc, *N*-acetylglucosamine; GlcA, glucuronic acid; Gro, glycerol; ManNAc, *N*-acetylmannosamine; P, phosphate; Rha, rhamnose. Adapted from Geno et al., 2015.

By comparing the genome of different serotypes, it was observed that acquisition, and/or loss, of particular capsular genes is the underlying cause for the emergence of many serotypes, being the average capsular rate of recombination much higher than the recombination rate of the rest of the genome (Mostowy et al*.,* 2017; Mavroidi et al*.,* 2007). This higher rate of recombination can result from two particular factors: the abundance of transposable and insertion sequence (IS) elements at the capsule locus; the similarity found in the ORFs that in different clinical isolates flank the capsular operon. This is in accordance to the notion that the *cps* cluster behaves as a pathogenicity island (Groisman and Ochman, 1996). In fact, Venkateswaran and collegues observed in vivo switching from one capsule type to another in pneumococcal cultures. In this case, authors reported that the difference observed in the pneumococcal serotypes was a consequence of the presence of an O-acetyl group in one of the capsular polysaccharides (Venkateswaran, Stanton and Austrian, 1983). This serotype transformation of pneumococcal bacteria, which may facilitate their evolution and adaptation to different host environments, implies that, by introducing the *cps* locus of the donor strain into the recipient, the latter gains new capsular genes but loses its own capsular cluster.

1.2.2 Role of the S. pneumoniae *capsular polysaccharide*

A century of research has shown that the capsule of *Streptococcus pneumoniae* has an essential role in the colonization of the infected host and in the virulence of a particular clinical isolate. Indeed, several studies demonstrated that unencapsulated mutant strains, or mutant strains that produce reduced amounts of capsule, are avirulent (Avery and Dubos, 1931; Bender and Yother, 2001; Morona et al*.,* 2004). Moreover, the attachment of the capsular polysaccharide to the cell wall is also an important factor to pneumococcal virulence (Morona, Morona and Paton, 2006).

The CPS of *S. pneumoniae* has distinct functional roles both in colonization and during infection of the host. When the pneumococcus enters the nasal cavity, it encounters an environment full of mucus secretions that are part of an innate response of the respiratory tract. To initiate a stable host colonization, bacteria need to pass through the luminal mucus and migrate to the epithelial surface. Nelson et al. showed that the capsule reduces bacterial entrapment by the mucus, possibly due to electrostatic repulsion, which may facilitate access

and attachment of pneumococcal bacteria to the surface of epithelial cells (Figure 1.2). This hypothesis emerged as both the sialic acid-rich mucopolysaccharides, present in the composition of the human mucus, and almost all pneumococcal capsular polysaccharides, are negatively charged (Nelson et al., 2007; Kamerling et al., 2000). Once at the epithelial surface, the expression of a thick capsule seems to be disadvantageous as it diminishes access of pneumococcal surface proteins (such as adhesins and teichoic acids) to host cell receptors. As a consequence, bacterial cell adherence can get compromised (Cundell et al., 1995b; Kim and Weiser, 1998). The contact of these surface proteins to the host epithelial receptors allows the establishment of colonizing bacteria in the nasopharynx and enhances their capacity to cross the blood-brain barrier (Figure 1.2). Despite its diverse composition, pneumococcal CPS has a major role in helping bacteria to escape host's immune system. During the progression from colonization to invasive infection, the capsule forms an inert shield that prevents antibody deposition and complement binding to structures at the bacterial cell surface, such as teichoic acids and cell surface proteins. In the absence of CPS, binding of antibodies and C3b molecules to the surface of bacterial cells serve as a red flag that permit their recognition by specific receptors produced by the host's phagocytes. Thus, acting as a mechanical barrier, CPS renders the pneumococcal cells resistant to phagocytosis (Musher, 1992; Winkelstein, 1981). Moreover, the presence of capsule can interfere with the host-pathogen interactions through a different mechanism. A well-known host response upon neutrophil stimulation is the production of neutrophil extracellular traps (NETs) that can bind, disarm, and kill pathogens extracellularly (Brinkmann et al., 2004; Urban et al., 2006). NET trapping seems to be a way of confining the infection and preventing systemic bacterial spread. Interestingly, it has also been reported that *S. pneumoniae* CPS can contribute to pathogenesis by reducing the trapping of bacteria by NETs structures (Wartha et al., 2007).

Based on the above, it is accepted that a successful pneumococcal colonization requires an optimal strategy that balances the CPS expression (Figure 1.2) and that pneumococci have the capacity to spontaneously vary CPS expression between two phases that have been designated as opaque and transparent. The opaque phase is characterized by an opaque, enriched in CPS, phenotype, which is present in colonies of bacteria that are more resistant to opsonophagocytosis but less able to adhere to the host epithelia. Bacteria that are present in the transparent phase, produce colonies with a transparent morphology and are associated with a low-capsule phenotype. These bacteria are more capable of adhesion to host

cells, but are susceptible to opsonophagocytosis (Weiser et al., 1994; Kim and Weiser, 1998). Furthermore, studies suggest that pneumococcus actively downregulates or upregulates CPS production in different host habitats (Ogunniyi, Giammarinaro and Paton, 2002; Hammerschmidt et al., 2005). This feature allows the selection of variants with optimal adaptation or fitness in different steps of colonization and infection.

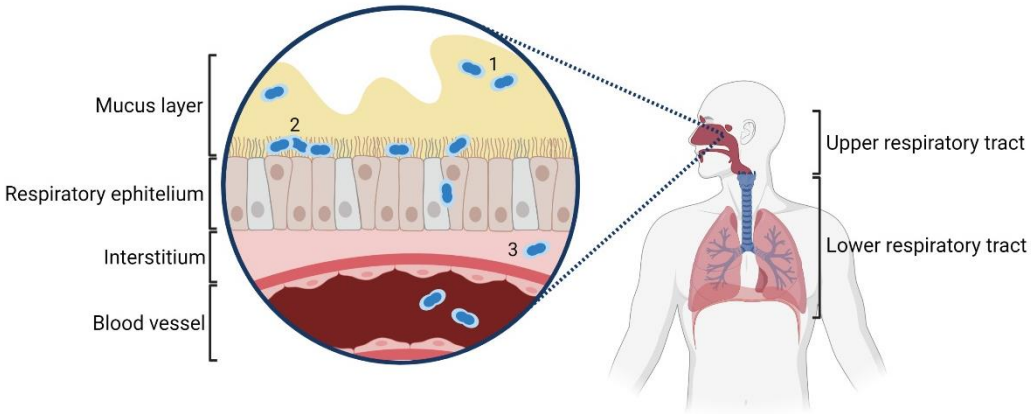

Figure 1.2: Variation of the thickness of the CPS during colonization and infection. During colonization of the nasopharynx, *S. pneumoniae* encounters the mucus environment that serve as a host barrier defence to invading microorganisms. The production of a thicker capsule reduces entrapment of bacteria by the mucus, probably due to electrostatic repulsion, helping the migration of bacteria to the epithelial cells (1). Then, at the epithelial surface, *S. pneumoniae* bacteria need to reduce capsule expression to establish colonization, as the presence of a thick capsule diminishes the access of pneumococcal surface proteins to host cell receptors (2). When pneumococcal bacteria progress to invasive infection, which involves crossing the blood-brain barrier, an enhancement of capsule expression is required to help bacteria escape the host's immune system (3).

Certain capsular serotypes appear to be better adapted to cause invasive disease while others seem to appear more frequently in carriage, considering that different serotypes show different rates of colonization and virulence (Melin et al., 2010; Orio et al., 2011). Although CPS is not the only element involved in the interaction between pneumococcal bacteria and the infected host, there are several studies that demonstrate a direct correlation between the capsule type expressed and accessibility of surface adhesins, resistance to complement deposition, and, in general, virulence (Kelly, Dillard and Yother, 1994; Sanchez et al., 2011).

Even though the amount of CPS expressed is diverse among serotypes, the difference in virulence is related to the biological properties of the capsule and not simply to the capsule thickness (Austrian, 1981).

Recent studies have shown that "nontypable" pneumococci can be found among those isolates capable of pneumococcal carriage and disease (Chewapreecha et al., 2014; Dixit et al., 2016). Although some of these isolates might produce a novel CPS that does not react with the existing typing sera, in most cases, the *cps* locus is absent or carry mutations that prevents production of capsule. The loss of CPS significantly decreases the chance of invasive pneumococcal disease and the occasional cases of pneumococcal infections reported to be caused by nonencapsulated strains are, more commonly, noninvasive diseases like otitis media or conjunctivitis (Park et al., 2014; Xu et al., 2011; Valentino et al., 2014). This observation suggests that pneumococcal isolates can compensate for the absence of capsule and cause disease in the infected host. Hence, as the capsule polysaccharide plays a critical role in virulence, its study is crucial for the development of new tools to fight this pathogen.

1.2.3 Genetic organization of the capsule locus of S. pneumoniae

Streptococcus pneumoniae circular genome is composed of about 2 million base pairs (bp) and has approximately 40% of G/C content (Hoskins et al., 2001).

The genes coding for enzymes involved in the synthesis of the capsular polysaccharide are located in a specific region of the pneumococcal chromosome - the *cps* operon - that has a cassette-like organization and that it is structured as a single transcriptional unit (Wen et al., 2015). In pneumococcal isolates from certain serotypes, there are enzymes essential for CPS synthesis that are encoded elsewhere in the pneumococcal chromosome. These enzymes are involved in the metabolism of particular capsular monosaccharides that are common to other cellular pathways and that are synthesized by housekeeping metabolic pathways (Morona, Morona and Paton, 1997; Hardy, Caimano and Yother, 2000; Yother, 2011). Except for serotype 37, the *cps* operon is flanked by the *dexB* and *aliA* genes, which are highly homologous amongst strains of different capsular serotypes (Bentley et al., 2006).

The organization of the *cps* operon (Figure 1.3) is similar to operons that in several lactic acid bacteria are responsible for the biosynthesis of exopolysaccharides of various composition (de Vuyst and Degeest, 1999). The upstream end of the *cps* locus is highly

conserved between clusters of different serogroups, and it includes the *wzg, wzh, wzd* and *wze* genes (also known as *cpsABCD*) (Figure 1.3). Immediately upstream of the first gene of the operon, *wzg*, there is a conserved promoter sequence, which is in accordance with the transcriptional start point of the *cps* operon that has been identified. However, full transcription of the *cps* genes requires additional elements that localize upstream of the core promoter (Muñoz et al*.,* 1997; Wen et al*.,* 2015). The fifth gene of the operon encodes the initiating glycosyltransferase, which is constituted by *wchA* (*cpsE*) in the majority of serotypes, where glucose is the first sugar of the capsule repeating unit (Kolkman, van der Zeijst and Nuijten, 1998; Bentley et al*.,* 2006; Yother, 2011). The sequence of *wzg* is the most conserved one between serogroups, whereas the sequences of *wzh*, *wzd* and *wze* (and *wchA* when present) can be divided in two different clusters. One of the clusters is associated with the ancestral form of the genes, while the second cluster probably emerged by lateral gene transfer and is correlated with serotypes that are more prone to cause disease (Morona et al*.,* 1999; Mavroidi et al*.,* 2007; Varvio et al,. 2009).

The downstream region of the *cps* locus is not as conserved as that encoding the first four *cps* genes being considered serotype specific (Figure 1.3). In each *S. pneumoniae* strain only one type of capsule is produced as there is normally only one set of type-specific genes. In addition, there is little homology between type-specific genes from different capsular serotypes (Bentley et al*.,* 2006). The variable region of the *cps* operon encodes for enzymes responsible for polymer-specific functions, such as the synthesis of specific NDP-sugars repeating units to each serotype, glycosyltransferases, and enzymes involved in particular sugar modifications (Kolkman, van der Zeijst and Nuijten, 1998; Bentley et al*.,* 2006). Moreover, in this region there are genes that encode the polymerase responsible for connecting individual repeating units and assembling high molecular weight CPS, *wzy*, and that encode the flippase responsible for transport of assembled CPS across the membrane to the cell surface, *wzx* (Bentley et al*.,* 2006; Yother, 2011).

Despite the conserved organization of the *cps* operons found in most pneumococcal isolates, there are two serotypes whose *cps* operons have a peculiar organization: serotype 3 and serotype 37.

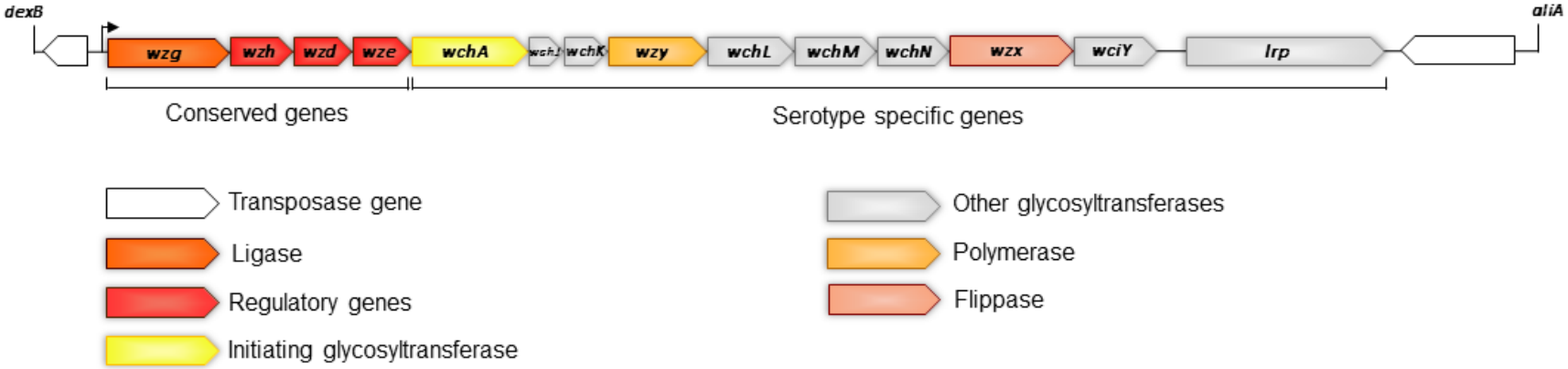

Figure 1.3: Schematic representation of the genetic organization of the *cps* operon of *S. pneumoniae* serotype 14. The conserved region between serotypes and the serotype specific region are shown. The arrow boxes represent the direction of transcription of each gene and are coloured according to the gene key, each colour corresponding to the function of the gene. This locus is flanked by the genes *dexB* and *aliA*. The black arrow shows the localization of the *cps* locus promoter. Adapted from Bentley at al., 2006

Pneumococcal bacteria of serotype 3 produce capsule of a relatively simple structure that is composed of alternating units of glucuronic acid (GlcA) and glucose (Glc). In these bacteria, the *cps* locus also localizes between genes *dexB* and *aliA* but there are only two genes that are absolutely required for the synthesis of capsule: *ugd* (*cps3D*), a UDP-Glucose dehydrogenase, and *wchE* (*cps3S*), the capsule synthase. In fact, the expression of WchE is sufficient for the synthesis of high molecular size type 3 polysaccharide in *Escherichia coli* (*E. coli*) and in unencapsulated *S. pneumoniae* strains that are capable of producing UDP-glucuronic acid (García et al*.,* 1997). It is noteworthy to highlight that in pneumococcal isolates of serotype 3, the *cps* locus has the corresponding DNA sequence of the regulatory conserved genes at its 5′, however, except for *wzd*, these genes are truncated or mutated, which prevents expression of the encoded proteins and indicates that these genes are not required for type 3 capsule synthesis (Arrecubieta, Garcia and López, 1995; Dillard, Vandersea and Yother, 1995; García et al*.,* 1997; Caimano, Hardy and Yother, 1998).

In the chromosome of bacteria that belong to serotype 37, there is a cryptic copy of type 33F *cps* locus between the genes *dexB* and *aliA*. However, this operon does not play a part in the production of serotype 37 capsular polysaccharide. In these bacteria, there is only one gene that is necessary for serotype 37 CPS synthesis, the *tts*, which codifies for a β-glucosyltransferase and is localized outside the *dexB*/*aliA* region of the chromosome. Surprisingly, when Llull et al*.* transformed other pneumococcal serotypes and Gram-positive organisms with the gene *tts*, they observed an acquisition of binary capsule types. These bacteria expressed two chemically and immunologically distinguishable capsules, i.e., serotype 37 plus the initial serotype of the transformed strain (García, Llull and López, 1999; Llull et al*.,* 1999; Llull, García and López, 2001).

1.2.4 Capsule Biosynthesis

Despite the structural diversity of the capsule in the different serotypes, there are only two known mechanisms of CPS synthesis in *S. pneumoniae*: the Wzy-dependent mechanism and the synthase-dependent mechanism. In the majority of pneumococcal serotypes the capsular polysaccharide is synthesized through the Wzy-dependent assembly pathway (Bentley et al*.,* 2006). This mechanism of polysaccharide synthesis is widely found in many Gram-negative bacteria, for example in *E. coli* strains producing group 1 and 4 capsules, and

in almost all Gram-positive bacteria, including staphylococcus (Whitfield and Paiment, 2003; Ericsson et al., 2012). Gram-negative and Gram-positive bacteria share common aspects in processes used to regulate and synthesize their capsular polymers. Mechanistically, the initial reaction of CPS polymerization proceeds similarly to other bacterial polymers, like peptidoglycan or lipopolysaccharides, whereby repeating units are built on the inner leaflet of the cytoplasmic membrane, transported across it to the outer face by a Wzx flippase, and then polymerized in a nonprocessive manner by a Wzy polymerase (Yother, 2011).

Only in pneumococcal bacteria of serotypes 3 and 37 is the CPS synthesis performed by the synthase-dependent assembly pathway. In these bacteria, a single enzyme is responsible for the initiation, the polymerization, and the transport of the capsular polysaccharide polymer across the bacterial membrane. In this process, individual nascent sugar units are added progressively to the reducing end of the growing chain through a mechanism that is still not clear. The composition of the resulting polysaccharides are generally simpler than those assembled through a Wzy-dependent assembly pathway, consisting usually of only one or two sugars (Llull et al., 1999; Cartee et al., 2000; Yother, 2011).

1.2.4.1 Synthase-dependent synthesis

Pneumococcal types 3 and 37 use the synthase-dependent mechanism for CPS synthesis. Serotype 3 has a simple disaccharide repeat unit comprising glucose (Glc) and glucuronic acid (GlcA) and requires only one membrane associated enzyme, the synthase WchE (Cps3S). This enzyme is responsible for the transport and linkage of the alternating Glc and GlcA moieties via distinct glycosidic bonds (Cartee et al., 2000). This processive β-glycosyltransferase has a similar predicted architecture as other bacterial polysaccharide synthases (e.g., HasA, the hyaluronic acid capsule of group A streptococci synthase), which includes four transmembrane domains and a large central cytoplasmic domain (Dillard, Vandersea and Yother, 1995; Kumari and Weigel, 1997). Synthesis initiates with the addition of one of the sugar residues, Glc from UDP-Glc, to phosphatidylglycerol, which serves as a primer for polymer synthesis (Cartee, Forsee and Yother, 2005b). After that, synthesis proceeds by the alternate addition of GlcA and Glc to the primer. Initially, the oligosaccharide is loosely associated to the synthase. If the UDP-sugar concentrations becomes limiting, the oligosaccharide-lipid fails to achieve a critical length and dissociates from the enzyme, in an

abortive translocation reaction, accumulating in the membrane (Forsee, Cartee and Yother, 2000). However, if GlcA and Glc are present in sufficient concentrations, a rapid oligomerization occurs reaching the necessary length for recognition (i.e., approximately 8 monomers) (Forsee, Cartee and Yother, 2006). Subsequently, the growing chain becomes tightly associated with the synthase and shifts the enzyme to a highly processive mode, leading to the production of high molecular weight polymers. This process suggests that the concentration of UDP-sugars regulate the rate of polymer synthesis (Forsee, Cartee and Yother, 2006; Ventura et al,. 2006). Moreover, in contrast to Wzy-dependent capsules, the type 3 CPS is not covalently linked to the cell wall (Sørensen et al., 1990). Instead, it remains connected to the cell either by the phosphatidylglycerol membrane anchor or by interactions with the synthase (Cartee, Forsee and Yother, 2005b). Consequently, the polysaccharide is not covalently linked to the peptidoglycan, resulting in its release during growth. Importantly, Choi and coworkers suggested that the CPS release is responsible for the verified lower efficacy of type 3 Pneumococcal Conjugated Vaccine. Two hypotheses emerged to explain this phenomenon, either because anti-CPS antibody binds to free unbound CPS, that functions as a decoy, which reduces opsonization, or because CPS release after antibody binding also prevents opsonization (Choi et al., 2015).

Serotype 37 produces a very thick homopolysaccharide branched capsule. The synthase encoded by *tts* has an apparent bifunctional activity that can either use UDP-Glc (UDP-Glucose) or UDP-Gal (UDP-Galactose) as a substrate. In addition, the gene *tts* is sufficient for the synthesis of a type 37 capsule in different Gram-positive bacteria, which strongly suggests that the nascent polysaccharide chain does not use specific transporters to cross the membrane (Llull et al., 1999; Llull, García and López, 2001).

1.2.4.2 Wzy-dependent synthesis

In *S. pneumoniae* the synthesis of most CPS is carried out by the Wzy-dependent mechanism, which is initiated with a reversible transfer of an activated sugar to a lipid carrier (undecaprenyl-phosphate, Und-P) present on the cytoplasmic face of the cell membrane (Figure 1.4). In the serotypes where glucose is the first sugar of the repeating unit, this step is

carried out by the Glc-1-phosphate (Glc1-P) transferase WchA (CspE) (Kolkman et al., 1997a; Cartee et al., 2005a).

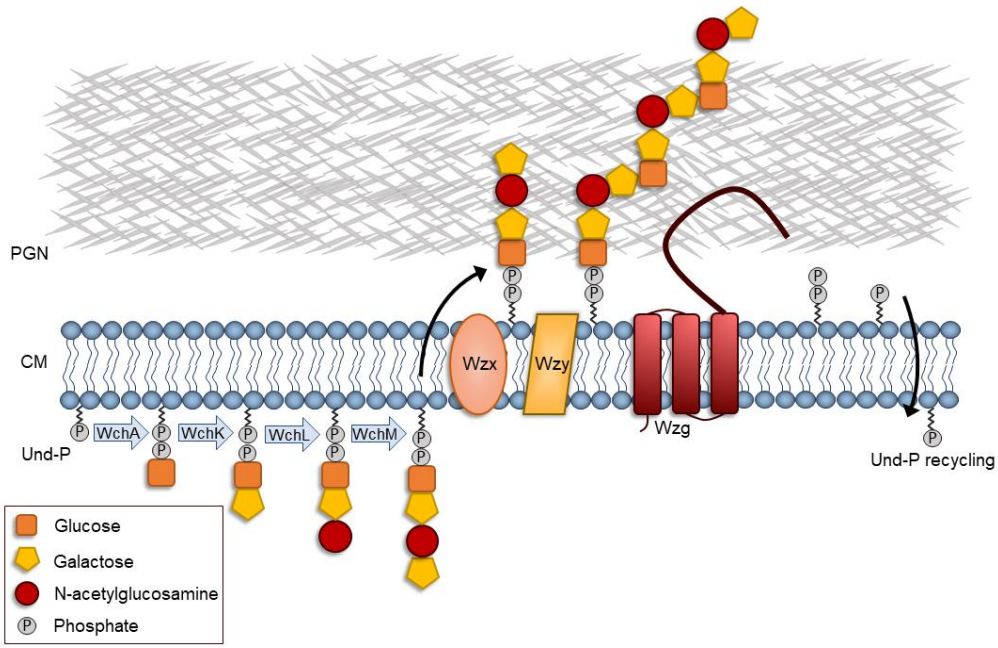

Figure 1.4: Model for *S. pneumoniae* capsular polysaccharide Wzy-dependent synthesis. This model represents serotype 14 CPS synthesis as an example. CPS synthesis initiates with the transfer of a glucose-1-phosphate to the lipid carrier, undecaprenyl phosphate (Und-P), by the initial glycosyltransferase WchA. Afterwards, other glycosyltransferases catalyse the sequential transfer of the other sugars: WchK adds a galactose, WchL adds an *N*-acetylglucosamine and WchM adds another galactose. The assembled lipid-linked capsule repeating unit is then transported across the membrane by the Wzx flippase. Exported capsular repeating units are then linked in a block-wise fashion by the polymerase Wzy, forming a high-molecular weight capsular polysaccharide. Finally, the last step in capsule synthesis requires the covalent attachment of CPS to the peptidoglycan by the ligase Wzg. This last step releases the lipid carrier Und-PP. Then, hydrolysis of the pyrophosphate bond of Und-PP by a phosphatase allows its recycling so that it is available for further cycles of this process. PGN, peptidoglycan; CM, cytoplasmic membrane.

Following initiation, other glycosyltransferases, encoded in the capsule locus, catalyze the sequential transfer of the other sugars, synthesized in the cytoplasm, to form the capsular repeating unit (Figure 1.4). These subsequent reactions occur accordingly to the substrate specificities of the glycosyltransferases to form type-specific CPS repeating units. Particularly for serotype 14, the capsular polysaccharide is composed of a tetrasaccharide repeating unit that is assemble by four different glycosyltransferases. The initial step, where Glc-1-P is linked to Und-P forming Und-PP-Glc, is catalyzed by the WchA transferase. The second assembly step is performed by WchK, a β-1,4-galactosyltransferase, that links galactose to the lipid-

linked glucose. After that, the third sugar, an *N*-acetylglucosamine residue, is added by WchL, a β-1,3-*N*-acetylglucosaminyltransferase. Finally, galactose is the last sugar to be added to the repeating unit and this reaction is catalyzed by WchM, another β-1,4-galactosyltransferase than links the galactose residue to the *N*-acetylglucosamine previously assembled (Kolkman et al*.,* 1997a; Kolkman, van der Zeijst and Nuijten, 1997b).

Once a repeating unit is assembled in the inner leaflet of the cytoplasmic membrane, it can be transported to the extracellular side by the Wzx flippase. Afterwards, in a reaction catalyzed by the Wzy polymerase, the translocated repeating unit is added in a block-wise fashion to others previously translocated, extending the polysaccharide at the reducing terminus, which is linked to the lipid carrier, and forming a high molecular weight capsular polysaccharide (Figure 1.4) (Yother, 2011).

1.2.5 Attachment of sugar polymers to the cell wall

Cell surface attachment of the newly synthesized polymers is the final step in the process of CPS synthesis and has been the subject of recent research developments.

Recently, it has been proposed that to allow the mature CPS to be covalently tethered to the cell wall, there is an unknown enzyme capable of catalyzing a direct covalent linkage, via a 1,6 glycosidic bond, between the capsular polysaccharide and the peptidoglycan at the pneumococcal cell surface. This linkage occurs in the reducing end sugar (usually Glc) of the polymer to the GlcNAc residue of the cell wall peptidoglycan (Larson and Yother, 2017). Moreover, phosphodiester bonds and oligosaccharide linkers – that are common to other polysaccharide-peptidoglycan linkages – seem to be missing in the CPS-peptidoglycan linkage (Larson and Yother, 2017).

Similar to peptidoglycan synthesis, transfer of the polysaccharide chain to the final acceptor releases Und-P-P, hydrolysis of the pyrophosphate bond by a phosphatase occurs and then Und-P is transported back to the cytoplasm. This recycling of Und-P, which is now available at the cytoplasm side of the bacterial membrane, allows the process to start all over again (Bouhss et al*.,* 2008). Xayarath et al. showed that knockout mutants of the flippase Wzx and the polymerase Wzy were only obtained in the presence of suppressor mutations. Interestingly, in most cases, the suppressor mutations were mapped in *wchA*, in the non-conserved extracytoplasmic and in the conserved cytoplasmic glycosyltransferase domains of

the protein. Thus, this observation indicates both domains have important roles in capsule synthesis (Xayarath and Yother, 2007). Most of these suppressor mutations led to a reduction in the amount of capsule synthesized, presumably to a degree that did not seriously affect the levels of available Und-P (Xayarath and Yother, 2007). This is especially important since mutations that originate reduced turnover of Und-P and/or accumulation of this intermediate seem to be lethal. The accumulation of Und-P linked capsule intermediates might be responsible for membrane destabilization or for the sequestration of Und-P, whose recycling is critical since this universal lipid carrier is necessary for other essential pathways, such as peptidoglycan, lipopolysaccharides and wall teichoic acids synthesis (Brown et al., 2013; Valvano, 2003; Bouhss et al., 2008).

On a different note, Kawai and colleagues have proposed that Wzg (CpsA) is the enzyme responsible for the capsule-cell wall ligase (Kawai et al., 2011). This protein, encoded by the first gene of the *cps* operon, is a LCP (LytR-CpsA-Psr) protein family member. Genes that are members of the LCP protein family are widely spread in Gram-positive bacteria (Hübscher et al., 2008). LCP protein family comprises a class of transmembrane proteins, with one or more transmembrane domains, that share a characteristic long extracellular tail where the LCP catalytic domain is localized (Figure 1.5). These proteins seem to be important in cell envelope biogenesis, proper cell division, and biofilm formation. Many of them are also upregulated under stress conditions (Mella-Herrera, Ramona Neunuebel and Golden, 2011; Utaida et al., 2003; Hübscher et al., 2008). Moreover, different bacterial species contain between one to eleven LCP proteins (Hübscher et al., 2008) that can be separated into several different subgroups based on sequence phylogeny, which could reflect functional diversification (Hübscher et al., 2008). For example, in *Streptococcus mutans*, mutation of the LCP family member *brpA* led to major defects in cell division and cell wall morphology; additionally, deletion of *lytR* showed dysregulated cell division, as cells grow in long chains (Chatfield, Koo and Quivey, 2005; Bitoun et al., 2013). LCP proteins may also have some redundant roles, as only the *Staphylococcus aureus* triple *lcp* mutant presented an ability to grow that was severely impaired and cells formed large amorphous complexes containing multiple incomplete septa (Hanson, Lowe and Neely, 2011; Over et al., 2011). In the case of *S. pneumoniae*, which produces three different LCP proteins (LytR, Wzg and Psr), the *lytR* mutant strain grew more slowly and presented septa placed in aberrant locations (Johnsborg and Håvarstein, 2009).

For a long time, LCP proteins were defined as transcriptional regulators due to the pleiotropic phenotypes observed in LCP mutant strains of different bacterial species and due to its sequence homology with LytR from *Bacillus subtilis*, which was thought to be a transcriptional regulator (Cieslewicz et al*.,* 2001). However, more recently, all three LCP proteins (LytR, Wzg and Psr) have been implicated in anchoring cell wall-related anionic glycopolymers to the peptidoglycan, like capsular polysaccharides, arabinogalactan, and secondary cell wall polymers, such as wall teichoic acids (WTAs) (Kawai et al*.,* 2011; Chan et al*.,* 2014; Harrison et al*.,* 2016). In various organisms, LCP proteins are often localized in the septum, where the peptidoglycan is intensively synthesized during cell division, accommodating the need to incorporate different polysaccharides into the aging meshwork (Eberhardt et al*.,* 2012; Baumgart et al*.,* 2016; Maréchal et al*.,* 2016). Additionally, the *wzg* knockout mutant of the serotype 2 D39 strain, which presents a significant less amount of CPS production, is not significantly affected in the transcription of the *cps* locus, which strongly suggests that Wzg is not a transcriptional regulator (Wen et al*.,* 2015).

Wzg predicted topology shows that this integral membrane protein has a small N-terminal cytoplasmic domain (with 27 amino acids), three transmembrane domains, and a large extracellular C-terminal tail. In the extracellular domain, Wzg shares the same characteristics of the family LCP domain, with a mixed α/β-structure, and an additional domain, called the accessory domain, which makes it unique among the family of LCP proteins (Figure 1.5). Notations in the genomic databases identify this accessory domain through its homology to the DNA polymerase processivity factor (DNA-PPF) (Hübscher et al*.,* 2008). Usually, the function of DNA-PPF proteins is to bind to and tether polymerases to the duplex DNA template, ensuring a firm contact with DNA during high-speed replication (Kuriyan and O'donnell, 1993). However, in the case of Wzg, due to its extracellular location and actual sequence divergence from the family of DNA-binding sliding clamp proteins, it is not likely that this domain plays a role in DNA replication (Hübscher et al*.,* 2008). Instead, this domain is predicted to be involved in protein–protein interactions with other CPS biosynthesis proteins (Hanson et al*.,* 2012; Rowe et al*.,* 2015). Thus, it is possible that the accessory domain is involved in regulation of the capsule synthesis. In *S. pneumoniae*, crystallographic studies have suggested the phosphotransferase activity of the serotype 2 Wzg protein, supporting the proposed enzymatic function of this protein (Kawai et al*.,* 2011; Eberhardt et al*.,* 2012).

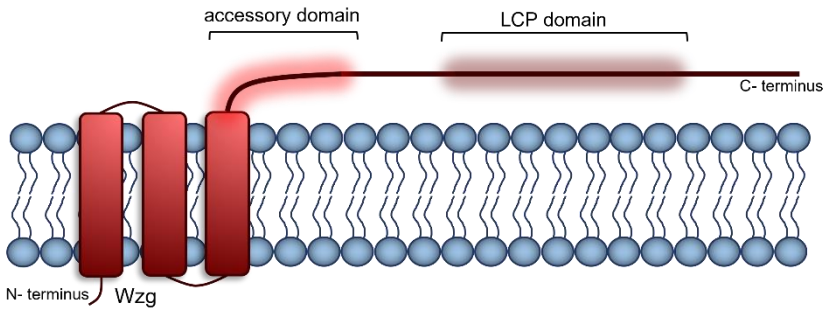

Figure 1.5: Scheme of Wzg protein domains. Wzg has a small N-terminal cytoplasmic domain followed by three transmembrane domains and a long extracytoplasmic C-terminal tail, which can be partitioned in two domains: the accessory domain and the LCP (LytR-CpsA-Psr) domain.

In agreement with the hypothesis that Wzg is the so long searched ligase, several studies have shown that the deletion of *wzg* results in a reduction of the amount of capsule attached to the cell wall in *S. pneumoniae* (Morona et al., 2000a; Bender, Cartee and Yother, 2003; Eberhardt et al., 2012). Also, inactivation of the *lytR* gene showed a severe defect in growth and impaired retention of CPS and teichoic acids (TA) on the surface of pneumococci (Ye et al., 2018). This observation indicates that LytR may have redundant roles as Wzg as it may function as a ligase of both CPS and TA to the cell wall. The growth defect phenotype is consistent with this hypothesis since it is similar to what has been observed when genes involved in TA biosynthesis are repressed (Liu et al., 2017). In addition, in vivo experiments revealed that *lytR* deletion significantly attenuated pneumococcal virulence (Ye et al., 2018). This apparent redundancy of the LCP family proteins is also observed in *S. aureus* and *B. subtilis*. In *S. aureus*, the LCP proteins LcpA, LcpB and LcpC have been implicated in the attachment of polysaccharides to peptidoglycan. LcpA and LcpB seem to be targeted on the attachment of WTA and LcpC on the attachment of the capsule to the peptidoglycan. Nonetheless, a functional overlap between LcpA, LcpB, and LcpC may exist, since mutations in each of these proteins can be partially compensated by the others (Chan et al., 2013; 2014). In fact, mutation of each LCP family protein in *B. subtilis* does not reflect in a major phenotype until all three genes are inactivated, indicating that these enzymes are not absolutely specific and suggesting a redundant role (Kawai et al., 2011; Gale et al., 2017). In conclusion, LCP proteins may not recognize the repeating chain of the anionic polymer, but the lipid and pyrophosphorylated parts instead. Although it seems that some LCP family enzymes have substrate preferences they also appear to be able to compensate or substitute for one another

to varying degrees (Eberhardt et al*.,* 2012). By giving bacteria some flexibility, protein redundancy ensures that mutations in one of these proteins do not result in a complete loss of function and/or in cell death.

1.2.6 Regulation of the capsule synthesis

The interactions between pathogens and their host are controlled by factors that are crucial for in vivo fitness and persistence of pathogens in adverse host niches. So, to be able to adapt and survive in different host environments – and cause invasive disease – *Streptococcus pneumoniae* must be able to modulate capsule production, as mentioned previously. Although most underlying molecular mechanisms controlling capsule production remain largely unknown, several points of control can regulate the process of CPS synthesis: the transcriptional regulation of the capsule operon, the availability of CPS precursors or cofactors required by enzymes involved in CPS synthesis, and the phosphoregulatory system constituted by the Wzh, Wzd and Wze enzymes.

1.2.6.1 Transcriptional regulation of the cps *operon*

One of the primary mechanisms of capsule synthesis regulation in *S. pneumoniae* involves the transcriptional regulation of the *cps* locus in response to surrounding stimuli. Transcriptional regulation of the *cps* operon is recognised to be an efficient way of controlling capsule expression. Thus, several studies have shown that the core promoter of the *cps* operon and sequence elements upstream of the core promoter are essential for full transcription of the *cps* genes (Shainheit, Mulé and Camilli, 2014; Wen et al*.,* 2015; Wu et al*.,* 2016). Expression of many proteins involved in the regulation of sugar pathways also appear to influence the transcription of the *cps* locus and capsular expression; nonetheless, the underlying mechanisms of these interactions are not yet fully understood.

Some examples of proteins whose expression influences the transcription of the *cps* operon are the phosphoglucomutase Pgm and the uridine diphosphate glucose pyrophosphorylase GalU. Pgm catalyses the conversion of glucose-6-phosphate to glucose-1-phosphate and GalU catalyses the formation of uridine diphosphate-glucose from glucose-1-phosphate (Mollerach, López and García, 1998; Hardy et al*.,* 2001). Pgm and GalU activities ultimately result in the formation of UDP-Glc, which is an essential intermediate in the

biosynthesis of polysaccharides (it is the substrate of WchA, which links the first sugar of the capsular repeating unit to Und-P). When each of *galU* or *pgm* genes were disrupted, *S. pneumoniae* mutants presented almost no capsule and exhibited growth defects, resulting in decreased virulence (Mollerach, López and García, 1998; Hardy et al., 2001; Cools et al., 2018). Considering that glucose is an important nutrient for the pneumococcal metabolism, it may serve as a specific environmental signal that can regulate the expression of proteins involved in the pneumococcal capsule synthesis. Accordingly, in the nasopharynx, where for optimal adhesion and colonization pneumococci requires less CPS, very low levels of glucose are detected. Conversely, high concentrations of glucose are found in blood and in the lungs, where pneumococcal bacteria have to produce high levels of CPS that is essential for their virulence (Baker et al., 2007; Philips et al., 2003). Hence, glucose may function as a host signal that trigger mechanisms accounting for the transition from carriage to invasive disease in *S. pneumoniae*.

Recently two other proteins were discovered as response regulators of the expression of the *cps* locus, CpsR and ComE, whose expression also seems to be regulated by the presence of glucose in the medium. CpsR, named as *cps* locus repressor, is a GntR family regulator that binds directly to the *cps* promoter region and negatively regulates CPS production (Wu et al., 2016). Moreover, CpsR binding activity to *cps* promoter is influenced by glucose in a dose dependent manner. In fact, Wu et al. showed a positive correlation between glucose concentrations and the amount of capsule synthesized. Also, binding of CpsR to *cps* promoter could be hindered with the addition of glucose. This suggests that glucose is a positive regulator for capsule synthesis by interacting with CpsR, controlling its repressor activity (Wu et al., 2016). The second protein, ComE, belongs to the ComD/E two component signalling system, responsible for the activation of competence upon accumulation of the competence-stimulating peptide (CSP) outside the bacterium (Pestova, Håvarstein and Morrison, 1996). When phosphorylated, ComE plays not only an important role during the induction of competence, but also negatively regulates the transcription of the *cps* locus, reducing capsule synthesis, and thus attenuating virulence (Martin et al., 2013; Kumar et al., 2017). Previous studies have long shown that the capsule reduces the natural competence of the pneumococcus for genetic transformation by acting as a barrier and preventing the CSP to reach its receptors (Yother, McDaniel and Briles, 1986; Weiser and Kapoor, 1999). In fact, it has been demonstrated that type IV pilus T4P system is crucial for the binding and intake of DNA

(Laurenceau et al., 2013). A thinner capsule may facilitate exposure of the pilus, enhancing the probability of exogenous DNA to be imported into the periplasm during transformation. Thus, the ability of the CSP-ComD/E competence system to regulate negatively capsule production is in accordance with a model where bacteria decrease the capsule layer that surrounds them in order to promote their ability to be transformed by DNA present in the surrounding medium. Moreover, a ticker capsule decreases the exposure of surface structures that are important in the pneumococcal adherence to respiratory epithelial cells (Talbot, Paton and Paton, 1996; Voss, Gámez and Hammerschmidt, 2012). In agreement, the deletion of *comE* resulted in reduction of colonization of the upper respiratory tract and virulence enhancement in a mice model (Kumar et al., 2017). In addition, Zheng et al. showed that glucose may reduce the expression of *comE*, positively regulating CPS production (Kumar et al., 2017). In conclusion, ComE acts as a transcription regulator of the capsule operon and its synthesis could be influenced by extracellular glucose concentrations.

1.2.6.2 Availability of precursors or cofactors

An additional potential point of control used by pneumococcus to indirectly modulate capsule synthesis is the availability of capsule precursors and cofactors required by enzymes involved in CPS production. One example is Glc-1-P, a precursor for the synthesis of both the capsule and other cell surface structures like teichoic acids. Hence, a limiting amount of this precursor in the cell will probably have an extreme impact in capsule production (Paton and Trappetti, 2019). Another example is the lipid acceptor Und-P, which besides its key role in CPS production, is also essential for the synthesis of peptidoglycan and teichoic acids. Thus, and because it is a relatively low-abundance lipid, Und-P may represent a central point in the regulation of the synthesis of surface structures (Brown et al., 2013; Valvano, 2003; Bouhss et al., 2008).

1.2.6.3 Wzh, Wzd and Wze phosphoregulatory system

The production of *S. pneumoniae* capsule, and the length of the assembled glycopolymer chains, is also modulated at a posttranscriptional level. This key regulation takes place through a phosphoregulatory system, constituted by Wzh, Wzd and Wze, that controls the polysaccharide assembly machinery. As mentioned above, the three genes that encode

proteins of this system, *wzh*, *wzd* and *wze*, are cotranscribed together at the 5′ end of the capsule transcript and are conserved in all serotypes, except serotypes 3 and 37. Wze is an autophosphorylating tyrosine kinase that belongs to the Bacterial Tyrosine Kinase (BY-kinase) family and that is involved in the phosphorylation of other proteins (Morona et al., 2000a). Importantly, several kinases have been shown to be crucial in bacterial environmental signalling (Hoch, 2000). Tyrosine phosphorylation is a strategic regulatory device often involved in the regulation of a myriad of physiological processes, including gene expression, stress response, cell division, and virulence (Klein, Dartigalongue and Raina, 2003; Minic et al., 2007; Petranovic et al., 2007; Lacour et al., 2008). Most of the characterized BY-kinases regulate the biosynthesis and export of capsular and extracellular polysaccharides (Chao, Wong and Av-Gay, 2014). Widespread among bacterial species and highly conserved in both Gram-negative and Gram-positive species, these enzymes use the ATP/GTP-binding Walker motif to catalyse phosphorylation of tyrosine residues (Grangeasse, Nessler and Mijakovic, 2012; Jadeau et al., 2008). Besides being able to autophosphorylate, these enzymes are very promiscuous, as they are capable of controlling several enzyme activities by phosphorylating their protein substrates. Additionally, BY-kinases relaxed specificity has been shown to be important for ensuring the correct cellular localization of its protein substrates, affecting mediation of protein interactions (Jers et al., 2010; Standish, Whittall and Morona, 2014).

BY-kinases share no homology to their eukaryotic counterparts and have a different structure and activation mechanism (Lee et al., 2008). In fact, BY-kinases are composed of a sensor membrane domain and a catalytic cytoplasmic domain. The sensor domain has two transmembrane domains with an extracellular hairpin loop between them, which is proposed to act as a sensor for outside signals. The catalytic cytoplasmic domain, that has the kinase function, possesses conserved Walker A and B ATP binding motifs and a tyrosine cluster at its C-terminal end for autophosphorylation (Grangeasse et al., 2007). In most Gram-negatives and in Actinobacteria the sensor and the catalytic domains are present in a single protein. Two well studied examples are ExoP from *Sinorhizobium meliloti* and Wzc from *E. coli* (González et al., 1998; Vincent et al., 1999). However, in the Gram-positive Firmicutes phylum, such as *S. pneumoniae*, the two domains are divided into two independent interacting proteins, encoded by two separate genes (Chao, Wong and Av-Gay, 2014). The splitting of the two domains into different polypeptide chains suggests that the dissociation of the phosphorylated kinase domains from their cognate transmembrane activator could occur to add an extra level of

regulation to the process of CPS synthesis or allow the interaction of each protein with other endogenous substrates or protein modulators, potentially cytoplasmatic. In *S. pneumoniae*, Wzd – which belongs to the Polysaccharide Co-Polymerase (PCP) family – contains the sensor domain (Morona, van den Bosch and Daniels, 2000b). This protein has two membrane-spanning hydrophobic domains and the N and C termini are localized in the cytoplasm, while the central portion is outside of the cell, exposed to the environment (Figure 1.6) (Bender and Yother, 2001). On the other hand, Wze has the catalytic domain and is the only BY-kinase known in pneumococcus. Characteristic of the BY-kinase family, Wze also possesses a Walker A and B ATP binding motif and a C-terminal tyrosine cluster (Morona et al., 2000a). This tyrosine-rich region is where autophosphorylation occurs and has an ordered (YGX) motif that varies from two to four repeats, depending on the serotype, four being the most prevalent (Paton and Trappetti, 2019). The multiple tyrosine residues at the C-terminal region of Wze became phosphorylated initially via ATP binding and then via transphosphorylation (Figure 1.6). Although the interaction with Wzd and the binding of ATP are prerequisites for initial Wze tyrosine autophosphorylation, the interaction with Wzd is not necessary for transphosphorylation between Wze proteins (Morona, van den Bosch and Daniels, 2000b; Bender and Yother, 2001).

Structural studies of BY-kinases, *S. aureus* CapB and *E. coli* Wzc and Etk, homologues of Wze, showed that these BY-kinases form a conserved ring-shaped octamer. In addition, these studies revealed that the last tyrosine of the tyrosine cluster of each subunit is bound into the active site of the neighbouring molecule, which could explain the trans-autophosphorylation event, common in the tyrosine cluster of BY-kinases. The crystal structure of these phosphorylated and non-phosphorylated BY-kinases suggest that intermolecular autophosphorylation dissociation of the subunit's active sites allows these kinases to interact with other substrate proteins (Olivares-Illana et al., 2008; Bechet et al., 2010). Hence, the cycling between phosphorylation/dephosphorylation of BY-kinases seem to lead to crucial conformational changes that can affect the function of other proteins of the CPS synthesis machinery (Figure 1.6). For this cycling to take place it is necessary the action of a third protein, a phosphatase. In *S. pneumoniae* this is accomplished by Wzh, which is a manganese-dependent phosphotyrosine-protein phosphatase that belongs to the Polymerase and Histidinol Phosphatase (PHP) family (Morona et al., 2002). Wzh is required for Wze

dephosphorylation and by binding to Wze it can prevent transphosphorylation (Figure 1.6) (Morona et al., 2000a).

All three genes responsible for the phosphoregulatory system, *wzh*, *wzd* and *wze* are essential for complete encapsulation of the pneumococcus (Morona et al., 2000a; 2002). In the *wzh* null mutant, the capsule is expressed all around the pneumococcal cells, but it is produced at lower levels than in the wild-type pneumococci (Morona et al., 2000a; Morona et al., 2004). In addition, the CPS ladder pattern observed in immunoblot experiments showed that the synthesized CPS has a chain size that is identical to that observed with wild-type pneumococci (Bender, Cartee and Yother, 2003). When Wzh is absent or inactivated – by point mutations at conserved residues involved in catalysis and metal binding – the levels of phosphorylated Wze increase (Morona et al., 2002). On the other hand, *wzd* and *wze* null mutants presented the same phenotype. In these mutants, colonies exhibit a rough phenotype, contrasting with the smooth phenotype that is characteristic of fully encapsulated pneumococcal cells. Additionally, immunofluorescence experiments that detected the presence of CPS at the surface of pneumococcal cells showed that CPS is absent from the septum of dividing cells or from the cell poles. Moreover, low levels of CPS-related material were detected all around the lateral cell surface, which are probably constituted by very short CPS chains (Morona et al., 2000a; 2004; Henriques et al., 2011).

Although Wzh, Wzd and Wze are clearly involved in modulation of capsule synthesis, the mode of action of this regulatory mechanism is still not fully understood. Indeed, phenotypic differences between mutants constructed in different backgrounds and conflicting results obtained by different authors hinder the complete comprehension of the system. Different studies have reported opposite results on CPS synthesis upon Wze phosphorylation. Morona and colleagues observed that Wze phosphorylation reduced capsule synthesis (Morona et al., 2000a). On the other hand, Bender et al. reported a direct correlation between phosphorylated Wze and the amount of capsule produced, suggesting that tyrosine phosphorylation could positively regulate CPS synthesis (Bender, Cartee and Yother, 2003). Interestingly, Weiser et al. demonstrated that changes in the levels of environmental oxygen influence the amount of capsule produced. Under high levels of oxygen available, both Wze phosphorylation and CPS production decreased, which is in accordance with the hypothesis that tyrosine phosphorylation positively regulates capsule synthesis (Weiser et al., 2001). Geno et al. further advanced that Wzh phosphatase activity also increases under high oxygen conditions (Geno

et al*.,* 2014). Hence, the levels of environmental oxygen seem to be a signal that affects capsule production. This observation concurs with the fact that decreased capsule synthesis is advantageous during colonization, which occurs in a highly oxygenated environment, the nasopharynx. As mentioned above, during colonization a thinner capsule layer allows exposure of adhesins and other surface structures, necessary for bacteria establishment in the host. Once bacteria invade systemic sites that have low oxygen concentrations, like the bloodstream or the brain, a thick capsule becomes essential for its escape from the host's immune system (Weiser et al*.,* 1994; Kim and Weiser, 1998). Moreover, elimination of the extracytoplasmatic portion of Wzd (which is proposed to be the environment sensor) leads to a desensitization of the system, responding to high or low oxygen levels with the same amount of tyrosine phosphorylation (Yother, 2011).

The interaction between the membrane protein Wzd and the cytoplasmic Wze is crucial for their localization at the division septum. The recruitment of Wzd/Wze complex occurs early in the cell cycle, as the observed fluorescent signal corresponding to fluorescent derivatives of Wzd and Wze appears before the onset of invagination (Henriques et al*.,* 2011). Nourikyan et al. later showed that the C-terminal cytoplasmic end of Wzd is responsible for the Wzd/Wze interaction and, consequently, for the autophosphorylation activity of Wze (Nourikyan et al*.,* 2015). When one of these two proteins (Wzd or Wze) is not produced, the remaining protein is unable to localize at the division septum, the capsule is still synthesized and attached to the cell surface, but it is absent from the division septum. Thus, it is proposed that Wzd/Wze act as spatial regulators of capsule metabolism, making sure that, upon cell division, CPS production and peptidoglycan synthesis occurs synchronously (Henriques et al*.,* 2011).

Interestingly, due to structural similarities, Wze and other BY-kinases have been categorized into the same protein superfamily as MinD and ParA proteins (Leipe et al*.,* 2002). MinD is responsible for positioning the division site correctly at mid-cell and ParA is involved in chromosome segregation (Bramkamp and van Baarle, 2009; Gerdes, Howard and Szardenings, 2010). Pneumococcus is devoid of ParA and MinD proteins and of a nucleoid occlusion system (Pinho, Kjos and Veening, 2013). Fleurie et al. showed that in *S. pneumoniae* proper localization of the septum is guided by MapZ, that directly interacts with FtsZ and guarantee the correct positioning of the division machinery (Fleurie et al*.,* 2014). Therefore, it is unlikely that Wze participates in division site selection in *S. pneumoniae*. ParA is an ATPase, member of the large P loop GTPase superfamily, which is involved in chromosome segregation

(Leipe et al., 2002). Although its role is not completely understood, it is thought to interact with and assist ParB during chromosome segregation (Gerdes, Howard and Szardenings, 2010). As shown in several studies, ParA-like proteins are involved in protein localization linked with the cell cycle (Lutkenhaus, 2012). Bearing this in mind, and because Wze has structural similarities with ParA, Nourikyan and co-workers speculate that Wze might have a role in chromosome segregation, behaving as a ParA-like protein. These authors showed that Wze interacts directly with ParB and that Wze phosphorylation modulates ParB/Wze complex stability (Nourikyan et al., 2015). Defective autophosphorylation of Wze not only acts by impairing capsule production, but also reduces ParB mobility (Figure 1.6), which promotes aberrant pneumococcal chromosome segregation and cell elongation (Nourikyan et al., 2015). The fact that bacteria of nonencapsulated strains lacking Wze can segregate their chromosomal DNA, indicates that Wze does not represent an authentic ParA protein but may be necessary for the network between cell cycle and the capsule synthesis machinery. Recently, the same authors discovered that another pneumococcal protein, the Regulator of Chromosome Segregation (RocS), interacts with DNA and with ParB to ensure the correct chromosome partitioning (Mercy et al., 2019). Of notice, RocS can also interact with Wze, which suggests that depending on Wze phosphorylation state, cell division can be blocked to make sure capsule secretion occurs properly and avoids nucleoid truncation (Figure 1.6). In fact, the non-phosphorylated *wze* null mutant, where each tyrosine from the tyrosine cluster of Wze was replaced by a phenylalanine, presented elongated cells and were hampered in both capsule synthesis and chromosome segregation. Moreover, RocS can interact with FtsZ, which suggests that cell division blocking may be accomplished by a direct action of RocS on the Z-ring (Figure 1.6). Considering that in the non-phosphorylated *wze* null mutant the Z-ring was correctly placed at mid-cell it seems that RocS blocks the constriction of the cells instead of the assembly of the FtsZ (Mercy et al., 2019). Although different from the typical nucleoid occlusion mechanisms, that prevent the assembly of the FtsZ ring, this regulation of constriction that is dependent on RocS represents a true nucleoid protection system. These findings reinforce the model where Wze cycling phosphorylation represents a signalling system that communicate the CPS synthesis status to the pneumococcal machinery involved in chromosome segregation. A crosstalk between several machineries, like chromosome segregation, peptidoglycan synthesis and capsule synthesis is crucial in bacterial cell division

in order to ensure proper CPS concealment of daughter cells and their ability to evade the host immune system.

Besides its role in the regulation of capsule synthesis, Standish and co-workers also showed that Wze directly influences the level of tyrosine phosphorylation of the autolysin LytA (Standish, Whittall and Morona, 2014). LytA is a virulence factor involved in autolysis and fratricidal induced lysis. This enzyme binds to phosphorylcholine residues present in the pneumococcal cell wall, which is essential for its amidase activity. Moreover, LytA can be phosphorylated in one tyrosine residue and because Wze is the only BY-kinase identified in pneumococcus so far, its involvement in LytA phosphorylation was enquired (Sun et al*.,* 2010). Indeed, Wze seems to be responsible for LytA phosphorylation, while Wzh is involved in its dephosphorylation (Figure 1.6). LytA phosphorylation appears to enhance its amidase activity, as well as its ability to bind to choline (Standish, Whittall and Morona, 2014). Furthermore, similar to Wze, LytA is also localized at the division septum (Henriques et al*.,* 2011; Mellroth et al*.,* 2012). This and the fact that Wze apparently modulates LytA function points to an important link between capsule synthesis and autolysis.

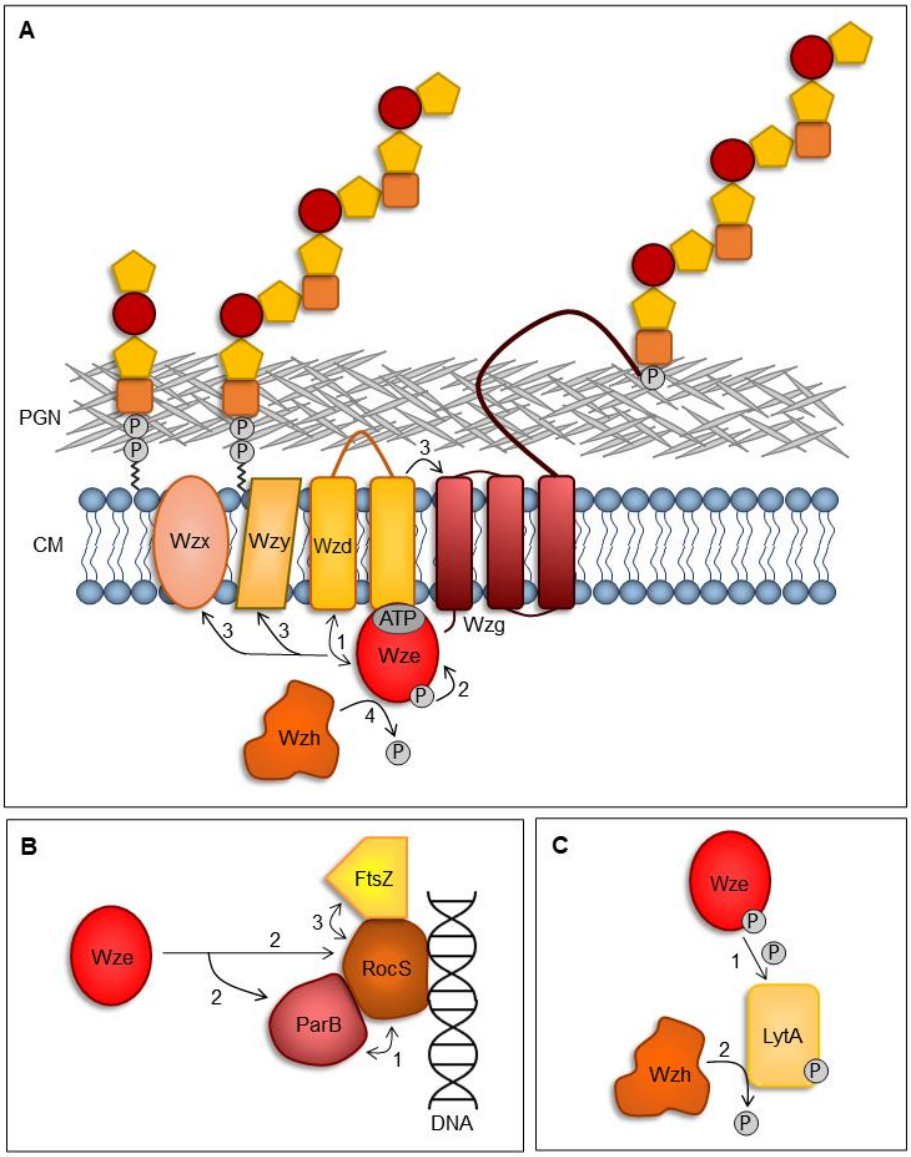

Figure 1.6: Regulation of capsule synthesis and its coordination with chromosome segregation and autolysis. A) Although Wzh, Wzd and Wze are clearly involved in modulation of capsule synthesis, the mode of action of this regulatory mechanism is still not fully understood. Upon interaction with Wzd, ATP binds to the Walker A motif of Wze, allowing Wze to hydrolyze ATP (1). After this step, Wze undergo autophosphorylation (2). Then, the complex Wzd/Wze may control the export (by Wzx) and polymerization (by Wzy) of the capsular polysaccharide polymer or its linkage to the pneumococcal cell surface (by Wzg) (3). Wze can afterwards be dephosphorylated by the phosphatase Wzh allowing the cycle to be repeated (4). PGN, peptidoglycan; CM, cytoplasmic membrane. **B)** RocS interacts with DNA and with ParB to ensure the correct chromosome segregation (1). In a nonphosphorylated state Wze can interact with ParB and with RocS delaying chromosome segregation to guarantee the coordination between capsule production and chromosome partitioning (2). The delay in chromosome segregation and consequent cell division blocking may be accomplished by a direct action of RocS on the Z-ring, since RocS also interacts with FtsZ (3). **C**- Phosphorylated Wze is responsible for the phosphorylation of

the autolysin LytA (1). LytA phosphorylation appears to enhance its amidase activity, as well as its ability to bind to choline. This points to an important link between capsule synthesis and autolysis. On the other hand, Wzh is involved in LytA dephosphorylation (2).

1.3 Other virulence factors

Streptococcus pneumoniae features a wide range of factors that are important in survival, colonization, and evasion of host defenses (Mitchell and Mitchell, 2010). These proteins, which contribute to the overall virulence of pneumococcal clinical isolates, are serious candidates for the development of new anti-infective molecules or to design new vaccines capable of preventing colonization or disease caused by strains from all pneumococcal serotypes. Consequently, the study of how pneumococcus bacteria interact with host cells has been encouraged and has increased greatly in the last decade. The mediation of this interaction occurs mainly through external components of this bacterium: the capsular polysaccharide, the bacterial cell wall and several surface proteins that are anchored to the pneumococcal cell surface.

In Gram-positive bacteria, the cell wall is constituted by different types of macromolecules that have a key role in the interaction of the bacterial cell with its surroundings (Figure 1.7). These macromolecules include covalently and noncovalently linked proteins, carbohydrates, polysaccharides, and teichoic acids, embedded in a peptidoglycan matrix. (Wiley and Schneewind, 1999).

As previously described, the CPS is considered a paramount virulence factor, since nonencapsulated strains are avirulent (Avery and Dubos, 1931). Thus, by serving as a shield, the capsule prevents the recognition by the host's immune system of bacterial peptidoglycan or proteins that are also crucial for virulence of pneumococcal bacteria and its viability in the infected host. Examples of such proteins are the pore-forming toxin pneumolysin (Ply) and different surface associated proteins that, depending on how they are retained in the cell wall upon secretion across the bacterial membrane, can be divided into three groups: (i) choline-binding proteins (which include autolysins and the pneumococcal surface protein C), (ii) lipoproteins, and (iii) LPXTG anchored proteins (Figure 1.7). Next there is a brief resume of the function and action of some of these proteins that are important for pneumococcal virulence.

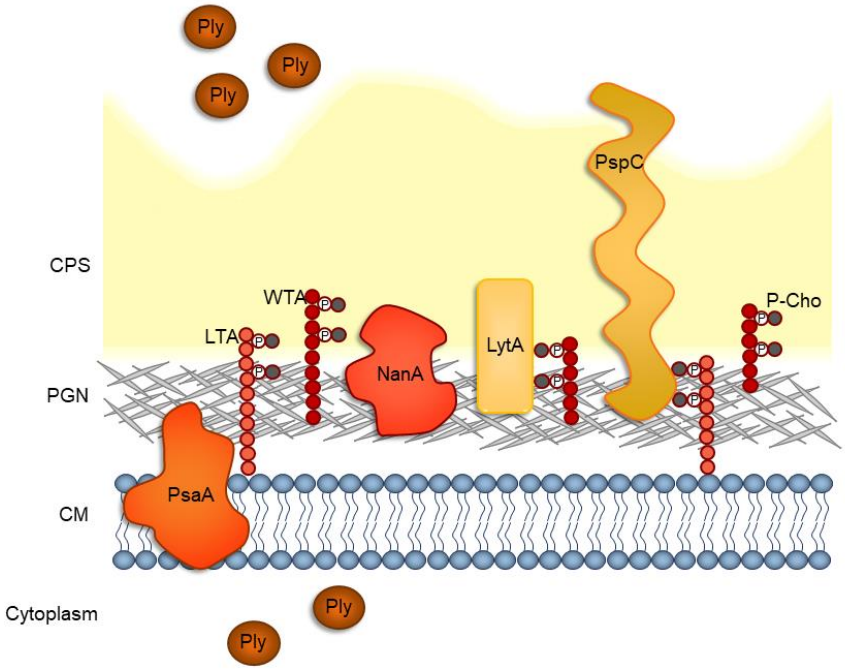

Figure 1.7: Schematic representation of *S. pneumoniae* cell wall and several important virulence factors. Pneumococcal cell wall is constituted by different types of macromolecules that have a key role in the interaction of the bacterial cell with its surroundings. These macromolecules include covalently and noncovalently linked proteins, carbohydrates, polysaccharides, and teichoic acids, embedded in a peptidoglycan matrix. The capsule is the major virulence factor. However, there are proteins that are also crucial for the viability and virulence of pneumococcal bacteria, like the pore-forming toxin pneumolysin (Ply) and other surface associated proteins. The various pneumococcal cell surface proteins can be divided into three groups, depending on how they are retained in the cell wall upon secretion: (i) choline-binding proteins (which include LytA and PspC) that bind to the phosphorylcholine (P-Cho) residues of wall teichoic acids (WTA) and lipoteichoic acids (LTA), (ii) lipoproteins (like PsaA), and (iii) LPXTG anchored proteins (like NanA). CPS, capsule polysaccharide; PGN, peptidoglycan; CM, cytoplasmic membrane.

1.3.1 Pneumolysin

Pneumolysin (Ply) is a pore forming toxin that belongs to the family of cholesterol dependent cytolysins (CDCs) and has a multifaceted and crucial role in pneumococcal disease (Figure 1.7). Mutants in which *ply* has been deleted are attenuated in virulence, compared with the wild-type pneumococci (Berry and Paton, 2000). This cytolysin can cause direct damage of host cells by binding to host cell membranes, which contain cholesterol, and by forming a ring-shaped pore that inserts into the membrane and that is assembled through the side-by-

side packing of several Ply proteins. The integration of numerous pore-forming Ply complexes and consequent membrane destabilization results in the host cell death (Rayner et al., 1995; Marshall et al., 2015). Thereby, due to the cytotoxic activity of Ply, bacteria are more capable to penetrate into sterile environments, like the bloodstream, and spread through the host's tissues. Moreover, expression of Ply can also contribute to inflammation, which facilitates bacterial invasion, and can interfere with the deposition of a complement response, which will help bacteria to escape the host's immune system. The capacity of Ply to activate the complement may seem disadvantageous to bacteria, but, in fact, it is a strategy that deviates this system from the surface of healthy bacterial cells. Ply can only interact with the complement system when it is secreted, which causes depletion of complement components in the serum, reducing complement binding to pneumococcus (Paton, Rowan and Ferrante, 1984). In addition, Ply is a key element in host-to-host pneumococcal transmission and establishment. First, because of its inflammatory effect, this toxin contributes to shedding of bacteria in secretions. Secondly, Ply also enhances survival of *S. pneumoniae* in an outside environment (Zafar et al., 2017).

Pneumolysin is generally conserved between serotypes, and it is essential for invasive disease. Nonhemolytic forms of pneumolysin have been identified in certain clinical isolates, yet they remain virulent and are still capable of causing invasive disease (Kirkham et al., 2006).

1.3.2 Choline-binding proteins

Streptococcus pneumoniae has a complex cell wall that is composed of a thick multi-layered murein (peptidoglycan) with covalently attached teichoic acids (WTA), membrane-bound lipoteichoic acids (LTA) and the capsular polysaccharide (Vollmer, Massidda and Tomasz, 2019). The peptidoglycan is a mesh-like structure that maintains cell shape, conferring protection against mechanical and osmotic lysis (Figure 1.7). It is composed of glycan chains cross-linked through short peptides. The glycan chains are usually amino-acylated sugars, and the most frequent ones are alternating β-1,4-linked *N*-acetylglucosamine (GlcNAc) and *N*-acetylmuramic acid (MurNAc) (Vollmer, Blanot and de Pedro, 2008). In addition, in *Streptococcus pneumoniae* the N-acetylglucosamine deacetylase A (PgdA) is able to deacetylate the peptidoglycan glycan chains leading to resistance to the hydrolytic action of lysozyme, a host muramidase known to accumulate in high concentrations in infection sites

(Vollmer and Tomasz, 2000). WTA and LTA render the pneumococcus cell wall unique because they contain an unusual complex repeating unit decorated with phosphorylcholine (P-Cho) residues (Behr et al., 1992). These P-Cho residues are found in pneumococcus and closely related species. They are involved in many physiological functions of the cell (e.g., their interaction with host epithelial cells promotes adherence) and represent specific attachment ligands for surface proteins, commonly called choline-binding proteins (CBPs) (Hakenbeck et al., 2009; Cundell et al., 1995a). Choline-binding proteins are polypeptides that bind to P-Cho residues and are present in all pneumococcal serotypes. This group of proteins include, among others, peptidoglycan hydrolases (such as LytA) and host-cell adhesins (such as PspC) (Figure 1.7).

1.3.2.1 LytA amidase (major pneumococcal autolysin)

Streptococcus pneumoniae has several cell wall hydrolases that cleave the covalent bonds of the peptidoglycan. These enzymes have fundamental roles in cell growth, cell wall turnover, separation of daughter cells, and genetic transformation (Vermassen et al., 2019). LytA, the major autolysin of pneumococcus, is responsible for the autolytic response induced during the stationary growth phase.

LytA has an N-terminal catalytic *N*-acetylmuramyl-L-alanine amidase domain and a C-terminal choline binding domain (CBD). The CBD allows the enzyme to attach noncovalently to the P-Cho residues present in the teichoic acids of the pneumococcal wall. This interaction is required for LytA activity, since this enzyme cannot hydrolyse the cell walls where P-Cho is replaced by other units, such as ethanolamine. Additionally, high concentrations of choline, which inhibits adsorption of LytA to the cell wall, prevents autolysis (Giudicelli and Tomasz, 1984).

Under conditions that hinder cell wall biosynthesis, such as nutrient starvation, LytA can be activated, which culminates in cell lysis (Mitchell et al., 1997). As an *N*-acetylmuramyl-L-alanine amidase (NAM-amidase), LytA cleaves the lactyl-amide bond between the first amino acid in the stem peptide and the *N*-acetylmuramic acid (MurNAc) of the peptidoglycan (Howard and Gooder, 1974). The *lytA* gene is highly conserved among serotypes and is present in virtually all clinical isolates, emphasizing its role in pathogenesis (Pozzi, Oggioni and Tomasz, 1989). Furthermore, mutant strains deficient in LytA showed strikingly reduced virulence in

mouse models of infection, compared to parental wild-type strains (Berry et al*.,* 1989). Nonetheless, how LytA contributes to virulence and how autolysis is beneficial for pneumococcus is still controversial. One hypothesis suggests that releasing the cytoplasmic content of the cell after bacterial lysis allows the inflammatory toxin pneumolysin (Ply) to be discharged in high local concentrations (Mitchell et al*.,* 1997). Because Ply does not contain a predicted signal peptide for export, lysis of the bacterial cell was thought to be the mechanism for secretion of this toxin (Walker et al*.,* 1987). Price and Camilli have demonstrated that during in vitro growth and in the absence of autolysis, exported Ply is localized in the cell wall compartment (Price and Camilli, 2009). However, autolysin independent release of Ply has been reported, as well as the release of Ply in early growth phases, in some strains, when the autolytic cascade is yet inactive (Benton, Paton and Briles, 1997; Balachandran et al*.,* 2001). Furthermore, another possibility is that lysis releases highly inflammatory cell wall components and proteins involved in immune evasion that may interfere with the host immune response and/or damage epithelial barriers, allowing pneumococci to disseminate through the body (Majcherczyk et al*.,* 1999; Martner et al*.,* 2009). A third theory proposes that the release of DNA upon autolysis of a subset of the pneumococcal population will favour DNA recombination of the surviving cells, enabling genetic variation and survival (Steinmoen, Knutsen and Håvarstein, 2002; Guiral et al*.,* 2005). In agreement, the *lytA* gene is upregulated during competence (Mortier-Barrière et al*.,* 1998).

1.3.2.2 Pneumococcal surface protein C (PspC)

Pneumococcal surface protein C (PspC) (also known as choline binding protein A - CbpA, SpsA, PbcA or Hic) is a highly polymorphic and multifunctional protein that decorates the surface of pneumococcus and that it is capable of interacting with a variety of host proteins. The analysis of *pspC* knockout mutants showed that they have a diminished capacity to adhere to epithelial host cells and a reduced ability for nasopharyngeal colonization (Rosenow et al*.,* 1997). PspC binds to the polymeric immunoglobulin receptor that transports IgA, expressed in epithelial cells, probably mediating adherence and helping in translocation across the mucosal barrier (Zhang et al*.,* 2000). Additionally, PspC interacts with factor H, a regulatory protein of the alternative complement pathway, inhibiting complement activation and

preventing pneumococcal opsonization (Janulczyk et al., 2000; Dave et al., 2004; Pathak et al., 2018).

1.3.3 Lipoproteins

Approximately 50 different pneumococcal cell surface lipoproteins have been identified and several of those have important roles in virulence (Pérez-Dorado, Galan-Bartual and Hermoso, 2012). The most studied example is the pneumococcal surface adhesin A (PsaA) (Figure 1.7). PsaA was initially believed to be an adhesion protein but, in fact, it is part of an ABC transporter complex. This metal-binding protein in combination with PsaB, the ATP-binding protein, and PsaC, the permease, allows the intake of manganese and zinc (Dintilhac et al., 1997; Johnston et al., 2004). The analysis of *psaA* knockout mutants showed that they present pleiotropic effects, including severe reduction of virulence, decreased adhesion to host cells, and increased sensitivity to oxidative stress (Marra et al., 2002; Tseng et al., 2002; Romero-Steiner et al., 2003). Moreover, PsaA might be an important player in the regulation of the capsule synthesis, since the tyrosine phosphatase, Wzh, requires manganese for its activity (Morona et al., 2002).

1.3.4 LPXTG anchored proteins

LPXTG motif (where X represents any amino acid) is a signature sequence usually present at the C-terminal of several proteins. The LPXTG sequence is recognized by a membrane associated transpeptidase called sortase. This enzyme cleaves between T and G residues of the LPXTG motif and catalyses the covalent attachment of these proteins to the peptidoglycan (Navarre and Schneewind, 1994). Of notice, neuraminidase NanA binds to the cell wall in a sortase-dependent fashion (Figure 1.7). The enzyme NanA is yet another virulence factor that is virtually present in all pneumococcal serotypes and it acts by cleaving sialic acid from host cells. The removal of sialic acid from host cells may cause direct damage and unmask potential binding sites for the bacteria, being important in colonization (Krivan and Roberts, 1988). Furthermore, removal of sialic acids from host cells by NanA resulted in complement activation (Syed et al., 2019).

1.4 State of the art

A full comprehension of how bacteria divide and how essential mechanisms for survival inside the host occur and are regulated is key for the design of new and improved strategies to fight bacterial infections. To achieve this goal, it is crucial to have a detailed understanding of the function, localization, and role inside the molecular machineries of the proteins involved in important mechanisms for cell division and survival. Initially, protein localization studies in *S. pneumoniae* used mainly immunofluorescent techniques. However, this procedure poses several disadvantageous. First, it requires cell fixation and permeabilization, and, thus, cell death, to grant access to the antibodies that cannot penetrate cell membranes. Consequently, this method impedes the study of protein dynamics and interactions during the cell cycle. Secondly, immunostaining is prone to the emergence of artifacts, representing a huge obstacle in protein localization studies and proper date analysis (Schnell et al*.,* 2012).

Over the last 30 years, after the discovery and implementation of the green fluorescent protein (GFP) as a molecular probe, several fluorescent-based imaging techniques were developed. This breakthrough marked a new era in microscopy that enabled a boost in protein localization and life cell studies, by increasing spatial and temporal resolution (Cambré and Aertsen, 2020). Molecular reporters, such as GFP, were successful because they allow in vivo visualization, provide highly specific output, are minimally invasive, and do not require external cofactors for its fluorescence. Nevertheless, the last step for chromophore maturation requires oxidation of the protein, which was a bottleneck for its use in microaerophiles like *S. pneumoniae* (Reid and Flynn, 1997). This prompt the study of chromophore variants to be used in these cases. In 2000, the first study on GFP expression in *S. pneumoniae* was published and, in 2009, it was reported for the first time the localization of fluorescent protein derivatives in pneumococcus (Acebo et al*.,* 2000; Eberhardt et al*.,* 2009). Fortunately, the toolbox available for in vivo studies of protein localization, as well as of spatial and temporal dynamics between proteins, has experienced great improvement over the last years. In our laboratory we constructed a set of plasmids that permit efficient expression of both N- and C-terminal fusions of proteins of interest to fluorescent proteins mCherry, Citrine, CFP and GFP. We were able to significantly improve the expression of N- terminal fusions by introducing a 10 amino acid tag, named i-tag, before the fluorescent protein, that enhanced translation efficiency (Henriques et al., 2013).

Chapter 2

Optimization of fluorescent tools for cell biology studies in Gram-positive bacteria

2.1 Abstract

The understanding of how Gram-positive bacteria divide and ensure the correct localization of different molecular machineries, such as those involved in the synthesis of the bacterial cell surface, is crucial to design strategies to fight bacterial infections. In order to determine the correct subcellular localization of fluorescent proteins in *Streptococcus pneumoniae*, we have previously described tools to express derivatives of four fluorescent proteins, mCherry, Citrine, CFP and GFP, to levels that allow visualization by fluorescence microscopy, by fusing the first ten amino acids of the *S. pneumoniae* protein Wze (the i-tag), upstream of the fluorescent protein. Here, we report that these tools can also be used in other Gram-positive bacteria, namely *Lactococcus lactis*, *Staphylococcus aureus* and *Bacillus subtilis*, possibly due to optimized translation rates. Additionally, we have optimized the i-tag by testing the effect of the first ten amino acids of other pneumococcal proteins in the increased expression of the fluorescent protein Citrine. We found that manipulating the structure and stability of the 5′ end of the mRNA molecule, which may influence the accessibility of the ribosome, is determinant to ensure the expression of a strong fluorescent signal.

2.2 Introduction

Streptococcus pneumoniae is a Gram-positive bacterium usually found in association with a range of different types of infections. It is a common respiratory pathogen, capable of causing low severity otitis media or more serious infections such as pneumonia or meningitis, as well as a frequent cause of community-acquired pneumonia in developed countries (Kadioglu et al., 2008).

Pneumococcal bacteria can colonize the mucosal surface of the upper respiratory tract, while remaining undetected and asymptomatic (Bogaert et al., 2004). However, when pneumococcal bacteria gain access to normally sterile locations of the organism, they are capable of successfully propagating, in spite of the different defence mechanisms of the host immune system (Kadioglu et al., 2008).

The understanding of how bacteria divide or perform specific tasks important for their survival inside the host is a requirement for the design of efficient strategies to fight bacterial infections. This implies a detailed knowledge not only of the function of proteins required for

the infection process, but also of their localization and role in complex molecular machineries. The availability of genetic and cell biology tools that allow controlled expression of proteins of interest, as well as the study of their localization, is therefore particularly important for the study of bacterial pathogens.

We have recently described tools that can contribute to the study of the pneumococcal biology by ensuring the expression of fusions of *S. pneumoniae* proteins to different fluorescent proteins, namely mCherry, Citrine, CFP and GFP (Henriques et al., 2013). This was achieved through the introduction of an upstream tag, named ''i-tag'', which increased the efficiency of protein translation.

We have now constructed different plasmids to demonstrate that this tag is also efficient in increasing expression of fluorescent proteins in different Gram-positive bacteria, such as *Lactococcus lactis*, *Bacillus subtilis* and *Staphylococcus aureus*.

In order to understand how the efficiency of protein translation is improved, we have determined the molecular requirements of the sequence encoding the i-tag that ensure the expression of the fluorescent proteins. We have identified additional 10 amino acid tags, derived from different pneumococcal proteins, which could also increase expression of fluorescent proteins by decreasing the stability of the structure of 5′ end of the transcribed mRNA molecule.

2.3 Materials and methods

2.3.1 Bacterial strains and growth conditions

All bacterial strains and plasmids used in this study are listed in Table 2.1. *Streptococcus pneumoniae* was grown in C + Y liquid medium (Lacks and Hotchkiss, 1960) at 37˚C, without aeration, or in tryptic soy agar (TSA, Difco) plates supplemented with 5% sheep blood (Probiologica). Tetracycline was added to the media at 1 μg/ml final concentration. *Bacillus subtilis* was grown in Luria-Bertani broth (LB; Difco) or Luria-Bertani agar (LA; Difco) medium at 37˚C with aeration. When needed, erythromycin (Ery, Sigma Aldrich) was added at final concentration of 1 μg/ml. *Lactococcus lactis* LL108 strain was grown in M17 broth (Difco), supplemented with sucrose (0.5 M) and glucose (0.5% w/v) at 30˚C without aeration. Tetracycline was used when required at 4 μg/ml. *Staphylococcus aureus* strains were grown at 30˚C with aeration in Tryptic Soy Broth (TSB; Difco) or on Tryptic Soy Agar (TSA; Difco). Medium

was supplemented when required with Ery, at 1 μg/ml. *Escherichia coli* was routinely grown in Luria-Bertani (LB; Difco) medium at 37˚C or Luria-Bertani agar (LA; Difco). Ampicillin was used when required at 100 μg/ml.

2.3.2 DNA manipulation procedures

All plasmids used in this study are listed in Table 2.1 and the sequences of the primers used are listed in Table 2.2. PCR products and plasmid DNA were purified with kits Wizard SV Gel and PCR Clean-up System and Wizard Plus SV Minipreps, respectively (Promega). PCR fragments were amplified with Phusion High-fidelity DNA polymerase (Finnzymes). Restriction enzymes were from New England Biolabs.

Table 2.1: Bacterial strains and plasmids

Name	Relevant Characteristics	Source/Reference
Strains		
Streptococcus pneumoniae		
R36A	Non-encapsulated laboratory strain.	(Avery et al., 1944)
BCSJC001	R36ApBCSJC001, Tet^r.	(Henriques et al., 2013)
BCSJC006	R36ApBCSJC006, Tet^r.	(Henriques et al., 2013)
BCSJC011	R36ApBCSJC011, Tet^r.	This work.
BCSJC012	R36ApBCSJC012, Tet^r.	This work.
BCSJC013	R36ApBCSJC013, Tet^r.	This work.
BCSJC014	R36ApBCSJC014, Tet^r.	This work.
BCSJC015	R36ApBCSJC015, Tet^r.	This work.
BCSJC016	R36ApBCSJC016, Tet^r.	This work.
BCSJC017	R36ApBCSJC017, Tet^r.	This work.
BCSJC018	R36ApBCSJC018, Tet^r.	This work.
BCSJC019	R36ApBCSJC019, Tet^r.	This work.
BCSJC020	R36ApBCSJC020, Tet^r.	This work.
BCSJC021	R36ApBCSJC021, Tet^r.	This work.
BCSJC022	R36ApBCSJC022, Tet^r.	This work.
BCSJC023	R36ApBCSJC023, Tet^r.	This work.
BCSJC024	R36ApBCSJC024, Tet^r.	This work.

Name	Relevant Characteristics	Source/Reference
Strains		
BCSJC025	R36ApBCSJC025, Tet^r.	This work.
BCSJC026	R36ApBCSJC026, Tet^r.	This work.
BCSJC027	R36ApBCSJC027, Tet^r.	This work.
BCSJC028	R36ApBCSJC028, Tet^r.	This work.
BCSJC029	R36ApBCSJC029, Tet^r.	This work.
BCSJC030	R36ApBCSJC030, Tet^r.	This work.
BCSJC031	R36ApBCSJC031, Tet^r.	This work.
BCSJC032	R36ApBCSJC032, Tet^r.	This work.
BCSJC033	R36ApBCSJC033, Tet^r.	This work.
BCSJC034	R36ApBCSJC034, Tet^r.	This work.
BCSJC035	R36ApBCSJC035, Tet^r.	This work.
BCSJC036	R36ApBCSJC036, Tet^r.	This work.
BCSJC037	R36ApBCSJC037, Tet^r.	This work.
BCSJC038	R36ApBCSJC038, Tet^r.	This work.
BCSJC047	R36ApBCSJC043, Tet^r.	This work.
BCSMH008	R36ApBCSMH007, Tet^r.	(Henriques et al., 2013)
BCSMH030	R36ApBCSLF001, Tet^r.	(Henriques et al., 2013)
BCSMH033	R36ApBCSMH002, Tet^r.	(Henriques et al., 2013)
BCSMH063	R36ApBCSMH061, Tet^r.	This work.
Lactococcus lactis		
LL108	RepA$^+$ MG1363, Cm^r.	(Leenhouts et al., 1996)
BCSJC039	LL108pBCSMH002, Tet^r.	This work.
BCSJC040	LL108pBCSJC001, Tet^r.	This work.
Staphylococcus aureus		
RN4220	Restriction deficient derivative of *S. aureus* NCTC8325-4 strain capable of receiving foreign DNA	R. Novick
BCSJC041	RN4220pBCSJC039, Amp^r; Ery^r; LacZ$^+$.	This work.
BCSJC042	RN4220pBCSJC040, Amp^r; Ery^r; LacZ$^+$.	This work.
Bacillus subtilis		
MB24	trpC2 metC3	Laboratory stock.
BCSJC043	MB24pBCSJC039, Amp^r; Ery^r; LacZ$^+$.	This work.
BCSJC044	MB24pBCSJC040, Amp^r; Ery^r; LacZ$^+$.	This work.

Name	Relevant Characteristics	Source/Reference
Plasmids		
Streptococcus pneumoniae plasmids		
pBCSJC001	pBCSMH004 derivative, allowing expression of Citrine containing the first 10 aa of Wze at its N-terminus, Tet^r	(Henriques et al., 2013)
pBCSJC006	pBCSJC001 derivative, TTA→CTC change in codon 4 of Wze, Tet^r.	(Henriques et al., 2013)
pBCSJC011	pBCSMH007 derivative, allowing expression of Citrine containing the first 10 aa of Wzd at its N-terminus, Tet^r.	This work.
pBCSJC012	pBCSJC037 derivative, allowing expression of Citrine containing the first 12 aa of MurM at its N-terminus, Tet^r.	This work.
pBCSJC013	pBCSJC038 derivative, allowing expression of Citrine containing the first 10 aa of MurN at its N-terminus, Tet^r.	This work.
pBCSJC014	pBCSJC001 derivative, allowing expression of Citrine containing the sequence MLEPTIAQKKL at its N-terminus, Tet^r.	This work.
pBCSJC015	pBCSJC001 derivative, allowing expression of Citrine containing the sequence MPLETIAQKKL at its N-terminus, Tet^r.	This work.
pBCSJC016	pBCSJC001 derivative, allowing expression of Citrine containing the sequence MPTILEAQKKL at its N-terminus, Tet^r.	This work.
pBCSJC017	pBCSJC001 derivative, allowing expression of Citrine containing the sequence MPTIALEQKKL at its N-terminus, Tet^r.	This work.
pBCSJC018	pBCSJC001 derivative, allowing expression of Citrine containing the sequence MPTIAQLEKKL at its N-terminus, Tet^r.	This work.
pBCSJC019	pBCSJC001 derivative, allowing expression of Citrine containing the sequence MPTIAQKLEKL at its N-terminus, Tet^r.	This work.

Name	Relevant Characteristics	Source/Reference
Plasmids		
pBCSJC020	pBCSJC001 derivative, allowing expression of Citrine containing the sequence MPTIAQKKLEL at its N-terminus, Tet^r.	This work.
pBCSJC021	pBCSJC001 derivative, allowing expression of Citrine containing the sequence MPTIAQKKLLE at its N-terminus, Tet^r.	This work.
pBCSJC022	pBCSJC001 derivative, TTA→TTG change in codon 4 of Wze, Tet^r.	This work.
pBCSJC023	pBCSJC001 derivative, TTA→CTT change in codon 4 of Wze, Tet^r.	This work.
pBCSJC024	pBCSJC001 derivative, TTA→CTA change in codon 4 of Wze, Tet^r.	This work.
pBCSJC025	pBCSJC001 derivative, TTA→CTG change in codon 4 of Wze, Tet^r.	This work.
pBCSJC026	pBCSJC001 derivative, GAA→GAG change in codon 5 of Wze, Tet^r.	This work.
pBCSJC027	pBCSJC001 derivative, TTA→TTG change in codon 4 of Wze and GAA→GAG change in codon 5 of Wze, Tet^r.	This work.
pBCSJC028	pBCSJC001 derivative, TTA→CTC change in codon 4 of Wze and GAA→GAG change in codon 5 of Wze, Tet^r.	This work.
pBCSJC029	pBCSJC001 derivative, TTA→CTA change in codon 4 of Wze and GAA→GAG change in codon 5 of Wze, Tet^r.	This work.
pBCSJC030	pBCSJC001 derivative, TTA→CTT change in codon 4 of Wze and GAA→GAG change in codon 5 of Wze, Tet^r.	This work.
pBCSJC031	pBCSJC001 derivative, TTA→CTG change in codon 4 of Wze and GAA→GAG change in codon 5 of Wze, Tet^r.	This work.
pBCSJC032	pBCSJC013 derivative CTC→CTG change in codon 6 of MurN, Tet^r.	This work.
pBCSJC033	pBCSJC013 derivative CTC→CTT change in codon 6 of MurN, Tet^r.	This work.
pBCSJC034	pBCSJC013 derivative CTC→CTA change in codon 6 of MurN, Tet^r.	This work.

Name	Relevant Characteristics	Source/Reference
Plasmids		
pBCSJC035	pBCSJC013 derivative CTC→TTG change in codon 6 of MurN, Tet^r.	This work.
pBCSJC036	pBCSJC013 derivative CTC→TTA change in codon 6 of MurN, Tet^r.	This work.
pBCSJC037	pBCSMH002 containing *murM-Citrine*, Tet^r.	This work.
pBCSJC038	pBCSMH002 containing *murN-Citrine*, Tet^r.	This work.
pBCSJC043	pBCSJC001 derivative, TTA→CTC change in codon 4 of Wze, GAA→GAG change in codon 5 of Wze and ATA→AGA change in codon 6 of Wze, Tet^r.	This work.
pBCSLF001	High-copy-number vector, contains the -10 constitutive promoter of *SigA* from *S. pneumoniae*, Tet^r.	(Henriques et al., 2011)
pBCSMH002	pBCSLF001 derivative, allows expression of Citrine fusion proteins, Tet^r.	(Henriques et al., 2011)
pBCSMH007	pBCSMH002 containing *wzd-Citrine*, Tet^r.	(Henriques et al., 2011)
pBCSMH060	pBCSMH002 containing *wchA-Citrine*, Tet^r.	This work.
pBCSMH061	pBCSMH060 derivative allowing expression of Citrine containing the first 11 aa of WchA at its N-terminus, Tet^r.	This work.
S. aureus/B. subtilis plasmids		
pMAD	*E. coli – S. aureus* shuttle vector with a thermosensitive origin of replication for Gram-positive bacteria, Amp^r; Ery^r; LacZ$^+$.	(Arnaud et al., 2004)
pBCSJC039	pMAD derivative containing the -10 constitutive promoter of *SigA* from *S. pneumoniae*, the ribosome-binding site and *citrine*, Amp^r; Ery^r; LacZ$^+$.	This work.
pBCSJC040	pMAD derivative containing the -10 constitutive promoter of *SigA* from *S. pneumoniae*, the ribosome-binding site and *icitrine*, Amp^r; Ery^r; LacZ$^+$.	This work.

2.3.3 Construction of plasmids for protein expression in S. pneumoniae

Construction of the plasmids that allowed the expression of Citrine fused to the first 10 amino acids of Wzd, WchA and MurN at its N-terminus was carried out by ligation of the PCR products resulting from the amplification of plasmids pBCSMH007, pBCSMH060 or pBCSJC038 with primer 1 combined with primers 2–4, respectively originating plasmids pBCSJC011, pBCSMH061 and pBCSJC013. Plasmid pBCSJC012 allowing expression of Citrine fused to the first 12 amino acids of MurM was obtained by amplification of plasmid pBCSJC037 with primers 1/5.

For expression of Citrine fused to modified versions of the first 10 amino acids of Wze, the pBCSJC001 plasmid was amplified with primers 6 and 20–21 and the resulting PCR products were digested and ligated producing plasmids pBCSJC014-pBCSJC021, respectively.

Construction of the plasmids encoding silent mutations in the leucine amino acid located at position 4 of Wze, was obtained by ligation of the PCR products resulting from the amplification of plasmid pBCSJC001 with primer 6 combined with primers 7–10. The plasmids obtained in this way were named pBCSJC022–025. Plasmid pBCSJC026 encoding the GAA→GAG silent mutation in the glutamate amino acid at position 5 of Wze was constructed by amplification of plasmid pBCSJC001 with primers 6/15.

In order to express double silent mutations in the leucine located at position 4 of Wze and glutamate at position 5 of Wze we constructed plasmids pBCSJC027- pBCSJC031. This was done by restriction and ligation of the PCR products resulting from amplification of plasmid pBCSJC001 using primers 6 and 11–14 and 6/16, respectively.

Construction of the plasmid pBCSJC043, which allowed the expression of Citrine in fusion with mutations TTA→CTC (silent mutation - leucine), GAA→GAG (silent mutation - glutamate) and ATA→AGA (mutation from isoleucine to an arginine) at positions 4–6 of Wze, was carried out by ligation of the PCR product resulting from the amplification of plasmid pBCSJC001 with primer 6 combined with primer 17.

Plasmids pBCSJC032-036 that allow Citrine expression fused, at its N-terminus, with an ''i-tag'' whose *murN* nucleotide sequence was modified so that it carried silent mutations in the leucine located at position 6, were obtained by restriction and ligation of the PCR product resulting from amplification of plasmid pBCSJC013 using primers 6 and 26–30.

Construction of the plasmids pBCSJC039 and pBCSJC040, which allowed the expression of Citrine and the improved form of Citrine in *S. aureus* and *B. subtilis*, was done by amplifying from pBSCMH002 or pBCSJC001 a fragment containing the −10 constitutive promoter of *SigA* from *S. pneumoniae*, the ribosome-binding site and Citrine or the −10 constitutive promoter of *SigA* from *S. pneumoniae*, the ribosome-binding site and iCitrine, respectively, with primers 31/32. The PCR fragments were purified, digested with BamHI and BglII and cloned into the same sites of plasmid pMAD or pBSCMH037.

The nucleotide sequences of the modified regions of the constructed plasmids were confirmed by sequencing.

Table 2.2: Primers used in this work.

Primer	Sequence 5'→3'	Restriction Site
1	GATGAGCTCGGTACCTCGGCTG	SacI
2	GCGGAGCTCTACATCGATTTCCAAAGTGTTTTG	SacI
3	GCGGAGCTCTGCCAGAAAAATTTCCAATCC	SacI
4	GCGGAGCTCAAACTCTTCTTTCGTGAGTGTAG	SacI
5	GCGGAGCTCATATTCTAATGTGGGAATGCC	SacI
6	GCGGCTAGCCTACCTCCTTAAGCTTATTATACC	NheI
7	GCGGCTAGCATGCCGACATTGGAAATAGCAC	NheI
8	GCGGCTAGCATGCCGACACTTGAAATAGCAC	NheI
9	GCGGCTAGCATGCCGACACTAGAAATAGCAC	NheI
10	GCGGCTAGCATGCCGACACTGGAAATAGCAC	NheI
11	GCGGCTAGCATGCCGACATTGGAGATAGCAC	NheI
12	GCGGCTAGCATGCCGACACTTGAGATAGCAC	NheI
13	GCGGCTAGCATGCCGACACTAGAGATAGCAC	NheI
14	GCGGCTAGCATGCCGACACTAGAGATAGCAC	NheI
15	GCGGCTAGCATGCCGACATTAGAGATAGCAC	NheI
16	GCGGCTAGCATGCCGACACTCGAGATAGCAC	NheI
17	GCGGCTAGCATGCCGACACTCGAGAGAGCAC	NheI
18	GCGGCTAGCATGTTAGAACCGACAATAGCAC	NheI
19	GCGGCTAGCATGCCGTTAGAAACAATAGCAC	NheI
20	GCGGCTAGCATGCCGACAATATTAGAAGCACAAAAAAAACTG	NheI
21	GCGGCTAGCATGCCGACAATAGCATTAGAACAAAAAAAACTG	NheI

Primer	Sequence 5'→3'	Restriction Site
22	GCGGCTAGCATGCCGACAATAGCACAATTAGAAAAAAAACTG	NheI
23	GCGGCTAGCATGCCGACAATAGCACAAAAATTAGAAAAACTG	NheI
24	GCGGCTAGCATGCCGACAATAGCACAAAAAAAATTAGAACTG	NheI
25	GCGGCTAGCATGCCGACAATAGCACAAAAAAAACTGTTAGAAGAG	NheI
26	GCGGCTAGCATGGTACTAACTACATTAACG	NheI
27	GCGGCTAGCATGGTACTAACTACACTTACG	NheI
28	GCGGCTAGCATGGTACTAACTACATTGACG	NheI
29	GCGGCTAGCATGGTACTAACTACACTAACG	NheI
30	GCGGCTAGCATGGTACTAACTACACTGACG	NheI
31	GCGGGATCCGAATTCGGATCTAAAG	BamHI
32	GCGAGATCTGGATCTGGAGCTGTAATATAAAAACC	BglII
33	GAGCTGAAGGGCATCGACTT	
34	CTTGTGCCCCAGGATGTTG	
35	AATGGTTGTAGTTGCGCGCTAT	
36	AATGCTTTACCCCTATTTTCCTTTG	

2.3.4 Microscopy

S. pneumoniae strains were grown until early exponential phase ($OD_{(600\ nm)}$=0.2–0.3) and observed by fluorescence microscopy on a thin layer of 1% agarose in PreC medium (Lacks and Hotchkiss, 1960). Images were obtained using a Zeiss Axio Observer Z1 microscope equipped with a Plan-Apochromat objective (100x/1.4 Oil Ph3; Zeiss) and a Photometrics CoolSNAP HQ2 camera (Roper Scientific). The following Semrock filter was used to visualize fluorescent signals: YFP-2427A-ZHE-ZERO for Citrine tagged proteins. After acquisition, images were analysed and cropped using Metamorph software (Meta Imaging series 7.5) and Image J software (Abràmoff et al., 2004). Fluorescence quantification was done using the Metamorph software by measuring the integrated fluorescence intensity in a defined region of 2 by 2 pixels and subtracting the minimum background fluorescence from every value. Quantification was performed for at least 100 cells of each strain. Statistical analysis of the fluorescence intensity data was performed using GraphPad Prism 6 (GraphPad Software, Inc.).

2.3.5 RNA isolation and Quantitative Real-Time PCR

S. pneumoniae strains were grown in C+Y until early-exponential phase for RNA extraction. Prior to harvesting, RNA protect Bacteria Reagent (twice the culture volume, QIAGEN) was added to the culture and the mixture was immediately vortexed for 10 sec. The cells were harvested, the pellet was frozen in liquid N_2 and stored at –80˚C overnight. The next day, the pellet was resuspended with 200 µl of sodium deoxycholate 0.25 mg/ml for 30 min at 37˚C. RNA was extracted with RNeasy Mini kit (QIAGEN) and resuspended in milli-Q water. During the RNA extraction assay, an on-column DNA digestion, using 30 U of RNase-free DNase (QIAGEN), was performed for further removal of residual contaminant DNA. Total RNA was quantified using a GeneQuant*pro* Spectrophotometer (GeneQuant).

cDNA was generated from 250 ng of each RNA sample using TaqMan RT Reagents (Applied Biosystems, Branchburg, NJ, USA). The reaction mix included 5.5 mM $MgCl_2$, 500 µM dNTPs, 2.5 µM random hexamers, 1 x RT Buffer, 0.8 U/µl RNase Inhibitor and 1.25 U/µl MultiScribe RT in a final volume of 25 µl. The Reverse Transcription conditions were 10 min at 25˚C, 15 min at 42˚C and 5 min at 99˚C. Quantification of Citrine expression was achieved using the LightCycler 480 (Roche, Indianapolis, In, USA), SYBR Green chemistry, and the standard curve method for relative quantification. The PCR reagents consisted of: 2 x LightCycler 480 SYBR Green I Master (Roche), 400 nM of each primer, and 5 µl of sample cDNA, in a final volume of 25 µl. The thermocycling profile was: 10 min at 95˚C followed by 40 cycles of 15 s at 95˚C and 1 min at 60˚C. qPCR primers for Citrine (33 and 34) and tetracycline (35 and 36) were designed using the Primer Express (Applied Biosystems).

Optical plates included plasmid standard curves for Citrine, and duplicates of each cDNA sample. ''No template'' and ''no RT'' controls were also included in every qPCR assays. For each sample, the expression of Citrine was determined from the respective standard curve by conversion of the mean threshold cycle values, and normalization was obtained by dividing the quantity of Citrine cDNAs by the quantity of cDNA amplified within the gene encoding for the tetracycline resistance protein (used as the endogenous control), which is cloned in the same plasmid. The specificity of the amplified products was verified by analysis of the dissociation curves generated by the LightCycler 480 SYBR software based on the specific melting temperature for each amplicon. The final qPCR results were based on two independent experiments.

2.3.6 Protein analysis

The analysis of the expression of the fluorescent Citrine protein linked to different N-terminal tags was done as previously described (Henriques et al., 2013). Bacterial cell aliquots of 1 ml of culture were harvested at mid-exponential growth phase. Cells were incubated at 37˚C during 30 minutes in deoxycholate (0.25 mg/ml), RNase (10 mg/ml), DNase (10 mg/ml) and PMSF (1 mM). For the fluorescent protein analysis, proteins were incubated with solubilization buffer (200 mM Tris-HCl pH 8.8, 20% glycerol, 5 mM EDTA pH 8.0, 0.02% bromophenol blue, 4% SDS, 0.05 M DDT) at 37˚C for 5 minutes and separated on SDS-PAGE. Gel images were acquired on a FUJI FLA 5100 laser scanner (Fuji Photo Film Co.) with 635 nm excitation and >665 nm band pass emission filter for protein molecular weight marker detection and 473 nm excitation and >510 nm band pass emission filter for Citrine detection.

For western-blot analysis, cell extracts were boiled during 5 minutes before being separated on SDS-PAGE. Proteins were transferred into a Hybond PVDF Membrane (Amersham) and probed with Living Colors Av. Peptide Antibody (Clontech) for the detection of Citrine, used at 1:500, followed by 1:100000 of goat anti-rabbit conjugated to horseradish peroxidase. Detection was done with ECL Plus Western Blotting Detection Reagents (Amersham).

2.4 Results and discussion

2.4.1 The first ten amino acids of the protein Wze, named the i-tag, can increase the expression of the Citrine fluorescent signal in different bacterial models

We have previously described the construction of a set of plasmids for the expression of fluorescent protein fusions in the low-GC Gram-positive *S. pneumoniae* bacteria (Henriques et al., 2013). These plasmids were designed in order to improve expression of the fluorescent proteins mCherry, Citrine, CFP and GFP by including a sequence encoding the first ten amino acids of the capsular protein Wze, which we named the i-tag, upstream of the fluorescent proteins. We proposed that this i-tag extension might facilitate ribosome accessibility to the ribosome-binding site, thus enhancing protein translation (Henriques et al., 2013).

In order to determine if we could apply a similar strategy to other bacterial models, we inquired whether the i-tag could likewise increase expression of fluorescent proteins in other Gram-positive bacteria, namely *Lactococcus lactis*, *Staphylococcus aureus* and *Bacillus subtilis*.

We transformed *L. lactis* with the previously constructed plasmid pBCSJC001, which allows the expression of the improved form of the fluorescent protein Citrine (iCitrine) (Henriques et al., 2013), and with pBCSMH002, which should allow expression of Citrine fusion protein without any tag (Henriques et al., 2011). These vectors are derivatives of the plasmid pLS1 that was shown to efficiently replicate and confer tetracycline resistance in Gram-positive bacteria (Lacks et al., 1986) including *L. lactis* (Fernandez de Palencia et al., 2000). Quantification of the fluorescent signal expressed by *L. lactis* strains encoding Citrine alone (BCSJC039) or the improved form of Citrine (BCSJC040), showed that, as formerly observed for *S. pneumoniae* (Henriques et al., 2013) the fusion of the first ten amino acids of Wze (i-tag) increased expression of fluorescence. *L. lactis* strain BCSJC039, expressing only the untagged fluorescent protein Citrine, showed low levels of fluorescence (Figure 2.1A). We then enquired whether the i-tag could likewise increase expression of fluorescent proteins in other Gram-positive bacteria besides *L. lactis*. As we did not succeed to transform these plasmids into other Gram-positive bacteria, we cloned the DNA fragment containing both the promoter and the coding sequence of the fluorescent proteins into the pMAD vector, which could be transformed into other Gram-positive bacteria. The pMAD plasmid contains a thermosensitive replication origin and replicates at 30˚C degrees (Arnaud et al., 2004).

We constructed two additional vectors by cloning the conserved −10 constitutive promoter region of *SigA* from *S. pneumoniae*, the ribosome-binding site, and Citrine (from plasmid pBCSMH002) or iCitrine (from plasmid pBCSJC001) in pMAD, which generated plasmids pBCSJC039 and pBCSJC040, respectively. The resulting plasmids were transformed in *S. aureus* and *B. subtilis* originating strains BCSJC041 to BCSJC044 and Citrine expression was detected by fluorescence microscopy. We observed an increase in fluorescence intensity only when the i-tag was fused to Citrine both in *S. aureus* strain BCSJC042 and *B. subtilis* strain BCSJC044. Heterogeneity in fluorescence intensity was observed in both bacterial species, which may be due to plasmid copy number instability at 30˚C degrees even under the selective pressure of erythromycin antibiotic. The observed heterogeneity may be reduced using other replicative plasmids or by expressing the fluorescent proteins from the chromosome. Low

levels of fluorescence were detected when Citrine (without the i-tag) was expressed in *S. aureus* BCSJC041 and *B. subtilis* BCSJC043 strains (Figure 2.1B).

Therefore, as observed for *S. pneumoniae* (Henriques et al., 2013), the presence of the nucleotide sequence encoding the i-tag upstream of the fluorescent protein Citrine results in increased fluorescence intensity, possibly due to optimized translation rates, in the Gram-positive bacteria *L. lactis*, *S. aureus* and *B. subtilis*.

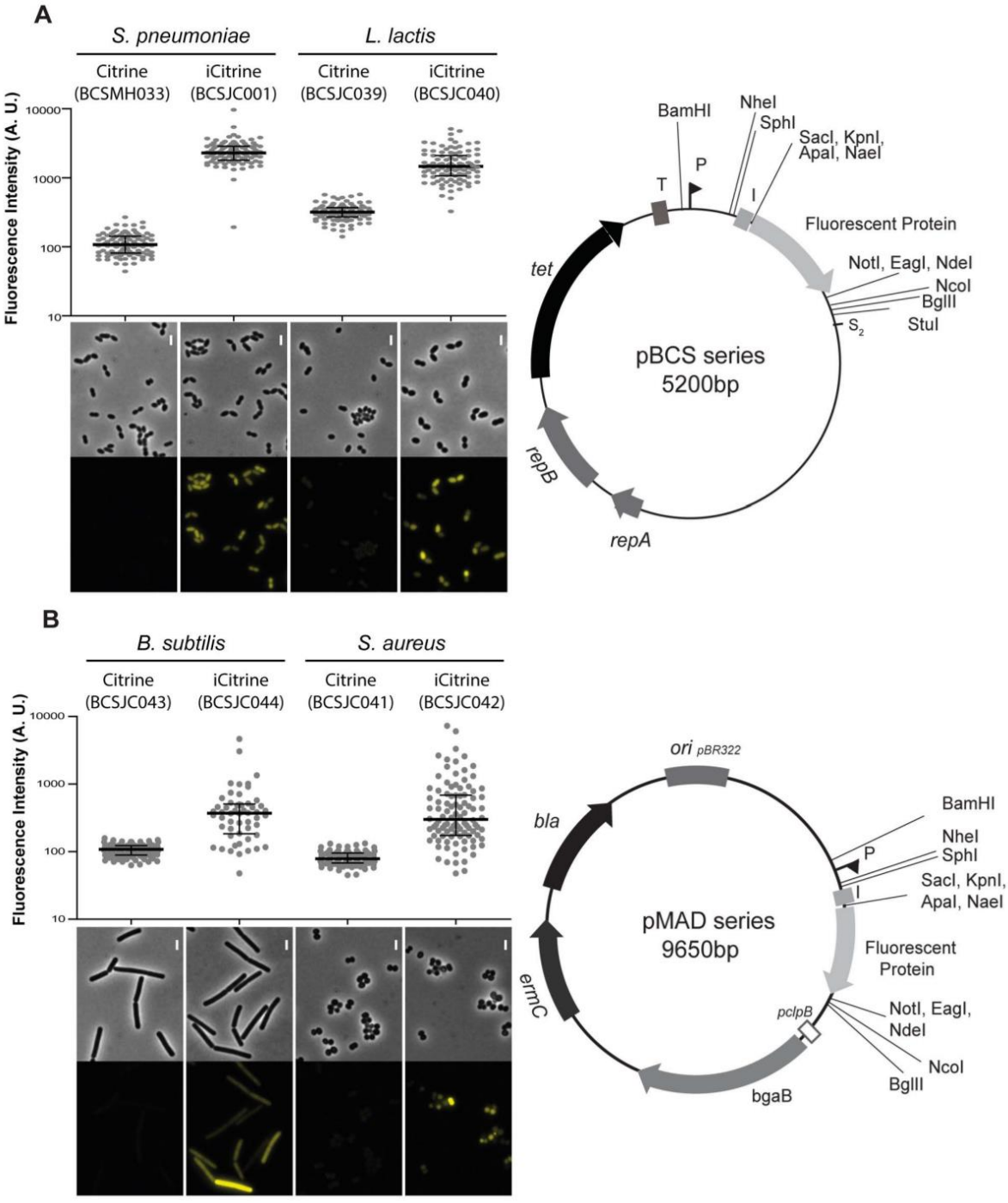

Figure 2.1: Linking the i-tag to Citrine improves the expression of fluorescence in Gram-positive bacteria. A) (Left panel) Median fluorescence, with 25% and 75% inter-quartile range (black lines) of the fluorescence signal detected in *S. pneumoniae* unencapsulated bacteria, in arbitrary units (A. U.), expressing Citrine (strain BCSMH033) or iCitrine (strain BCSJC001), and *L. lactis*, expressing Citrine (strain BCSJC039) and iCitrine (strain BCSJC040). At least 100 cells of each strain were quantified. Representative images of each strain are shown below the graph. Scale bar: 1 μm. (Right panel) Map of the pBCS plasmids. Fluorescent protein refers to Citrine and iCitrine. *repA*, *repB*, plasmid replication genes. *tet*, tetracycline resistance marker. T, transcription terminator. P, promoter. S2, stop codon. **B)** (Left panel) Median fluorescence, with 25% and 75% inter-quartile range (black lines) of the fluorescence signal emitted by Citrine and iCitrine detected in *S. aureus* bacteria, in arbitrary units (A. U.), expressing Citrine (strain BCSJC041) and iCitrine (strain BCSJC042), or *B. subtilis*, expressing Citrine (strain BCSJC043) or iCitrine (strain BCSJC044). At least 100 cells of each strain were quantified. Representative images of each strain are shown below the graph. Scale bar: 1 μm. (Right panel) Map of the pMAD plasmids. Fluorescent protein refers to Citrine and iCitrine. Unique restriction sites are indicated. *ermC*, erythromycin resistance marker.

2.4.2 Determination of the N-terminal tag requirements to improve expression of fluorescent proteins in Streptococcus pneumoniae

In order to determine how the sequence of the i-tag permitted an efficient expression of the fluorescent proteins, we decided to investigate if the N-terminal of other highly expressed pneumococcal capsular proteins were also capable of increasing the expression of fluorescent proteins in *S. pneumoniae*. We had observed a strong fluorescent signal when some of these proteins had their C-terminus end fused to the Citrine fluorescent protein (Henriques et al., 2013). For this purpose, we initially redesigned plasmid pBCSJC001 and substituted the i-tag encoding the first ten amino acids of Wze, for the sequences encoding the first ten amino acids of Wzd (originating plasmid pBCSJC011) and the first eleven amino acids of WchA (originating plasmid pBCSMH061), two proteins involved in capsular biosynthesis (Bentley et al., 2006). These plasmids were transformed in *S. pneumoniae* R36A originating strains BCSJC011 and BCSMH063, which expressed Citrine with a N-terminal tag constituted by 10/11 amino acids of Wzd or WchA, respectively. When protein expression was determined by fluorescence microscopy, we noticed that the fluorescence signal in strain BCSMH063, encoding $WchA_{10aa}$-Citrine, was higher than the signal observed in BCSJC001 strain, encoding the original iCitrine fusion, Wze_{10aa}-Citrine (Figure 2.2). The expression of

Wzd_{10aa}-Citrine also resulted in higher fluorescent signal but in this case only in a sub-population of cells (Figure 2.2).

We also designed two additional plasmids in which the fluorescent protein Citrine was fused, at its N-terminus, to the first amino acids of MurM (pBCSJC012) or MurN (pBCSJC013), two *S. pneumoniae* enzymes that are involved in the synthesis of a branched peptidoglycan (Filipe et al., 2000), originating strains BCSJC012 and BCSJC013, respectively. Fluorescence microscopy analysis showed that in both cases, the expression of fluorescence was lower than for iCitrine. This was particularly noticeable for the expression of $MurN_{10aa}$-Citrine fusion, which did not result in fluorescent bacteria (Figure 2.2).

Amino acid sequence alignment of the N-terminal regions of Wze, Wzd, WchA, MurM and MurN showed that a motif of two amino acids, a leucine (L) and a glutamate (E), are conserved in those that allowed the expression of higher fluorescent signals (Wze, Wzd, WchA and MurM). However, neither the leucine codon (UUG or UUA) nor its distance to the start codon was conserved (Figure 2.2).

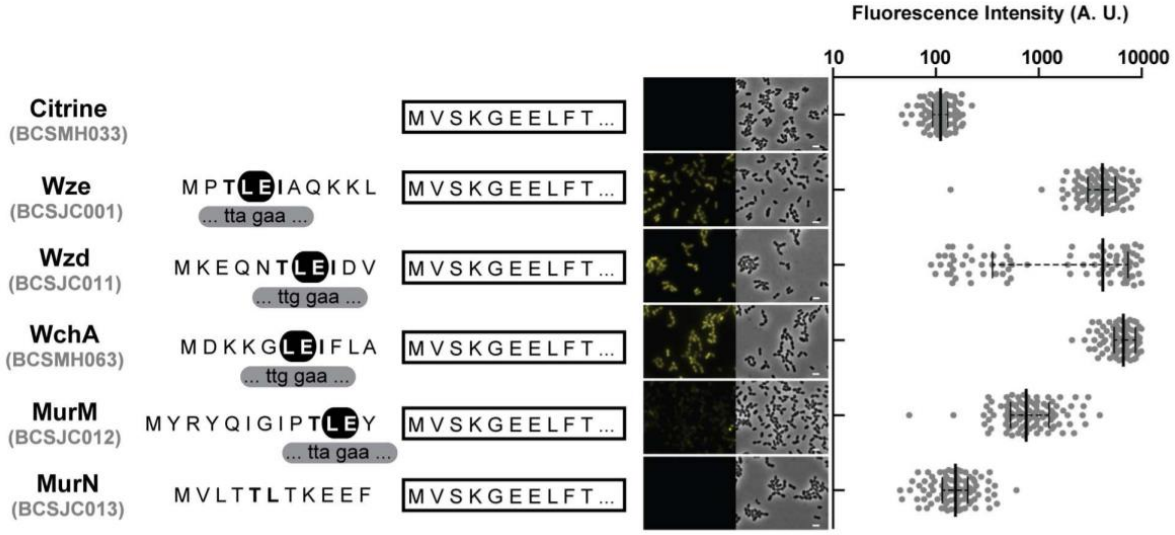

Figure 2.2: The amino terminal end of different *S. pneumoniae* proteins ensures expression of the Citrine fluorescent signal when a conserved LE motif is present. (Left panel) Sequence of the first amino acids of proteins WchA, MurM, MurN, Wze and Wzd that were linked to Citrine (shown as a white rectangle) are shown. Highlighted (black) are the conserved amino acids L (leucine) and E (glutamic acid). (Right panel) Median fluorescence, with 25% and 75% inter-quartile range (black lines) of the fluorescence signal detected in *S. pneumoniae* R36A unencapsulated bacteria, in arbitrary units (A. U.), emitted by Citrine (BCSMH033), $WchA_{(1-10)}$-Citrine (BCSMH063), $MurM_{(1-10)}$-Citrine (BCSJC012), $MurN_{(1-10)}$-Citrine (BCSJC013), $Wze_{(1-10)}$-Citrine (BCSJC001) and $Wzd_{(1-10)}$-Citrine (BCSJC011). At least 100 cells of each strain were quantified. Representative images of each strain are shown. Scale bar: 1 μm.

In order to determine the optimal distance of this conserved LE motif to the start codon, we constructed a set of plasmids (pBCSJC014 to pBCSJC021) in which the LE encoding codons were 0 to 9 codons away from the start codon (Figure 2.3). *S. pneumoniae* R36A strains BCSJC014 to BCSJC021 expressing these plasmids were analysed by fluorescence microscopy. The highest fluorescent signal was observed for BCSJC014 and BCSJC019 strains, in which the LE motif was located immediately next to or six amino acids far from the starting methionine, respectively (Figure 2.3). In all other cases, fluorescence levels were about 50% lower than for iCitrine (Figure 2.3). Therefore, the distance of the LE motif to the N-terminal end of the protein was not a crucial factor to ensure increased expression of Citrine.

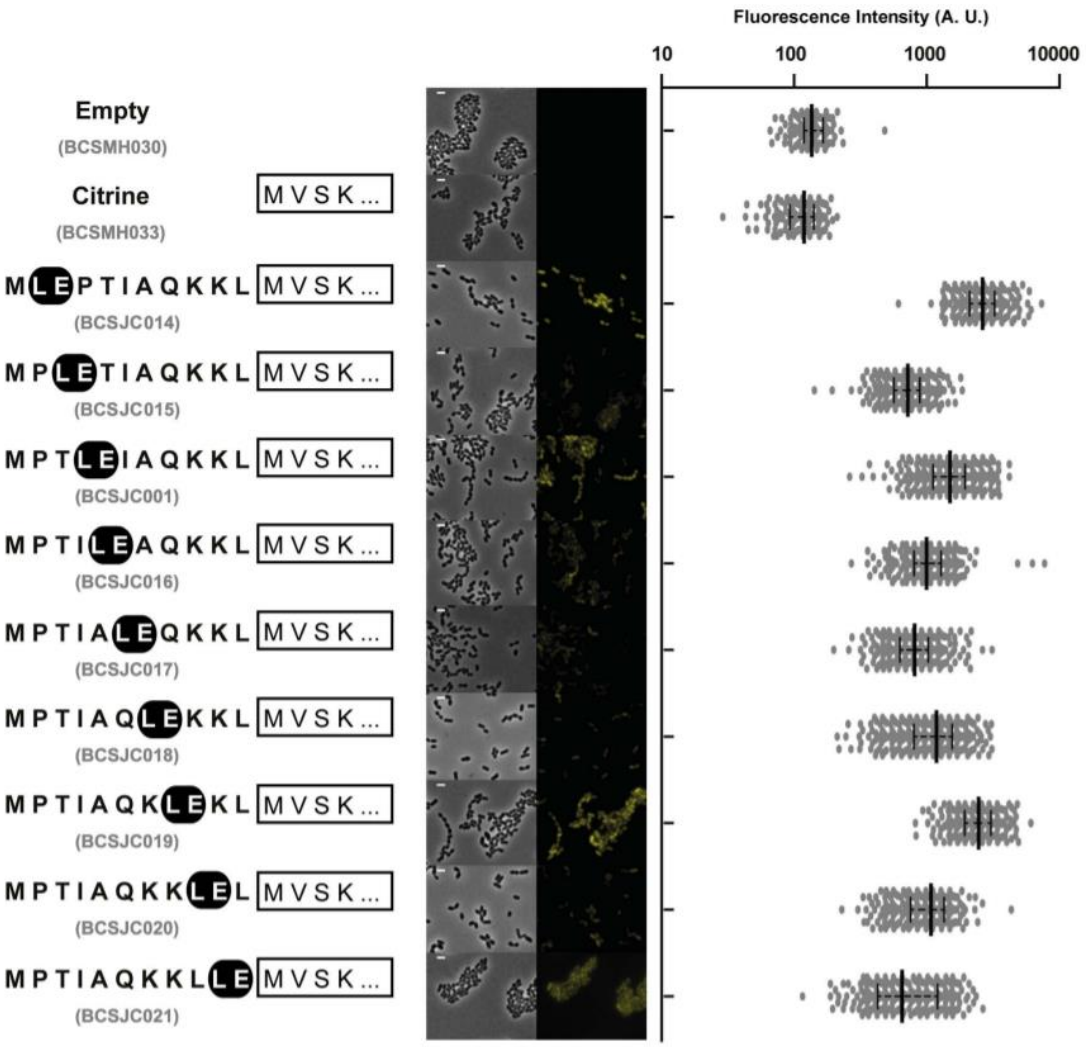

Figure 2.3: Expression of the Citrine fluorescent signal is not dependent on the distance of the conserved LE motif to its N-terminal end. Amino acid sequence of the different tags, containing the LE motif successively positioned 0 to 9 amino acids distant from the starting methionine, linked to Citrine (shown as a white rectangle) is shown. Median fluorescence, with 25% and 75% inter-quartile range (black lines) of the fluorescence signal emitted by the following unencapsulated bacteria *S. pneumoniae*

R36A strains, in arbitrary units (A. U.): Empty plasmid (BCSMH030), Citrine (BCSMH033), i*(MLEPTIAQKKL)-Citrine (BCSJC014), i*(MPLETIAQKKL)-Citrine (BCSJC015), i*(MPTLEIAQKKL)-Citrine (BCSJC001), i*(MPTILEAQKKL)-Citrine (BCSJC016), i*(MPTIALEQKKL)-Citrine (BCSJC017), i*(MPTIAQLEKKL)-Citrine (BCSJC018), i*(MPTIAQKLEKL)-Citrine (BCSJC019), i*(MPTIAQKKLEL)-Citrine (BCSJC020), and i*(MPTIAQKKLLE)-Citrine (BCSJC021). The strains BCSMH030 and BCSMH033 were used as a negative control. At least 100 cells of each strain were quantified. Representative images of each strain are shown. Scale bar: 1 μm.

As the Leucine codon also varied in the different N-terminal regions that were tested (Figure 2.2), we speculated whether the use of less frequently used codons could prevent the successful expression of the Citrine fluorescent protein, as the introduction of less frequently used codons in the beginning of mRNA molecules may result in the reduction of the translation of the encoded proteins. This hypothesis had been previously suggested for *B. subtilis*, where a sequence encoding the first eight amino acids of specific ComGA was proposed to overcome the slow translation initiation caused by the eukaryotic codon bias present in fluorescent proteins (Veening et al., 2004). This is due to the fact that the absence of tRNA molecules can result in a stalled translation process, which consequently may lead to the disassembly of the complex ribosome/mRNA (Gustafsson et al., 2004; Lee et al., 2009).

We therefore constructed different pBCSJC001 derivative plasmids (pBCSJC006, pBCSJC022 to pBCSJC025), where the leucine codon in the fourth position of the i-tag (UUA, codon usage frequency of 0.0198) was replaced by the alternative leucine codons, which are predicted to be differently used by *S. pneumoniae* CUG (0.0092), CUA (0.0116), CUC (0.0127), CUU (0.0207) and UUG (0.0287) (Zhu et al., 2010). Pneumococcal strains carrying the iCitrine fusion expressing these silent mutations were observed by fluorescence microscopy and the fluorescent signal obtained was quantified. The highest fluorescence signal was obtained for the strain expressing the original iCitrine fusion where leucine is coded by the UUA codon (BCSJC001) (Figure 2.4). Interestingly, we also observed high fluorescence signals for the strains expressing the modified iCitrine fusion where the UUA leucine codon was replaced by either the lowest frequency leucine CUG (BCSJC025) or the highest frequency leucine codon UUG (BCSJC022), indicating that codon usage does not determine the efficiency of the i-tag.

We also tested the effect of exchanging the glutamate codon in the fifth position of the i-tag (GAA, codon usage frequency of 0.0517) for the alternative glutamate codon (GAG,

codon usage frequency of 0.0211), which resulted in lower levels of fluorescent signal (Figure 2.4).

The observation that the combination of the less frequently used codons or of the more frequently used codons did not always result in non-fluorescent or highly fluorescent pneumococcal bacteria, respectively, allowed us to conclude that fluorescence stabilization is codon-sequence specific in a way that seems not to be influenced by the usage of less frequently used codons.

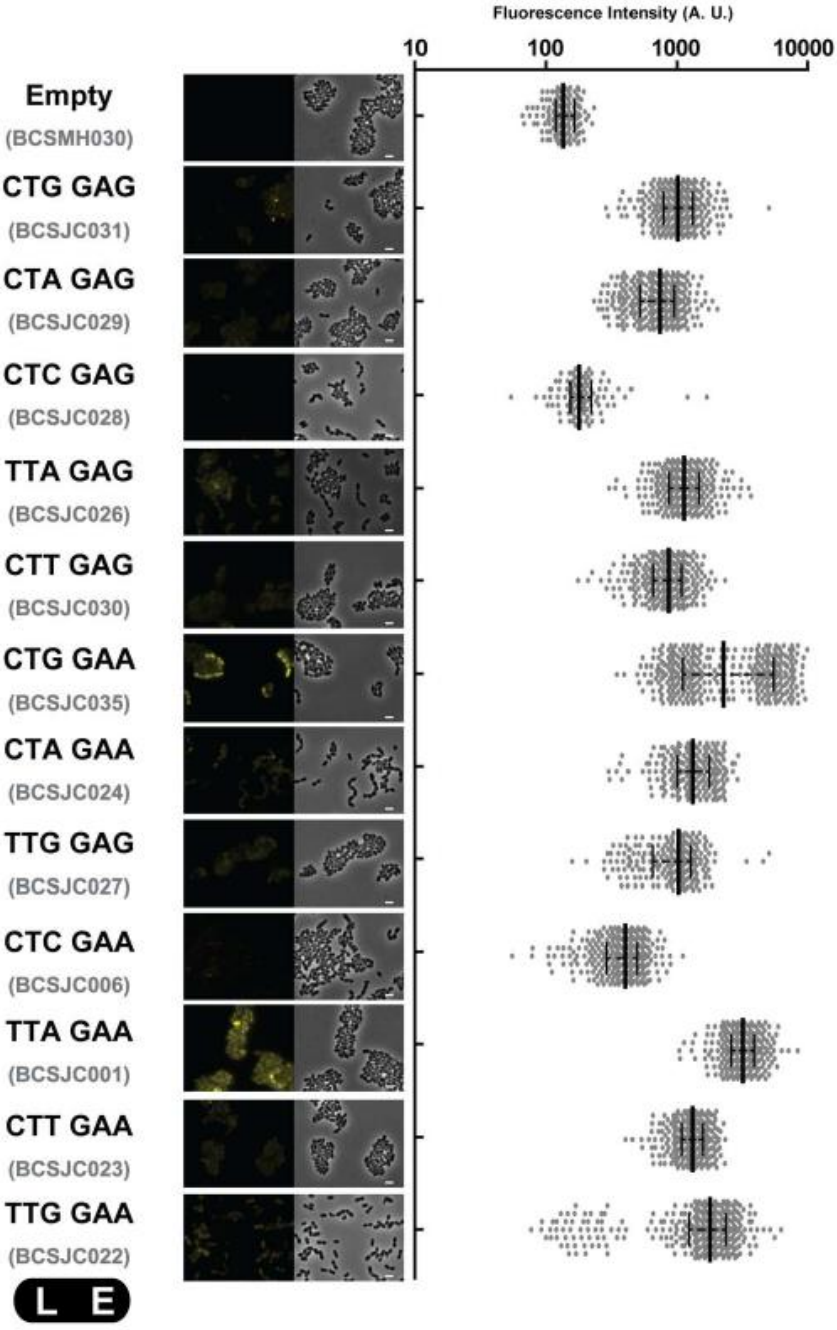

Figure 2.4: Fluorescence intensity is not only dependent on codon usage. Different pBCSJC001 derivative plasmids were constructed where the leucine codon in the fourth position of the i-tag (TTA) was replaced by the alternative leucine codons (TTG, CTT, CTA, CTG), and/or the glutamate codon in the fifth position of the i-tag (GAA) was replaced by the alternative glutamate codon (GAG). Median fluorescence, with 25% and 75% inter-quartile range (black lines) of the fluorescence signal emitted by the following unencapsulated bacteria *S. pneumoniae* R36A strains, in arbitrary units (A. U.): Empty plasmid (strain BCSMH030 used as a negative control), CTGGAG (frequency of 0.0002, strain BCSJC031), CTAGAG (frequency of 0.0002, strain BCSJC029), CTCGAG (frequency of 0.0003, strain BCSJC028), TTAGAG (frequency of 0.0004, strain BCSJC026), CTTGAG (frequency of 0.0004, strain BCSJC030), CTGGAA (frequency of 0.0005, strain BCSJC025), CTAGAA (frequency codon usage of 0.0006, strain BCSJC024), TTGGAG (frequency of 0.0006, strain BCSJC027), CTCGAA (frequency of 0.0007, strain BCSJC006), TTAGAA (frequency of 0.0010, strain BCSJC001), CTTGAA (frequency of 0.0011, strain BCSJC023) and TTGGAA (frequency of 0.0015, strain BCSJC022). At least 100 cells of each strain were quantified. Representative images of each strain are shown. Scale bar: 1 μm.

2.4.3 Fluorescence intensity seems to be dependent on the stability of the 5′ end of the mRNA structure

We hypothesized that the effect of N-terminal i-tag on the expression of the Citrine protein could be related to the structure of the 5′ end of the mRNA molecule produced or to its stability, which consequently could improve the accessibility of the ribosome. Therefore, the 5′ ends of the mRNAs originated by the introduction of the different tags described above were evaluated by the RNAfold program available at the ViennaRNA Web Services (Gruber et al., 2008). When we plotted the intensity of the fluorescent signal detected in the pneumococcal strains expressing Citrine with different N-terminal ends, with the respective minimum free energy predicted for the 5′ end of the corresponding mRNA molecules (Figure 2.5A), we observed an apparent inverse correlation between the stability of mRNA structures and the intensity of the fluorescent signals (Figure 2.5B). The highest fluorescent signal was observed with strain BCSMH063 that expressed the $WchA_{10aa}$-Citrine.

We also noticed that in the strains with the lowest levels of fluorescence, such as that encoding $MurN_{10aa}$-Citrine, the AGGAGG ribosome-binding site was stably paired with the leucine codon (Figure 2.5C) possibly impairing ribosome binding to the mRNA molecule. Therefore, we asked whether replacing the leucine codon for an alternative codon, which would not pair with the RBS and would decrease the stability of the predicted structure of the 5′ end of the mRNA, could allow protein translation initiation and the expression of a

fluorescent signal. For this, we constructed plasmids pBCSJC35 and pBCSJC036 in which the *murN* wild-type CUC leucine codon, present in plasmid pBCSJC013, was substituted by the alternative leucine codons (the less frequently used UUG and the more frequently used UUA, respectively). As expected, resulting strains BCSJC035 and BCSJC036 showed higher levels of fluorescence (Figure 2.5C).

Similar results could be obtained by mutating the codon located next to the leucine CUC and glutamate GAG codons in the iCitrine expressed by BCSJC028 strain. Although the presence of these codons prevented the expression of any fluorescent signal, mutating the codon next to them, from AUA to AGA, which converts an isoleucine to an arginine, resulted in increased fluorescence in accordance with the predicted decrease in the stability the 5' end mRNA structure and the improved accessibility to the ribosome binding site (Figure 2.5D).

In order to determine if the increased fluorescence observed for strains BCSJC035, BCSJC036 and BCSJC047 could result from higher mRNA levels or higher protein translation, we quantified by qPCR, also known as real-time PCR the levels of mRNA of these strains in exponentially growing bacteria, relatively to the mRNA of the tetracycline resistance marker, encoded in the plasmid backbone.

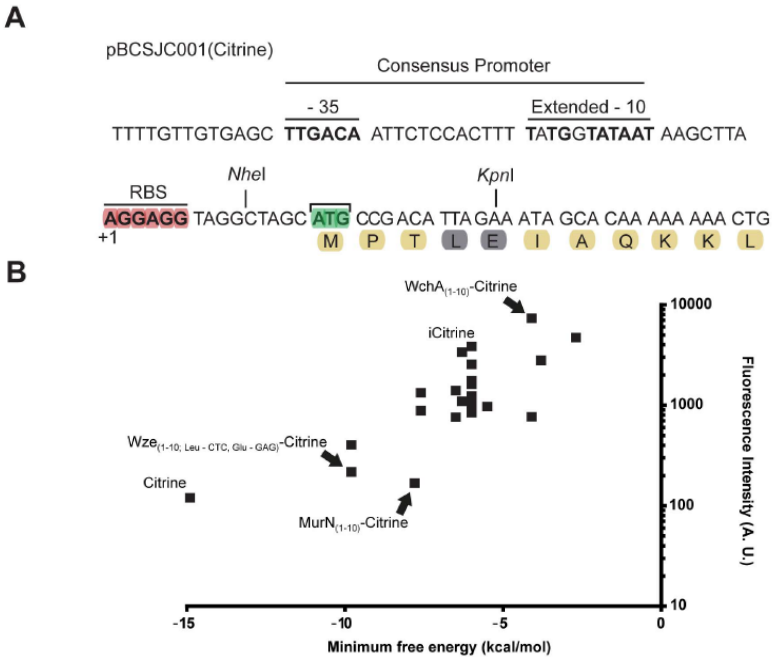

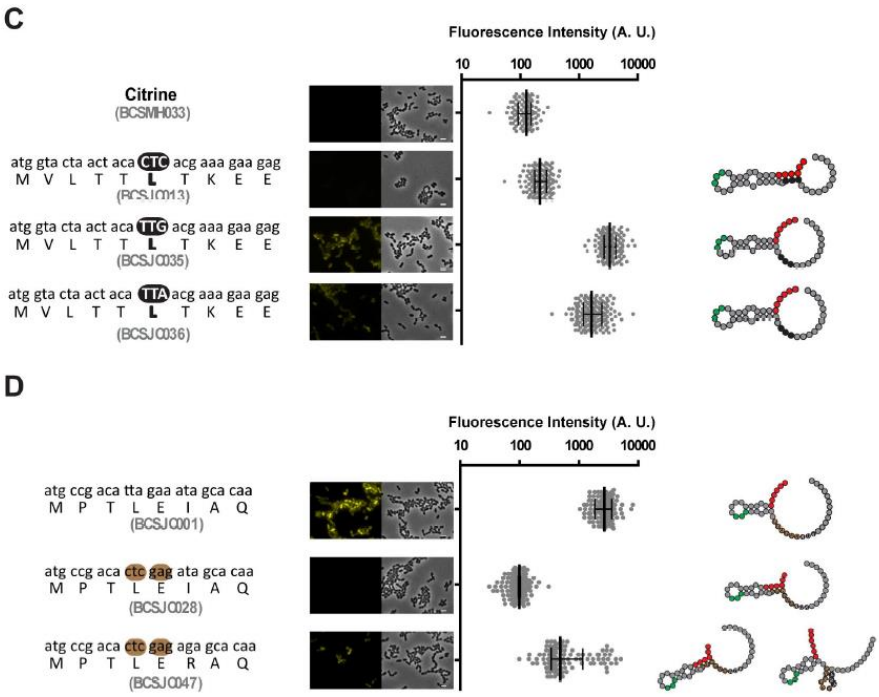

Figure 2.5: Expression of Citrine derivatives containing N-terminal tags is dependent on ribosome binding site accessibility. A) Partial sequence of plasmid pBCSJC001 highlights the consensus promoter region, the ribossome-binding site, the proposed transcription start site (+1) and translation start site (AUG) (Sabelnikov et al., 1995; Lacks et al., 2000). **B)** The mean fluorescence measured for the different constructs where Citrine has been fused to different tags at its N-terminal end is plotted relatively to the predicted thermal stability (minimum free energy in kcal/mol) of the 5′ end of the mRNA (+1 to +45) structures. The values for some Citrine derivatives are highlighted: Citrine (expressed in strain BCSMH033), iCitrine (strain BCSJC001), $WchA_{(1-10)}$-Citrine (strain BCSMH063), $MurN_{(1-10)}$-Citrine (strain BCSJC012) and $Wze_{(1-10)}$-Citrine with mutated leucine (CTC) and glutamate (GAG) codons (strain BCSJC028). **C)** Replacing the wild-type CTC leucine codon in pBCSJC006 for the alternative TTG and TTA codons in the tag derived from the N-terminal end of MurN resulted in increased cell fluorescence. Median fluorescence, with 25% and 75% inter-quartile range (black lines) emitted by unencapsulated R36A *S. pneumoniae* strains expressing Citrine (used as a negative control, strain BCSMH033), $MurN_{(1-10)}$-Citrine with CTC codon (strain BCSJC013), with TTG codon (strain BCSJC035) and with TTA (strain BCSJC036). At least 100 cells of each strain were quantified. (Left) Representative images of each strain as well as the peptide and nucleotide sequences of the N-terminal tag. Scale bar: 1 μm. (Right) Representation of the 5′-end mRNA structure. Ribosome binding site (Red), AUG codon (Green) and mutated nucleotides (black) are highlighted. **D)** Mutating the ATA isoleucine codon in pBCSJC028 to the AGA arginine codon in the tag derived from the N-terminal end of Wze resulted in increased cell fluorescence. Median fluorescence, with 25% and 75% inter-quartile range (black lines) emitted by unencapsulated R36A *S. pneumoniae* strains expressing iCitrine (used as a positive control, strain BCSJC011), $Wze_{(1-10)}$-Citrine with CTC leucine and glutamate GAG codons (strain BCSJC028), $Wze_{(1-10)}$-Citrine with CTC leucine, glutamate GAG and arginine AGA codons (strain BCSJC047). At least 100 cells of each strain were quantified. (Left) Representative images of each strain as well as the peptide and nucleotide sequences of the N-terminal tag. Scale bar: 1 μm. (Right) Representation of the 5′-end mRNA

structure. Ribosome binding site (Red), AUG codon (Green) and mutated nucleotides (black) are highlighted.

We observed that levels of the different mRNAs were not sufficiently different to explain the variability in fluorescence expression amongst the fluorescent and non-fluorescent strains (Figure 2.6A). Citrine protein levels were also quantified using a fluorescent image analyser and Western-blot analysis. We observed that Citrine could be detected only in fluorescent strains, namely those encoding for $MurN_{CTC\text{-}TTG}$-Citrine (strain BCSJC035), $MurN_{CTC\text{-}TTA}$-Citrine (strain BCSJC036), $MurM_{CTC\text{-}GAG\text{-}AGA}$-Citrine (strain BCSJC47) and strain Wze_{10aa}-Citrine (strain BCSJC001 which encodes iCitrine) (Figure 2.6B). Taken together these results show that the stability of the 5′ end of the transcribed mRNA, and the pairing with ribosome-binding site, which may prevent the access of the ribosome, determine the efficiency of the expression of Citrine derivatives in *S. pneumoniae*.

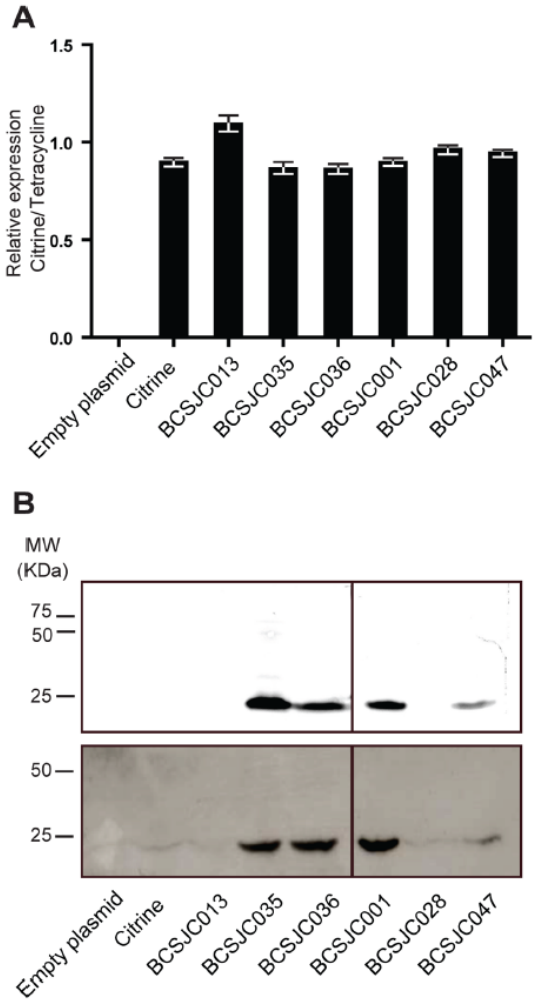

Figure 2.6: Increased fluorescence resulting from the presence of different tags is due to increased protein levels. A) mRNA encoding Citrine was quantified by qPCR in strains expressing specific amino acid sequences from different tags fused to Citrine, relatively to the mRNA for the tetracycline resistance protein which is encoded in the plasmid backbone. Strains analysed were BCSMH030 (transformed with an empty vector), BCSJC013 (expressing $MurN_{10aa}$_Citrine), BCSJC035 (expressing $MurN_{10aa(CTC\text{-}TTG)}$-Citrine), BCSJC036 (expressing $MurN_{10aa(CTC\text{-}TTA)}$-Citrine), BCSJC001 (expressing $Wze_{(1–10)}$-Citrine), BCSJC028 (expressing $Wze_{10aa(TTA\text{-}CTC,\ GAA\text{-}GAG)}$-Citrine), BCSJC047 (expressing $Wze_{10aa(TTA\text{-}CTC,\ GAA\text{-}GAG,\ ATA\text{-}AGA)}$-Citrine). **B)** Cell extracts from these strains were separated by SDS-Page and analysed using a Fluorescent Image Analyzer (top panel) and by Western-blot analysis using an antibody that recognizes Citrine protein (bottom panel), showing that Citrine fluorescence results from increased protein levels and not increased mRNA levels.

2.5 Final remarks

The study of protein localization in different bacterial species requires the development of flexible tools. Here we have shown that tools previously developed for the Gram-positive pathogen *S. pneumoniae*, can be used in other pathogenic bacteria, namely *S. aureus*, in the model organism *B. subtilis* or in *L. lactis*, a species of great industrial interest, suggesting that these tools can have a widespread application. Furthermore, we have optimized the sequence of the i-tag in order to maximize the production of the Citrine fluorescent protein in *S. pneumoniae* by manipulating the structure and stability of the mRNA 5′ end encoded by the i-tag. The 5′ end of mRNA transcripts plays a major role in the translation initiation and determines the translation rate and consequently the total amount of protein produced (Kudla et al., 2009). We propose that the determination of minimum free energy predicted for the 5′ end of the mRNAs molecules originated by the introduction of the different tags may predict whether the expression of a specific fluorescent protein will be successful.

Chapter 3

Efficient encapsulation of the newly synthesized cell wall protects *Streptococcus pneumoniae* from peptidoglycan hydrolases and host defenses

3.1 Abstract

Synthesis of the capsular polysaccharide, a major virulence factor for many pathogenic bacteria, is required for bacterial survival within the infected host. In *Streptococcus pneumoniae*, Wze, an autophosphorylating tyrosine kinase, and Wzd, a membrane protein required for Wze autophosphorylation, co-localize at the division septum and guarantee the presence of capsule at this subcellular location.

To determine how bacteria regulate capsule synthesis, we searched for pneumococcal proteins that interact with Wzd and Wze. We found that Wzg, the ligase that attaches capsule to the bacterial cell wall, interacts with Wzd, and that this interaction recruits Wzg to the septum. Pneumococcal mutants unable to produce Wzd, that therefore lack capsule at midcell, become more exposed to peptidoglycan binding receptors, have increased susceptibility to lysis induced by peptidoglycan hydrolases and have decreased survival in a zebrafish embryo infection model.

We propose that the Wzd/Wze pair ensures full encapsulation of pneumococcal bacteria by adjusting the number of Wzg molecules recruited to the division septum, which in turn tunes the pace of capsule attachment to match the rate of peptidoglycan synthesis. Impairing the encapsulation process, at localized subcellular sites, facilitates elimination of bacteria by strategies that target the pneumococcal peptidoglycan.

3.2 Introduction

Streptococcus pneumoniae is an important Gram-positive bacterial pathogen, which can colonize asymptomatically the nasopharynx of healthy individuals (Austrian, 1986) or spread to other sites of the human host, causing disease such as otitis media, pneumonia, or meningitis (Kadioglu et al., 2008). The presence of a capsule, a polysaccharide that, together with wall teichoic acids, covers the peptidoglycan (PGN) macromolecule at the bacterial cell surface (Vollmer et al., 2008), is crucial for the ability of pneumococcus to cause invasive disease, since less encapsulated or non-encapsulated strains are less virulent or avirulent (Magee et al., 2001; Hyams et al., 2010; Wu et al., 2016). The capsule surrounds the surface of bacteria and acts as a shield that confers protection against the host's immune system (Abeyta, Hardy and Yother, 2003; Wartha et al., 2007; Winkelstein et al., 1981). A tight control of the

amount of capsular polysaccharide (CPS) expressed or linked to the cell surface is expected to occur during the infection process, as a thick capsule may be disadvantageous during the colonization stage of infection, by preventing the exposure of bacterial molecules required for surface adhesion (Kadioglu et al., 2008).

To date, more than one hundred capsular serotypes have been identified in pneumococcal bacteria (Geno et al., 2015; Calix et al., 2012; Ganaie et al., 2020). The genes encoding proteins involved in CPS synthesis and regulation are, in most cases, located in the same region of the *S. pneumoniae* chromosome: the *cps* operon (Bentley et al., 2006). Most proteins encoded within the *cps* operon are serotype specific including those involved in the assembly of the repeating CPS unit, responsible for the transport of the CPS repeating unit from the inner to the outer face of the plasma membrane, involved in the polymerization of different repeating units and in the assembly of a mature CPS. However, the proteins encoded by the first four genes at the 5' end of the *cps* operon are highly conserved between serotypes and are proposed to be involved in the regulation of CPS synthesis (Bentley et al., 2006). The first gene in the *cps* operon encodes Wzg, also known as CpsA, an enzyme that belongs to the LCP (**L**ytR – **C**ps2A – **P**sr) protein family. The pleiotropic phenotypes of LCP mutant strains of various species led to the initial characterization of these proteins as transcriptional regulators of cell wall processes (Lazarevic et al., 1992; Guidolin et al., 1994). However, a more recent study from Kawai and colleagues provided strong evidence that LCP proteins are in fact phosphotransferase enzymes implicated in anchoring anionic cell wall polymers, such as teichoic acids, and capsular polysaccharides, to peptidoglycan (Kawai et al., 2011). Moreover, crystallography studies by Eberhardt and colleagues support the proposed phosphotransferase activity for the serotype 2 Wzg protein (Eberhardt et al., 2012). Pneumococcal *wzg* mutant strains contain significantly less capsule material attached to the cell wall (Morona et al., 2006), while a *wzg-lytR* double mutant has strongly distorted morphology and retains much less capsule material compared with the single *wzg* mutant (Eberhardt et al., 2012). Recently, it was demonstrated that a *lytR* single mutant is impaired in the retention of both CPS and teichoic acids (Wu et al., 2018). Importantly, it seems that all three LCP homologs have semi-redundant roles in the attachment of CPS and teichoic acids precursor chains to peptidoglycan (Eberhardt et al., 2012).

Besides *wzg*, the conserved region of the *cps* operon contains *wzh*, *wzd*, and *wze*, which encode three proteins that are part of a phosphoregulatory system required to control the synthesis of the capsule and its attachment to the cell wall. Wze, also known as CpsD, is an autophosphorylating tyrosine kinase that belongs to the Bacterial Tyrosine Kinase family (Grangeasse et al., 2007). It has the conserved motifs characteristic of this protein family: a Walker A ATP binding motif and a C-terminal tyrosine cluster (Morona et al., 2000a). Wzd, also known as CpsC, is a membrane protein required for the autophosphorylation of Wze (Bender and Yother, 2001). Wzh, also known as CpsB, is a phosphotyrosine protein phosphatase of the PHP family that dephosphorylates Wze (Morona et al., 2002). For years, the role of tyrosine phosphorylation in capsular polysaccharide synthesis has been the subject of debate, with different reports presenting conflicting results, either supporting that Wze phosphorylation reduces capsule synthesis (Morona et al., 2000a) or that it positively regulates CPS synthesis (Bender et al., 2003; Weiser et al., 2001).

Previously, we identified a novel role for Wzd and Wze as spatial regulators of capsule synthesis (Henriques et al., 2011). Wzd and Wzae localize at the division septum in a manner that is dependent on the presence of both proteins, but independent of all other proteins encoded in the *cps* operon. In the absence of Wzd or Wze, capsule is synthesized and attached to the cell wall, but it is absent from the division septum, the site where cell wall synthesis occurs during division. Therefore, we proposed that Wzd and Wze function as spatial regulators of capsule synthesis, ensuring that it occurs at the division septum, possibly to conceal newly synthesized cell wall (Henriques et al., 2011). A second role for the Wzd/Wze complex is to recruit the polysaccharide polymerase Wzy to the division site (Nourikyan et al., 2015). This suggests that CPS is produced only at the division septum by a single machinery (Nourikyan et al., 2015). In a *wzd* or *wze* null mutant, capsule is absent from the septum, but present in the rest of the cell surface, probably due to the observed delocalization of the CPS synthesis machinery (Nourikyan et al., 2015). This shows that these mutants are still able to export and attach polysaccharides to the cell surface.

Currently, the model for regulation of *S. pneumoniae* capsular polysaccharide synthesis proposes that when non-phosphorylated Wze interacts with Wzd, both proteins localize to the division septum. Upon interaction with Wzd, Wze undergoes a conformational switch, promoting ATP binding and allowing autophosphorylation of its C-terminal tyrosine cluster. Wze can then be dephosphorylated by the phosphatase Wzh and the cyclic

phosphorylation/dephosphorylation of Wze could regulate the activity of the capsule assembly machinery. Likely, Wzd and Wze capture the CPS synthesis machinery at the division site and trigger CPS export by the flippase Wzx, followed by polymerization by Wzy and anchoring to the peptidoglycan mesh by the phosphotransferase Wzg (Nourikyan et al. 2015).

In this work, we wanted to determine the mechanism by which septal Wzd/Wze ensure CPS attachment to the septal cell wall. We demonstrate that this process is mediated by the recruitment of the Wzg ligase. When Wzg is not recruited to the division septum, there is an absence of septal CPS that results in bacteria with septal cell wall more exposed to external PGN hydrolases or host PGN receptors.

3.3 Materials and methods

3.3.1 Bacterial strains and growth conditions

Bacterial strains and plasmids used in this study are listed in Table 3.1. *Escherichia coli* bacteria were routinely grown in Luria Broth (LB) medium at 37ºC, unless otherwise indicated. When appropriate, ampicillin (100 µg/ml) or kanamycin (50 µg/ml) were added to the growth media. For bacterial two-hybrid assays, MacConkey agar medium (Difco) and Maltose 1% (w/v) (Difco) were used. *Streptococcus pneumoniae* bacteria were grown in liquid semi-defined C + Y medium (Lacks and Hotchkiss, 1960) at 37ºC, without aeration, or on tryptic soy agar (TSA, Difco) plates supplemented with 5% (v/v) sheep blood (ThermoScientific). When needed, tetracycline (1 µg/ml) was added to the growth media.

3.3.2 DNA manipulation procedures

E. coli and *S. pneumoniae* competent cells preparation and transformation were performed as previously described (Sambrook et al., 1989; Martin et al., 1995). PCR products and plasmid DNA were purified with Wizard® SV Gel and PCR Clean-up System and Wizard® Plus SV Minipreps, respectively (Promega). PCR fragments were amplified with Phusion High-Fidelity DNA polymerase (Finnzymes). Restriction enzymes used were acquired from New England Biolabs or from Fermentas. Primers used in this work are listed in Table 3.2.

Table 3.1: Bacterial strains and plasmids

Name	Relevant Characteristics	Source/Reference
Strains		
Escherichia coli		
DH5α	*recA endA1 gyrA96 thi-1 hsdR17 supE44 relA1* ϕ80 d*lacZ* M15	Gibco-BRL
BL21(DE3)	*F–ompT gal dcm lon hsdSB(rB-mB-) λ(DE3 [lacI lacUV5-T7 gene 1 ind1 sam7 nin5])*	Lab Stock
BTH101	Reporter strain for BTH system, *F- cya-99, araD139, galE15, galK16, rpsL1* (Str^r), *hsdR2, mcrA1, mcrB1*	(Karimova et al., 1998)
BCSRN001	DH5α transformed with pBCSRN001 (pET21aLytA-GFP)	This work.
Streptococcus pneumoniae		
ATCC6314	Encapsulated strain, serotype 14	American Type Culture Collection
R36A	Non-encapsulated laboratory strain	(Avery, 1944)
BCSMC001	ATCC6314Δ*cps*	(Henriques et al., 2011)
BCSMH001	ATCC6314Δ*wzd*	(Henriques et al., 2011)
BCSMH002	ATCC6314Δ*wze*	(Henriques et al., 2011)
BCSMH022	BCSMH001 transformed with pBCSMH007 (*wzd-citrine*)	(Henriques et al., 2011)
BCSMH036	R36A transformed with pBCSMH020 (*sfGFP*)	(Henriques et al., 2011)
BCSMH061	BCSMH001 transformed with pBCSMH064 (*wzdY39C-citrine*)	This work.
BCSMH062	BCSMH001 transformed with pBCSMH065 (*wzdV56A-citrine*)	This work.
BCSMH064	BCSMH001 transformed with pBCSMH066 (*wzdY82F-citrine*)	This work.
BCSMH065	BCSMH001 transformed with pBCSMH067 (*wzdV116A-citrine*)	This work.
BCSMH070	ATCC6314 transformed with pBCSMH070 (*wchA-CFP*)	This work.
BCSMH071	ATCC6314Δ*cps* transformed with pBCSMH070 (*wchA-CFP*)	This work.
BCSMH072	ATCC6314 transformed with pBCSMH071 (*iCFP-wzg*)	This work.
BCSMH073	ATCC6314Δ*cps* transformed with pBCSMH071 (*iCFP-wzg*)	This work.
BCSMH074	ATCC6314Δ*wze* transformed with pBCSMH071 (*iCFP-wzg*)	This work.
BCSMH075	ATCC6314Δ*wzd* transformed with pBCSMH071 (*iCFP-wzg*)	This work.

Name	Relevant Characteristics	Source/Reference
Strains		
BCSMH076	ATCC6314Δ*cps* transformed with pBCSMH072 (*iCFP-wzgwzd*)	This work.
BCSMH077	ATCC6314Δ*wzd* transformed with pBCSMH072 (*iCFP-wzgwzd*)	This work.
BCSJF005	ATCC6314 transformed with pBCSJF005 (*iGFP-wzg*)	This work.
BCSJF006	BCSMC001 transformed with pBCSJF005 (*iGFP-wzg*)	This work.
BCSJF007	BCSMH002 transformed with pBCSJF005 (*iGFP-wzg*)	This work.
BCSJF008	BCSMH001 transformed with pBCSJF005 (*iGFP-wzg*)	This work.
BCSJF009	BCSMC001 transformed with pBCSJF006 (*iGFP-wzgwzd*)	This work.
BCSJF010	BCSMH001 transformed with pBCSJF006 (*iGFP-wzgwzd*)	This work.
BCSJF011	BCSMH001 transformed with pBCSJF007 (*iGFP-wzgwzdV56A*)	This work.
BCSJF012	BCSMH001 transformed with pBCSJF008 (*iGFP-wzgwzdY82F*)	This work.
BCSJC048	BCSMH036 transformed with pBCSJC044 (*lytA-GFP*)	This work.
Name	**Relevant Characteristics**	**Source/Reference**
Plasmids		
Plasmids for protein purification		
pET21a	T7p, T7t, His-Tag, lacI, Amp^r	Lab Stock
pBCSRN001	pET21a allowing expression of LytA-GFP, Amp^r	This work.
Plasmids for bacterial two-hybrid assay		
pUT18C	BTH plasmid, N-terminal *cyaA*T18 fusion, Amp^r.	(Karimova et al., 1998)
pUT18	BTH plasmid, C-terminal *cyaA*T18 fusion, Amp^r.	(Karimova et al., 1998)
pKT25	BTH plasmid, N-terminal *cyaA*T25 fusion, Kan^r.	(Karimova et al., 1998)
pKNT25	BTH plasmid, C-terminal *cyaA*T25 fusion, Kan^r.	(Karimova et al., 1998)
pKT25zip	BTH control plasmid, Kan^r.	(Karimova et al., 1998)
pUT18Czip	BTH control plasmid, Amp^r.	(Karimova et al., 1998)
pBCSMC001	BTH plasmid containing *cyaA*T25-*wzd* fusion.	(Henriques et al., 2011)
pBCSMC002	BTH plasmid containing *cyaA*T18-*wze* fusion.	(Henriques et al., 2011)

Name	Relevant Characteristics	Source/Reference
Plasmids		
pBCSMC005	BTH plasmid containing *cyaA*T18-*wzd* fusion.	This work.
pBCSMC006	BTH plasmid containing *wze-cyaA*T18 fusion.	This work.
pBCSMC007	BTH plasmid containing *wzd-cyaA*T25 fusion.	This work.
pBCSMC008	BTH plasmid containing *cyaA*T25-*wze* fusion.	This work.
pBCSMC009	BTH plasmid containing *wze-cyaA*T25 fusion.	This work.
pBCSMH040	BTH plasmid containing *wzd-cyaA*T18 fusion.	This work.
pBCSMH049	BTH plasmid containing *cyaA*T18-*wzg* fusion.	This work.
pBCSMH050	BTH plasmid containing *wzg-cyaA*T18 fusion.	This work.
pBCSMH051	BTH plasmid containing *cyaA*T25-*wzg* fusion.	This work.
pBCSMH052	BTH plasmid containing *wzg-cyaA*T25 fusion.	This work.
pBCSMH053	BTH plasmid containing *cyaA*T18-*wchA*fusion.	This work.
pBCSMH054	BTH plasmid containing *wchA-cyaA*T18 fusion.	This work.
pBCSMH062	BTH plasmid containing *wzdV56A-cyaA*T18 fusion.	This work.
pBCSMH063	BTH plasmid containing *wzdY82F-cyaA*T18 fusion.	This work.
pBCSJF009	BTH plasmid containing *cyaA*T25-*wchA* fusion.	This work.
pBCSJF010	BTH plasmid containing *wchA-cyaA*T25 fusion.	This work.
Replicative plasmids in *S. pneumoniae*		
pBCSLF001	High-copy-number vector, contains the -10 constitutive promoter of *SigA* from *S. pneumoniae*, Tet^r	(Henriques et al., 2011)
pBCSMH002	Allows expression of Citrine fusion proteins, Tet^r.	(Henriques et al., 2011)
pBCSMH007	pBCSMH002 containing *wzd-citrine*, Tet^r.	(Henriques et al., 2011)
pBCSMH018	Allows expression of CFP fusion proteins, Tet^r.	(Henriques et al., 2013)
pBCSMH020	pBCSLF001 derivative, allows expression of sfGFP fusion proteins, Tet^r.	(Henriques et al., 2011)
pBCSMH031	Allows expression of CFP containing the first 10 aa of Wze at its N-terminus, Tet^r.	(Henriques et al., 2013)
pBCSMH032	Expression of sfGFP containing the first 10 aa of Wze at its N-terminus, Tet^r.	(Henriques et al., 2013)
pBCSMH064	pBCSMH002 containing *wzdY39C-citrine*, Tet^r.	This work.
pBCSMH065	pBCSMH002 containing *wzdV56A-citrine*, Tet^r.	This work.
pBCSMH066	pBCSMH002 containing *wzdY82F-citrine*, Tet^r.	This work.
pBCSMH067	pBCSMH002 containing *wzdV116A-citrine*, Tet^r.	This work.

Name	Relevant Characteristics	Source/Reference
Plasmids		
pBCSMH070	pBCSMH018 containing *wchA-CFP*, Tet^r.	This work.
pBCSMH071	pBCSMH031 containing *iCFP-wzg*, Tet^r.	This work.
pBCSMH072	pBCSMH031 containing *iCFP-wzgwzd*, Tet^r.	This work.
pBCSJF005	pBCSMH032 containing *iGFP-wzg*, Tet^r.	This work.
pBCSJF006	pBCSMH032 containing *iGFP-wzgwzd*, Tet^r.	This work.
pBCSJF007	pBCSMH032 containing *iGFP-wzgwzdV56A*, Tet^r.	This work.
pBCSJF008	pBCSMH032 containing *iGFP-wzgwzdY82F*, Tet^r.	This work.
pBCSJC044	pBCSMH020 containing *lytA-GFP*, Tet^r.	This work.

Table 3.2: Primers used in this work.

Primer	Sequence 5'→3'	Restriction Site
1	CGGGATCCCGGAGAAAATATGAAGG	BamHI
2	GGAATTCCCCTCTCTCCTATTTC	EcoRI
3	CTAGTCTAGAGATGAAGGAACAAAACACTTTGG	XbaI
4	CGCGGATCCCCTTTCAACTTACTCAAGTTTGG	BamHI
5	CGGGATCCTAAGGAGGAAATATGA	BamHI
6	GGAATTCCATTTCAACTTACTCAAG	EcoRI
7	CGGGATCCTAGGAGGGAGGAATGCCG	BamHI
8	GGAATTCCATTTTTTACCATAATTTCC	EcoRI
9	CGGGATCCAATGCCGACATTAGA	BamHI
10	GGAATTCCCCTAAGTTATTTTTTACC	EcoRI
11	CGCGGATCCAATGAGTAGACGTTTTAAAAAATCACG	BamHI
12	CCGGAATTCTCATCTACCCTCCATCACATCC	EcoRI
13	CCGGAATTCTTTCTACCCTCCATCACATCC	EcoRI
14	AACTGCAGAATGGATAAAAAAGGATTGG	PstI
15	CGCGGATCCTTACTTCGCTCCATTTCTC	BamHI
16	CGCGGATCCTTCTTCGCTCCATTTCTC	BamHI
17	GGCTGCAGAGATGGATAAAAAAGGATTGG	PstI
18	CGCGGATCCTTACTTCGCTCCATTTCTC	BamHI

Primer	Sequence 5′→3′	Restriction Site
19	AACTGCAGAATGGATAAAAAAGGATTGG	PstI
20	CGCGGATCCTTCTTCGCTCCATTTCTC	BamHI
21	CTAGCTAGCATGAAGGAACAAAACACTTTGG	NheI
22	GTACTGCAGGCAAAAGC	Mutation Y→C
23	GCTTTTGCCTGCAGTAC	Mutation Y→C
24	GGGGTACCTTTCAACTTACTCAAG	KpnI
25	CGGTTAACTGCATAAATCCG	Mutation V→A
26	CGGATTTATGCAGTTAACCG	Mutation V→A
27	GATAATTTCACGAAAGTCTTTAAC	Mutation Y→F
28	GTTAAAGACTTTCGTGAAATTATC	Mutation Y→F
29	GTATCAACTGGTGCTGTTAC	Mutation V→A
30	GTAACAGCACCAGTTGATAC	Mutation V→A
31	ATAAGAATGCGGCCGCAATGAGTAGACGTTTTAAAAAATCACG	NotI
32	GAAGATCTTCATCTACCCTCCATCACATCC	BglII
33	GGAAGATCTTAAGGAGGTGCTGCGGCCATGAAGGAACAAAACAC	BglII; RBS
34	GAAGGCCTCTATTTCAACTTACTCAAG	StuI
35	CTAGCTAGCATGGATAAAAAAGGATTGG	NheI
36	CGCGCCGGCCTTCGCTCCATTTCTCATAAATAC	NaeI
37	GGCGCTAGCATGGAAATTAATGTGAGTAAATTAAG	NheI
38	GCGGTACCTTTTACTGTAATCAAGCCATC	KpnI
39	GCGGGATCCATGGAAATTAATGTGAGTAAATTAAG	BamHI
40	GCGCTCGAGGTCGACTTTGTATAGTTCATC	XhoI

3.3.3 Construction of plasmids for Bacterial two-hybrid assays

Plasmids to test Wzd and Wze interactions with other capsule proteins, were constructed using inserts amplified from ATCC6314 chromosomal DNA, unless otherwise indicated. Plasmids pBCSMC005, pBCSMH040 and pBCSMC007, encoding fusion proteins T18-Wzd, Wzd-T18 and Wzd-T25, were constructed by amplification of *wzd* with primers 1/2, 3/4 and 5/6, respectively, followed by restriction and ligation into plasmids pUT18C, pUT18 and pKNT25. Plasmids pBCSMC006 and pBCSMC009, encoding fusions Wze-T18 and Wze-T25

were constructed by amplification of *wze* with primers 7/8, followed by restriction and ligation into pUT18 and pKNT25, respectively. Plasmid pBCSMC008, encoding fusion T25-Wze, was obtained by amplification of *wze* with primers 9/10 and cloning into pKT25. Plasmids pBCSMH049 and pBCSMH051, encoding T18-Wzg and T25-Wzg, were constructed by amplification of *wzg* with primers 11/12, restriction and ligation into pUT18C and pKT25. Amplification of *wzg* with primers 11/13, restriction and ligation into pUT18 and pKNT25 produced plasmids pBCSMH050 and pBCSMH052, encoding the fusions Wzg-T18 and Wzg-T25, respectively. Plasmids pBCSMH053 and pBCSMH054, encoding T18-WchA and WchA-T18, were constructed by amplification of *wchA* with primer pairs 14/15 and 14/16, followed by restriction and ligation into pUT18C and pUT18, respectively. Plasmids pBCSJF009 and pBCSJF010, encoding fusions T25-WchA and WchA-T25 were constructed by amplification of *wchA* with primer pairs 17/18 and 19/20, respectively, restriction and ligation into pKT25 and pKNT25. Plasmids pBCSMH062 and pBCSMH063, encoding fusions WzdV56A-T18 and WzdY82F-T18, were constructed using primers 3/4 to amplify the mutated *wzd* genes from plasmids pBCSMH064 and pBCSMH066, respectively, followed by restriction and ligation into pUT18. The nucleotide sequences of the inserts of the constructed plasmids were confirmed by sequencing.

3.3.4 Bacterial two-hybrid assays

Bacterial Two-hybrid assays were done in *E. coli* strain BTH101. Transformants with plasmids mentioned above were plated in MacConkey media, supplemented with ampicillin, kanamycin, and maltose. Plates were incubated at 30ºC and screened for pink/white colonies, in which pink indicated a positive interaction. Single colonies were grown at 30ºC in the presence of 0.5 mM of IPTG and the interactions confirmed by β-galactosidase activity measurements as described (Karimova et al., 2005). Part of these cultures (3 µl) were also used to spot fresh plates to visualize differences in the color of the bacterial lawn. Representative images of the bacterial lawn obtained after spotting fresh mannitol plates were acquired on different days and light conditions.

3.3.5 Construction of plasmids for protein expression in S. pneumoniae

To determine the localization of Wzd proteins containing the point mutations Y39C, V56A, Y82F and V116A, plasmids expressing Citrine C-terminal fusions of the mutated proteins were constructed. The mutated *wzd* genes were amplified in two different fragments using primers 21/22 and 23/24 for *wzdY39C*; 21/25 and 26/24 for *wzdV56A*; 21/27 and 28/24 for *wzdY82F*; 21/29 and 30/24 for *wzdV116A*. In each case, the two fragments were joined by overlapping PCR using primers 21/24 and cloned in pBCSMH002, producing plasmids pBCSMH064-067. Plasmid pBCSJF005, encoding a fluorescent derivative of Wzg, was constructed by amplification of *wzg* from the ATCC6314 chromosomal DNA with primers 31/32, restriction and ligation into pBCSMH032. Plasmids pBCSJF006-008 were constructed by amplification of *wzd*, *wzdV56A* and *wzdY82F*, respectively, with primers 33/34 using plasmids pBCSMH007, pBCSMH065 and pBCSMH066 as templates, restriction and ligation into pBCSJF005. In the resulting plasmids, the protein fusion iGFP-Wzg is expressed in the presence of Wzd, WzdV56A or WzdY82F. CFP fluorescent derivatives of Wzg were expressed through the construction of plasmid pBCSMH071 by amplification of *wzg* from the ATCC6314 chromosomal DNA with primers 31/32, restriction and ligation into pBCSMH031. Amplification of *wzd* with primers 33/34 using plasmid pBCSMH007 as template, restriction, and ligation into pBCSMH071 produced plasmids pBCSMH072. In this plasmid, the protein fusion iCFP-Wzg is expressed in the presence of Wzd. Plasmid pBCSMH070, was constructed by amplification of *wchA* from the ATCC6314 chromosomal DNA with primers 35/36, restriction and ligation into pBCSMH018. Plasmid pBCSJC044, encoding a LytA fluorescent derivatives, was constructed by amplification of *lytA* with primers 37/38, restriction and ligation into pBCSMH020. The nucleotide sequences of the inserts of the constructed plasmids were confirmed by sequencing.

3.3.6 Construction of plasmids for protein expression in E. coli

To express in *E. coli* and purify the protein LytA-GFP, amplification of *lytA-GFP* was done using primers 39 and 40 and the plasmid pBCSJC044 as template. Restriction and ligation into pET21a, produced plasmid pBCSRN001.

3.3.7 Protein purification

The protocol for the purification of *S. pneumoniae* LytA-GFP was adapted from (García et al., 1987). Briefly, *E. coli* BL21(DE3) cells were transformed with the plasmid pBCSRN001 and incubated overnight at 37°C, with vigorous shaking, in LB supplemented with 100 μg/ml ampicillin and 2% lactose. Cells were harvested by centrifugation, resuspended in 20 mM sodium phosphate buffer, pH 6.9, and broken by sonication. Clarified lysate was applied to DEAE-cellulose resin (DEAE Sephacel™, GE Healthcare) and incubated at 4°C for 1 h with stirring. Bound protein was washed five times with 20 mM sodium phosphate buffer containing 1.5 M NaCl, then eluted in the same buffer containing 2% choline. Protein was dialyzed against 20 mM sodium phosphate buffer, pH 6.9 to remove the salts and aliquots were stored at 4°C.

3.3.8 Lysis assays

For lysis assays, encapsulated ATCC6314, its capsule null mutant (BCSMC001) and the *wzd* null mutant (BCSMH001) strains were grown O/N in 50ml of C+Y until $OD_{(600nm)}$~0.9, centrifuged, washed once with fresh C+Y medium, resuspended in 50 ml, and placed for 20 minutes in an ice bath. Cell suspensions were added to boiling water, at a flow that did not stop boiling, and further boiled for 40 minutes. Cell suspensions were then diluted to $OD_{(600nm)}$~1 and divided in two tubes, one of which received purified LytA-GFP at a final concentration of 6,75 μg/ml. $OD_{(600nm)}$ was followed in a Cary 100 UV-Vis Spectrophotometer (Agilent) using 10x10 mm cuvettes (Sarstedt) containing 3ml of culture, with a sterile gauze lid and a cuvette-adapted stirring bar (VWR) to allow continuous slow stirring. Lysis was followed by the decrease in $OD_{(600nm)}$ measured every 5 minutes for 150 minutes.

3.3.9 Growth assays

S. pneumoniae cells were grown O/N at 37ºC without aeration in liquid semi-defined C + Y medium. When stationary phase was reached, at an $OD_{(600nm)}$~0.8, cultures were diluted to $OD_{(600nm)}$~0.05. The $OD_{(600nm)}$ was measured every 30 minutes until $OD_{(600nm)}$~0.2 and then

every 15 minutes. Absorbance values obtained during exponential growth were selected and used to determine duplication times (presented as a median value and n=10).

3.3.10 Dot blot assays

Cell samples were prepared by harvesting cells at exponential growth-phase ($OD_{(600nm)}$ ~ 0.5) and resuspending them in water. After adjusting the samples to same cell density, cells were lysed with deoxycholate and boiled for 3 min before use. Samples were loaded into Nitrocellulose (Amersham) membranes, pre-equilibrated in PBS and placed on top of PBS-soaked Hybond Blotting Paper. 3µl of each sample was loaded in triplicates and the membranes were allowed to air-dry for 30 min, and then blocked during 1 h in Blocking Buffer (5% non-fat dried milk in PBS). Membranes were washed in PBS-T (PBS + 0.05% Tween 20) and incubated overnight at 4°C with primary antibody Anti-CPS14 diluted 3/1000 in PBS-T, purified as previously described (Xayarath and Yother, 2007; Henriques et al., 2011). After washing with PBS-T, membranes were incubated during 1 h at room temperature with secondary antibody Anti-Rabbit StarBright Blue 700 (BioRad) diluted 1/5000 in PBS-T. Membranes were again washed with PBS-T and detected using the iBright FL1500 Imaging System.

3.3.11 Microscopy

S. pneumoniae strains were grown until early exponential phase and observed by fluorescence microscopy on a thin layer of 1% agarose in PreC medium (Lacks and Hotchkiss, 1960). Images were acquired in a Zeiss Axio Observer microscope, equipped with a Photometrics CoolSNAP HQ2 camera (Roper Scientific), with appropriate exposure times (500-1000 ms for GFP; 5000 ms for Citrine and CFP; 100 ms for AlexaFluor secondary antibody), and analyzed using FIJI software (Schindelin et al., 2012) as well as eHooke software (Saraiva et al., 2021), which was developed in-house.

Determination of the fluorescence ratio (FR) was performed as previously described (Pereira et al., 2007). Briefly, the intensity of the fluorescent signal at the division septum was

divided by the fluorescent signal at the peripheral membrane. Average background fluorescence was subtracted from every value. An FR value higher than 2 is indicative of septal enrichment. Quantification was performed for at least 100 cells of each strain.

In vivo detection of the capsule produced at the surface of *S. pneumoniae* cells was performed as previously described (Henriques et al., 2011), but Anti-rabbit Alexa Fluor 594 antibody (Invitrogen) was used as a secondary antibody. When necessary LytA-GFP purified protein was added to the media at 5 μg/ml concentration and incubated for 10 min at 37ºC.

3.3.12 Infection assays using zebrafish embryos

Wild-type AB zebrafish were obtained from the Zebrafish International Resource Center (Eugene). Embryos were raised at 28°C in E3 medium. Larvae were anaesthetized with 200 μg/ml tricaine (Sigma) for the injection procedure. For injection of zebrafish larvae, cells were grown at 37ºC without aeration in liquid semi-defined C + Y medium, harvested (1 ml) at exponential growth ($OD_{(600nm)}$~0.6), washed with fresh C+Y medium and resuspended in 100 μl of C+Y medium. A 70 kDa rhodamine dextran (Invitrogen/Molecular Probes) tracer was added in a proportion of 1:1 just before injection. Anaesthetized zebrafish larvae, 3 days post-fertilization (dpf), were microinjected in the hindbrain ventricle with 0.5–2 nl of bacterial suspension (Mostowy et al., 2013), so that a group of 12 embryos for each bacterial strain were injected with the same glass microcapillary needle filled with bacterial suspension. This experiment was repeated four times. Bacterial load upon infection was determined by plating at least three alive larvae onto TSA 5% blood agar before and 2 hours post-injection, which confirmed that the number of bacteria injected for each strain were very similar. Each larvae was collected into an Eppendorf with 200 μl of lysis solution and then were mechanically smashed, dilutions in C+Y were plated. Infected larvae were transferred into individual wells (containing 1 ml of E3 in 24 well plates), incubated at 30°C and regularly observed under a stereomicroscope (Rounioja et al., 2012).

3.3.13 Statistical analysis

Statistical analyses of data presented in the figures were done using GraphPad Prism 8 software (GraphPad Software).

Analysis of data of the beta-galactosidase activity presented in Figures 3.1, 3.3, 3.5 and Supplementary Figure 3.2; of the Fluorescence ratios (FR) presented in Figures 3.2, 3.5, 3.7, and Supplementary Figures 3.3 and 3.4 and of the Area of bacteria in Supplementary Figure 3.6 was done using a Mann-Whitney Test. Results are available in Supplementary Table 3.1. P values ≤ 0.05 were considered as significant for all analysis performed and are indicated with asterisks: *P ≤ 0.05, **P ≤ 0.01, ***P ≤ 0.001 and ****P ≤ 0.0001.

Survival rates of the zebrafish embryos in the experiments reported in Figure 3.8, were also analyzed with the Graph Pad Prism 8 software. The statistical significance in these assays was measured using the Log-rank (Mantel-Cox) test. p values of <0.05 were considered significant.

3.4 Results

3.4.1 The CPS-cell wall ligase Wzg interacts with Wzd

We have previously found that Wzd and Wze act as spatial regulators of the *S. pneumoniae* capsule synthesis, to ensure that capsule is present at midcell, at the newly produced cell surface (Henriques et al., 2011). However, the mechanism mediating this regulation has remained unclear. We hypothesized that the Wzd/Wze complex either activates or recruits particular proteins of the CPS machinery synthesis to the division site (Henriques et al., 2011). We have now used a Bacterial Two-Hybrid (BTH) assay to screen for possible interactions between Wzd or Wze proteins from *S. pneumoniae* ATCC6314 strain, which produces a serotype 14 capsular polysaccharide, and two candidate proteins that could have a role in the control of the total amount of capsule present at the bacterial surface: WchA, the glycosyl transferase that links the first glucose residue of the capsule repeating unit to the lipid anchor present in the membrane of pneumococci (Kolkman et al., 1997a); and Wzg, the putative CPS-cell wall ligase that links assembled capsule molecules, which have been exported across the bacterial membrane but are still linked to a lipid anchor, to the

peptidoglycan macromolecule, preventing the release of capsule to the surrounding medium (Kawai et al., 2011). An interaction was found only between Wzd and Wzg (Figure 3.1, column 18), which was dependent on the T25/T18 tag that was linked to the interacting proteins (Figure 3.1, column 12), while no interactions were found between Wzd/Wze and WchA. Wzg interactions were observed when the T25-tag was fused to the N-terminal of the protein (Figure 3.1), but not when it was fused to the C-terminal (Supplementary Figure 3.1). Wzg was also found to interact with itself (Figure 3.1, column 23). In accordance with what has been previously reported (Henriques et al., 2011), we were also able to detect an interaction between Wzd and Wze (Figure 3.1, columns 3-4 and 10-11).

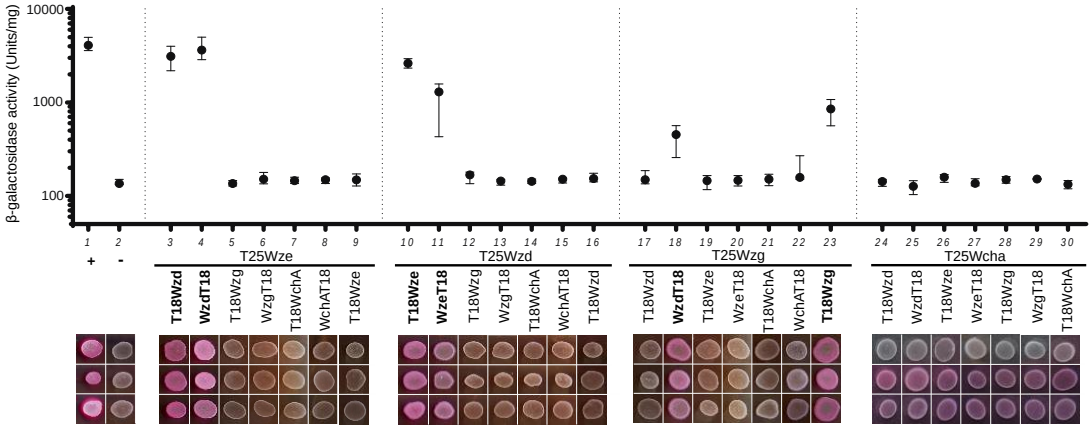

Figure 3.1: Wzg, a putative CPS-cell wall ligase, interacts with Wzd and with itself. Interactions between Wze, Wzd, Wzg and WchA were tested using Bacterial Two-Hybrid *E. coli* system. β-galactosidase activity of cells expressing putative interaction partners was measured in cell extracts in at least three independent replicates. Black circles indicate median values and brackets show the 25% and 75% percentiles. Representative images of the bacterial lawn obtained after spotting a liquid culture of *E. coli* cells expressing putative interacting partners in fresh mannitol plates are shown below each measurement. Positive control (+): *E. coli* expressing T18 and T25 fragments linked to leucine zipper domains that can dimerize; Negative control (-): *E. coli* expressing untagged T18 and T25 fragments. Interactions were detected between T25-Wzg/Wzd-T18 and T25-Wzg/T18-Wzg. As previously described (Henriques et al. 2011) combinations of plasmids expressing Wzd and Wze indicate that these proteins interact.

3.4.2 Wzg septal localization is dependent on the presence of Wzd/Wze proteins

Given that Wzg interacted with Wzd in the BTH assay, and that Wzd has been shown to localize at the septum of encapsulated *S. pneumoniae* cells (Henriques et al., 2011), we decided to determine whether the septal localization of Wzg in dividing pneumococcal bacteria (Eberhardt et al., 2012) was dependent on the expression, or localization, of Wzd. For that, we constructed pneumococcal strains expressing a N-terminal fusion of Wzg linked to iGFP, an improved version of GFP for in vivo localization of proteins in *S. pneumoniae* (Henriques et al., 2013). A pneumococcal plasmid expressing iGFP-Wzg was transformed into the wild-type ATCC6314 encapsulated strain (generating strain BCSJF005), into its unencapsulated isogenic strain that lacks the entire *cps* operon (generating strain BCSJF006), into the ATCC6314 *wze* null mutant in which Wzd is unable to localize at the septum, (Henriques et al., 2011) (generating strain BCSJF007), and into the ATCC6314 *wzd* null mutant (generating strain BCSMH008). When the resulting strains were observed by fluorescence microscopy, the fluorescent signal from iGFP-Wzg was found to be more enriched at the septal region of cells from the encapsulated strain (BCSJF005), than in cells from the unencapsulated strain or from the *wze* and *wzd* null mutant strains (Figure 3.2). In these, iGFP-Wzg was spread throughout the cell membrane, in accordance with the presence of three predicted transmembrane spanning domains in Wzg protein (Hübscher et al., 2008). A quantitative analysis of these results was done by determining the ratio of the fluorescence signal at the septum versus the peripheral membrane (FR), as described in the Materials and Methods section. Notice that the septum contains two membranes, so only FR values higher than ~2 indicate preferential septal localization (Pereira et al., 2007; Atilano et al., 2010). The encapsulated strain had a median FR value of 2.4, while strains lacking the *cps* operon, or the *wze* or *wzd* genes, had median FR values below 2 (1.6, 1.5 and 1.4, respectively, Figure 3.2), suggesting that Wzd is required for septal localization of Wzg. In agreement, complementation of the *wzd* null mutant with plasmid encoded Wzd (strain BCSJF010) caused an increase in recruitment of Wzg to the septum (median FR value of 2.0, Figure 3.2). It is possible that full complementation was not achieved because Wzd in the plasmid is under the control of a constitutive promoter, instead of the *cps* promoter. Septal enrichment of Wzg was not recovered upon complementation of the unencapsulated strain BCSJF009 with plasmid encoded Wzd (median FR value of 1.5, Figure

3.2). In this strain Wzd is present but it is delocalized due to the absence of Wze (Henriques et al., 2011). Therefore, septal Wzd appears to be required for the recruitment of Wzg to the septum, as expected if a physical interaction between the two proteins was responsible for Wzg localization. Similar data was obtained using a CFP fusion to Wzg (Supplementary Figure 3.2) showing that septal Wzg enrichment is independent of the fluorescent tag used.

In contrast to Wzg, WchA localization does not show septal enrichment, as expression of WchA-CFP in an encapsulated or a non-encapsulated strain resulted in bacteria with a fluorescence signal dispersed throughout the membrane (Supplementary Figure 3.3).

Together, these results indicate that Wzg localizes at the division septum of pneumococcal cells, in a process that requires the correct expression and septal localization of Wzd/Wze.

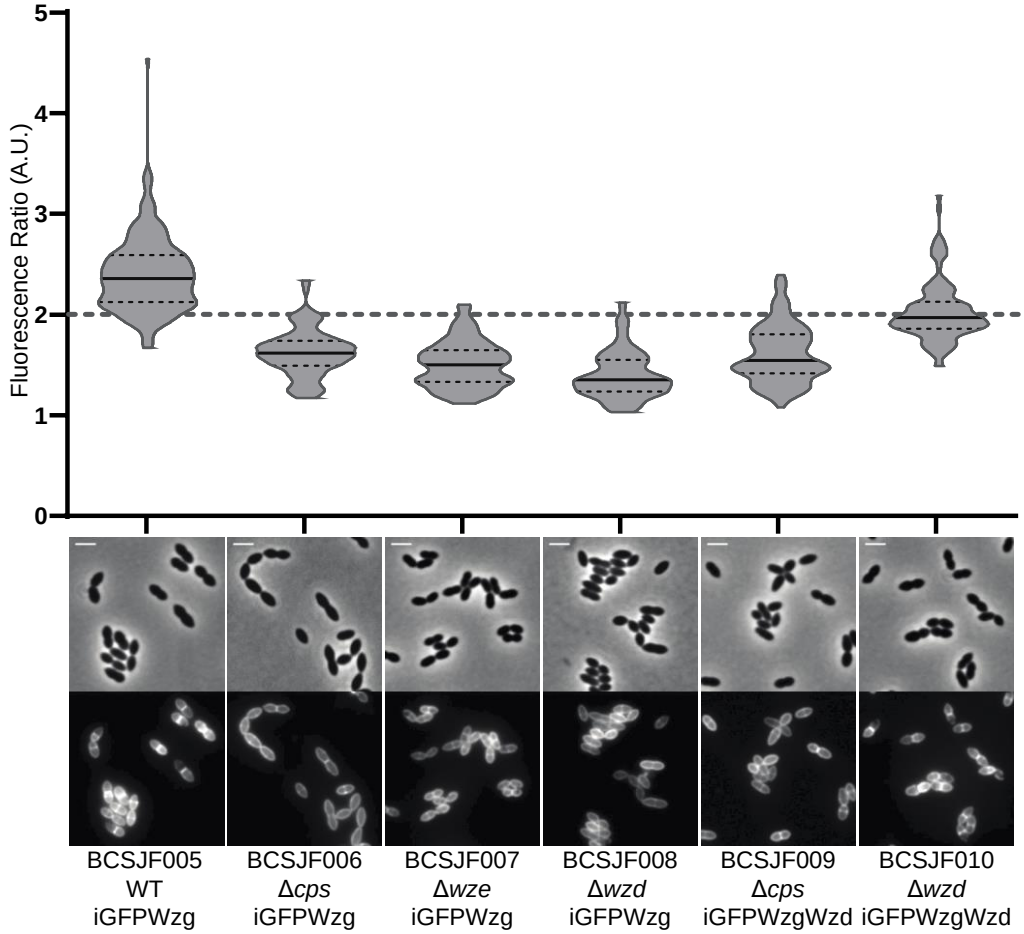

Figure 3.2: Septal localization of Wzg is dependent on the expression of Wzd/Wze. Graph shows the ratio of iGFP-Wzg fluorescence measured at the septum versus the peripheral wall in the *S. pneumoniae* wild-type encapsulated strain (BCSJF005, n=194), in the capsule null mutant (BCSJF006, n=121), in the *wze* null mutant (BCSJF007, n=106), in the *wzd* null mutant (BCSJF008, n=107) and in the *cps* and *wzd* null mutants expressing Wzd from a constitutive promoter (BCSJF009, n=112, and BCSJF010, n=109, respectively). Enrichment of Wzg at the septum is only observed when Wzd is expressed and is localized at the division septum. Solid lines indicate median, and dashed lines indicate 25% and 75% percentiles. Representative phase contrast and fluorescence microscopy images of each strain are shown below the graph. Scale bar, 2 μm.

3.4.3 The transmembrane and DNA-PPF domains of Wzg are required for its interaction with the membrane protein Wzd and with itself

Wzg is constituted by a small intracellular domain at its N-terminus, followed by three membrane spanning domains and a large extracellular C-terminal domain (Figure 3.3A). This large extracellular protein region contains an accessory domain, named DNA-PPF, present in some proteins of the LCP family, and the LytR-CpsA-PsR domain (Figure 3.3A), considered to be the core catalytic domain, present in all proteins of this family (Hübscher et al., 2008). To determine which regions are involved in Wzg interactions, we used again a BTH assay. For this purpose, 6 different fragments of Wzg, shown in Figure 3.3A, were tested, showing that the transmembrane domain and the first 120 amino acids of the extracellular domain (containing the accessory DNA-PPF domain), are required for self-interaction of Wzg monomers (Figure 3.3B, see columns 8/9 and 14/15) and for the interaction between Wzg and Wzd (Figure 3.3B, see columns 21 and 22). These results suggest that Wzd recruits Wzg to the pneumococcal division septum through interaction with the membrane anchored accessory DNA-PPF domain.

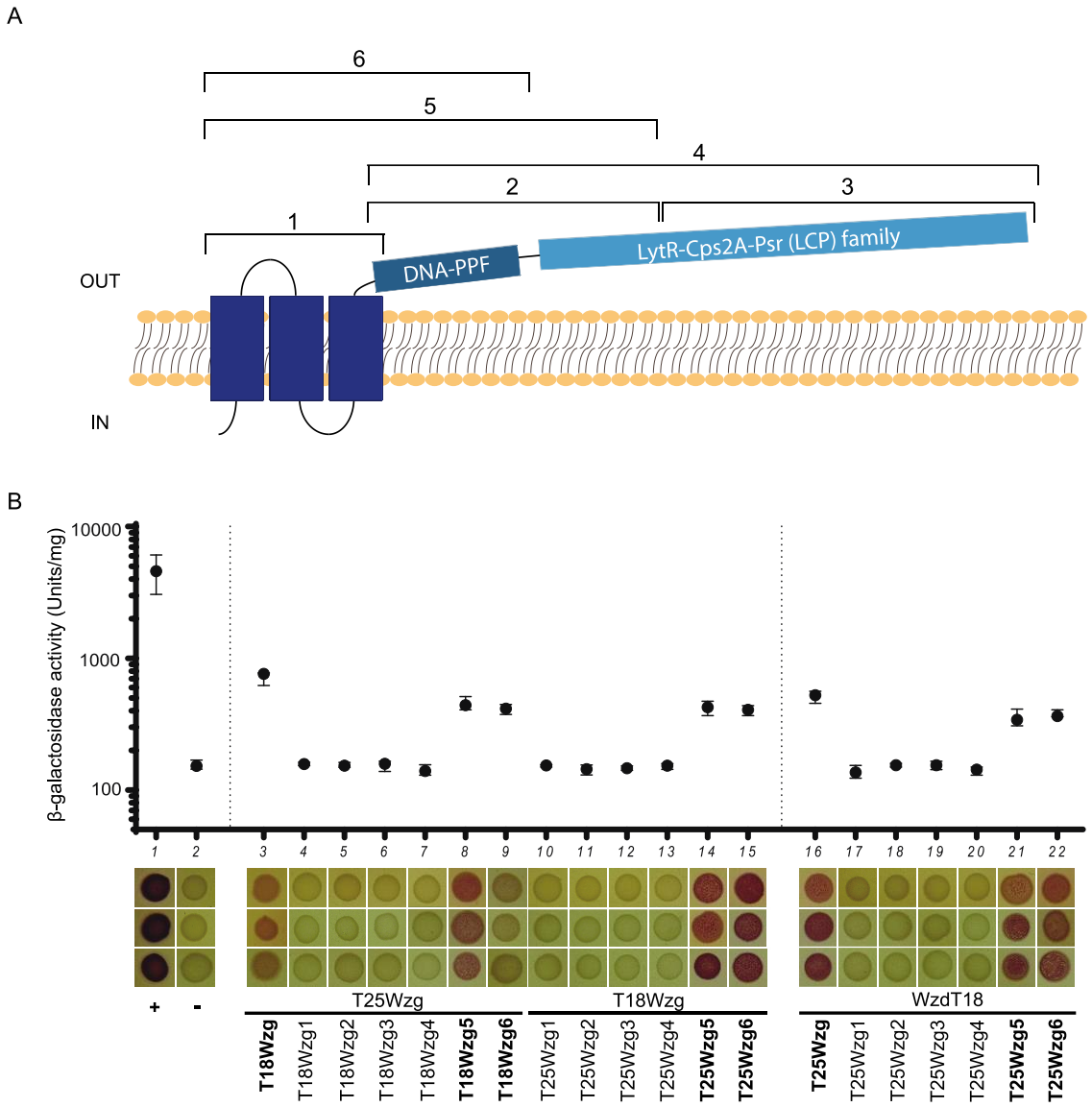

Figure 3.3: The transmembrane and DNA-PPF domains of Wzg are required for its self-interaction and interaction with Wzd. A) Scheme indicating the 6 different regions of Wzg tested for interaction with Wzd by BTH. **B)** Interactions between Wzg and the Wzg1-6 constructs were analyzed by BTH. Black circles indicate median values and brackets show the 25% and 75% percentiles of β-galactosidase activity measured in cell extracts of at least three independent replicates. Representative images of the bacterial lawn obtained after spotting fresh mannitol plates with a liquid culture of *E. coli* cells expressing putative interacting partners are shown below each measurement. Positive control (+): *E. coli* expressing T18 and T25 fragments linked to leucine zipper domains that can dimerize; Negative control (-): *E. coli* expressing untagged T18 and T25 fragments. Only the Wzg5 and Wzg6 constructs, which include the three transmembrane domains and the DNA-PPF domain, interact with full-length Wzg and with Wzd.

3.4.4 Wzd V56 residue is critical for interaction with, and septal recruitment of, Wzg

Having determined the region of the Wzg ligase required for interaction with Wzd, we then enquired which region of the Wzd regulator was involved in this interaction.

Morona and colleagues have previously described that specific point mutations in Wzd, when in the presence of a mutated Wzh phosphatase, are associated with deficient attachment of capsular polysaccharide (CPS) to the cell wall (Morona et al., 2006). Mutants bearing these alterations present a mucoid phenotype, in which total CPS levels are similar to the wild-type strain, but levels of CPS attached to the cell wall are much lower (Morona et al., 2006). These observations indicate that the specific residues that were identified are important for the ligation of CPS to the cell wall, but how this takes place has remained elusive. We hypothesized that these residues could be involved in Wzd interaction with the Wzg ligase. To test this hypothesis, and as the reported mucoid mutants carried other mutations beside those reported in Wzd, we first tested whether four of the reported mutations, namely Y39C, V56A, Y82F and V116A (Morona et al., 2006), impaired expression, or septal localization, of Wzd. All these residues are located in the extracellular loop of Wzd (Figure 3.4A), which could be responsible for its interaction with and recruitment of Wzg. We therefore expressed fluorescent derivatives of the four Wzd mutant alleles in a *wzd* null mutant and determined their septal localization by fluorescence microscopy (Figure 3.4B). The ability of a mutated Wzd to localize at the division septum indicates that the protein is able to interact with Wze and may still regulate the synthesis of the pneumococcal CPS synthesis. The Y39C mutation likely affects expression or stability of the Wzd protein, as no fluorescent cells were observed in the strain expressing WzdY39C. The V116A mutation impaired correct localization of Wzd at the septum, which became spread throughout the entire cell membrane. This mislocalization could be due to lack of interaction with Wze, which is required for septal localization of Wzd. In contrast, mutations V56A and Y82F did not impair correct septal Wzd localization (Figure 3.4B). We then asked whether WzdV56A and WzdY82F mutants were altered in their ability to interact with Wzg and to recruit the capsule ligase to the division septum of pneumococci.

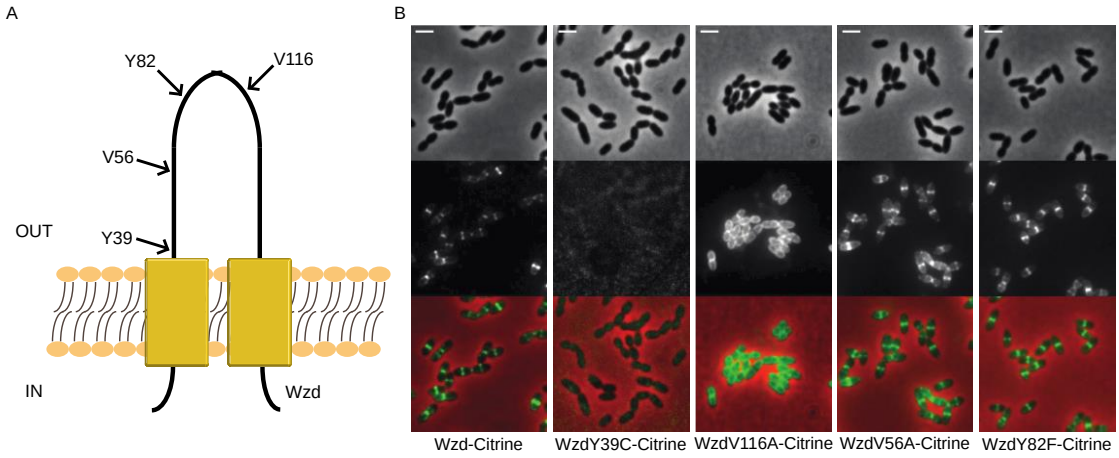

Figure 3.4: Point mutations in Wzd affect its localization. A) Scheme of Wzd protein indicating the localization, in the extracellular loop, of four mutations that were associated with a mucoid colony phenotype (Morona, Morona and Paton, 2006). **B)** Localization of Citrine fluorescent derivatives of Wzd single-residue mutants expressed in a *wzd* null mutant strain. Strain BCSMH022, expressing Wzd-Citrine was used as control. V56A and Y82F mutations did not interfere with the ability of Wzd to localize at the division septum upon interaction with Wze. Scale bar, 2 μm.

In the BTH assay WzdV56A, but not WzdY82F, lost the ability to interact with Wzg (Figure 3.5A, columns 66 and 67) indicating that V56 is critical for Wzd/Wzg interaction. We next tested whether WzdV56A was also unable to interact with Wzg in pneumococcal cells, leading to Wzg mis-localization. For this purpose, we co-expressed, in a *wzd* null mutant, the fusion protein iGFP-Wzg with either Wzd (strain BCSJF010), WzdY82F (strain BCSJF012) or WzdV56A (strain BCSJF011). As described above, when Wzd was constitutively expressed from a plasmid in a strain lacking *wzd*, iGFP-Wzg was able to localize at the division septum (median FR of 2.0). Similarly, WzdY82F was able to recruit iGFP-Wzg to the septum (median FR of 2.2) (Figure 3.5B). On the contrary, complementation with WzdV56A, did not recruit iGFP-Wzg to the division septum, as the fluorescent signal was distributed over the cell membrane (median FR of 1.3), similarly to the non-complemented strain BCSJF008 (median FR of 1.4) (Figure 3.5B).

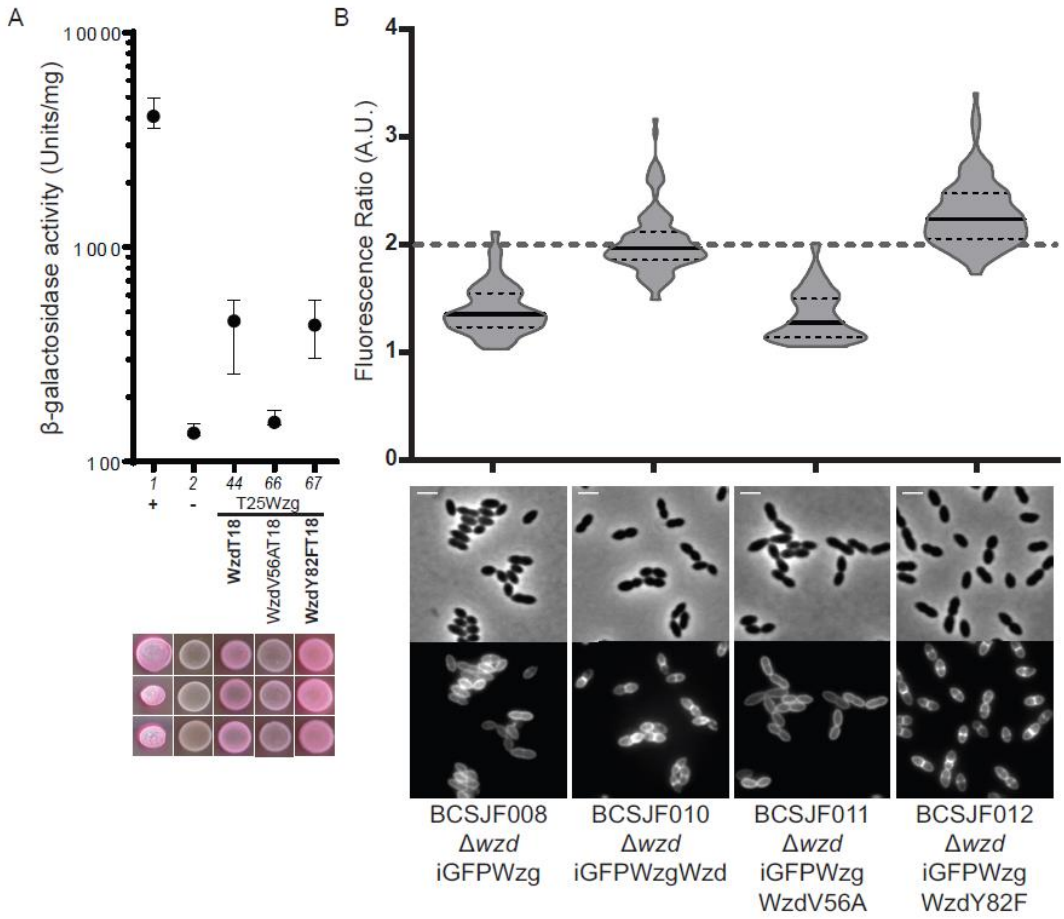

Figure 3.5: The valine residue at position 56 of Wzd is required for its interaction with Wzg, and for the recruitment of Wzg to the division septum. A) Interaction between Wzg and Wzd, WzdV56A and WzdY82F point mutants was tested by BTH. Black circles indicate median values and brackets show the 25% and 75% percentiles of β-galactosidase activity measured in cell extracts of at least three independent replicates. Representative images of the bacterial lawn obtained after spotting fresh mannitol plates a liquid culture of *E. coli* cells expressing putative interacting partners are shown below each measurement. Positive control (+): *E. coli* expressing T18 and T25 fragments linked to leucine zipper domains that can dimerize; Negative control (-): *E. coli* expressing untagged T18 and T25 fragments. WzdV56A-T18 lost the ability to interact with T25-Wzg. **B)** Graph shows the ratio of iGFP-Wzg fluorescence measured at the septum versus the peripheral wall in the *S. pneumoniae wzd* null mutant strain (BCSJF008, n=107) and in the *wzd* null mutant strain expressing Wzd or Wzd point mutants from a constitutive promoter (non-mutated Wzd strain BCSJF010, n=109, mutant WzdV56A strain BCSJF011, n=106, and mutant WzdY82F strain BCSJF012, n=128). WzdY82F, but not WzdV56A, can recruit Wzg to the division septum of pneumococcal bacteria.

3.4.5 Wzg recruitment to the septum by Wzd is required for the presence of capsular polysaccharide at midcell

Given that Wzg attaches capsule polysaccharide to the peptidoglycan, we questioned if the WzdV56A mutant, which can localize at the division septum, but is unable to recruit the Wzg ligase, was affected in capsule distribution at the bacterial surface. In encapsulated pneumococcal cells, the capsule is distributed throughout the surface, while in a strain lacking Wzd, the capsule is detected at the cell surface, but it is absent from the division septum (Henriques et al., 2011) (Figure 3.6). This is not due to an increased growth rate induced by the lack of capsule as the wild-type ATCC6314 and its *wzd* null mutant (BCSMH001) strains have identical duplication times (33 min for both strains).

We transformed the *wzd* null mutant with plasmids encoding (i) iGFP-Wzg alone (strain BCSJF008); (ii) iGFP-Wzg and Wzd (strain BCSJF010); (iii) iGFP-Wzg and one of the variants WzdY82F (strain BCSJF012) or WzdV56A (strain BCSJF011) and visualized the presence of the capsule by immunofluorescence microscopy (Figure 3.6). Complementation of the *wzd* null mutant with a plasmid co-expressing iGFP-Wzg and Wzd, or WzdY82F, resulted in bacteria encapsulated, including at the septum. However, complementation with a plasmid co-expressing iGFP-Wzg with WzdV56A, resulted in bacteria that produce capsule (Supplementary Figure 3.4), but have a completely different pattern of CPS, as it was no longer homogeneously detected around the cells. Instead, CPS was absent from most regions of the cell and accumulated in dots near the division septum or at the cell poles. These CPS foci may reflect the subcellular localization of the machinery responsible for the polymerization and translocation of the CPS.

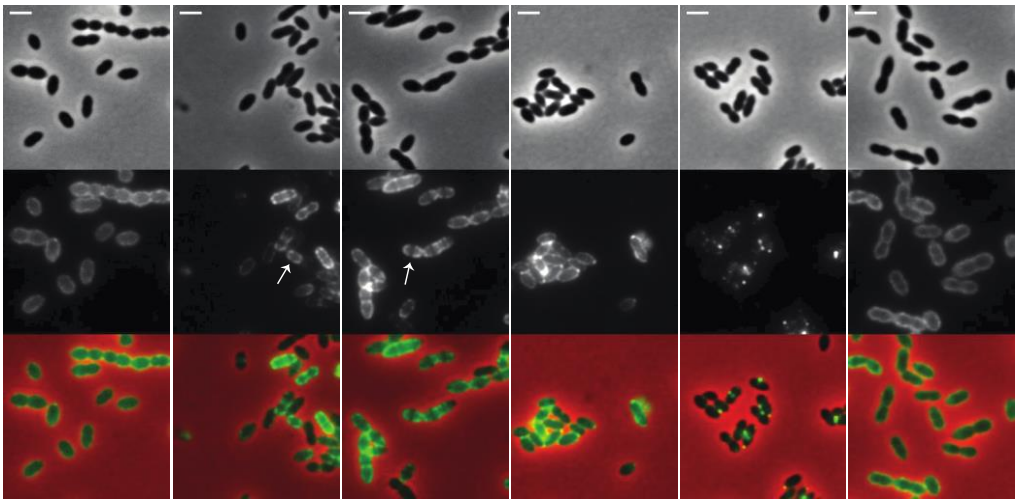

Figure 3.6: Expression of WzdV56A impairs the Wzg ability to produce a pneumococcal cell surface fully surrounded by capsule. Immunofluorescence microscopy images using a serotype-14 specific serum to detect the presence of the capsular polysaccharide at the cell surface. Wild-type encapsulated ATCC6314 expressed capsule all over the surface, while *wzd* null mutant strain BCSMH001 lacked capsule at midcell. Cells of *wzd* null mutant strain were transformed with plasmids expressing (i) iGFP-Wzg alone (BCSJF008), resulting in cells where the capsule is absent from the division septum; (ii) iGFP-Wzg and Wzd, or with WzdY82F (strains BCSJF010 and BCSJF012, respectively), resulting in cells with homogeneous distribution of CPS at their surface or (iii) iGFP-Wzg and WzdV56A (strain BCSJF011), resulting in cells where CPS accumulated in spots and was absent from most of the bacterial cell surface. Scale bar, 2 μm.

3.4.6 Capsule absence at midcell results in increased exposure of bacterial septal cell wall

The coordination of the Wzd/Wze complex with the Wzg ligase may ensure that newly synthesized cell wall is simultaneously produced and masked by CPS, so that bacteria permanently present a fully concealed cell wall. Absence of CPS at the division septum, caused by lack of Wzd, may result in exposure of particular cell surface components, such as PGN or wall teichoic acids, to receptors produced by the host immune system.

To determine if wall teichoic acids are differently exposed at the bacterial cell surface in the absence of CPS, we used a recombinant and purified fluorescent derivative of LytA, a peptidoglycan hydrolase produced by *S. pneumoniae*, that binds phophorylcholine residues

present in pneumococcal wall teichoic acids (Giudicelli et al., 1984). We hypothesized that localized or complete absence of capsule, in the *wzd* or in the *cps* null mutants respectively, could lead to an increased number of LytA-GFP molecules bound to the surface of bacteria. Addition of LytA-GFP to growing cultures of the wild-type ATCC6314 strain, its *wzd* null mutant (BCSMH001) and the capsule null mutant (BCSMC001), followed by epifluorescence microscopy to quantify levels of bound protein, showed that the fluorescent signal of bound LytA-GFP was ~1.5 times higher in the *wzd* null mutant than in the parental encapsulated strain. As expected, this increase was more pronounced in the unencapsulated strain (BCSMC001), where the fluorescent signal from bound LytA-GFP was ~6 times higher than for the parental strain (Figure 3.7A and B). The observed increased levels of LytA-GFP were not a consequence of an increased cell volume, as *wzd* mutant cells were significantly smaller than parental and non-encapsulated bacteria (Supplementary Figure 3.5 and Supplementary Table).

Increased exposure of the cell wall of *wzd* mutant to LytA-GFP could be deleterious for bacteria, as it could increase susceptibility to lysis by external PGN hydrolases. To test this hypothesis, purified LytA-GFP was added to previously boiled bacterial cultures (required to inactivate native PGN hydrolases). Both the *wzd* null mutant and *cps* null mutant were more susceptible to lysis than the parental encapsulated ATCC6314 strain (Figure 3.7C). Interestingly, the *wzd* null mutant, with partial exposure of the bacterial cell surface, was as susceptible to LytA-GFP induced lysis as *cps* null mutant, with complete absence of capsule. This suggests that even a small breach in the concealment provided by CPS to the bacterial cell wall is sufficient to expose bacteria to cell wall binding molecules present in the growth medium, such as PGN hydrolases or host immune receptors.

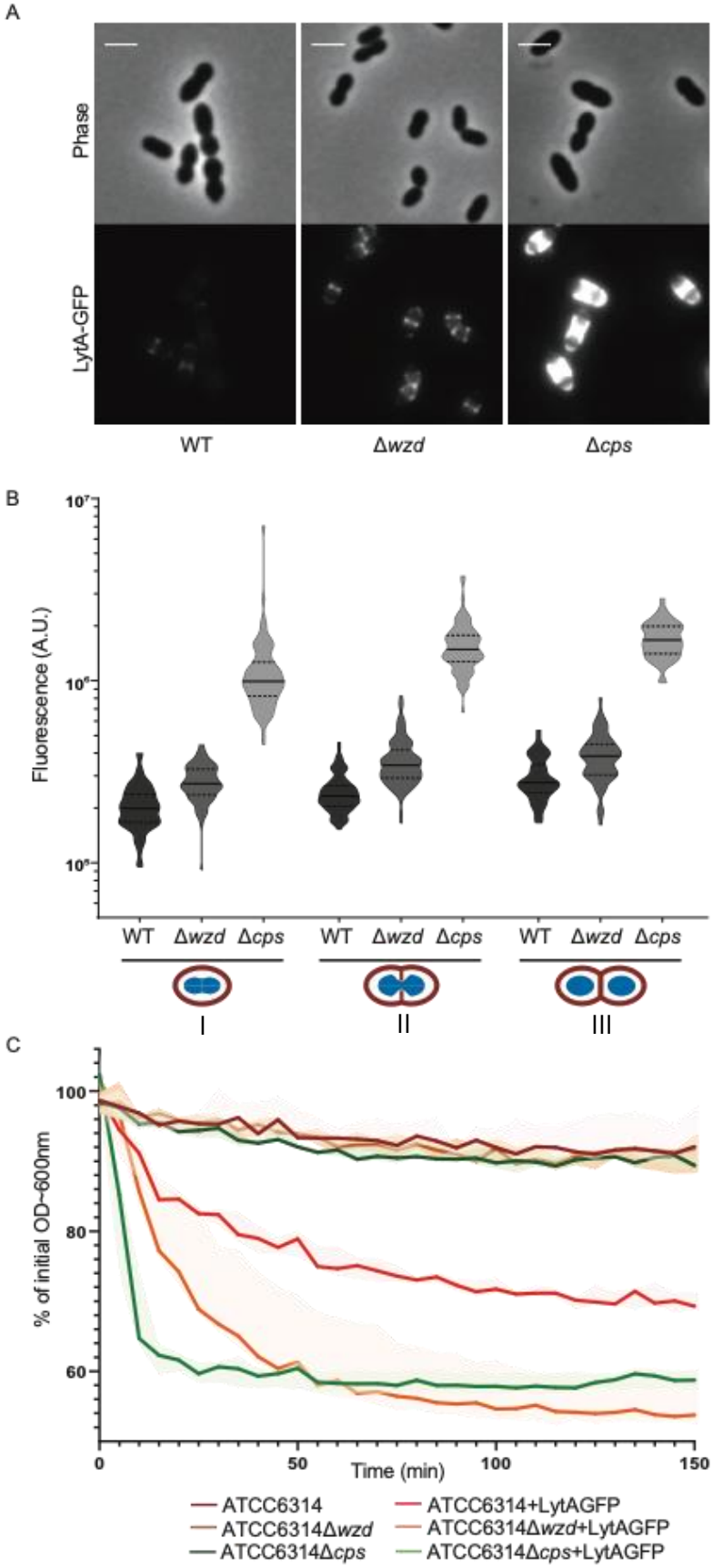
A
Phase
LytA-GFP
WT
Δwzd
Δcps
B
Fluorescence (A.U.)
WT Δwzd Δcps WT Δwzd Δcps WT Δwzd Δcps
I
II
III
C
% of initial OD-600nm
Time (min)
ATCC6314
ATCC6314Δwzd
ATCC6314Δcps
ATCC6314+LytAGFP
ATCC6314Δwzd+LytAGFP
ATCC6314Δcps+LytAGFP

Figure 3.7: Absence of capsule at the division septum results in increased exposure of bacteria cell wall and susceptibility to lysis. A) Epifluorescence microscopy images of wild-type ATCC6314 strain (WT), its capsule null mutant (BCSMC001; Δ*cps*) and the *wzd* null mutant (BCSMH001; Δ*wzd*) incubated with LytA-GFP. Scale bar, 2 μm. **B)** Quantification of cell bound LytA-GFP fluorescence. Bacteria were grouped in three different classes (n> 50), depending on their cell cycle stage: (I) recently divided cells; (II) cells initiating division as seen from invagination of cell surface; (III) cells at the final steps of division, with deep invagination at division septum. Lack of capsule (at mid-cell or over the entire cell wall) results in bacteria that bind more LytA-GFP than the parental encapsulated bacteria. **C)** Lysis of boiled bacterial cells of wild-type ATCC6314, unencapsulated (ATCC6314Δ*cps*) and *wzd* null mutant (ATCC6314Δ*wzd*) strains was assessed by the decrease in $OD_{(600nm)}$ in the absence (n=3) or presence (n=7) of LytA-GFP. Lysis curves show that the lack of capsule at particular sub-cellular sites of the bacterial cell surface increase bacteria susceptibility to lysis. Solid lines represent the curve obtained with the median values for each timepoint. Shaded areas associated with each solid line represent the interquartile range.

3.4.7 Absence of capsule at midcell impairs virulence

To test the consequences of the absence of capsule at midcell on virulence, we used a zebrafish infection model. Due to its small size and rapid generation time, zebrafish (*Danio rerio*) is a powerful vertebrate model for studying host-pathogen interactions (Neely et al., 2002; Miller et al., 2004; van der Sar et al., 2006; Mesquita et al., 2017). In particular, zebrafish embryos have been used as a model for host immune responses in systemic *S. pneumoniae* infections (Rounioja et al., 2012).

We performed survival assays by infecting zebrafish embryos, 3 days post-fertilization, with *S. pneumoniae* strains ATCC6314 (encapsulated), BCSMC001 (unencapsulated) and BCSMH001 (*wzd* null mutant). As observed in Figure 3.8, less than 30h post-infection, 0% of zebrafish embryos infected with the wild-type strain survived. However, 33% of embryos infected with the *wzd* null mutant strain (BCSMH001) were able to survive, even 72h after infection, close to the 47% of embryos that survive when infected with unencapsulated strain (BCSMC001). These results demonstrate that absence of capsule at the septum results in bacteria severely impaired in the ability to kill zebrafish embryos.

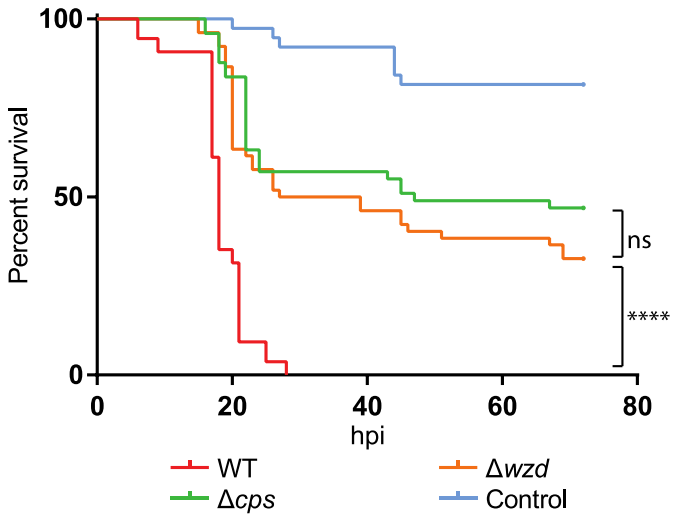

Figure 3.8: Full encapsulation of the cells is necessary for virulence. Survival graph of zebrafish embryos injected, three days post-fertilization, with wild-type ATCC6314 (WT), unencapsulated BCSMC001 (Δ*cps*), *wzd* null mutant BCSMH001 (Δ*wzd*) and medium used to resuspend bacteria (Control). The *wzd* null mutant was severely impaired in virulence, similarly to the unencapsulated BCSMC001 strain. The assay was performed with at least 50 embryos for each condition that were injected in four different days and the obtained survival curves, except those obtained with the *cps* and *wzd* mutants, were significantly different ($p<0.0001$). (hpi) hours post infection.

3.5 Discussion

We have previously proposed that Wzd and Wze act as spatial regulators of capsule synthesis, to ensure that it occurs at the division septum, possibly to conceal the newly synthesized cell wall (Henriques et al., 2011). Therefore, Wzd and Wze guarantee that the *S. pneumoniae* cell wall is completely surrounded and protected by the capsular polysaccharide during the entire cell cycle. However, how Wzd and Wze perform this role was not known. Two hypotheses could be envisioned: Wzd/Wze recruit other members of the CPS synthesis machinery to the division septum or, alternatively, Wzd/Wze interact and activate other members of the CPS synthesis machinery already present at that site. To understand the role of Wzd/Wze, we used a BTH assay and tested whether WchA, the first glycosyltransferase in the synthesis of the CPS repeating unit, or Wzg, the CPS-cell wall ligase, interacted with Wzd or Wze. While no interactions were detected between Wzd/Wze and WchA, we found that Wzg interacts with Wzd, as well as with itself. LCP enzymes such as Wzg are generally thought

to work as monomers (Li et al., 2020), although LcpA from *Corynebacterium glutamicum* can dimerize under particular conditions (Baumgart et al., 2016), and that may also be the case in *S. pneumoniae*.

Importantly, this work showed that Wzd/Wzg interaction is critical for correct localization of Wzg. As expected for a protein with three transmembrane domains, Wzg was found to be present at the membrane of pneumococcal cells. A Wzg fluorescent derivative was enriched at the septum of wild-type encapsulated ATCC6314 (serotype 14) cells, as previously described for the *S. pneumoniae* encapsulated D39 (serotype 2) and unencapsulated R6 strains (Eberhardt et al., 2012). However, contrary to what was previously reported, we observed that the localization of Wzg was dependent on the ability of bacteria to produce capsule. Wzg lost its septal enrichment in a mutant strain lacking the *cps* operon and, specifically, in the absence of the Wzd or Wze proteins. It is possible that the role of Wzd on Wzg localization varies for different serotypes, explaining the discrepancies in data obtained by different groups.

Morona and colleagues have previously proposed that alterations in Wzd/Wze expression could influence the levels of capsule associated with the cell wall or released into the growth medium (Morona et al., 2006). These authors found that the change of a valine to an alanine at position 56 of Wzd, or of a tyrosine to a phenylalanine at position 82, in bacteria that lack the Wzh phosphatase, causes a mucoid phenotype in pneumococcal serotype 2 colonies (Morona et al., 2006). These mutants produce total CPS levels that are similar to the parental strain, but the levels of CPS actually attached to the cell wall are lower, suggesting a decreased activity of the CPS ligase. As we showed that Wzd and Wzg interact, leading to Wzg septal recruitment, we hypothesized that the V56A and Y82F mutations in Wzd might interfere with its interaction with and recruitment of Wzg. Indeed, WzdV56A did not interact with Wzg in a BTH assay and did not recruit Wzg to the division septum of pneumococcal cells. This was not the case for WzdY82F, which interacted with and recruited Wzg, indicating that the mucoid phenotype of this mutant arises via a different mechanism (Morona et al., 2006). As substitution of Wzd tyrosine 82 by a cysteine was reported to cause a decrease in the phosphorylation of Wze (Byrne et al., 2011), it is possible that this residue has a major role in the interaction between these two proteins or in the promotion of Wze phosphorylation by Wzd.

Wzg was initially thought to regulate transcription of the *cps* operon (Cieslewicz et al., 2001). This was based on the homology of its C-terminal domain with LytR (Guidolin et al., 1994), a *B. subtilis* transcriptional regulator (Lazarevic et al., 1992), as well as on the fact that in *Streptococcus agalactiae*, the homologue protein CpsIA functions as a transcriptional regulator (Cieslewicz et al., 2001). Moreover, Wzg homologues from *Streptococcus iniae* and *S. agalactiae* bind specifically to DNA containing the capsule operon promoter region (Hanson et al., 2012; Hanson et al., 2011). It seems therefore plausible that Wzg has two roles in the regulation of the CPS assembly: to attach the capsular polysaccharide to PGN, through its extracellular domain, and to control the transcription of the *cps* operon, through its short cytoplasmic N-terminal end. The fact that in a BTH assay the transmembrane domain and the first part of the extracellular domain of Wzg are required for an interaction with Wzd, and that a point mutation in the extracellular domain of Wzd prevents this interaction, highlights the importance of the extracellular regions of both proteins in *S. pneumoniae* CPS synthesis.

More recently, the polymerase Wzy and the flippase Wzx were shown to localize exclusively at septum, suggesting that CPS synthesis occurs only at that place (Nourikyan et al., 2015). Interestingly, delocalization of Wzy was seen in a *wze* null mutant, which led to a sequential model where Wzd/Wze complex localize at the septum and then Wze captures Wzy resulting in its subsequent septal localization (Nourikyan et al., 2015). Considering these results, together with the data presented in this work, it is tempting to speculate that Wzd/Wze could control the elongation of the CPS chain (through recruitment of Wzy), as well as its ligation to the peptidoglycan (through recruitment of Wzg). Septal enrichment of Wzg may be crucial for CPS attachment to occur at a rate which is synchronized with the rate of PGN synthesis at the division septum. When this synchronization is lost, as it happens in the *wzd* mutant, where septal enrichment of Wzg is lost, *S. pneumoniae* cells synthesize PGN at the septum which is not immediately concealed by CPS. This results in cells where the cell wall at midcell is exposed to external WTA- or PGN-binding proteins. In agreement with this idea the *wzd* null mutant bound higher amounts of the PGN hydrolase LytA to its surface and was more susceptible to lysis by LytA than the fully encapsulated parental strain. More importantly, a *wzd* null mutant was dramatically impaired in virulence, in a zebrafish embryo infection model, showing that full encapsulation of bacterial cells, covering the entire cell wall, is crucial for virulence.

3.6 Supplementary information

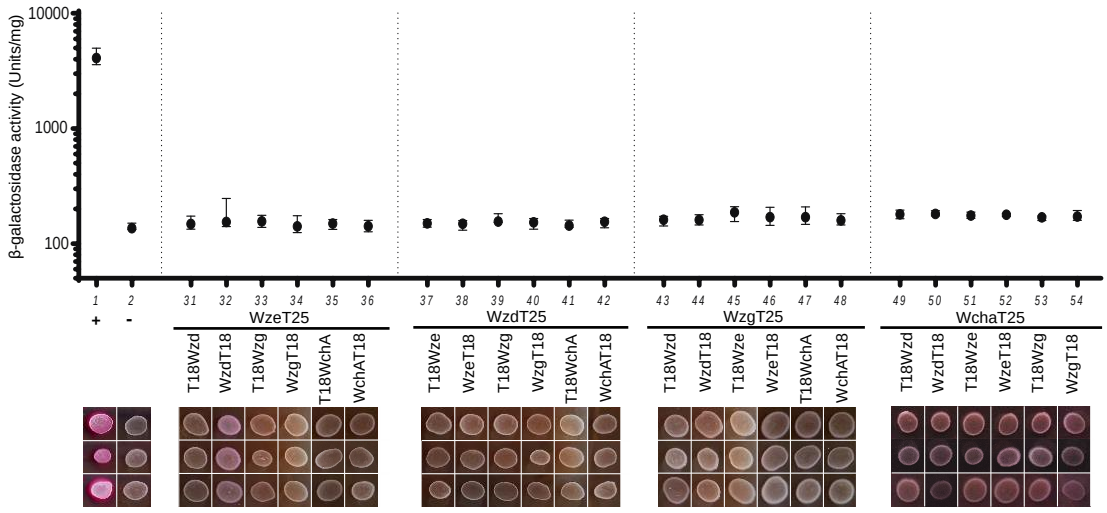

Supplementary Figure 3.1: Introduction of the T25 tag at the C-terminal of different capsule synthesis proteins may prevent their interaction with partner proteins. Wze, Wzd, Wzg and WchA interactions were tested using Bacterial Two-Hybrid *E. coli* system. β-galactosidase activity of cells expressing putative interaction partners was measured in cell extracts in at least three independent replicates. Black circles indicate median values and brackets show the 25% and 75% percentiles. Representative images of the bacterial lawn obtained after spotting fresh mannitol plates with a liquid culture of *E. coli* cells expressing putative interacting partners, are shown below each measurement. Positive control (+): *E. coli* expressing T18 and T25 fragments linked to leucine zipper domains that can dimerize; Negative control (-): *E. coli* expressing untagged T18 and T25 fragments. No interactions were detected between tested proteins.

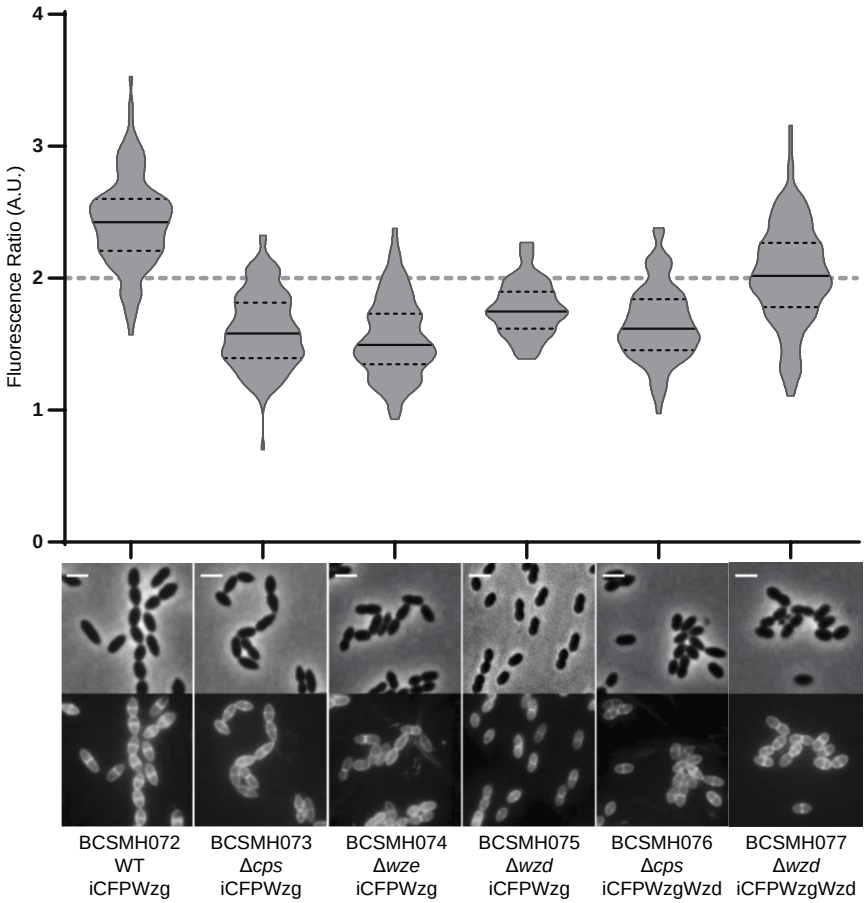

Supplementary Figure 3.2: Septal localization of Wzg is dependent on the expression of Wzd/Wze. Graph shows the ratio of iCFP-Wzg fluorescence measured at the septum versus the peripheral wall in the *S. pneumoniae* wild-type encapsulated strain (BCSMH072, n=132), the capsule null mutant (BCSMH073, n=129), the *wze* null mutant (BCSMH074, n=130), the *wzd* null mutant (BCSMH075, n=112) and in the *cps* and *wzd* null mutants expressing Wzd from a constitutive promoter (BCSMH076, n=135, and BCSMH077, n=154, respectively). Enrichment of Wzg at the septum is only observed when Wzd is expressed and is localized at the division septum. Solid lines indicate median, and dashed lines indicate 25% and 75% percentiles. Representative phase contrast and fluorescence microscopy images of each strain are shown below the graph. Scale bar, 2 μm.

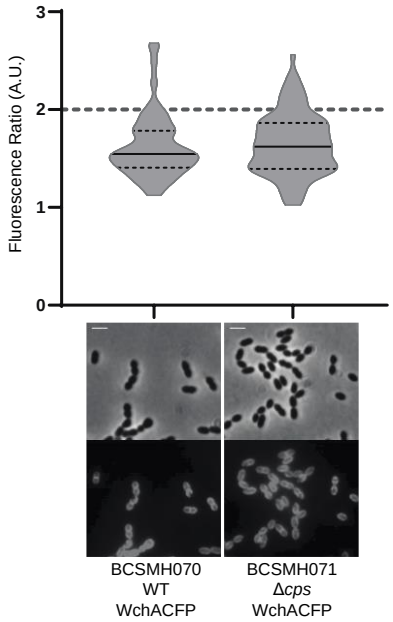

Supplementary Figure 3.3: Membrane localization of WchA is independent of the expression of capsule. Graph shows the ratio of WchA-CFP fluorescence measured at the septum versus the peripheral wall in the *S. pneumoniae* wild-type encapsulated strain (BCSMH070, n=101) and in the capsule null mutant (BCSMH071, n=101). No difference in the localization of WchA was observed between encapsulated and non-encapsulated bacteria. Solid lines indicate median, and dashed lines indicate 25% and 75% percentiles. Representative phase contrast and fluorescence microscopy images of each strain are shown below the graph. Scale bar, 2 µm.

Supplementary Figure 3.4: Expression of capsular polysaccharide in the presence of different Wzd proteins. Dot blot assays performed with cells from exponentially growing cultures of ATCC6314 (encapsulated parental strain, WT), BCSMC001 (non-encapsulated Δ*cps* mutant strain), BCSMH001 (Δ*wzd* mutant strain) and its derivatives strains that carry a plasmid expressing iGFPWzg in the presence of Wzd (BCSJF010 strain); of the mutated WzdV56A protein (BCSJF011 strain) and of the mutated

WzdY82F protein (BCSJF012 strain). Expression of both WzdV56A and WzdY82F protein result in bacteria capable of producing capsular polysaccharide.

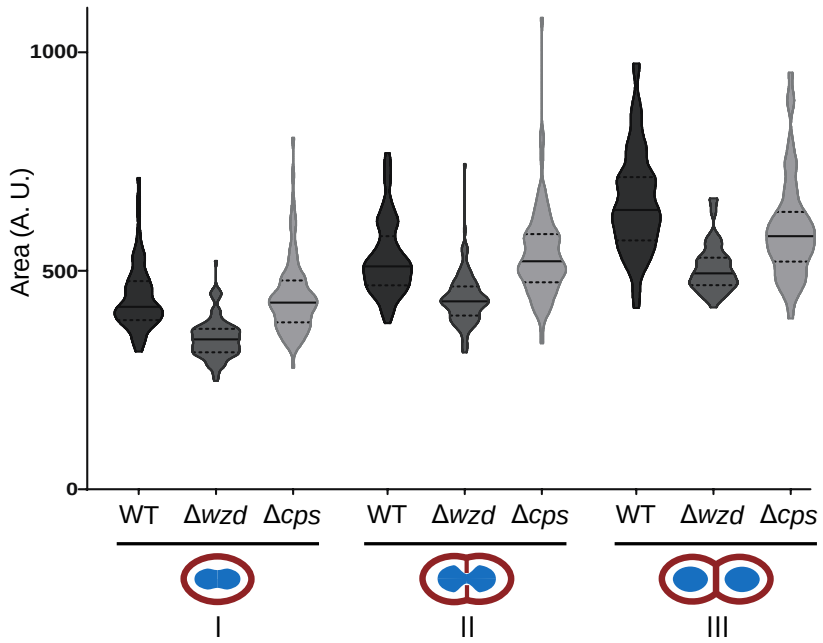

Supplementary Figure 3.5: Absence of Wzd results in smaller cell size. Phase contrast microscopy images of wild-type ATCC6314 strain (WT), its capsule null mutant (BCSMC001; Δ*cps*) and the *wzd* null mutant (BCSMH001; Δ*wzd*) were used to determine cell size. Bacteria were grouped in three different classes depending on their cell cycle stage: (I) recently divided cells; (II) cells initiating division as seen from invagination of cell surface; (III) cells at the final steps of division, with deep invagination at division septum. Lack of Wzd, but not of CPS, results in smaller cells.

Supplementary Table 3.1: Statistical analysis of all figures

Figure 3.1						
A	**B**	**P value**	**P value summary**	**Significantly different (P < 0.05)?**	**Median of column B**	**Median of column A**
1	**2**	<0,0001	****	Yes	136,0, n=15	4090, n=16
3	**1**	0,0402	*	Yes	4090, n=16	3109, n=6
	2	<0,0001	****	Yes	136,0, n=15	3109, n=6
4	**1**	0,4494	ns	No	4090, n=16	3637, n=6
	2	<0,0001	****	Yes	136,0, n=15	3637, n=6
5	**1**	<0,0001	****	Yes	4090, n=16	135,7, n=5
	2	0,8001	ns	No	136,0, n=15	135,7, n=5
6	**1**	0,0004	***	Yes	4090, n=16	151,0, n=4
	2	0,307	ns	No	136,0, n=15	151,0, n=4
7	**1**	0,0004	***	Yes	4090, n=16	145,7, n=4
	2	0,3155	ns	No	136,0, n=15	145,7, n=4
8	**1**	0,0004	***	Yes	4090, n=16	149,1, n=4
	2	0,307	ns	No	136,0, n=15	149,1, n=4

9	**1**	<0,0001	****	Yes	4090, n=16	148,7, n=5
	2	0,5531	ns	No	136,0, n=15	148,7, n=5
10	**1**	0,0008	***	Yes	4090, n=16	2619, n=6
	2	<0,0001	****	Yes	136,0, n=15	2619, n=6
11	**1**	<0,0001	****	Yes	4090, n=16	1295, n=11
	2	<0,0001	****	Yes	136,0, n=15	1295, n=11
12	**1**	<0,0001	****	Yes	4090, n=16	168,0, n=6
	2	0,0467	*	Yes	136,0, n=15	168,0, n=6
13	**1**	<0,0001	****	Yes	4090, n=16	144,7, n=6
	2	0,6222	ns	No	136,0, n=15	144,7, n=6
14	**1**	<0,0001	****	Yes	4090, n=16	143,5, n=5
	2	0,3056	ns	No	136,0, n=15	143,5, n=5
15	**1**	0,0004	***	Yes	4090, n=16	151,1, n=4
	2	0,2208	ns	No	136,0, n=15	151,1, n=4
16	**1**	0,0004	***	Yes	4090, n=16	153,4, n=4
	2	0,08	ns	No	136,0, n=15	153,4, n=4
17	**1**	<0,0001	****	Yes	4090, n=16	149,0, n=15
	2	0,1485	ns	No	136,0, n=15	149,0, n=15
18	**1**	<0,0001	****	Yes	4090, n=16	453,4, n=19
	2	<0,0001	****	Yes	136,0, n=15	453,4, n=19
19	**1**	0,0004	***	Yes	4090, n=16	145,4, n=4
	2	0,5965	ns	No	136,0, n=15	145,4, n=4
20	**1**	0,0004	***	Yes	4090, n=16	146,8, n=4
	2	0,5304	ns	No	136,0, n=15	146,8, n=4
21	**1**	0,0004	***	Yes	4090, n=16	151,0, n=4
	2	0,4208	ns	No	136,0, n=15	151,0, n=4
22	**1**	<0,0001	****	Yes	4090, n=16	158,0, n=10
	2	0,0012	**	Yes	136,0, n=15	158,0, n=10
23	**1**	<0,0001	****	Yes	4090, n=16	851,3, n=6
	2	<0,0001	****	Yes	136,0, n=15	851,3, n=6
24	**1**	0,0004	***	Yes	4090, n=16	142,6, n=4
	2	0,7363	ns	No	136,0, n=15	142,6, n=4
25	**1**	0,0004	***	Yes	4090, n=16	126,6, n=4
	2	0,469	ns	No	136,0, n=15	126,6, n=4
26	**1**	0,0004	***	Yes	4090, n=16	158,4, n=4
	2	0,1244	ns	No	136,0, n=15	158,4, n=4
27	**1**	0,0004	***	Yes	4090, n=16	136,7, n=4
	2	0,9613	ns	No	136,0, n=15	136,7, n=4
28	**1**	0,0004	***	Yes	4090, n=16	149,1, n=4
	2	0,1847	ns	No	136,0, n=15	149,1, n=4
29	**1**	0,0004	***	Yes	4090, n=16	151,9, n=4
	2	0,0485	*	Yes	136,0, n=15	151,9, n=4
30	**1**	0,0004	***	Yes	4090, n=16	133,0, n=4
	2	0,5304	ns	No	136,0, n=15	133,0, n=4

Figure 3.2						
A	**B**	**P value**	**P value summary**	**Significantly different (P < 0.05)?**	**Median of column B**	**Median of column A**
BCSJF005	**BCSJF006**	<0,0001	****	Yes	1,616, n=121	2,354, n=194
BCSJF005	**BCSJF007**	<0,0001	****	Yes	1,499, n=106	2,354, n=194
BCSJF005	**BCSJF008**	<0,0001	****	Yes	1,351, n=107	2,354, n=194
BCSJF005	**BCSJF009**	<0,0001	****	Yes	1,542, n=112	2,354, n=194
BCSJF005	**BCSJF010**	<0,0001	****	Yes	1,969, n=109	2,354, n=194
BCSJF006	**BCSJF007**	0,0001	***	Yes	1,499, n=106	1,616, n=121
BCSJF006	**BCSJF008**	<0,0001	****	Yes	1,351, n=107	1,616, n=121
BCSJF006	**BCSJF009**	0,354	ns	No	1,542, n=112	1,616, n=121
BCSJF006	**BCSJF010**	<0,0001	****	Yes	1,969, n=109	1,616, n=121

Figure 3.3						
A	**B**	**P value**	**P value summary**	**Significantly different (P < 0.05)?**	**Median of column B**	**Median of column A**
1	**2**	0,0286	*	Yes	152,1, n=4	4578, n=4
3	**1**	0,0286	*	Yes	4578, n=4	761,7, n=4
	2	0,0286	*	Yes	152,1, n=4	761,7, n=4
4	**1**	0,0286	*	Yes	4578, n=4	157,0, n=4
	2	0,6857	ns	No	152,1, n=4	157,0, n=4
5	**1**	0,0286	*	Yes	4578, n=4	152,7, n=4
	2	>0,9999	ns	No	152,1, n=4	152,7, n=4
6	**1**	0,0286	*	Yes	4578, n=4	158,1, n=4
	2	>0,9999	ns	No	152,1, n=4	158,1, n=4
7	**1**	0,0286	*	Yes	4578, n=4	139,4, n=4
	2	0,3429	ns	No	152,1, n=4	139,4, n=4
8	**1**	0,0286	*	Yes	4578, n=4	439,3, n=4
	2	0,0286	*	Yes	152,1, n=4	439,3, n=4
9	**1**	0,0286	*	Yes	4578, n=4	414,0, n=4
	2	0,0286	*	Yes	152,1, n=4	414,0, n=4
10	**1**	0,0286	*	Yes	4578, n=4	153,4, n=4
	2	>0,9999	ns	No	152,1, n=4	153,4, n=4
11	**1**	0,0286	*	Yes	4578, n=4	143,9, n=4
	2	0,3429	ns	No	152,1, n=4	143,9, n=4
12	**1**	0,0286	*	Yes	4578, n=4	146,3, n=4
	2	0,3143	ns	No	152,1, n=4	146,3, n=4
13	**1**	0,0286	*	Yes	4578, n=4	152,7, n=4
	2	0,8857	ns	No	152,1, n=4	152,7, n=4
14	**1**	0,0286	*	Yes	4578, n=4	423,9, n=4
	2	0,0286	*	Yes	152,1, n=4	423,9, n=4
15	**1**	0,0286	*	Yes	4578, n=4	405,8, n=4
	2	0,0286	*	Yes	152,1, n=4	405,8, n=4
16	**1**	0,0286	*	Yes	4578, n=4	524,3, n=4
	2	0,0286	*	Yes	152,1, n=4	524,3, n=4

17	**1**	0,0286	*	Yes	4578, n=4	136,0, n=4
	2	0,2	ns	No	152,1, n=4	136,0, n=4
18	**1**	0,0286	*	Yes	4578, n=4	154,1, n=4
	2	0,8857	ns	No	152,1, n=4	154,1, n=4
19	**1**	0,0286	*	Yes	4578, n=4	154,0, n=4
	2	>0,9999	ns	No	152,1, n=4	154,0, n=4
20	**1**	0,0286	*	Yes	4578, n=4	142,6, n=4
	2	0,2	ns	No	152,1, n=4	142,6, n=4
21	**1**	0,0286	*	Yes	4578, n=4	341,1, n=4
	2	0,0286	*	Yes	152,1, n=4	341,1, n=4
22	**1**	0,0286	*	Yes	4578, n=4	364,4, n=4
	2	0,0286	*	Yes	152,1, n=4	364,4, n=4

Figure 3.5A						
A	**B**	**P value**	**P value summary**	**Significantly different (P < 0.05)?**	**Median of column B**	**Median of column A**
1	**2**	<0,0001	****	Yes	136,0, n=15	4090, n=16
46	**1**	<0,0001	****	Yes	4090, n=16	453,4, n=19
	2	<0,0001	****	Yes	136,0, n=15	453,4, n=19
66	**1**	<0,0001	****	Yes	4090, n=16	152,7, n=10
	2	0,0029	**	Yes	136,0, n=15	152,7, n=10
67	**1**	<0,0001	****	Yes	4090, n=16	434,2, n=10
	2	<0,0001	****	Yes	136,0, n=15	434,2, n=10

Figure 3.5B					
A **B**	**BCSJF008** **BCSJF010**	**BCSJF008** **BCSJF011**	**BCSJF008** **BCSJF012**	**BCSJF010** **BCSJF011**	**BCSJF010** **BCSJF012**
P value	<0,0001	0,0199	<0,0001	<0,0001	<0,0001
P value summary	****	*	****	****	****
Significantly different (P < 0.05)?	Yes	Yes	Yes	Yes	Yes
Median of line A	1,351, n=107	1,351, n=107	1,351, n=107	1,969, n=109	1,969, n=109
Median of line B	1,969, n=109	1,271, n=106	2,240, n=128	1,271, n=106	2,240, n=128

Figure 3.7B						
A	**B**	**P value**	**P value summary**	**Significantly different (P < 0.05)?**	**Median of column B**	**Median of column A**
WT1	***Δwzd1***	<0,0001	****	Yes	272075, n=133	198617, n=68
WT1	***Δcps1***	<0,0001	****	Yes	991751, n=95	198617, n=68
Δwzd1	***Δcps1***	<0,0001	****	Yes	991751, n=95	272075, n=133
WT2	***Δwzd2***	<0,0001	****	Yes	342969, n=114	232748, n=126
WT2	***Δcps2***	<0,0001	****	Yes	1484402, n=95	232748, n=126
Δwzd2	***Δcps2***	<0,0001	****	Yes	1484402, n=95	342969, n=114
WT3	***Δwzd3***	<0,0001	****	Yes	385568, n=79	275639, n=66
WT3	***Δcps3***	<0,0001	****	Yes	1672209, n=53	275639, n=66
Δwzd3	***Δcps3***	<0,0001	****	Yes	1672209, n=53	385568, n=79

Figure 3.8								
WT vs Δcps			**WT vs Δ*wzd***			***Δcps vs Δwzd***		
Log-rank (Mantel-Cox) test			Log-rank (Mantel-Cox) test			Log-rank (Mantel-Cox) test		
Chi square	60,33		Chi square	47,01		Chi square	1,769	
df	1		df	1		df	1	
P value	<0,0001		P value	<0,0001		P value	0,1835	
P value summary	****		P value summary	****		P value summary	ns	
Are the survival curves sig different?	Yes		Are the survival curves sig different?	Yes		Are the survival curves sig different?	No	
Median survival			Median survival			Median survival		
WT	18		WT	18		*Δcps*	47	
Δcps	47		*Δwzd*	33		*Δwzd*	33	
Ratio (and its reciprocal)	0,383	2,611	Ratio (and its reciprocal)	0,5455	1,833	Ratio (and its reciprocal)	1,424	0,7021
95% CI of ratio	0,2399 to 0,6115	1,635 to 4,169	95% CI of ratio	0,3565 to 0,8346	1,198 to 2,805	95% CI of ratio	0,8574 to 2,366	0,4227 to 1,166
Hazard Ratio (Mantel-Haenszel)	A/B	B/A	Hazard Ratio (Mantel-Haenszel)	A/C	C/A	Hazard Ratio (Mantel-Haenszel)	B/C	C/B
Ratio (and its reciprocal)	8,651	0,1156	Ratio (and its reciprocal)	6,135	0,163	Ratio (and its reciprocal)	0,702	1,424
95% CI of ratio	5,019 to 14,91	0,06706 to 0,1993	95% CI of ratio	3,652 to 10,30	0,09705 to 0,2738	95% CI of ratio	0,4168 to 1,182	0,8457 to 2,399
Hazard Ratio (logrank)	A/B	B/A	Hazard Ratio (logrank)	A/C	C/A	Hazard Ratio (logrank)	B/C	C/B
Ratio (and its reciprocal)	4,304	0,2323	Ratio (and its reciprocal)	3,346	0,2988	Ratio (and its reciprocal)	0,7189	1,391
95% CI of ratio	2,696 to 6,870	0,1456 to 0,3709	95% CI of ratio	2,140 to 5,232	0,1911 to 0,4673	95% CI of ratio	0,4352 to 1,188	0,8420 to 2,298

Supplementary Figure 3.2						
A	**B**	**P value**	**P value summary**	**Significantly different (P < 0.05)?**	**Median of column B**	**Median of column A**
1	**2**	<0,0001	****	Yes	136,0, n=15	4090, n=16
31	**1**	0,0004	***	Yes	4090, n=16	148,3, n=4
	2	0,3571	ns	No	136,0, n=15	148,3, n=4
32	**1**	<0,0001	****	Yes	4090, n=16	154,4, n=13
	2	0,0026	**	Yes	136,0, n=15	154,4, n=13
33	**1**	0,0004	***	Yes	4090, n=16	156,1, n=4
	2	0,1522	ns	No	136,0, n=15	156,1, n=4
34	**1**	0,0004	***	Yes	4090, n=16	141,0, n=4
	2	0,6646	ns	No	136,0, n=15	141,0, n=4
35	**1**	0,0004	***	Yes	4090, n=16	149,6, n=4
	2	0,4107	ns	No	136,0, n=15	149,6, n=4
36	**1**	<0,0001	****	Yes	4090, n=16	141,8, n=5
	2	0,8001	ns	No	136,0, n=15	141,8, n=5
37	**1**	<0,0001	****	Yes	4090, n=16	149,7, n=5
	2	0,1974	ns	No	136,0, n=15	149,7, n=5
38	**1**	<0,0001	****	Yes	4090, n=16	148,7, n=5
	2	0,5991	ns	No	136,0, n=15	148,7, n=5
39	**1**	<0,0001	****	Yes	4090, n=16	155,6, n=5
	2	0,0077	**	Yes	136,0, n=15	155,6, n=5
40	**1**	<0,0001	****	Yes	4090, n=16	153,3, n=5
	2	0,2661	ns	No	136,0, n=15	153,3, n=5
41	**1**	<0,0001	****	Yes	4090, n=16	143,3, n=5
	2	0,168	ns	No	136,0, n=15	143,3, n=5
42	**1**	0,0004	***	Yes	4090, n=16	154,9, n=4
	2	0,1847	ns	No	136,0, n=15	154,9, n=4
43	**1**	<0,0001	****	Yes	4090, n=16	161,4, n=5
	2	0,0328	*	Yes	136,0, n=15	161,4, n=5
44	**1**	<0,0001	****	Yes	4090, n=16	160,6, n=5
	2	0,0328	*	Yes	136,0, n=15	160,6, n=5
45	**1**	0,0004	***	Yes	4090, n=16	187,3, n=4
	2	0,0036	**	Yes	136,0, n=15	187,3, n=4
46	**1**	0,0004	***	Yes	4090, n=16	169,6, n=4
	2	0,0196	*	Yes	136,0, n=15	169,6, n=4
47	**1**	0,0004	***	Yes	4090, n=16	169,8, n=4
	2	0,0273	*	Yes	136,0, n=15	169,8, n=4
48	**1**	0,0004	***	Yes	4090, n=16	159,4, n=4
	2	0,0273	*	Yes	136,0, n=15	159,4, n=4
49	**1**	0,0004	***	Yes	4090, n=16	180,0, n=4
	2	0,0036	**	Yes	136,0, n=15	180,0, n=4

50	**1**	0,0004	***	Yes	4090, n=16	180,9, n=4
	2	0,001	**	Yes	136,0, n=15	180,9, n=4
51	**1**	0,0004	***	Yes	4090, n=16	175,2, n=4
	2	0,0021	**	Yes	136,0, n=15	175,2, n=4
52	**1**	0,0004	***	Yes	4090, n=16	178,4, n=4
	2	0,001	**	Yes	136,0, n=15	178,4, n=4
53	**1**	0,0004	***	Yes	4090, n=16	169,4, n=4
	2	0,0062	**	Yes	136,0, n=15	169,4, n=4
54	**1**	0,0004	***	Yes	4090, n=16	171,7, n=4
	2	0,0062	**	Yes	136,0, n=15	171,7, n=4

Supplementary Figure 3.3						
A	**B**	**P value**	**P value summary**	**Significantly different (P < 0.05)?**	**Median of column B**	**Median of column A**
BCSMH072	**BCSMH073**	<0,0001	****	Yes	1,582, n=129	2,426, n=132
BCSMH072	**BCSMH074**	<0,0001	****	Yes	1,749, n=112	2,426, n=132
BCSMH072	**BCSMH075**	<0,0001	****	Yes	1,496, n=130	2,426, n=132
BCSMH072	**BCSMH076**	<0,0001	****	Yes	1,620, n=135	2,426, n=132
BCSMH072	**BCSMH077**	<0,0001	****	Yes	2,017, n=154	2,426, n=132
BCSMH073	**BCSMH074**	<0,0001	****	Yes	1,749, n=112	1,582, n=129
BCSMH073	**BCSMH075**	0,1103	ns	No	1,496, n=130	1,582, n=129
BCSMH073	**BCSMH076**	0,1189	ns	No	1,620, n=135	1,582, n=129
BCSMH073	**BCSMH077**	<0,0001	****	Yes	2,017, n=154	1,582, n=129

Supplementary Figure 3.4	
P value	0,3097
P value summary	ns
Significantly different (P < 0.05)?	No
Median of column A	1,545, n=101
Median of column B	1,622, n=101

Supplementary Figure 3.6						
A	**B**	**P value**	**P value summary**	**Significantly different (P < 0.05)?**	**Median of column B**	**Median of column A**
WT1	***Δwzd1***	<0,0001	****	Yes	343,0, n=133	417,5, n=68
WT1	***Δcps1***	0,9104	ns	No	427,0, n=94	417,5, n=68
Δwzd1	***Δcps1***	<0,0001	****	Yes	427,0, n=94	343,0, n=133
WT2	***Δwzd2***	<0,0001	****	Yes	430,0, n=114	510,0, n=126
WT2	***Δcps2***	0,4659	ns	No	522,0, n=95	510,0, n=126
Δwzd2	***Δcps2***	<0,0001	****	Yes	522,0, n=95	430,0, n=114
WT3	***Δwzd3***	<0,0001	****	Yes	494,0, n=79	639,0, n=66
WT3	***Δcps3***	0,0011	**	Yes	579,0, n=53	639,0, n=66
Δwzd3	***Δcps3***	<0,0001	****	Yes	579,0, n=53	494,0, n=79

Chapter 4

Strategies to interfere with the capsule synthetic machinery of *S. pneumoniae*

4.1 Abstract

Streptococcus pneumoniae is a widespread respiratory pathogen and a frequent cause of community-acquired pneumonia. Despite the contributions that antibiotics and the development of vaccines have introduced in the strategies used to tackle with pneumococcal infections, the emergence of antibiotic resistance and serotype replacement observed in clinical isolates is compromising the success of this battle. Consequently, the development of new classes of drugs, capable of eliminating this pathogen or of preventing its ability to infect the host, is imperative. The capsule polysaccharide surrounding the surface of most pneumococcal cells, is the major virulence factor, whose synthesis is regulated by Wzd and Wze enzymes that are part of a phosphoregulatory system. As Wze, an autophosphorylating tyrosine kinase, and Wzd, a membrane protein required for Wze autophosphorylation, co-localize at the division septum to successfully regulate the synthesis of capsule, we have designed a method that allows the in vivo screening of inhibitory peptides or compounds capable of interfering with the Wzd/Wze interaction, or its septal localization, and that are capable of preventing the complete encapsulation of pneumococcal cells. We constructed a pneumococcal mutant strain capable of producing the Wzd and Wze interacting partners attached to different fluorescent proteins, Wzd-CFP and Wze-Citrine, that allow the observation of the complex Wzd/Wze delocalization, or its dissociation resulting in the delocalization of Wzd-CFP through the membrane and the dispersion of Wze-Citrine to the cytoplasm. We propagate this mutant strain in the presence of different compounds and identify one that, if present in the growth medium, results in the delocalization of the complex Wzd/Wze and is capable of preventing the full encapsulation of pneumococcal cells. This, and other compounds found through this screening, are candidates for the development of new pneumococcal anti-infective compounds, whose mechanism of action requires further investigation.

4.2 Introduction

Streptococcus pneumoniae is the most common agent of community acquired pneumonia, which is the third leading cause of death worldwide and the major cause of death of children under 5 years old (Marangu and Zar, 2019). Although vaccination strategies against

this pathogen have proven to be successful, cases of serotype replacement observed with particular clinical pneumococcal strains, which can increase the proportion of nonvaccine serotypes found associated with pneumococcal colonization and infection cases, is driving a re-emergence of pneumococcal infections (Hanage et al., 2015). Likewise, the increased expansion of resistance to multiple classes of antibiotics also observed in different pneumococcal isolates confirms the expected *S. pneumoniae* fast adaptation to selective pressure. The rise of antibiotic resistance worldwide prompted the Centers for Disease Control and Prevention (CDC) to consider *S. pneumoniae* a serious and urgent public health threat that demands immediate attention and response (CDC's 2019 Antibiotic Resistance Threats Report). Consequently, the development of anti-infective agents, of new classes of antibacterial drugs, of newer formulations of older drugs and/or the combination of antibiotic agents with other therapeutic options desperately needs to be explored. Bacteria of *S. pneumoniae* use the capsule polysaccharide (CPS), which is essential for pneumococcal virulence, to escape the host's immune system. Therefore, the molecular machineries involved in CPS synthesis and its translocation to the surface of bacteria are an alluring therapeutic target.

Almost all the more than 100 different serotypes that have been described in *S. pneumoniae* carry a highly conserved 5′ end *cps* locus (Ganaie et al., 2020). Amongst the conserved genes, there are those that encode members of a phosphoregulatory system of the capsule synthesis, *wzh*, *wzd*, and *wze*. Wzd and Wze belong to the bacteria-specific BY-kinases (bacterial tyrosine kinases) family. Tyrosine phosphorylation is a regulatory bacterial strategy often involved in the regulation of a myriad of physiological processes, including gene expression, stress response, cell division, and virulence (Klein, Dartigalongue and Raina 2003; Minic et al., 2007; Petranovic et al., 2007; Lacour et al., 2008). Wzd is a transmembrane protein, which may be able to sense and transmit signals from the environment to the cell interior, and Wze is an autophosphorylating tyrosine kinase. The interaction between Wzd and Wze and the ability of the later to bind phosphorylated ribonucleosides, such as ATP, are prerequisites for initial Wze tyrosine autophosphorylation. Also important, is the action of the third protein, the phosphatase Wzh, which can dephosphorylate Wze molecules carrying phosphorylated tyrosines (Morona et al., 2002). The cycling between phosphorylation/dephosphorylation reactions of BY-kinases seem to lead to crucial conformational changes that can affect the

function of other proteins of the CPS synthesis machinery (Morona, van den Bosch and Daniels 2000; Bender and Yother 2001).

The presence of both Wzd and Wze at the division septum is important for pneumococcal bacteria as *wzd* and *wze* null mutants lack CPS, detected through immunofluorescence, at the division septum (Henriques et al., 2011). Moreover, *wze* null mutant and the *wzd* null mutant were dramatically impaired in virulence, in mice and in the zebrafish embryo infection model, respectively, showing that full encapsulation of bacterial cells, covering the entire cell wall, is crucial for virulence (Morona et al., 2004; Figueiredo et al, 2021 submitted).

BY-kinases might be ideal drug targets due to their absence in Eukarya and as they seem to be essential in the control of bacterial growth, capsule synthesis and antibiotic resistance, and due to the crucial role, they play in virulence (Grangeasse et al., 2007; Lee et al., 2008; Sun et al., 2010). Small-molecule drugs capable of targeting human Ser/Thr and Tyr kinases are already used in the clinic to treat cancer (Bhullar et al., 2018). Their clinical success has encouraged the search for similar compounds that can inhibit bacterial kinases. Optimally, these new drugs should be highly selective bacterial kinases and not be able to affect host kinases. Thus, small-molecule kinase inhibitor libraries that are already established, can help find such promising candidates in bacterial studies. High-throughput screenings to find inhibitors of PknB, an essential serine-threonine protein kinase present in *Mycobacterium tuberculosis* using kinase inhibitor libraries, have already been made. However, despite the promising in vitro results observed with some candidate compounds, they presented only a moderate effectiveness in vivo and presented additional concerns due to their toxicity (Lougheed et al., 2011; Chapman et al., 2012). Differences in vitro and in vivo could be due to low cell wall permeability, which will not allow the compound to reach the target molecule present in the bacterial cytoplasm, or the presence of other interaction partners, which are not present in vitro, and that may prevent binding of a compound to the protein target.

In this work, we designed a system that allows the screening for molecules capable of interfering with the localization and interaction of Wzd and/or Wze enzyme, in order to select for compounds capable of interfering with the synthesis of capsule in propagating encapsulated bacteria. We constructed a mutant strain capable of expressing fluorescent Wzd and Wze interacting enzymes, each attached to a different fluorescent protein, enabling the

search for compounds that would either delocalize the complex Wzd/Wze or inhibit their interaction. As a proof of concept, we performed a small screening process and found that the presence of a serine protease inhibitor (Pefabloc SC) in the growth medium, results in the delocalization of the complex Wzd/Wze and is capable of prevent full encapsulation of pneumococcal encapsulated bacteria. These results show that it is possible to identify candidate compounds capable interfering with the CPS synthesis in pneumococcal bacteria.

4.3 Materials and methods

4.3.1 Bacterial strains and growth conditions

The bacterial strains used in this study are listed in Table 4.1. *Streptococcus pneumoniae* bacteria were propagated in C + Y, a semi-chemically defined liquid medium (Lacks and Hotchkiss 1960) at 37˚C, without aeration, or in tryptic soy agar (TSA, Difco) plates supplemented with 5% (v/v) sheep blood (Probiologica). Tetracycline was added to the media at 1 μg/ml final concentration. *Lactococcus lactis* LL108 bacteria were grown in M17 broth (Difco), supplemented with sucrose (0.5 M) and glucose (0.5% w/v) at 30˚C without aeration. When needed, erythromycin (Ery, Sigma Aldrich) was added at final concentration of 100 μg/ml.

Table 4.1: Bacterial strains and plasmids

Name	Relevant Characteristics	Source/Reference
Strains		
Streptococcus pneumoniae		
ATCC6314	Encapsulated strain, serotype 14	American Type Culture Collection
R36A	Non-encapsulated laboratory strain	(Avery, 1944)
BCSMC001	ATCC6314Δ*cps*	(Henriques et al., 2011)
BCSMH001	ATCC6314Δ*wzd*	(Henriques et al., 2011)
BCSMH004	ATCC6314*wze::wzeCitrine*	(Henriques et al., 2011)
BCSJF015	ATCC6314 *wzd::wzd_CFP wze::wzeCitrine*	Master thesis

Name	Relevant Characteristics	Source/Reference
Strains		
BCSJF016	ATCC6314 *wzd::wzdCFP wze::wzeCitrine* pBCSMH017, Tet^r	Master thesis
BCSJF017	ATCC6314 *wzd::wzdCFP wze::wzeCitrine* pBCSLF001, Tet^r	Master thesis
BCSJF033	ATCC6314 *wzd::wzdCFP wze::wzeCitrine* pBCSMH005, Tet^r	This work.
BCSJF034	ATCC6314 *wzd::wzdCFP wze::wzeCitrine* pBCSMH006, Tet^r	This work.
BCSJF035	ATCC6314 *wzd::wzdCFP wze::wzeCitrine* pBCSMH003, Tet^r	This work.
BCSJF036	ATCC6314 *wzd::wzdCFP wze::wzeCitrine* pBCSJF018, Tet^r	This work.
BCSJF037	ATCC6314 *wzd::wzdCFP wze::wzeCitrine* pBCSJF019, Tet^r	This work.
BCSJF038	ATCC6314 *wzd::wzdCFP wze::wzeCitrine* pBCSJF020, Tet^r	This work.
BCSJF044	R36A pBCSJF018, Tet^r	This work.
BCSJF045	R36A pBCSJF019, Tet^r	This work.
BCSJF046	R36A pBCSJF020, Tet^r	This work.
BCSJF047	R36A pBCSJF023, Tet^r	This work.
BCSJF048	R36A pBCSJF024, Tet^r	This work.
BCSJF049	R36A pBCSJF025, Tet^r	This work.
BCSJF052	ATCC6314 *wzd::wzdCFP wze::wzeCitrine* pBCSJF024, Tet^r	This work.
BCSJF053	ATCC6314 *wzd::wzdCFP wze::wzeCitrine* pBCSJF025, Tet^r	This work.
BCSJF057	ATCC6314 *wzd::wzdCFP wze::wzeCitrine* pBCSJF023, Tet^r	This work.
Name	**Relevant Characteristics**	**Source/Reference**
Plasmids		
Streptococcus pneumoniae		
pBCSLF001	High-copy-number vector, contains the −10 constitutive promoter of *SigA* from *S. pneumoniae*, Tet^r	(Henriques et al., 2011)
pBCSMH003	Plasmid allowing expression of Wze-mCherry, Tet^r	(Henriques et al., 2011)
pBCSMH005	Plasmid allowing expression of Wze(WA)-mCherry, Tet^r	(Henriques et al., 2011)
pBCSMH006	Plasmid allowing expression of Wze(Tyr)-mCherry, Tet^r	(Henriques et al., 2011)
pBCSMH017	Plasmid expression of Wze, Tet^r	(Henriques et al., 2011)
pBCSJF018	Plasmid allowing expression of the first 10aa from Wze, Tet^r	This work.
pBCSJF019	Plasmid allowing expression of the first 25aa from Wze, Tet^r	This work.
pBCSJF020	Plasmid allowing expression of the first 50aa from Wze, Tet^r	This work.
pBCSJF023	Plasmid allowing expression of WzeΔN-mCherry, Tet^r	This work.

Name	Relevant Characteristics	Source/Reference
Plasmids		
pBCSJF024	Plasmid allowing expression of WzeΔcentral-mCherry, Tet^r	This work.
pBCSJF025	Plasmid allowing expression of WzeΔC-mCherry, Tet^r	This work.

4.3.2 DNA manipulation procedures

All plasmids used in this study are listed in Table 4.1 and the sequences of the primers used are listed in Table 4.2. Preparation of *S. pneumoniae* competent cells and their transformation with DNA were executed as previously described (Martin et al., 1995). PCR products and plasmid DNA were purified with kits Wizard SV Gel and PCR Clean-up System and Wizard Plus SV Minipreps, respectively (Promega). PCR fragments were amplified with Phusion High-fidelity DNA polymerase (Finnzymes). DNA fragments were digested with restriction enzymes acquired from New England Biolabs and the T4 DNA ligase used was acquired from ThermoFisher.

Table 4.2: Primers used in this work.

Primer	Sequence 5'→3'	Restriction Site
1	GCGGAGCTCTGTTGCTGTTACCAAG	SacI
2	GCGGAGCTCCAGTTTTTTTTGTGCTATTTC	SacI
3	GCGGAGCTCTGTACACAAGGCATTGTAATATTC	SacI
4	GCGGAGCTCAGTTGTTTTTCCTTCCCCAGG	SacI
5	GCGGAGCTCACTACTTCCGTAAATATAG	SacI
6	GTAGAGCTCCATGCTAGCCTACCTCCTTAAG	SacI
7	GATGAGCTCGGTGAGGCGAATAAACGTGATG	SacI
8	GATGAGCTCTGTTTTTCCTTCCCCAGGG	SacI
9	GATGAGCTCGGTACCAGCTCGGCTG	SacI

4.3.3 Construction of plasmids for protein expression in S. pneumoniae

Construction of pneumococcal plasmids that allow the expression of the first 10 aa, 25aa and 50aa of Wze was carried out through the amplification of the plasmid pBCSMH017 with primers 1 and 2-4, respectively, that were restricted with SacI prior their subsequent ligation. This originated plasmids pBCSJF018, pBCSJF019 and pBCSJF020. Plasmid pBCSJF023, which allows expression of WzeΔN protein where the N-terminal domain has been deleted (approximately 50 aa) fused to mCherry, was obtained through the amplification of plasmid pBCSMH003 with primers 5 and 6. For expression of WzeΔcentral where the Central portion has been deleted (approximately 130 aa) fused to mCherry, the pBCSMH003 plasmid was amplified with primers 7 and 8, digested with the appropriate restriction enzyme, subjected to a subsequent ligation, producing plasmid pBCSJF024. Construction of the plasmid encoding WzeΔC, where the C-terminal domain has been deleted (approximately 50 aa) fused to mCherry, was obtained by ligation of the PCR product resulting from the amplification of plasmid pBCSMH003 with primer 1 and 9, originating plasmid pBCSJF025.

The nucleotide sequences of the modified regions of the constructed plasmids were confirmed by sequencing.

4.3.4 Growth assays

S. pneumoniae cells were grown overnight at 37ºC without aeration in semi-defined C+Y liquid medium. When stationary phase was reached, at an $OD_{(600nm)}$~0.8, cultures were diluted to $OD_{(600nm)}$~0.01. The $OD_{(600nm)}$ was measured every 30 minutes.

4.3.5 Microscopy

Cultures of the different *S. pneumoniae* mutant strains used in this work were grown until early exponential phase ($OD_{(600nm)}$=0.2–0.3), harvested, resuspended in fresh C+Y medium and transferred to a thin layer of 1% agarose in PreC medium (Lacks and Hotchkiss 1960). Images resulting from fluorescence microscopy analysis were obtained using a Zeiss Axio Observer Z1 microscope equipped with a Plan-Apochromat objective (100x/1.4 Oil Ph3; Zeiss) and a Photometrics CoolSNAP HQ2 camera (Roper Scientific), with appropriate exposure times

(5000ms for Citrine and CFP, and 100ms for Anti-rabbit Alexa Fluor 594 antibody (Invitrogen)). After acquisition, images were analysed using FIJI software (Schindelin et al., 2012) as well as eHooke software (Saraiva et al., 2021), which was developed in-house (available at https://github.com/BacterialCellBiologyLab/eHooke). Determination of the fluorescence ratio (FR) was performed as previously described (Pereira et al., 2007; Atilano et al., 2010). Briefly, the intensity of the fluorescent signal at the division septum was divided by the fluorescent signal at the peripheral membrane. Average background fluorescence was subtracted from every value. An FR value higher than 2 was considered to be indicative of septal enrichment. Quantification was performed for at least 100 cells of each mutant strain.

To measure the Pearson Correlation Coefficient (PCC) between the signals from the two fluorescent proteins expressed in different mutant strains or when bacteria were propagated in presence of different compounds, images of each fluorescence channel were aligned and loaded side-by-side in the eHooke software. After automatic cell segmentation, cells that showed an Wzd-CFP signal at the septum were selected for PCC measurements. The intensity of the pixels corresponding to each bacterial cell, from the two channels that carry each fluorescence signal (derived from Wzd-CFP or from Wzd-Citrine) were determined and used to calculate the PCC value using an equation adapted from Dunn et al., 2011:

$$\mathrm{PCC} = \frac{\sum_i (X_i - \overline{X})(Y_i - \overline{Y})}{\sqrt{\sum_i (X_i - \overline{X})^2}\sqrt{\sum_i (Y_i - \overline{Y})^2}}$$

in which Xi and Yi correspond to each pixel intensity for two fluorescence channels and $\overline{X}$ and $\overline{Y}$ correspond to the mean intensities of the corresponding channel.

For the screening of compounds capable of interfering with capsule synthesis, which was carried out at different concentrations, the strain BCSJF015 was grown overnight in C+Y medium at 37ºC with no aeration. When the culture reached the stationary phase it was diluted to $OD_{(600nm)}$=0.2. This diluted culture was added to a 96 well plate, which had the compounds to be analysed, at different concentrations, and that was placed at 37ºC for 20 minutes. Using a replica plater, bacteria was then transferred to a microscope slide with an agarose layer, with a width of approximately 0.75mm. A cover slip was placed on top before analysis through fluorescence microscopy.

After performing the screening as explain in Supplementary Figure 4.2, the effect exerted by some candidate compounds were analysed again. However, in this case, compounds were added at different concentrations to Eppendorfs carrying 1ml of the diluted culture at $OD_{(600nm)}$=0.2 that were incubated at 37ºC for 40 minutes before microscopy analysis.

Detection of the capsule produced at the surface of *S. pneumoniae* cells in the presence of selected compounds was performed as previously described (Henriques et al., 2011), using an Anti-rabbit Alexa Fluor 594 antibody (Invitrogen) as a secondary antibody.

4.3.6 Statistical analysis

Statistical analysis of data presented in the figures were done using GraphPad Prism 8 (GraphPad Software). Analysis of data of the Fluorescence ratios (FR) presented in Figures 4.2, 4.4, and 4.5, and of the Area of bacteria in Figure 4.3 was done using a Mann-Whitney Test. P values ≤ 0.05 were considered as significant for all analysis performed and are indicated with asterisks: *P ≤ 0.05, **P ≤ 0.01, ***P ≤ 0.001, and ****P ≤ 0.0001.

4.4 Results and discussion

4.4.1 Development and optimization of a screening method to search for small peptides or compounds that could prevent Wzd/Wze interaction

Wzd is a membrane bound polypeptide, while Wze is a cytoplasmatic protein, but upon interaction, the enzymatic complex formed by these two proteins localizes to the division septum of bacteria (Henriques et al., 2011). We hypothesized that by attaching a different fluorescent protein to each Wzd and Wze interacting partner, it would be possible to verify when they were interacting with each other and how dynamic was this interaction. Thus, we decided to construct a pneumococcal mutant strain, BCSJF015, which produces fluorescent derivatives of Wzd and Wze, from their native genetic locus (Wzd-CFP and Wze-Citrine), allowing the determination of their temporal and spatial localization in live cells. When Wzd-CFP and Wze-Citrine interact, both co-localize at the division septum (Figure 4.1). However, if this interaction is prevented, Wze-Citrine should diffuse into the cytoplasm, as it lost its ability

to bind the partner protein, while Wzd-CFP should spread through the entire membrane (Figure 4.1). We hypothesized that the loss of the co-localization signal could be used to screen for small inhibitory peptides, or different chemical compounds, that either can prevent Wzd/Wze interaction, or delocalize this protein complex, from the division septum of pneumococcal encapsulated bacteria.

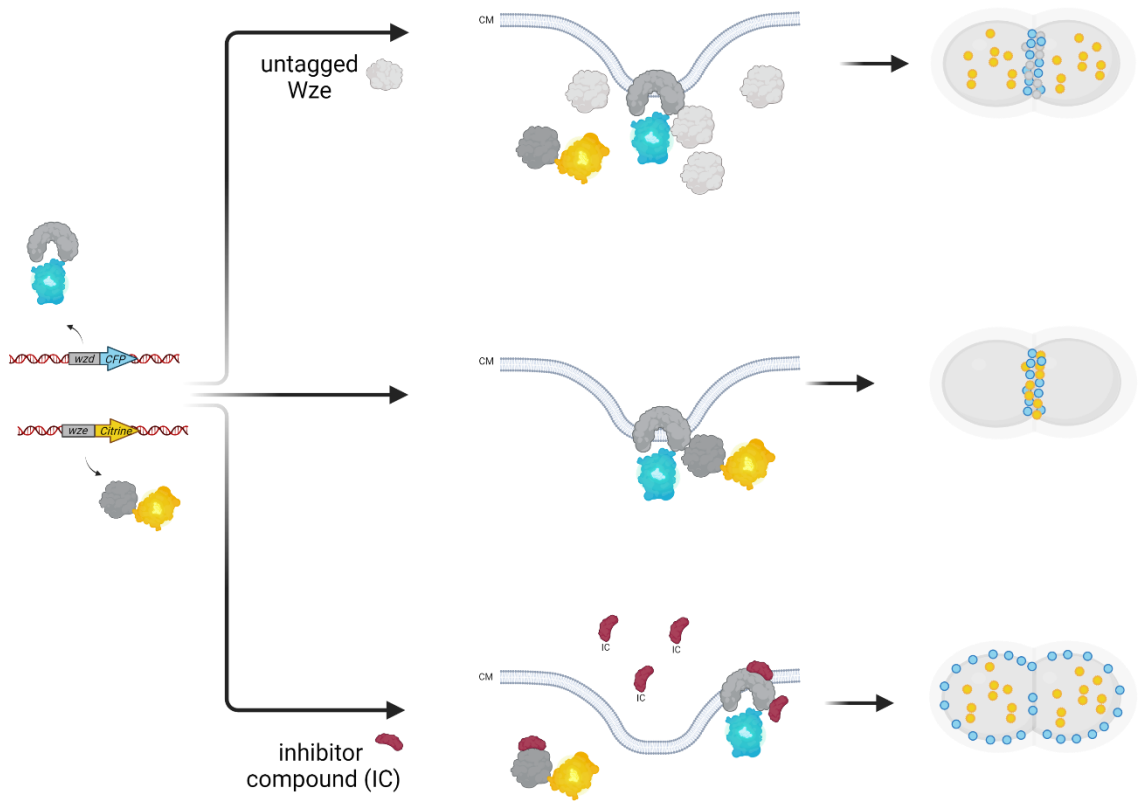

Figure 4.1: Schematic view of the screening method designed to find small inhibitory peptides or inhibitory compounds (IC). Both proteins Wzd and Wze are linked to two different tags (Wzd-CFP in blue and Wze-Citrine in yellow). When membrane tagged-Wzd and cytoplasmic tagged-Wze interact, they localize at the division septum (middle). However, in case there are other non-fluorescent proteins of Wze that are able to interfere with the interaction of the two fluorescent proteins, Wzd-CFP should localize at the division septum, while Wze-Citrine should be dispersed into the cytoplasm (top). If an inhibitory compound (IC in red) is present that is capable of disrupting the Wzd/Wze complex, the Wzd-CFP fluorescence should appear through the entire membrane, while Wze-Citrine fluorescence should be dispersed into the cytoplasm (bottom). CM, cytoplasmic membrane.

We started by confirming the septal localization of Wzd-CFP and Wze-Citrine proteins in our reporter strain BCSJF015 (Figure 4.2A). Then, to validate the screening method, we decided to enquire if the presence of an untagged Wze protein, encoded in a plasmid, could compete with the chromosomal encoded Wze-Citrine, for Wzd-CFP interaction. We observed

that in bacteria expressing Wze, Wzd-CFP kept its septal localization. However, in the same bacteria, Wze-Citrine was delocalized and spread in the cytoplasm. This indicates that both untagged Wze and Wze-Citrine can interact with Wzd-CFP (Figure 4.2A). The presence of the plasmid in BCSJF015 bacteria, or the presence of tetracycline in the growth medium, did not influence the localization of the fluorescent Wzd and Wze proteins as both proteins Wzd-CFP and Wze-Citrine maintained their septal localization (Figure 4.2A).

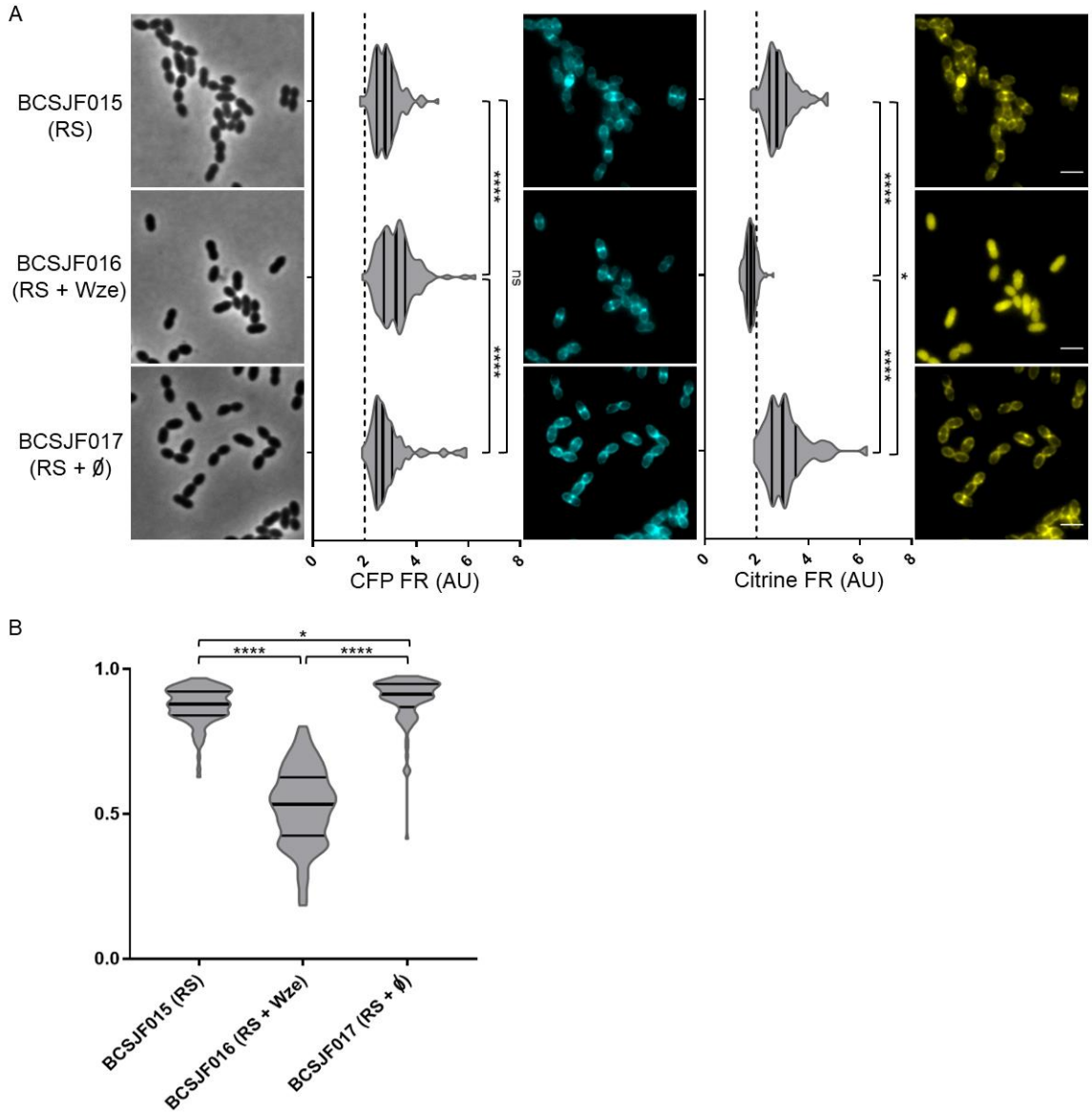

Figure 4.2: Constitutive expression of Wze prevents septal localization of the fluorescent Wze-Citrine being produced from its native *cps* locus. A) Epifluorescence microscopy images of the reporter strain BCSJF015, a derivative of the encapsulated ATCC6314 that was modified to express Wzd-CFP and Wze-Citrine proteins encoded from the *cps* operon (top panels). Also present are microscopy imagens obtained with BCSF015 bacteria transformed with a plasmid encoding for an untagged Wze (BCSJF016)

and with BCSF015 bacteria that had been transformed with the empty vector (BCSJF017). Scale bar, 2 μm. The fluorescence ratio obtained for both CFP and Citrine fluorescence signals, and determined in different pneumococcal bacteria, are shown on the left of each microscopy image. Data are represented in violin plots with the interior horizontal lines representing the median (thick) and the first-to-third quartiles (thin). The number of bacteria analysed are 117 (BCSJF015), 125 (BCSJF016) and 106 (BCSJF017). Statistical analysis was performed using a two-sided Mann–Whitney U test. **** $P < 0.0001$. RS, reporter strain. NS, not significant. AU, arbitrary units. **B)** Pearson Correlation Coeficient (PCC) values between Wzd-CFP and Wze-Citrine fluorescent signals detected in different bacteria from the three strains. A PCC of 1 indicates perfect co-localization of the CFP and the Citrine fluorescence signals. A value of -1 indicates that one protein is only detected when the other signal is absent. Data are represented from 0 to 1 for an easier visualization of the values, in violin plots, in which interior horizontal lines represent the median (thick) and the first-to-third quartiles (thin). The number of bacteria analysed are 117 (BCSJF015), 128 (BCSJF016) and 108 (BCSJF017). Statistical analysis was performed using a two-sided Mann–Whitney U test. **** $P < 0.0001$. RS, reporter strain.

A quantitative analysis of these results was done by determining the ratio of the fluorescence signal at the septum versus the peripheral membrane (FR) of pneumococcal cells from the different strains, as described in the Materials and Methods section. Since the septum contains two membranes, it is considered that FR values higher than ~2 indicate preferential septal localization (Pereira et al., 2007; Atilano et al., 2010). In this case, we observed that the expression of Wze resulted in the delocalization of the fluorescent signal of Wze-Citrine. Only in pneumococcal cells from the BCSJF016 mutant strain was possible to determine an FR value for Wze-Citrine bellow 2, having a median FR value of 1.8 (Figure 4.2A).

The interference exerted by the expression of Wze on the septal localization of Wze-Citrine can be also shown through the analysis of the colocalization between Wzd-CFP and Wze-Citrine fluorescence signals. Therefore, we decided to measure the Pearson's Correlation Coefficient (PCC) between the fluorescent signals from Wzd-CFP and Wze-Citrine proteins, as described in the Materials and Methods section (Figure 4.2B). In the case of a frequent colocalization between the two proteins the value of PCC is expected to be close to 1. This value can decrease to -1 when the presence of one protein always results in the absence of the other. As expected, the median PCC values determined in cells of the BCSJF016 strain, the reporter strain transformed with the plasmid encoding for the untagged Wze, were lower (0.53) than those determined in cells of the reporter strain BCSJF015 (0.88) and in cells of the BCSJF017 strain, the reporter strain transformed with an empty plasmid (0.91). These results show that the presence of a particular molecule (such as the untagged version of Wze, small

peptides, or chemical compounds), when present in the cytoplasm of pneumococcal cells can prevent the interaction between Wzd-CFP and Wze-Citrine (and most likely of the untagged versions), which will result in the mislocalization of the Wzd/Wze complex and in the perturbation of the process of capsule synthesis.

We also enquired if expression of Wzd-CFP and Wze-Citrine in the BCSJF015 reporter strain interferes with the metabolism of the bacterial cell surface or with the expression of the capsular polysaccharide. Growth curves were determined and compared with the parental encapsulated strain ATCC6314 and the strain ATCC6314*wze*::*wzeCitrine* (strain BCSMH004). No significative difference was observed in the growth rates (data not shown), strains have identical duplication times (approximately 30 min for the three strains). We also asked whether bacteria of the BCSJF015 reporter strain presented an altered size or ability to form chains as this would be indicative of altered activity of enzymes involved in the synthesis or degradation of the bacterial cell surface. We observed that BCSJF015 cells did not present filaments but were smaller, compared with the wild-type strain (Figure 4.3A). We further enquired whether the BCSJF015 reporter strain was capable of producing capsule by performing an immunofluorescence assay that could detect this glycopolymer at the surface of pneumococcal cells. In the parental and encapsulated ATCC6314 strain, as well as in the ATCC6314*wze*::*wzeCitrine* strain, the capsule is distributed throughout the surface of the cells. However, cells from the BCSJF015 reporter strain presented a result similar to that observed with cells of the *wzd* null mutant strain, where the capsule is present at the cell surface, but it is absent from the division septum (Figure 4.3B). This suggests that although both Wzd-CFP and Wze-Citrine can interact and co-localize at the division septum, their function or their interaction with other important proteins of the capsule machinery synthesis might be compromised. Therefore, the BCSJF015 reporter strain can be used to screen for small peptides or compounds capable of inhibiting Wzd/Wze interaction or delocalizing the Wzd/Wze complex. In order to screen for inhibitors of the capsule synthesis process, this reporter strain should be improved so that the presence of the fluorescent protein linked to Wzd does not interfere with the ability of bacteria to produce capsule (for example, by expressing iCFP-Wzd protein instead of Wzd-CFP).

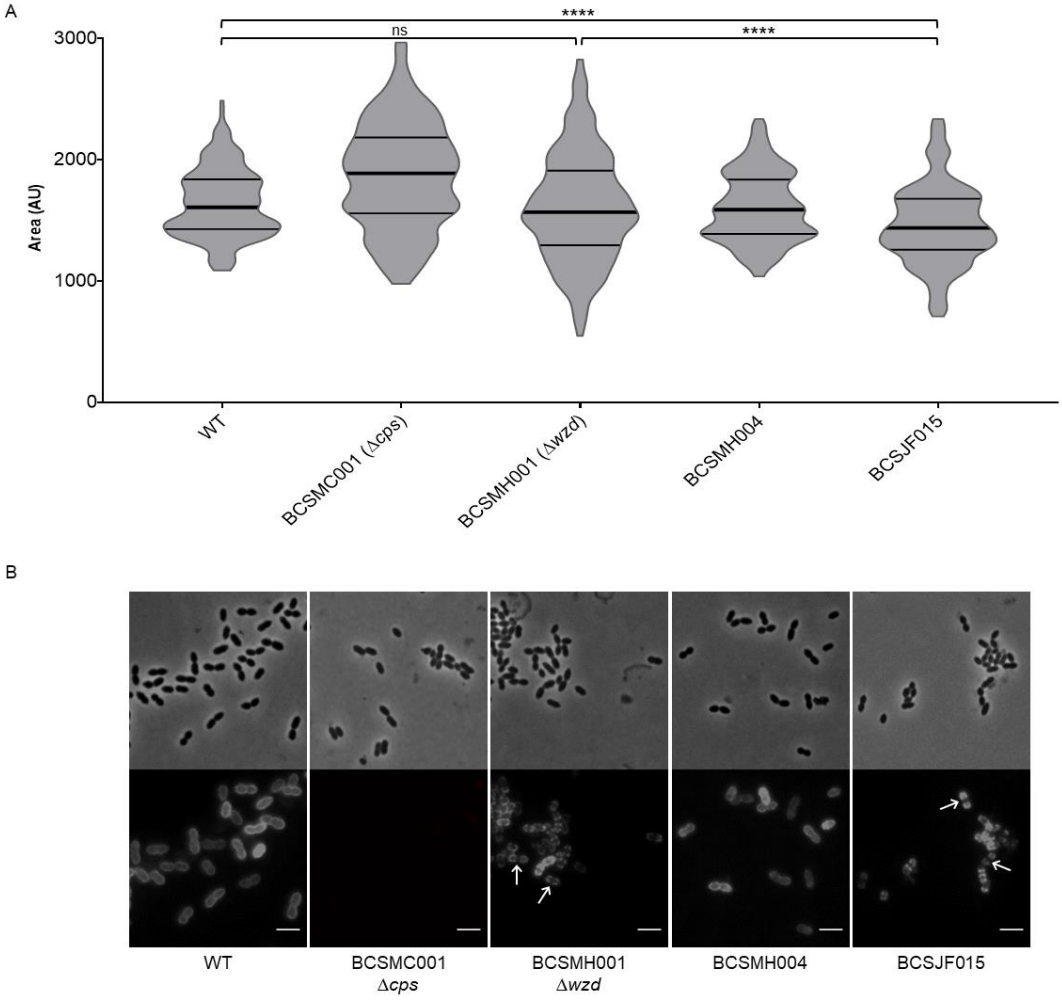

Figure 4.3: Characterization of the reporter strain BCSJF015. A) Phase contrast microscopy images of wild-type ATCC6314 strain (WT), its capsule null mutant (BCSMC001), the *wzd* null mutant (BCSMH001), the BCSMH004 strain, which express Wze-Citrine fluorescent derivative from its native locus and BCSJF015, expression of Wzd-CFP and Wze-Citrine fluorescent derivatives from their native locus, were used to determine cell size. Data are represented in violin plots with the interior horizontal lines representing the median (thick) and the first-to-third quartiles (thin). The number of bacteria analysed are 209 (WT), 137 (unencapsulated strain BCSMC001), 250 (*wzd* null mutant strain BCSMH001), 160 (BCSMH004 which express Wze-Citrine fluorescent derivative from its native locus) and 259 (BCSJF015 which express Wzd-CFP and Wze-Citrine fluorescent derivatives from their native locus). Statistical analysis was performed using a two-sided Mann–Whitney U test. **** $P < 0.0001$. NS, not significant. AU, arbitrary units. The unencapsulated strain BCSMC001 presented bigger cells while the strain BCSJF015 presented smaller cells, compared with the wild-type strain. **B)** Immunofluorescence microscopy images using a serotype-14 specific serum to detect the presence of the capsular polysaccharide at the cell surface. Wild-type encapsulated ATCC6314 (WT) expressed capsule all over the surface, while *wzd* null mutant strain BCSMH001 lacked capsule at midcell (white arrows). The unecapsulated strain BCSMC001 did not present any fluorescence as it is unable to produce the capsular polysaccharide. Bacteria from the BCSMH004 strain, which express Wze-Citrine fluorescent derivative from its native locus, presented a homogeneous distribution of CPS at their surface. However, in BCSJF015, expression of Wzd-CFP and Wze-Citrine fluorescent derivatives from their native locus, results

in bacteria with capsule absent from the division septum, a result that is similar to what happens in the *wzd* null mutant strain (BCSMH001, examples are highlighted by white arrows). Scale bar, 2 μm.

4.4.2 Screening of small peptides with a sequence identical to part of Wze or mutated forms of Wze

To enquire if we would be able to find a small peptide capable of preventing the interaction between Wzd and Wze, which may interfere with capsule synthesis, we started the screening by constructing pneumococcal mutant strains that express small peptides with an amino acid sequence identical to different regions of the Wze protein or that express mutated forms of Wze (Figure 4.4A). We first enquired if the first 10 aa, 25 aa and 50 aa of the protein Wze would be sufficient to compete for Wzd interaction. However, neither of the three tested peptides influenced Wzd-CFP or Wze-Citrine localization, indicating that they could not compete for Wzd-CFP interaction, as shown by FR and PCC values (Figure 4.4B and 4.4C). We further divided the Wze protein into three different segments and enquired whether deletion of each one resulted in a protein still able to compete for Wzd interaction (Figure 4.4A). However, neither of the mutated Wze forms could compete for Wzd interaction suggesting that the three parts of Wze are important for Wzd/Wze interaction (Figure 4.4B and 4.4C). Finally, we decided to test if the activities of either phosphorylation of the C-terminal tyrosine cluster or the binding of phosphorylated ribonucleosides in the Walker A motif, that are associated with the Wze protein, would influence Wze/Wzd interaction. We constructed pneumococcal strains that express Wze where we have mutated the Tyr cluster by substituting the tyrosines for phenylalanines, Wze(Tyr) or that express an altered Wze carrying mutations on the Walker A motif, Wze(WA), a previously described mutated form of Wze in which the Walker A motif is inactivated by the mutations $G_{48}A$ and $K_{49}A$ (Morona et al., 2000a). Using a bacterial two hybrid system, we have previously reported that, unlike Wze(Tyr), the Wze(WA) is not able to interact with Wzd (Henriques et al., 2011). As expected, in our screening, while Wze(Tyr) could interact with Wzd-CFP, promoting the delocalization of the chromosomal-encoded Wze-Citrine, the Wze(WA) mutant could not. These results confirm that for Wzd/Wze interaction, the presence of a functional Walker A motif in Wze is essential, while the ability of Wze to phosphorylate its C-terminal cluster is not.

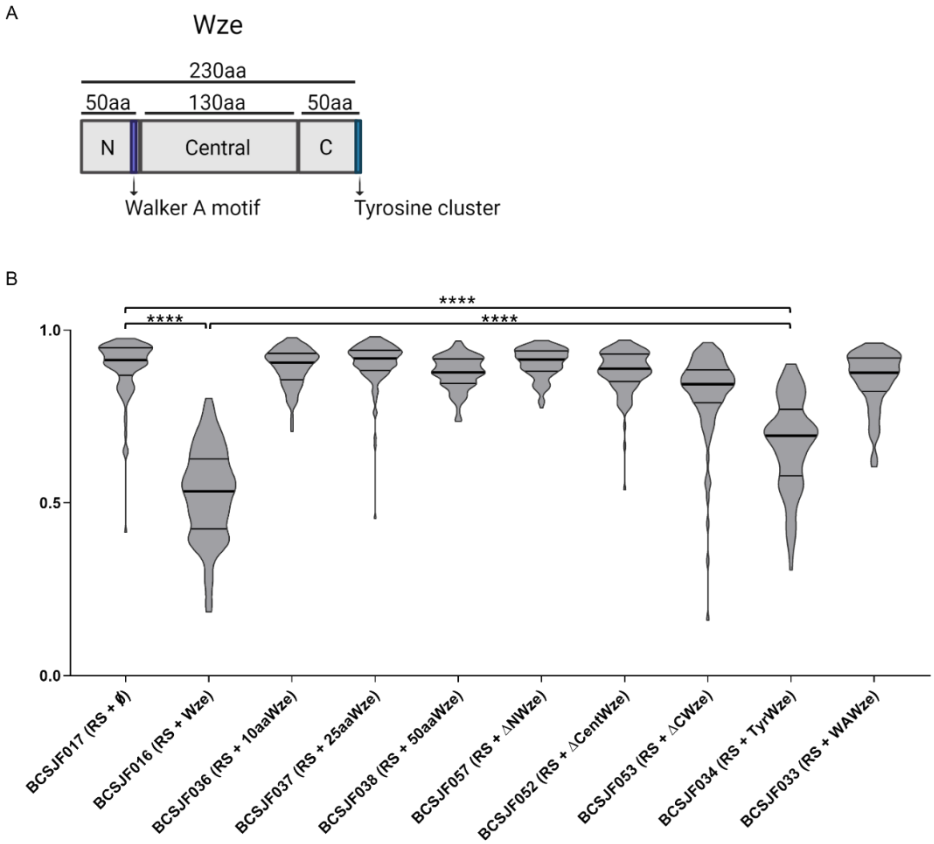
A
Wze
230aa
50aa
130aa
50aa
N
Central
C
Walker A motif
Tyrosine cluster
B
****
****
****
1.0
0.5
0.0
BCSJF017 (RS + ∅)
BCSJF016 (RS + Wze)
BCSJF036 (RS + 10aaWze)
BCSJF037 (RS + 25aaWze)
BCSJF038 (RS + 50aaWze)
BCSJF057 (RS + ΔNWze)
BCSJF052 (RS + ΔCentWze)
BCSJF053 (RS + ΔCWze)
BCSJF034 (RS + TyrWze)
BCSJF033 (RS + WAWze)

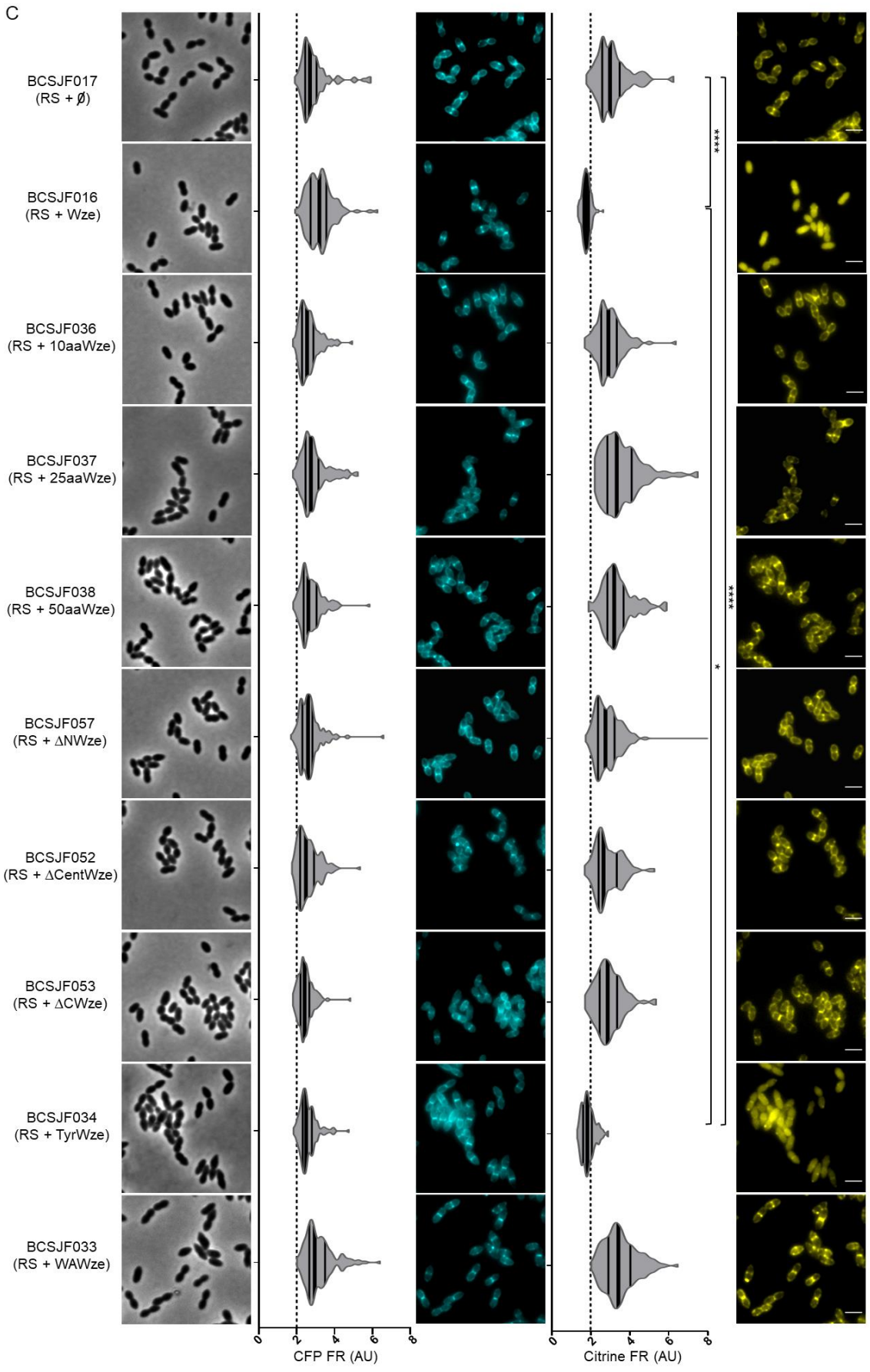
C
BCSJF017
(RS + Ø)
BCSJF016
(RS + Wze)
BCSJF036
(RS + 10aaWze)
BCSJF037
(RS + 25aaWze)
BCSJF038
(RS + 50aaWze)
BCSJF057
(RS + ΔNWze)
BCSJF052
(RS + ΔCentWze)
BCSJF053
(RS + ΔCWze)
BCSJF034
(RS + TyrWze)
BCSJF033
(RS + WAWze)
0
2
4
6
8
CFP FR (AU)
0
2
4
6
8
Citrine FR (AU)
****
***
*

Figure 4.4: Constitutive expression of Wze mutated in the Tyrosine cluster can delocalize the fluorescent Wze-Citrine produced from its native locus, the *cps* operon. A) Schematic representation of Wze divided portions, indicating their length, the position of the Walker A motif and the Tyrosine cluster. **B)** PCC values for Wzd-CFP and Wze-Citrine pair expressed in the same strain considering the whole cell. A PCC of 1 would indicate perfect co-localization and -1 indicate one protein would be absent in the presence of the other. Data are represented from 0 to 1 for an easier visualization of the values, in violin plots, in which the lines inside represent the median (thick) and the first-to-third quartiles (thin). From up to bottom, n = 108, 128, 104, 120, 109, 119, 111, 104, 112, 125. Statistical analysis was performed using a two-sided Mann–Whitney U test. **** $P < 0.0001$. RS, reporter strain. **C)** Epifluorescence microscopy images of the reporter strain BCSJF015 (a derivative of the encapsulated ATCC6314 modified to express Wzd-CFP and Wze-Citrine from the *cps* operon) transformed with plasmids encoding parts or mutated forms of Wze. BCSF016 (encoding for an untagged Wze), BCSJF017 (transformed with an empty vector), BCSJF036 (encoding the first 10aa of Wze), BCSJF037 (encoding the first 25aa of Wze), BCSJF038 (encoding the first 50aa of Wze), BCSJF057 (encoding Wze where the 50aa of the N-terminal portion were deleted), BCSJF052 (encoding Wze where the 130aa of the Central portion were deleted), BCSJF053 (encoding Wze where the 50aa of the C-terminal portion were deleted), BCSJF034 (encoding Wze with the Tyrosine cluster mutated to phenylalanines), BCSJF033 (encoding Wze with Walker A mutated to became inactive). Scale bar, 2 μm. Fluorescence ratio quantifications are shown on the left of each microscopy image. Data are represented in violin plots and the lines inside represent the median and the first-to-third quartiles. From up to bottom, n = 106, 125, 102, 120, 106, 116, 111, 104, 111, 125. Statistical analysis was performed using a two-sided Mann–Whitney U test. **** $P < 0.0001$. RS, reporter strain. AU, arbitrary units.

4.4.3 Screening of several compounds that prevent Wzd/Wze interaction

The next step was to perform the screening for compounds capable preventing Wzd/Wze interaction, using a small library of compounds commercially available, that were tested at different concentrations. In the first selection of compounds, we included antibiotics, sugars, detergents, minerals, protease inhibitors, among others, as shown in Supplementary Figure 4.1.

After performing the screening as explain in Supplementary Figure 4.2, the effect of some of the promising compounds were analysed again. In the confirmation assay, we used 1 ml pneumococcal cultures of the BCSJF015 reporter strain that were exposed to the candidate compounds for a short period of time (40 minutes), in Eppendorf tubes, before performing the analysis by fluorescence microscopy to determine the FR and PCC values of Wzd-CFP and Wzd-Citrine (Figure 4.5).

The analysis of FR values for Wzd-CFP and Wzd-Citrine in the BCSJF015 reporter strain, identified Tetracycline and the Pefabloc SC as compounds capable of decreasing the septal localization of both proteins. Bacteria exposed to Tetracycline showed a median FR value of 2.2 for Wze-Citrine and 2.3 for Wzd-CFP. Both values are lower that the median FR value of 2.8 observed for both Wze-Citrine and Wzd-CFP when the BCSJF015 reporter strain was propagated in C+Y medium. This suggests that Tetracycline can lead to delocalization of both Wze-Citrine and Wzd-CFP from the division septum. However, we also observed that Tetracycline did not influence the PCC value of Wze-Citrine and Wzd-CFP, 0.87 compared to 0.88 from the wild type. This can be explained by the maintenance of the interaction between Wze-Citrine and Wzd-CFP despite their delocalization from the division septum. However, we favour the hypothesis that the FR values are reduced due to the presence of tetracycline, which is a fluorescent compound, in the cytoplasm of pneumococcal cells.

Exposure of bacteria from the BCSJF015 reporter strain to Pefabloc SC resulted in FR values that were lower than those observed with tetracycline (FR of 1.8 for both Wze-Citrine and Wzd-CFP, compared with 2.8 observed with bacteria that were not exposed to the Pefabloc SC compound). The potential ability of Pefabloc SC to cause delocalization of Wze-Citrine and Wzd-CFP from the division septum was confirmed through the determination of the PCC associated with both fluorescent signals. The PCC value was determined to be 0.76 when bacteria were exposed to Pefabloc SC, a lower value than the one observed with bacteria propagated in C+Y, 0.88. This confirmed that not only Wze-Citrine and Wzd-CFP delocalized from the division septum, but their interaction was compromised.

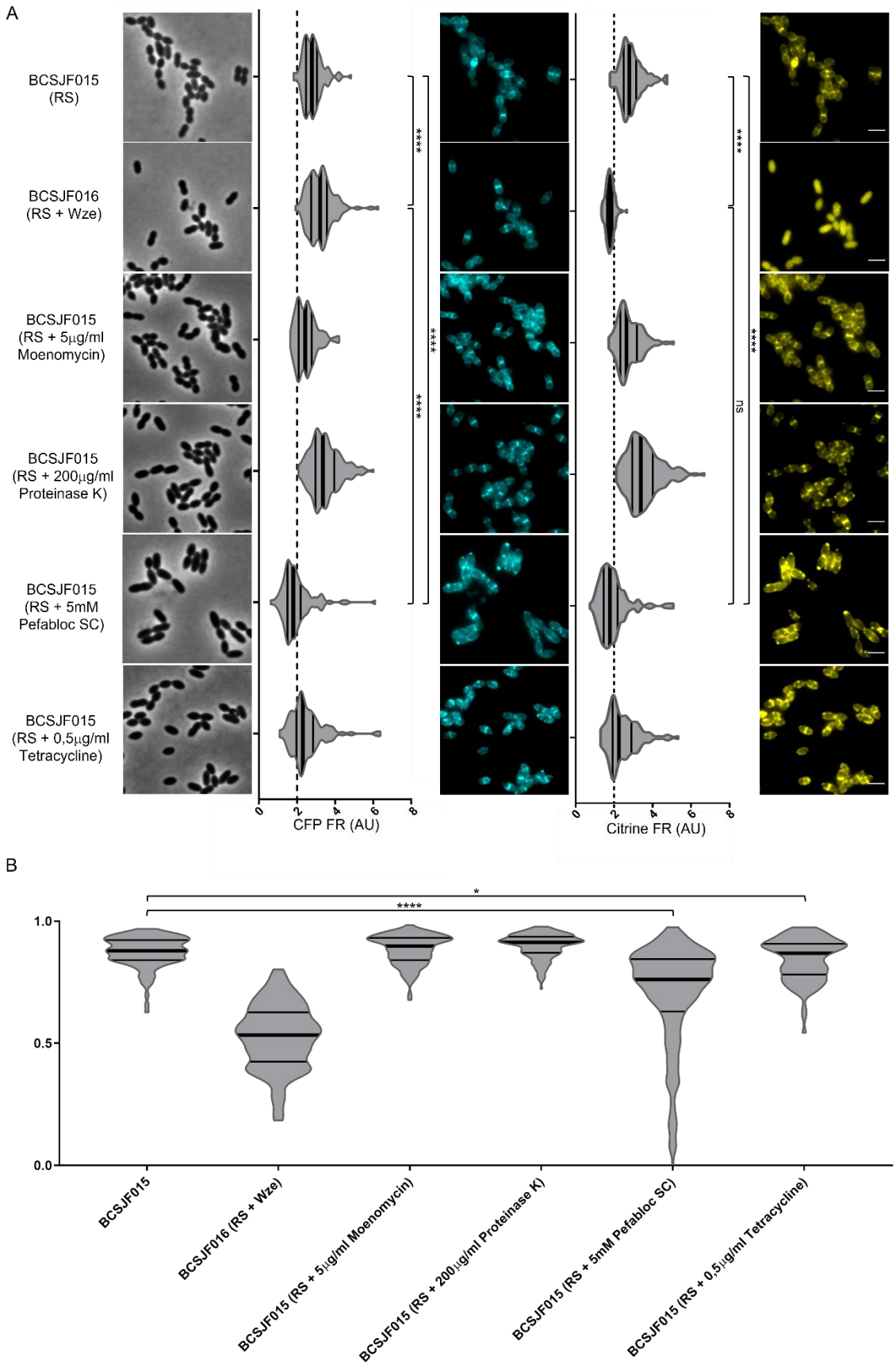
A
BCSJF015 (RS)
BCSJF016 (RS + Wze)
BCSJF015 (RS + 5μg/ml Moenomycin)
BCSJF015 (RS + 200μg/ml Proteinase K)
BCSJF015 (RS + 5mM Pefabloc SC)
BCSJF015 (RS + 0,5μg/ml Tetracycline)
****
****
****
****
ns
0
2
4
6
8
CFP FR (AU)
Citrine FR (AU)
B
*
****
1.0
0.5
0.0
BCSJF015
BCSJF016 (RS + Wze)
BCSJF015 (RS + 5μg/ml Moenomycin)
BCSJF015 (RS + 200μg/ml Proteinase K)
BCSJF015 (RS + 5mM Pefabloc SC)
BCSJF015 (RS + 0,5μg/ml Tetracycline)

Figure 4.5: Screening for compounds capable of hindering Wzd/Wze interaction identified Pefabloc SC. A) Epifluorescence microscopy images of bacteria from the reporter BCSJF015 strain (a derivative of the encapsulated ATCC6314 modified to express Wzd-CFP and Wze-Citrine from the *cps* locus) that were exposed to different compounds added to the growth medium. The compounds tested were, from up to bottom, Moenomycin (at 5μg/ml), Proteinase K (at 200μg/ml), Pefabloc SC (at 5mM) and Tetracycline (at 0.5μg/ml). Also included are the results obtained with BCSF016 strain (the Reporter Strain (RS) expressing an untagged Wze). Scale bar, 2 μm. Fluorescence ratio quantifications are shown on the left of each microscopy image. Data are represented in violin plots and the lines inside represent the median (thick) and the first-to-third quartiles (thin). From up to bottom, n = 117, 125, 105, 170, 106, 111. Statistical analysis was performed using a two-sided Mann–Whitney U test. **** P < 0.0001. RS, reporter strain. AU, arbitrary units. **B)** PCC values for the fluorescent signals from the Wzd-CFP and Wze-Citrine pair determined in different bacterial cells from the same strain. A PCC of 1 indicates a perfect co-localization between both CFP and Citrine values. A value of -1 indicates that one fluorescent signal is only observed if the other is absent. Data are represented from 0 to 1 for an easier visualization of the values, in violin plots, in which the lines inside represent the median (thick) and the first-to-third quartiles (thin). From left to right, n = 117, 128, 112, 171, 228, 112. Statistical analysis was performed using a two-sided Mann–Whitney U test. **** P < 0.0001. RS, reporter strain.

Pefabloc SC is a specific, potent, and irreversible inhibitor of serine proteases and it is nontoxic to cells, so it can be used on living cells. This compound belongs to the family of sulfonyl fluorides and has an activity comparable with PMSF or DFP. Furthermore, Pefabloc SC was also described as a potent serine threonine phosphatase inhibitor (Mintz et al., 1993; Dentan et al., 1996).

The discovery of Pefabloc SC as a possible candidate to inhibit Wzd and/or Wze shows that the screening method designed might be a powerful tool to successfully find other inhibitory compounds that could possibly be tested and help in the fight of pathogenic bacteria.

4.4.4 Effect of Pefabloc SC in capsule synthesis

After the discovery of Pefabloc SC as a potential inhibitor of Wzd/Wze interaction, we decided to confirm the effect of this protease inhibitor in the synthesis of the capsule in encapsulated bacteria. Therefore, we performed an immunofluorescence assay to enquire if the presence of Pefabloc SC in the medium alters the ability of bacteria to produce a cell surface fully concealed by the capsule (Figure 4.6). In the wild-type strain ATCC6314 the capsule covers the hole cell, but when Pefabloc SC is added to the medium it is possible to

see a decrease or even absence of capsule at the division septum. This could mean that this compound might decrease capsule synthesis, implicating a decrease in virulence. In the case of *wzd* null mutant and BCSJF015, that present an absence of capsule at the division septum, in the presence of Pefabloc SC cells seem to have even less capsule around and the absence of capsule at the septum appears larger. All together these results demonstrate that Pefabloc SC has an effect on the synthesis of the capsule which, among other things, might result from the delocalization of the complex Wzd/Wze and the inhibition of their interaction.

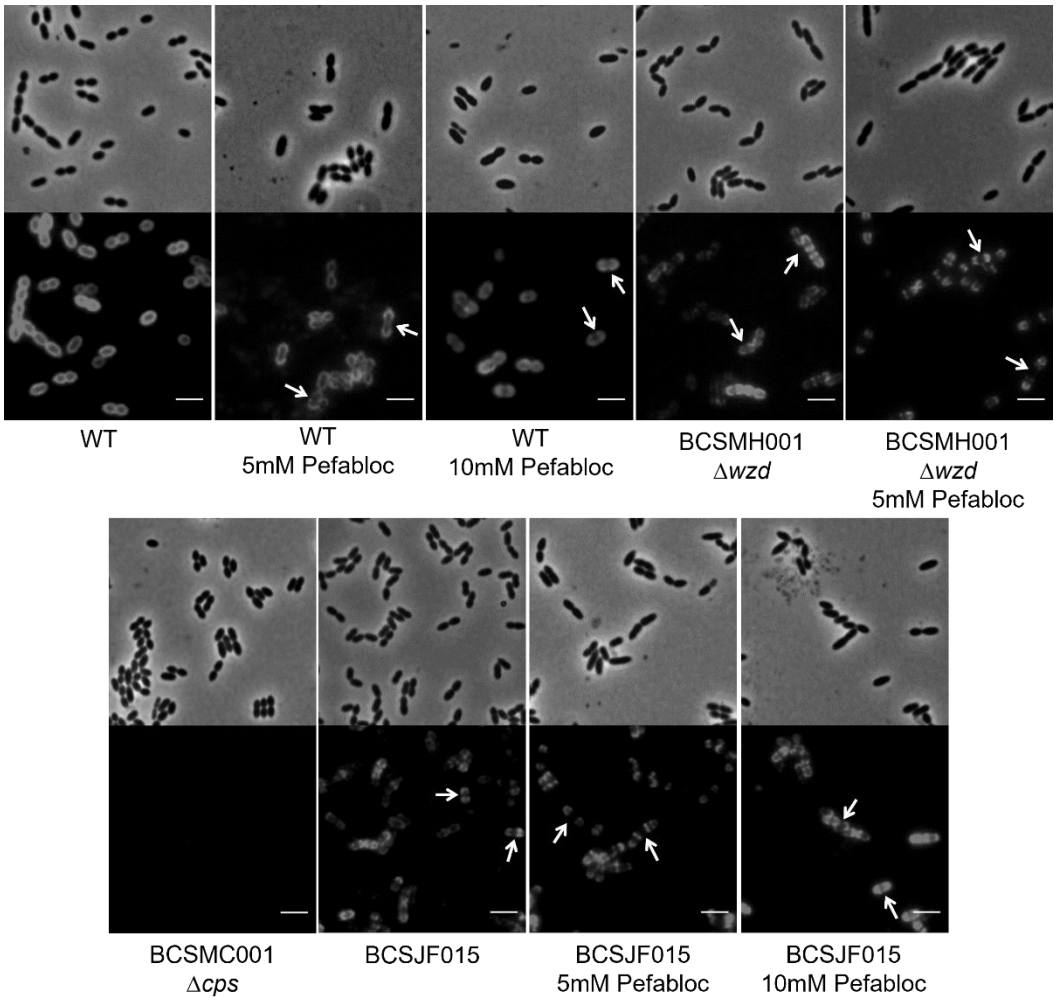

Figure 4.6: Pefabloc SC diminishes the synthesis of the capsule at the division septum. Immunofluorescence microscopy images using a serotype-14 specific serum to detect the presence of the capsular polysaccharide at the cell surface. Wild-type encapsulated ATCC6314 expressed capsule all over the surface, while *wzd* null mutant strain BCSMH001 lacked capsule at midcell. The unecapsulated strain BCSMC001 did not present any fluorescence. In the strain BCSJF015, expressing Wzd-CFP and Wze-Citrine fluorescent derivatives from their native locus, the capsule is absent from the division septum, similar to what happens in the *wzd* null mutant strain (examples are highlighted by white arrows). In the presence of Pefabloc SC the wild-type strain seems to have less capsule or even absence

of capsule at the septum, and the *wzd* null mutant and BCSJF015 showed even bigger gaps of capsule at the septum. Scale bar, 2 μm.

4.5 Final remarks

Despite the discovery of antibiotics and the development of vaccines against *Streptococcus pneumoniae*, the emergence of antibiotic resistance and serotype replacement observed among clinical pneumococcal isolates may compromise the current strategies that are used to tackle with pneumococcal infections. Here, we have designed a method that can screen for compounds capable of causing delocalization of the complex Wzd/Wze from the dividing septum, or that are capable of inhibiting the interaction between Wzd and Wze. Wzd and Wze belong to a phosphoregulatory system that control the synthesis of the capsular polysaccharide in most encapsulated pneumococcal strains. The dysregulation of the Wzd/Wze role leads to the absence or diminishment of capsule at the septum, which represents a major decrease in virulence probably by facilitating exposure of bacteria host immune defenses.

In this work, as a proof of concept, we found a promising candidate compound that may result in the inhibition of the Wzd/Wze interaction, Pefabloc SC. How this protease inhibitor is capable of not only delocalize Wzd/Wze from the dividing septum but also of hinder their interaction is currently being tackled. Moreover, using an immunofluorescence assay we observed a diminish of capsule at the septum in the wild-type strain ATCC6314 when Pefabloc SC is added to the medium. The next step will be to prove if this compound really has an impact on virulence, and to do a high throughput screening of other possible candidates perhaps using compound libraries already described.

4.6 Supplementary information

	1	2	3	4	5	6	7	8	9	10	11	12
A	Control	Control	Control	Control	Tetracycline 0,01µg/ml	Tetracycline 0,1µg/ml	Tetracycline 0,5µg/ml	Tetracycline 1µg/ml	-	-	-	-
B	Tunicamycin 0,5µg/ml	Tunicamycin 1µg/ml	Tunicamycin 7,5µg/ml	Tunicamycin 15µg/ml	Mitomycin C 0,001mg/ml	Mitomycin C 0,005mg/ml	Mitomycin C 0,01mg/ml	Mitomycin C 0,05mg/ml	-	-	-	-
C	Moenomycin 0,25µg/ml	Moenomycin 0,5µg/ml	Moenomycin 1µg/ml	Moenomycin 5µg/ml	Choline 0,5%	Choline 1%	Choline 2%	Choline 5%	-	-	-	-
D	Glucose 1%	Glucose 5%	Glucose 10%	Glucose 15%	Magnesium 1mM	Magnesium 5mM	Magnesium 10mM	Magnesium 20mM	-	-	-	-
E	EDTA 10mM	EDTA 25mM	EDTA 50mM	EDTA 75mM	Imipenem 0,15µg/ml	Imipenem 0,25µg/ml	Imipenem 0,5µg/ml	Imipenem 1µg/ml	-	-	-	-
F	Proteinase K 0,4µg/ml	Proteinase K 10µg/ml	Proteinase K 100µg/ml	Proteinase K 200µg/ml	Triton X-100 0,1%	Triton X-100 0,5%	Triton X-100 1%	Triton X-100 2%	-	-	-	-
G	Protease inhibitor cocktail diluted	Protease inhibitor cocktail diluted	Protease inhibitor cocktail 7x concentrated	Protease inhibitor cocktail 7x concentrated	Pefabloc SC 0,5mM	Pefabloc SC 1mM	Pefabloc SC 5mM	Pefabloc SC 10mM	-	-	-	-
H	Irgasan 0,1%	Irgasan 0,5%	Irgasan 1%	Irgasan 2%	Xilose 1%	Xilose 5%	Xilose 10%	Xilose 15%	Control	Control	-	-

Supplementary Figure 4.1: 96 well plate with the compounds and concentrations screened. The control (BCSJF015 with only C+Y medium) is repeated at the end of the plate to make sure that the time spent on taking photographs of each compound at different concentrations does not influence the result observed.

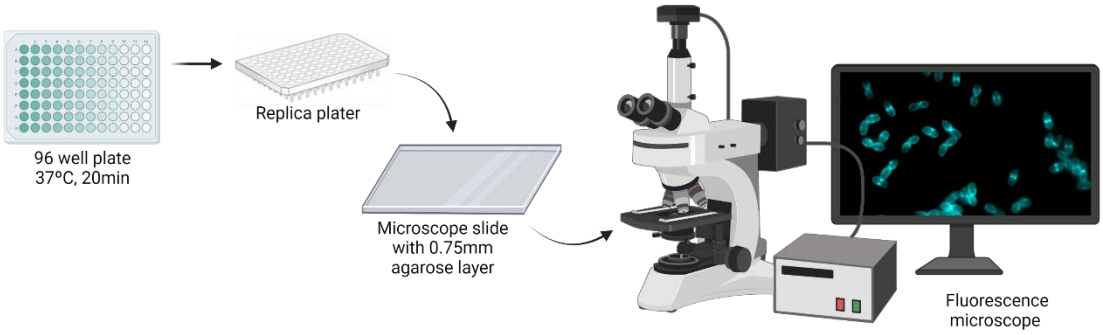

Supplementary Figure 4.2: Method for the screening of numerous compounds at various concentrations. After overnight growth and then dilution, the strain BCSJF015, a derivative of the encapsulated ATCC6314 modified to express Wzd-CFP and Wze-Citrine from the *cps* operon, is added to a 96 well plate at an $OD_{(600nm)}$=0.2. Then, several compounds at the different concentrations are added and the plate is placed at 37ºC for 20 minutes. Using a replica plater, bacteria are then transferred to a microscope slide with approximately 0.75mm agarose layer and then the cover slip is placed on top. Then, it is ready to be observed under the microscope.

Chapter 5

Conclusion and future perspectives

In order to find new and more efficient strategies to fight bacterial infections a full comprehension of how bacteria interact and survive inside the host is crucial. To be able to achieve this goal, the study of mechanisms essential for virulence and their regulation is of upmost importance. Specifically, the elucidation of the function and role of proteins that belong to molecular machineries involved in division, survival, and virulence, will probably revolutionize our capacity to fight bacterial pathogens. The determination of the subcellular localization of these molecular machineries, or the identity of the elements that share the same localization, can frequently help to understand how a specific protein contribute to viability of bacteria or to the strategies used by these microorganisms to interact with the infected host. Consequently, to enhance the toolbox available for in vivo studies of protein localization, as well as of spatial and temporal dynamics between proteins, we developed a set of plasmids which significantly improved the expression of N- terminal fusions of proteins of interest. For that, we designed a tag that increases translation efficiency of heterologous proteins, the i-tag. In this thesis, we showed that these new tools can be used in several Gram-positive bacteria, namely *S. aureus*, a pathogen of great clinical importance, *B. subtilis*, a well-known Gram-positive bacterial model, or *L. lactis*, a microorganism of great industrial interest, which suggests that the tools we have developed have widespread applications. Moreover, we also optimized the sequence of the i-tag in order to maximize the production of the Citrine fluorescent protein in *S. pneumoniae* by manipulating the structure and expected stability of the mRNA 5′ end encoded by the i-tag (Catalão et al., 2014). Kudla et al. showed that the stability of the mRNA folding at the 5′ end of the mRNA transcripts plays a major role in the translation initiation, determining the translation rate and consequently the total amount of protein produced (Kudla et al., 2009). With our work, we propose that the determination of minimum free energy predicted for the 5′ end of the mRNA molecules originated by the introduction of the different tags may predict whether the expression of a specific fluorescent protein will be successful. This knowledge could ultimately be used for other proteins or applications, guaranteeing higher levels of protein expression. We hope that the use of these tools might accelerate new discoveries and answer many questions the scientific community is eager to answer. Hence, holding this improved toolbox, we decided to use it in our research, particularly for the study of *Streptococcus pneumoniae* capsule synthesis.

Streptococcus pneumoniae can colonize its host, generally asymptomatically, in a healthy carriage mode. However, with the right conditions, it can become an opportunist

pathogen. It is still unclear how it regulates its own metabolism to be able to switch between the two lifestyles and what triggers this change between the two modes of host interaction. One most noteworthy feature is its capacity to regulate capsule synthesis to select the level of expression that best suits it – a thicker capsular polysaccharide to help migration through the mucus and its escape from the host immune system, a thinner capsule to permit exposure of adhesins, which seems to be required so that they can adhere to the host epithelium. The capsular polysaccharide, a key virulence factor and a major component of the cell wall, surrounds the pneumococcal bacterial cells, meaning that it is the first contact between *Streptococcus pneumoniae* and its host. In fact, the capsular polysaccharide is essential for the ability of pneumococcus to cause invasive disease, since less encapsulated or non-encapsulated strains are less virulent or avirulent (Magee et al., 2001; Hyams et al., 2010; Wu et al., 2016). Therefore, unravelling how regulation of the capsule synthesis occur may lead us one step forward to connect the dots and understand the relationship between these bacteria and its host.

Streptococcus pneumoniae has a phosphoregulatory system that is constituted by Wzh, Wzd and Wze proteins and that controls capsule synthesis. The genes that encode these three proteins are localized at the beginning of the *cps* operon and are conserved in almost all the more than 100 different *Streptococcus pneumoniae* serotypes described. Wze is an autophosphorylating tyrosine kinase that belongs to the Bacterial Tyrosine Kinase family and, at its C- terminal end, has several tyrosine residues, a "tyrosine cluster", that can be phosphorylated. Wzd is a membrane protein required for the autophosphorylation of Wze (Grangeasse et al., 2007; Bender and Yother, 2001). On the other hand, Wzh is a phosphotyrosine protein phosphatase of the PHP family that dephosphorylates Wze (Morona et al., 2002). Wzd and Wze have been proposed to be spatial regulators of capsule synthesis. These two proteins interact and localize at the division septum granting the accurate synthesis of the capsule at that place. In the absence of Wzd or Wze, capsule is synthesized and attached to the cell wall, but it is absent from the division septum, the site where cell wall synthesis occurs during division (Henriques et al., 2011). It is proposed that cycles of phosphorylation/ dephosphorylation of Wze can trigger a conformational switch that regulate capsule synthesis by affecting the activity of other protein components of the polysaccharide assembly machinery. Wzd is a membrane protein with two transmembrane domains and an N- and C-terminals cytoplasmatic ends. Nourikyan et al. showed that the C-terminal cytoplasmic end of

Wzd is responsible for the Wzd/Wze interaction and, consequently, for the autophosphorylation activity of Wze and its localization at the division septum (Nourikyan et al., 2015). But how Wzd/Wze complex control CPS synthesis is still not completely understood. We hypothesized that the complex Wzd/Wze either recruit other proteins important for the CPS synthesis to the division septum and/or they interact and activate other proteins important for the CPS synthesis that localize at the division septum (Henriques et al., 2011). In accordance with both these hypotheses are the results obtained by Nourikyan et al. that show that in the absence of Wzd C-terminal cytoplasmic end, or in the absence of Wze, the capsule polymerase Wzy is partially delocalized from the division septum. Additionally, the substitution of the C-terminal tyrosine residues of Wze by phenylalanines, which prevents Wze phosphorylation, results in bacteria with Wze localized at the division septum despite its phosphorylation state. This mutant has a hampered CPS production at the division septum and a partially delocalized Wzy from the septum (Nourikyan et al., 2015).

In this work, we present results that highlight the importance of the Wzd/Wze complex in spatial regulation of the CPS synthesis – by regulation of the septal localization and/or activation of additional proteins involved in the CPS synthesis. We demonstrated that Wzd can interact with Wzg, which is proposed to attach capsular polysaccharide to cell wall peptidoglycan, and that the prevention of this interaction affects the septal localization of Wzg. In the parental encapsulated ATCC6314 strain, we were able to observe that a fluorescent derivative of Wzg was enriched at the septum. However, in mutant strains that lack the *csp* operon, the *wzd* or the *wze* genes, the protein Wzg was not enriched at the division septum. These results, together with those from the Bacterial Two-Hybrid assay indicate that Wzg may be recruited to the division septum by Wzd, so that it can attach the capsular polysaccharide to the recently assembled PGN present at that site. Several reports show that in the absence of Wzg, the capsule is still produced and localized all around the bacterial cells, but with reduced amount of CPS and different levels between cells (Morona et al., 2004; Eberhardt et al., 2012). These results suggest that in the absence of Wzg, other ligases may take its role and attach the capsular polysaccharide to the peptidoglycan. The fact that *wzg* null mutant presents capsule attached to the cell wall is another result that indicates that LCP proteins, like Wzg, have semi-redundant roles, as suggested before for other proteins of this family (Hanson, Lowe and Neely, 2011; Over et al., 2011). Considering the results obtained by Nourikyan et al. and the data presented in this work we can conclude that Wzd and Wze guarantee that the *S.*

pneumoniae cell wall is completely surrounded and protected by the capsular polysaccharide during the entire cell cycle (Nourikyan et al., 2015). It is tempting to propose that Wzd/Wze, by recruiting Wzy, is able to control the elongation of the CPS chain and that by recruiting Wzg is able to regulate its attachment to the peptidoglycan.

Taking into account the role of Wzg in attaching CPS to the cell wall we wondered if the correct localization of Wzg and the timing of linking the CPS to the pneumococcal surface may be important for the survival of bacteria. In fact, what are the consequences for the bacteria if these organisms produce reduced levels of capsule and/or if the produced capsule is not homogeneously distributed through the entire cell surface and is absent from a particular subcellular site, such as the division septum? We speculated that septal enrichment of Wzg may be essential to ensure that CPS attachment rate occurs synchronously with PGN synthesis rate at the division septum. In the case of the *wzd* null mutant, in which Wzg is not enriched at the septum, the synchronization of PGN synthesis and CPS attached to PGN is altered as *S. pneumoniae* cells synthesize PGN at the septum which is not immediately concealed by CPS. This most likely results in cells carrying at their surface, molecules of WTA or PGN that are exposed, at the division septum, to external binding proteins. In agreement with this hypothesis, we observed that the *wzd* null mutant bound at its surface higher amounts of the PGN hydrolase LytA when compared with the parental fully encapsulated ATCC6314 strain. Additionally, the *wzd* null mutant strain was more susceptible to lysis by LytA than the fully encapsulated parental strain. Moreover, the increased exposure of the *wzd* null mutant to external receptors results in bacteria that have their virulence, in a zebrafish embryo infection model, dramatically impaired. This shows that full encapsulation of bacterial cells, covering the entire cell wall, is crucial for the strategies bacteria use to interact with the infected host. The same result, a significant reduction of virulence, was observed for the *wze* null mutant in mice, using both systemic and intranasal models of infection (Morona et al., 2004). Additionally, the *wze* null mutant that produces an enzyme where the C-terminal tyrosine residues have been substituted by phenylalanines, to impair the ability of the enzyme for autophosphorylation, was able to cause systemic disease in mice after intraperitoneal infection, but not after intranasal infection. This suggests that a loss of control of CPS synthesis regulation, via phosphorylation/ dephosphorylation of the tyrosines in the tyrosine cluster of Wze, impacts the capacity of *S. pneumoniae* to translocate from the lungs into the bloodstream (Morona et al., 2004). In light of all of these results we conclude and emphasize that the pair Wzd/Wze are

key elements in capsule synthesis that orchestrate and coordinate all steps for a correct and full encapsulation of pneumococcal bacterial cells. Nevertheless, some questions remain to be elucidated, for example (Grangeasse, 2016): how does Wzd/Wze/Wzh regulate the capsule assembly machinery? During the cell cycle, is there a hierarchical order for the phosphorylation of Wze targets? What is the molecular mechanism that synchronizes and coordinates PGN synthesis and CPS production?

As mentioned earlier, *S. pneumoniae* is an opportunist pathogen and a frequent cause of community-acquired pneumonia, which is a leading cause of morbidity and mortality worldwide (Welte and Köhnlein, 2009). Two strategies to fight bacterial infections have been frequently established and, until now, have been successful: the generalized use of an increasing diversified repertoire of antibiotics and the development of vaccination programs that employ different types of vaccines. However, with the emergence of resistance to multiple classes of antibiotics and serotype replacement observed in clinical isolates, it is imperative to promote the development of new classes of drugs that are capable of eliminating this pathogen or of preventing its ability to infect the host. Several lines of research are currently trying to develop new tactics capable of uncovering an Achilles heel of bacteria and to find new ways of tackling bacterial infections. Some of the most inventive and/or already developed proposals include: 1- The development of infection-killing polymers. It has been reported that a star shaped polymer, which is toxic to bacteria due to a multimodal antimicrobial mechanism, has the ability to rip apart their cell walls by disrupting the integrity of the outer membrane and the cytoplasmic membrane, unregulating ion efflux/influx and inducting apoptotic-like death (Lam et al., 2016); 2- The transformation of existing drugs. These re-engineer antibiotics, obtained by changing their structure to make them more powerful and more effective, may be used to prevent expression of resistance in bacteria and improve the durability of antibiotics. Vancomycin has been one antibiotic that scientists have successfully modified (Wu, Cameron and Boger, 2018). Moreover, already in progress, there is the use of super-computing to calculate parameters associated with alterations in the structure of candidate molecules that permits to make new and improved antibiotics from the existing ones (König et al., 2021). 3- Using organisms that are unable to damage the infected host but that can be used as weapons against bacteria. Bacteriophages, viruses that can invade and kill bacteria, might be manipulated in order to better target and destroy specific bacterial organisms. Phage therapy has been studied for a long time and, in some countries like Georgia,

Poland and Russia, it is already being used therapeutically to treat bacterial infections that do not respond to conventional antibiotics (Mousavi et al., 2021; Międzybrodzki et al., 2018). 4- Molecular tweezers, unique supramolecular artificial receptors, that modulate biofilm formation by *Staphylococcus aureus.* These tweezers may complement antibiotic treatment of bacterial infections as it constitutes a platform for disrupting the assembly of bacterial functional amyloid peptides and bacterial biofilms (Malishev et al., 2021). All these studies demonstrate the effort that the scientific community is spending on tackling with the current need of finding new bacterial disease-fighting strategies. In this work, we also developed an easy strategy to find drugs that are capable of interfering with the Wzd/Wze interaction, or its septal localization, and that can prevent the complete encapsulation of pneumococcal cells. This in vivo screening was possible through the construction of a mutant *S. pneumoniae* strain that is capable of expressing fluorescent Wzd and Wze interacting enzymes, each attached to a different fluorescent protein. The dysregulation of the Wzd/Wze role leads to the absence or to the diminishment of capsule at the septum, which is associated with a major decrease in virulence, probably by facilitating exposure of bacteria to host immune defenses. As a proof of concept, we propagated this mutant strain in the presence of different compounds to find a promising candidate that might result in the inhibition of the Wzd/Wze interaction. We have observed that the presence of Pefabloc SC, a protease inhibitor, results in the delocalization of Wzd/Wze from the dividing septum of pneumococcal bacteria. How this molecule hinders the interaction of these two proteins is currently being tackled. Furthermore, we also tested the effect of Pefabloc SC in the parental wild-type fully encapsulated ATCC6314 strain. Using an immunofluorescence assay we observed that the addition of Pefabloc SC to the medium of a ATCC6314 culture, results in bacteria with a reduction of capsule at the septum, which shows that this compound is capable of preventing the full encapsulation of pneumococcal cells. Next, we would like to prove if this compound really has an impact on virulence, and to do a high throughput screening of other possible candidates.

The results obtained in this thesis have contributed to the elucidation of the capsular synthesis process in *S. pneumoniae* and I hope that the development of the tools here described may help in the study of how these bacteria divide and survive, in liquid cultures and inside the host, leading to the discovery of new anti-microbial drugs.

REFERENCES

Abdullahi O, Karani A, Tigoi CC et al. The prevalence and risk factors for pneumococcal colonization of the nasopharynx among children in Kilifi district, Kenya. *PLoS One* 2012; 7(2):e30787, doi: 10.1371/journal.pone.0030787.

Abeyta M, Hardy GG, Yother J. Genetic alteration of capsule type but not PspA type affects accessibility of surface-bound complement and surface antigens of *Streptococcus pneumoniae*. *Infect Immun* 2003 Jan;71(1):218-25. doi: 10.1128/IAI.71.1.218-225.2003.

Abràmoff MD, Magalhães PJ, Ram SJ. Image processing with ImageJ. *Biophotonics International* 2004;11: 36–42.

Acebo P, Nieto C, Corrales MA et al. Quantitative detection of *Streptococcus pneumoniae* cells harbouring single or multiple copies of the gene encoding the green fluorescent protein. *Microbiology* 2000 Jun;146 (Pt 6):1267-1273. doi: 10.1099/00221287-146-6-1267.

Aguiar SI, Brito MJ, Gonçalo-Marques J et al. Serotypes 1, 7F and 19A became the leading causes of pediatric invasive pneumococcal infections in Portugal after 7 years of heptavalent conjugate vaccine use. *Vaccine* 2010 Jul 19;28(32):5167-73. doi: 10.1016/j.vaccine.2010.06.008.

Almeida ST, Paulo AC, Froes F, de Lencastre H, Sá-Leão R. Dynamics of pneumococcal carriage in adults: a new look at an old paradigm. *J Infect Dis*. 2021 May 20;223(9):1590-1600. doi: 10.1093/infdis/jiaa558.

Andam CP, Hanage WP. Mechanisms of genome evolution of Streptococcus. *Infect Genet Evol* 2015 Jul;33:334-42. doi: 10.1016/j.meegid.2014.11.007.

Arnaud M, Chastanet A, Debarbouille M. New vector for efficient allelic replacement in naturally nontransformable, low-GC-content, Gram-positive bacteria. *Appl Environ Microbiol* 2004 Nov;70(11):6887-91. doi: 10.1128/AEM.70.11.6887-6891.2004.

Arrecubieta C, García E, López R. Sequence and transcriptional analysis of a DNA region involved in the production of capsular polysaccharide in *Streptococcus pneumoniae* type 3. *Gene* 1995 Dec 29;167(1-2):1-7. doi: 10.1016/0378-1119(95)00657-5.

Atilano ML, Pereira PM, Yates J et al. Teichoic acids are temporal and spatial regulators of peptidoglycan cross-linking in *Staphylococcus aureus*. *Proc Natl Acad Sci USA* 2010 Nov 2;107(44):18991-6. doi: 10.1073/pnas.1004304107.

Austrian R. Some observations on the pneumococcus and on the current status of pneumococcal disease and its prevention. *Rev Infect Dis* 1981 Mar-Apr;3 Suppl:S1-17. doi: 10.1093/clinids/3.supplement_1.s1.

Austrian R. Some aspects of the pneumococcal carrier state. *J Antimicrob Chemother* 1986 Jul;18 Suppl A:35-45. doi: 10.1093/jac/18.supplement_a.35.

Avery OT, Dubos R. The protective action of a specific enzyme against type III pneumococcus infection in mice. *J Exp Med* 1931;54:73–89. doi:10.1084/jem.54.1.73

Avery OT, Macleod CM, Mccarty M. Studies on the chemical nature of the substance inducing transformation of pneumococcal types induction of transformation by a desoxyribonucleic acid fraction isolated from pneumococcus type III. *J Exp Med* 1944 Feb 1; 79(2): 137–158. doi:10.1084/jem.79.2.137

Baker EH, Clark N, Brennan AL et al. Hyperglycemia and cystic fibrosis alter respiratory fluid glucose concentrations estimated by breath condensate analysis. *J Appl Physiol* (1985) 2007 May;102(5):1969-75. doi: 10.1152/japplphysiol.01425.2006.

Balachandran P, Hollingshead SK, Paton JC et al. The autolytic enzyme LytA of *Streptococcus pneumoniae* is not responsible for releasing pneumolysin. *J Bacteriol* 2001 May;183(10):3108-16. doi: 10.1128/JB.183.10.3108-3116.2001.

van Bambeke F, Reinert RR, Appelbaum PC et al. Multidrug-resistant *Streptococcus pneumoniae* infections: current and future therapeutic options. *Drugs* 2007;67(16):2355-82. doi: 10.2165/00003495-200767160-00005.

Baumgart M, Schubert K, Bramkamp M et al. Impact of LytR-CpsA-Psr proteins on cell wall biosynthesis in *Corynebacterium glutamicum*. *J Bacteriol* 2016 Oct 21;198(22):3045-3059. doi: 10.1128/JB.00406-16.

Bechet E, Gruszczyk J, Terreux R et al. Identification of structural and molecular determinants of the tyrosine-kinase Wzc and implications in capsular polysaccharide export. *Mol Microbiol* 2010 Sep;77(5):1315-25. doi: 10.1111/j.1365-2958.2010.07291.x.

Behr T, Fischer W, Peter-Katalinić J et al. The structure of pneumococcal lipoteichoic acid. Improved preparation, chemical and mass spectrometric studies. *Eur J Biochemc* 1992 Aug 1;207(3):1063-75. doi: 10.1111/j.1432-1033.1992.tb17143.x.

Bender MH, Yother J. CpsB is a modulator of capsule-associated tyrosine kinase activity in *Streptococcus pneumoniae*. *J Biol Chem* 2001 Dec 21;276(51):47966-74. doi: 10.1074/jbc.M105448200.

Bender MH, Cartee RT, Yother J. Positive correlation between tyrosine phosphorylation of CpsD and capsular polysaccharide production in *Streptococcus pneumoniae*. *J Bacteriol* 2003 Oct;185(20):6057-66. doi: 10.1128/JB.185.20.6057-6066.2003.

Bentley SD, Aanensen DM, Mavroidi A et al. Genetic analysis of the capsular biosynthetic locus from all 90 pneumococcal serotypes. *PLoS Genet* 2006 Mar;2(3):e31. doi: 10.1371/journal.pgen.0020031.

Benton KA, Paton JC, Briles DE. Differences in virulence for mice among *Streptococcus pneumoniae* strains of capsular types 2, 3, 4, 5, and 6 are not attributable to differences in pneumolysin production. *Infect Immun* 1997 Apr;65(4):1237-44. doi: 10.1128/iai.65.4.1237-1244.1997.

Berry AM, Lock RA, Hansman D et al. Contribution of autolysin to virulence of *Streptococcus pneumoniae*. *Infect Immun* 1989 Aug;57(8):2324-30. doi: 10.1128/iai.57.8.2324-2330.1989.

Berry AM, Paton JC. Additive attenuation of virulence of *Streptococcus pneumoniae* by mutation of the genes encoding pneumolysin and other putative pneumococcal virulence proteins. *Infect Immun* 2000 Jan;68(1):133-40. doi: 10.1128/IAI.68.1.133-140.2000.

Bitoun JP, Liao S, McKey BA et al. Psr is involved in regulation of glucan production, and double deficiency of BrpA and Psr is lethal in *Streptococcus mutans*. *Microbiology (Reading)* 2013 Mar;159(Pt 3):493-506. doi: 10.1099/mic.0.063032-0.

Bhullar KS, Lagarón NO, McGowan EM et al. Kinase-targeted cancer therapies: progress, challenges and future directions. *Mol Cancer* 2018 Feb 19;17(1):48. doi: 10.1186/s12943-018-0804-2.

Bogaert D, de Groot R, Hermans PW. *Streptococcus pneumoniae* colonisation: the key to pneumococcal disease. *Lancet Infect Dis* 2004 Mar;4(3):144-54. doi: 10.1016/S1473-3099(04)00938-7.

Bouhss A, Trunkfield AE, Bugg TDH et al. The biosynthesis of peptidoglycan lipid-linked intermediates. *FEMS Microbiol Rev* 2008 Mar;32(2):208-33. doi: 10.1111/j.1574-6976.2007.00089.x.

Bramkamp M, van Baarle S. Division site selection in rod-shaped bacteria. *Curr Opin Microbiol*

2009 Dec;12(6):683-8. doi: 10.1016/j.mib.2009.10.002.
Brinkmann V, Reichard U, Goosmann C et al. Neutrophil extracellular traps kill bacteria. *Science*. 2004 Mar 5;303(5663):1532-5. doi: 10.1126/science.1092385.
Brown S, Santa Maria JP Jr, Walker S. Wall teichoic acids of Gram-positive bacteria. *Annu Rev Microbiol* 2013;67:313-36. doi: 10.1146/annurev-micro-092412-155620.
Brueggemann AB, Griffiths DT, Meats E et al. Clonal relationships between invasive and carriage *Streptococcus pneumoniae* and serotype- and clone-specific differences in invasive disease potential. *J Infect Dis* 2003 May 1;187(9):1424-32. doi: 10.1086/374624.
Byrne JP, Morona JK, Paton JC et al. Identification of *Streptococcus pneumoniae* Cps2C residues that affect capsular polysaccharide polymerization, cell wall ligation, and Cps2D phosphorylation. *J Bacteriol* 2011 May;193(9):2341-6. doi: 10.1128/JB.00074-11.
Caimano MJ, Hardy GG, Yother J. Capsule genetics in *Streptococcus pneumoniae* and a possible role for transposition in the generation of the type 3 locus. *Microb Drug Resist* 1998; 4(1):11-23. doi: 10.1089/mdr.1998.4.11.
Calix JJ, Porambo RJ, Brady AM et al. Biochemical, genetic, and serological characterization of two capsule subtypes among *Streptococcus pneumoniae* serotype 20 strains: Discovery of a new pneumococcal serotype. *J Biol Chem* 2012 Aug 10;287(33):27885-94. doi: 10.1074/jbc.M112.380451.
Cambré A, Aertsen A. Bacterial vivisection: how fluorescence-based imaging techniques shed a light on the inner workings of bacteria. *Microbiol Mol Biol Rev* 2020 Oct 28;84(4):e00008-20. doi: 10.1128/MMBR.00008-20.
Cartee RT, Forsee WT, Schutzbach JS et al. Mechanism of type 3 capsular polysaccharide synthesis in *Streptococcus pneumoniae*. *J Biol Chem* 2000 Feb 11;275(6):3907-14. doi: 10.1074/jbc.275.6.3907.
Cartee RT, Forsee WT, Bender MH et al. CpsE from type 2 *Streptococcus pneumoniae* catalyzes the reversible addition of glucose-1-phosphate to a polyprenyl phosphate acceptor, initiating type 2 capsule repeat unit formation. *J Bacteriol* 2005a Nov;187(21):7425-33. doi: 10.1128/JB.187.21.7425-7433.2005.
Cartee RT, Forsee WT, Yother J. Initiation and synthesis of the *Streptococcus pneumoniae* type 3 capsule on a phosphatidylglycerol membrane anchor. *J Bacteriol* 2005b Jul;187(13):4470-9. doi: 10.1128/JB.187.13.4470-4479.2005b.
Catalão MJ, Figueiredo J, Henriques MX et al. Optimization of fluorescent tools for cell biology studies in Gram-positive bacteria. *PLoS One* 2014 Dec 2;9(12):e113796. doi: 10.1371/journal.pone.0113796.
Chan YGY, Frankel MB, Dengler V et al. *Staphylococcus aureus* mutants lacking the LytR-CpsA-,Psr family of enzymes release cell wall teichoic acids into the extracellular medium. *J Bacteriol* 2013 Oct;195(20):4650-9. doi: 10.1128/JB.00544-13.
Chan YGY, Kim HK, Schneewind O et al. The capsular polysaccharide of *Staphylococcus aureus* is attached to peptidoglycan by the LytR-CpsA-Psr (LCP) family of enzymes. *J Biol Chem* 2014 May 30;289(22):15680-90. doi: 10.1074/jbc.M114.567669.
Chao JD, Wong D, Av-Gay Y. Microbial protein-tyrosine kinases. *J Biol Chem*. 2014 Apr 4;289(14):9463-72. doi: 10.1074/jbc.R113.520015.
Chapman TM, Bouloc N, Buxton RS et al. Substituted aminopyrimidine protein kinase B (PknB) inhibitors show activity against *Mycobacterium tuberculosis*. *Bioorg Med Chem Lett* 2012 May 1;22(9):3349-53. doi: 10.1016/j.bmcl.2012.02.107
Chatfield CH, Koo H, Quivey RG. The putative autolysin regulator LytR in *Streptococcus mutans* plays a role in cell division and is growth-phase regulated. *Microbiology (Reading)* 2005

Feb;151(Pt 2):625-631. doi: 10.1099/mic.0.27604-0.

Chen C, Cervero Liceras F, Flasche S et al. Effect and cost-effectiveness of pneumococcal conjugate vaccination: a global modelling analysis. *Lancet Glob Heal* 2019 Jan;7(1):e58-e67. doi: 10.1016/S2214-109X(18)30422-4.

Chewapreecha C, Harris SR, Croucher NJ et al. Dense genomic sampling identifies highways of pneumococcal recombination. *Nat Genet* 2014 Mar;46(3):305-309. doi: 10.1038/ng.2895.

Choi EH, Zhang F, Lu YJ et al. Capsular polysaccharide (CPS) release by serotype 3 pneumococcal strains reduces the protective effect of anti-type 3 CPS antibodies. *Clin Vaccine Immunol* 2015 Dec 16;23(2):162-7. doi: 10.1128/CVI.00591-15.

Cieslewicz MJ, Kasper DL, Wang Y et al. Functional analysis in type Ia group B Streptococcus of a cluster of genes involved in extracellular polysaccharide production by diverse species of streptococci. *J Biol Chem* 2001 Jan 5;276(1):139-46. doi: 10.1074/jbc.M005702200.

Cools F, Torfs E, Vanhoutte B et al. *Streptococcus pneumoniae* galU gene mutation has a direct effect on biofilm growth, adherence and phagocytosis in vitro and pathogenicity in vivo. *Pathog Dis* 2018 Oct 1;76(7). doi: 10.1093/femspd/fty069.

Cundell DR, Gerard NP, Gerard C et al. *Streptococcus pneumoniae* anchor to activated human cells by the receptor for platelet-activating factor. *Nature* 1995a Oct 5;377(6548):435-8. doi: 10.1038/377435a0.

Cundell DR, Weiser JN, Shen J et al . Relationship between colonial morphology and adherence of *Streptococcus pneumoniae*. *Infect Immun* 1995b Mar;63(3):757-61. doi: 10.1128/iai.63.3.757-761.1995.

Dave S, Carmicle S, Hammerschmidt S et al. Dual roles of PspC, a surface protein of *Streptococcus pneumoniae*, in binding human secretory IgA and factor H. *J Immunol* 2004 Jul 1;173(1):471-7. doi: 10.4049/jimmunol.173.1.471.

Dentan C, Tselepis AD, Chapman MJ et al. Pefabloc, 4-[2-aminoethyl]benzenesulfonyl fluoride, is a new, potent nontoxic and irreversible inhibitor of PAF-degrading acetylhydrolase. *Biochim Biophys Acta* 1996 Feb 16;1299(3):353-7. doi: 10.1016/0005-2760(95)00226-x.

Dillard JP, Vandersea MW, Yother J. Characterization of the cassette containing genes for type 3 capsular polysaccharide biosynthesis in *Streptococcus pneumoniae*. *J Exp Med* 1995 Mar 1;181(3):973-83. doi: 10.1084/jem.181.3.973.

Dintilhac A, Alloing G, Granadel C et al. Competence and virulence of *Streptococcus pneumoniae*: Adc and PsaA mutants exhibit a requirement for Zn and Mn resulting from inactivation of putative ABC metal permeases. *Mol Microbiol* 1997 Aug;25(4):727-39. doi: 10.1046/j.1365-2958.1997.5111879.x.

Dixit C, Keller LE, Bradshaw JL et al. Nonencapsulated *Streptococcus pneumoniae* as a cause of chronic adenoiditis. *IDCases* 2016 Apr 12;4:56-8. doi: 10.1016/j.idcr.2016.04.001.

Dochez AR, Avery OT. The elaboration of specific soluble substance by pneumococcus during growth. *J Exp Med* 1917 Oct; 1;26(4):477-93. doi: 10.1084/jem.26.4.477.

Dunn KW, Kamocka MM, McDonald JH. A practical guide to evaluating colocalization in biological microscopy. *Am J Physiol Cell Physiol* 2011 Apr;300(4):C723-42. doi: 10.1152/ajpcell.00462.2010.

Eberhardt A, Wu LJ, Errington J et al . Cellular localization of choline-utilization proteins in *Streptococcus pneumoniae* using novel fluorescent reporter systems. *Mol Microbiol* 2009 Oct;74(2):395-408. doi: 10.1111/j.1365-2958.2009.06872.x.

Eberhardt A, Hoyland CN, Vollmer D et al. Attachment of capsular polysaccharide to the cell wall in *Streptococcus pneumoniae*. *Microb Drug Resist* 2012 Jun;18(3):240-55. doi: 10.1089/mdr.2011.0232.

Ericsson DJ, Standish A, Kobe B et al. Wzy-dependent bacterial capsules as potential drug targets. *Curr Drug Targets* 2012 Oct;13(11):1421-31. doi: 10.2174/138945012803530279.

Eskola J, Kilpi T, Palmu A et al. Efficacy of a pneumococcal conjugate vaccine against acute otitis media. *N Engl J Med* 2001 Feb 8;344(6):403-9. doi: 10.1056/NEJM200102083440602.

Félix S, Handem S, Nunes S, et al. Impact of private use of the 13-valent pneumococcal conjugate vaccine (PCV13) on pneumococcal carriage among Portuguese children living in urban and rural regions. *Vaccine*. 2021 Jul 22;39(32):4524-4533. doi: 10.1016/j.vaccine.2021.06.035.

Figueiredo J, Henriques MX, Catalão MJ et al. Efficient encapsulation of the newly synthesized cell wall protects *Streptococcus pneumoniae* from peptidoglycan hydrolases and host defenses. *PLoS Pathog* 2021 - submitted.

File TM Jr, Marrie TJ. Burden of community-acquired pneumonia in North American adults. *Postgrad Med* 2010 Mar;122(2):130-41. doi: 10.3810/pgm.2010.03.2130.

Fleurie A, Lesterlin C, Manuse S et al. MapZ marks the division sites and positions FtsZ rings in *Streptococcus pneumoniae*. *Nature* 2014 Dec 11;516(7530):259-262. doi: 10.1038/nature13966.

Forsee WT, Cartee RT, Yother J. Biosynthesis of type 3 capsular polysaccharide in *Streptococcus pneumoniae*. Enzymatic chain release by an abortive translocation process. *J Biol Chem* 2000 Aug 25;275(34):25972-8. doi: 10.1074/jbc.M002613200.

Forsee WT, Cartee RT, Yother J. Role of the carbohydrate binding site of the *Streptococcus pneumoniae* capsular polysaccharide type 3 synthase in the transition from oligosaccharide to polysaccharide synthesis. *J Biol Chem* 2006 Mar 10;281(10):6283-9. doi: 10.1074/jbc.M511124200.

Fernandez de Palencia P, Nieto C, Acebo P, Espinosa M, Lopez P. Expression of green fluorescent protein in *Lactococcus lactis*. *FEMS Microbiol Lett* 2000 Feb 15;183(2):229-34. doi: 10.1111/j.1574-6968.2000.tb08963.x.

Fernebro J, Andersson I, Sublett J et al. Capsular expression in *Streptococcus pneumoniae* negatively affects spontaneous and antibiotic-induced lysis and contributes to antibiotic tolerance. *J Infect Dis* 2004 Jan 15;189(2):328-38. doi: 10.1086/380564.

Filipe SR, Pinho MG, Tomasz A. Characterization of the *murMN* operon involved in the synthesis of branched peptidoglycan peptides in *Streptococcus pneumoniae*. *J Biol Chem* 2000 Sep 8;275(36):27768-74. doi: 10.1074/jbc.M004675200.

Gale RT, Li FKK, Sun T, Strynadka NCJ, Brown ED. *B. subtilis* LytR-CpsA-Psr enzymes transfer wall teichoic acids from authentic lipid-linked substrates to mature peptidoglycan in vitro. *Cell Chem Biol* 2017 Dec 21;24(12):1537-1546.e4. doi: 10.1016/j.chembiol.2017.09.006.

Ganaie F, Saad JS, McGee L et al. A new pneumococcal capsule type, 10D, is the 100th serotype and has a large *cps* fragment from an oral streptococcus. *mBio* 2020; May 19;11(3):e00937-20. doi: 10.1128/mBio.00937-20.

García JL, García E, López R. Overproduction and rapid purification of the amidase of *Streptococcus pneumoniae*. *Arch Microbiol* 1987;149(1):52-6. doi: 10.1007/BF00423136.

García E, Arrecubieta C, Muñoz R et al. A functional analysis of the *Streptococcus pneumoniae* genes involved in the synthesis of type 1 and type 3 capsular polysaccharides. *Microb Drug Resist* 1997;3(1):73-88. doi: 10.1089/mdr.1997.3.73.

García E, Llull D, López R. Functional organization of the gene cluster involved in the synthesis of the pneumococcal capsule. *Int Microbiol* 1999 Sep;2(3):169-76.

Geno KA, Hauser JR, Gupta K et al. *Streptococcus pneumoniae* phosphotyrosine phosphatase CpsB and alterations in capsule production resulting from changes in oxygen availability.

J Bacteriol 2014 Jun;196(11):1992-2003. doi: 10.1128/JB.01545-14.

Geno KA, Gilbert GL, Song JY et al. Pneumococcal capsules and their types: past, present, and future. *Clin Microbiol Rev*. 2015 Jul;28(3):871-99. doi: 10.1128/CMR.00024-15.

Geno KA, Saad JS, Nahm MH. Discovery of Novel Pneumococcal Serotype 35D, a Natural WciG-Deficient Variant of Serotype 35B. *J Clin Microbiol*. 2017 May;55(5):1416-1425. doi: 10.1128/JCM.00054-17.

Gerdes K, Howard M, Szardenings F. Pushing and pulling in prokaryotic DNA segregation. *Cell* 2010 Jun 11;141(6):927-42. doi: 10.1016/j.cell.2010.05.033.

Giammarinaro P, Paton JC. Role of RegM, a homologue of the catabolite repressor protein CcpA, in the virulence of *Streptococcus pneumoniae*. *Infect Immun* 2002 Oct;70(10):5454-61. doi: 10.1128/IAI.70.10.5454-5461.2002.

Gibson GJ, Loddenkemper R, Sibille Y. European lung white book (2 edn.), European Respiratory Society/European Lung Foundation, Sheffield, UK. 2003.

Giudicelli S, Tomasz A. Attachment of pneumococcal autolysin to wall teichoic acids, an essential step in enzymatic wall degradation. *J Bacteriol* 1984 Jun;158(3):1188-90. doi: 10.1128/jb.158.3.1188-1190.1984.

Goebel WF, Avery OT. A study of pneumococcus autolysis. *J Exp Med* 1929 Jan 31;49(2):267-86. doi: 10.1084/jem.49.2.267.

González JE, Semino CE, Wang LX et al. Biosynthetic control of molecular weight in the polymerization of the octasaccharide subunits of succinoglycan, a symbiotically important exopolysaccharide of *Rhizobium meliloti*. *Proc Natl Acad Sci USA.* 1998 Nov 10;95(23):13477-82. doi: 10.1073/pnas.95.23.13477.

Grangeasse C, Cozzone AJ, Deutscher J et al. Tyrosine phosphorylation: an emerging regulatory device of bacterial physiology. *Trends Biochem Sci* 2007 Feb;32(2):86-94. doi: 10.1016/j.tibs.2006.12.004.

Grangeasse C, Nessler S, Mijakovic I. Bacterial tyrosine kinases: evolution, biological function and structural insights. *Philos Trans R Soc Lond B Biol Sci* 2012 Sep 19;367(1602):2640-55. doi: 10.1098/rstb.2011.0424.

Grangeasse C. Rewiring the pneumococcal cell cycle with Serine/Threonine- and Tyrosine-kinases. *Trends Microbiol* 2016 Sep;24(9):713-724. doi: 10.1016/j.tim.2016.04.004.

Griffith F. The significance of pneumococcal types. *J Hyg (Lond)* 1928 Jan; 27(2): 113–159. doi: 10.1017/s0022172400031879

Groisman EA, Ochman H. Pathogenicity islands: bacterial evolution in quantum leaps. *Cell*. 1996 Nov 29;87(5):791-4. doi: 10.1016/s0092-8674(00)81985-6.

Gruber AR, Lorenz R, Bernhart SH, Neubock R, Hofacker IL. The Vienna RNA website. *Nucleic Acids Res* 2008 Jul 1;36(Web Server issue):W70-4. doi: 10.1093/nar/gkn188.

Guidolin A, Morona JK, Morona R et al. Nucleotide sequence analysis of genes essential for capsular polysaccharide biosynthesis in *Streptococcus pneumoniae* type 19F. *Infect Immun* 1994 Dec;62(12):5384-96. doi: 10.1128/iai.62.12.5384-5396.1994.

Guiral S, Mitchell TJ, Martin B et al. Competence-programmed predation of noncompetent cells in the human pathogen *Streptococcus pneumoniae*: Genetic requirements. *Proc Natl Acad Sci USA* 2005 Jun 14;102(24):8710-5. doi: 10.1073/pnas.0500879102.

Gustafsson C, Govindarajan S, Minshull J. Codon bias and heterologous protein expression. *Trends Biotechnol* 2004 Jul;22(7):346-53. doi: 10.1016/j.tibtech.2004.04.006.

Hakenbeck R, Madhour A, Denapaite D et al. Versatility of choline metabolism and choline-binding proteins in *Streptococcus pneumoniae* and commensal streptococci. *FEMS Microbiol Rev* 2009 May;33(3):572-86. doi: 10.1111/j.1574-6976.2009.00172.x.

Hammerschmidt S, Wolff S, Hocke A et al. Illustration of pneumococcal polysaccharide capsule during adherence and invasion of epithelial cells. *Infect Immun*. 2005 Aug;73(8):4653-67. doi: 10.1128/IAI.73.8.4653-4667.2005.

Hanage WP, Kaijalainen TH, Syrjänen RK et al. Invasiveness of serotypes and clones of *Streptococcus pneumoniae* among children in Finland. *Infect Immun* 2005; Jan;73(1):431-5. doi: 10.1128/IAI.73.1.431-435.2005.

Hanson BR, Lowe BA, Neely MN. Membrane topology and DNA-binding ability of the streptococcal CpsA protein. *J Bacteriol* 2011 Jan;193(2):411-20. doi: 10.1128/JB.01098-10.

Hanson BR, Runft DL, Streeter C et al. Functional analysis of the CpsA protein of *Streptococcus agalactiae*. *J Bacteriol* 2012 Apr;194(7):1668-78. doi: 10.1128/JB.06373-11.

Hardy GG, Caimano MJ, Yother J. Capsule biosynthesis and basic metabolism in *Streptococcus pneumoniae* are linked through the cellular phosphoglucomutase. *J Bacteriol* 2000 Apr;182(7):1854-63. doi: 10.1128/JB.182.7.1854-1863.2000.

Hardy GG, Magee AD, Ventura CL et al. Essential role for cellular phosphoglucomutase in virulence of type 3 *Streptococcus pneumoniae*. *Infect Immun* 2001 Apr;69(4):2309-17. doi: 10.1128/IAI.69.4.2309-2317.2001.

Harrison J, Lloyd G, Joe M et al. Lcp1 is a phosphotransferase responsible for ligating arabinogalactan to peptidoglycan in *Mycobacterium tuberculosis*. *mBio* 2016 Aug 2;7(4):e00972-16. doi: 10.1128/mBio.00972-16.

Henriques MX, Catalão MJ, Figueiredo J et al. Construction of improved tools for proteinocalization in *Streptococcus pneumoniae*. *Appl Environ Microbiol* 2013;8(1):e55049. doi: 10.1371/journal.pone.0055049.

Henriques MX, Rodrigues T, Carido M et al. Synthesis of capsular polysaccharide at the division septum of *Streptococcus pneumoniae* is dependent on a bacterial tyrosine kinase. *Mol Microbiol* 2011 Oct;82(2):515-34. doi: 10.1111/j.1365-2958.2011.07828.x.

Hoch JA. Two-component and phosphorelay signal transduction. *Curr Opin Microbiol* 2000 Apr;3(2):165-70. doi: 10.1016/s1369-5274(00)00070-9.

Hortal M, Algorta G, Blanchi I et al. Capsular type distribution and susceptibility to antibiotics of *Streptococcus pneumoniae* clinical strains isolated from Uruguayan children with systemic infections. Pneumococcus Study Group. *Microb Drug Resist*. 1997; 3(2):159-63. doi: 10.1089/mdr.1997.3.159.

Hoskins J, Alborn WE, Arnold J et al. Genome of the bacterium *Streptococcus pneumoniae* strain R6. *J Bacteriol* 2001 Oct;183(19):5709-17. doi: 10.1128/JB.183.19.5709-5717.2001.

Howard LV, Gooder H. Specificity of the autolysin of *Streptococcus* (Diplococcus) *pneumoniae*. *J Bacteriol* 1974 Feb;117(2):796-804. doi: 10.1128/jb.117.2.796-804.1974.

Huang SS. Post-PCV7 changes in colonizing pneumococcal serotypes in 16 Massachusetts communities, 2001 and 2004. *Pediatrics* 2005 Sep;116(3):e408-13. doi: 10.1542/peds.2004-2338.

Hübscher J, Lüthy L, Berger-Bächi B et al. Phylogenetic distribution and membrane topology of the LytR-CpsA-Psr protein family. *BMC Genomics* 2008 Dec 19;9:617. doi: 10.1186/1471-2164-9-617.

Hyams C, Camberlein E, Cohen JM, Bax K, Brown JS. The *Streptococcus pneumoniae* capsule inhibits complement activity and neutrophil phagocytosis by multiple mechanisms. *Infect Immun* 2010 Feb;78(2):704-15. doi: 10.1128/IAI.00881-09. Epub 2009 Nov 30.

Jadeau F, Bechet E, Cozzone AJ et al. Identification of the idiosyncratic bacterial protein tyrosine kinase (BY-kinase) family signature. *Bioinformatics* 2008 Nov 1;24(21):2427-30. doi: 10.1093/bioinformatics/btn462.

Janulczyk R, Iannelli F, Sjöholm AG et al. Hic, a novel surface protein of *Streptococcus pneumoniae* that interferes with complement function. *J Biol Chem* 2000 Nov 24;275(47):37257-63. doi: 10.1074/jbc.M004572200.

Jers C, Pedersen MM, Paspaliari KD et al. *Bacillus subtilis* BY-kinase PtkA controls enzyme activity and localization of its protein substrates. *Mol Microbiol* 2010 Jul;77(2):287-99. doi: 10.1111/j.1365-2958.2010.07227.x.

Johnsborg O, Håvarstein LS. Pneumococcal LytR, a protein from the LytR-CpsA-Psr family, is essential for normal septum formation in *Streptococcus pneumoniae*. *J Bacteriol* 2009 Sep;191(18):5859-64. doi: 10.1128/JB.00724-09.

Johnston JW, Myers LE, Ochs MM et al. Lipoprotein PsaA in virulence of *Streptococcus pneumoniae*: Surface accessibility and role in protection from superoxide. *Infect Immun* 2004 Oct;72(10):5858-67. doi: 10.1128/IAI.72.10.5858-5867.2004.

Kadioglu A, Weiser JN, Paton JC, Andrew PW. The role of *Streptococcus pneumoniae* virulence factors in host respiratory colonization and disease. *Nat Rev Microbiol* 2008 Apr;6(4):288-301. doi: 10.1038/nrmicro1871.

Kamerling JP. 2000. Pneumococcal polysaccharides: a chemical view, p 81–114 *In* Tomasz A. (ed), *Streptococcus pneumoniae*: molecular biology & mechanisms of disease. Mary Ann Liebert, Inc., Larchmont, NY

Karimova G, Pidoux J, Ullmann A et al. A bacterial two-hybrid system based on a reconstituted signal transduction pathway. *Proc Natl Acad Sci USA* 1998 May 12;95(10):5752-6. doi: 10.1073/pnas.95.10.5752.

Karimova G, Dautin N, Ladant D. Interaction network among *Escherichia coli* membrane proteins involved in cell division as revealed by bacterial two-hybrid analysis. *J Bacteriol* 2005 Apr;187(7):2233-43. doi: 10.1128/JB.187.7.2233-2243.2005.

Kawai Y, Marles-Wright J, Cleverley RM et al. A widespread family of bacterial cell wall assembly proteins. *EMBO J* 2011 Sep 30;30(24):4931-41. doi: 10.1038/emboj.2011.358.

Kelly T, Dillard JP, Yother J. Effect of Genetic Switching of Capsular Type on Virulence of *Streptococcus Pneumoniae*. *Infect Immun* 1994 May;62(5):1813-9. doi: 10.1128/iai.62.5.1813-1819.1994.

Kim JO, Weiser JN. Association of intrastrain phase variation in quantity of capsular polysaccharide and teichoic acid with the virulence of *Streptococcus pneumoniae*. *J Infect Dis* 1998 Feb;177(2):368-77. doi: 10.1086/514205.

Kirkham LAS, Jefferies JMC, Kerr AR et al. Identification of invasive serotype 1 pneumococcal isolates that express nonhemolytic pneumolysin. *J Clin Microbiol* 2006 Jan;44(1):151-9. doi: 10.1128/JCM.44.1.151-159.2006.

Klein G, Dartigalongue C, Raina S. Phosphorylation-mediated regulation of heat shock response in *Escherichia coli*. *Mol Microbiol* 2003 Apr;48(1):269-85. doi: 10.1046/j.1365-2958.2003.03449.x.

Kolkman MA, Wakarchuk W, Nuijten PJ et al. Capsular polysaccharide synthesis in *Streptococcus pneumoniae* serotype 14: molecular analysis of the complete *cps* locus and identification of genes encoding glycosyltransferases required for the biosynthesis of the tetrasaccharide subunit. *Mol Microbiol* 1997a Oct;26(1):197-208. doi: 10.1046/j.1365-2958.1997.5791940.x.

Kolkman MA, van der Zeijst BA, Nuijten PJ. Functional analysis of glycosyltransferases encoded by the capsular polysaccharide biosynthesis locus of *Streptococcus pneumoniae* serotype 14. *J Biol Chem* 1997b Aug 1;272(31):19502-8. doi: 10.1074/jbc.272.31.19502.

Kolkman MA, van der Zeijst BA, Nuijten PJ. Diversity of capsular polysaccharide synthesis gene

clusters in *Streptococcus pneumoniae*. *J Biochem* 1998 May;123(5):937-45. doi: 10.1093/oxfordjournals.jbchem.a022028.

König G, Sokkar P, Pryk N et al. Rational prioritization strategy allows the design of macrolide derivatives that overcome antibiotic resistance. *Proc Natl Acad Sci USA* 2021 Nov 16;118(46):e2113632118. doi: 10.1073/pnas.2113632118.

Krivan HC, Roberts DD. Many pulmonary pathogenic bacteria bind specifically to the carbohydrate sequence GalNAc beta 1-4Gal found in some glycolipids. *Proc Natl Acad Sci USA* 1988 Aug;85(16):6157-61. doi: 10.1073/pnas.85.16.6157.

Kudla G, Murray AW, Tollervey D, Plotkin JB. Coding-sequence determinants of gene expression in *Escherichia coli*. *Science* 2009 Apr 10;324(5924):255-8. doi: 10.1126/science.1170160.

Kumar LS, Agarwal S, Atack JM et al. ComE, an essential response regulator, negatively regulates the expression of the capsular polysaccharide locus and attenuates the bacterial virulence in *Streptococcus pneumoniae*. *Front Microbiol* 2017 Mar 7;8:277. doi: 10.3389/fmicb.2017.00277.

Kumari K, Weigel PH. Molecular cloning, expression, and characterization of the authentic hyaluronan synthase from group C *Streptococcus equisimilis*. *J Biol Chem*. 1997 Dec 19;272(51):32539-46. doi: 10.1074/jbc.272.51.32539.

Kuriyan J, O'donnell M. Sliding clamps of DNA polymerases. *J Mol Biol* 1993 Dec 20;234(4):915-25. doi: 10.1006/jmbi.1993.1644.

Lacks S, Hotchkiss RD. A study of the genetic material determining an enzyme activity in Pneumococcus. *Biochimica et Biophysica Acta* 1960 Apr 22;39:508-18. doi: 10.1016/0006-3002(60)90205-5.

Lacks SA, Lopez P, Greenberg B, Espinosa M (1986) Identification and analysis of genes for tetracycline resistance and replication functions in the broad-host-range plasmid pLS1. *J Mol Biol* 1986 Dec 20;192(4):753-65. doi: 10.1016/0022-2836(86)90026-4.

Lacks SA, Ayalew S, de la Campa AG, Greenberg B. Regulation of competence for genetic transformation in *Streptococcus pneumoniae*: expression of *dpnA*, a late competence gene encoding a DNA methyltransferase of the *DpnII* restriction system. *Mol Microbiol* 2000 Mar;35(5):1089-98. doi: 10.1046/j.1365-2958.2000.01777.x.

Lacour S, Bechet E, Cozzone AJ et al. Tyrosine phosphorylation of the UDP-glucose dehydrogenase of *Escherichia coli* is at the crossroads of colanic acid synthesis and polymyxin resistance. *PLoS One* 2008 Aug 25;3(8):e3053. doi: 10.1371/journal.pone.0003053.

Lam SJ, O'Brien-Simpson NM, Pantarat N et al. Combating multidrug-resistant Gram-negative bacteria with structurally nanoengineered antimicrobial peptide polymers. *Nat Microbiol* 2016 Sep 12;1(11):16162. doi: 10.1038/nmicrobiol.2016.162.

Larson TR, Yother J. *Streptococcus pneumoniae* capsular polysaccharide is linked to peptidoglycan via a direct glycosidic bond to β-D- *N* -acetylglucosamine. *Proc Natl Acad Sci* 2017 May 30;114(22):5695-5700. doi: 10.1073/pnas.1620431114.

Laurenceau RL, Rard Pé Hau-Arnaudet G, Baconnais S et al . A type IV pilus mediates DNA binding during natural transformation in *Streptococcus pneumoniae*. *PLoS Pathog* 2013;9(6):e1003473. doi: 10.1371/journal.ppat.1003473.

Law J, Buist G, Haandrikman A et al. A system to generate chromosomal mutations in *Lactococcus lactis* which allows fast analysis of targeted genes. *J Bacteriol* 1995 Dec;177(24):7011-8. doi: 10.1128/jb.177.24.7011-7018.1995.

Lazarevic V, Margot P, Soldo B et al. Sequencing and analysis of the *Bacillus subtilis lytRABC* divergon: a regulatory unit encompassing the structural genes of the N-acetylmuramoyl-

L-alanine amidase and its modifier. *J Gen Microbiol* 1992 Sep;138(9):1949-61. doi: 10.1099/00221287-138-9-1949.

Lee CJ, Banks SD, Li JP. Virulence, immunity, and vaccine related to *Streptococcus pneumoniae*. *Crit Rev Microbiol* 1991; 18(2):89-114. doi: 10.3109/10408419109113510.

Lee DC, Zheng J, She Y-M et al. Structure of *Escherichia coli* tyrosine kinase Etk reveals a novel activation mechanism. *EMBO J* 2008 Jun 18;27(12):1758-66. doi: 10.1038/emboj.2008.97.

Lee YS, Shibata Y, Malhotra A et al. A novel class of small RNAs: tRNA-derived RNA fragments (tRFs). *Genes Dev* 2009 Nov 15;23(22):2639-49. doi: 10.1101/gad.1837609.

Leenhouts K, Buist G, Bolhuis A, et al. A general system for generating unlabelled gene replacements in bacterial chromosomes. *Mol Gen Genet*. 1996 Nov 27;253(1-2):217-24. doi: 10.1007/s004380050315.

Leipe DD, Wolf YI, Koonin E V. et al . Classification and evolution of P-loop GTPases and related ATPases. *J Mol Biol* 2002 Mar 15;317(1):41-72. doi: 10.1006/jmbi.2001.5378.

Li FKK, Rosell FI, Gale RT et al. Crystallographic analysis of *Staphylococcus aureus* LcpA, the primary wall teichoic acid ligase. *J Biol Chem* 2020 Feb 28;295(9):2629-2639. doi: 10.1074/jbc.RA119.011469.

Lindberg B, Lonngren J, Powell DA. Structural studies on the specific type-14 pneumococcal polysaccharide. *Carbohydr Res* 1977 Sep;58(1):177-86. doi: 10.1016/s0008-6215(00)83413-8.

Liu X, Gallay C, Kjos M et al. High-throughput CRISPRi phenotyping identifies new essential genes in *Streptococcus pneumoniae*. *Mol Syst Biol* 2017 May 10;13(5):931. doi: 10.15252/msb.20167449.

Llull D, Muñoz R, López R et al. A single gene (*tts*) located outside the cap locus directs the formation of *Streptococcus pneumoniae* type 37 capsular polysaccharide. Type 37 pneumococci are natural, genetically binary strains. *J Exp Med*. 1999 Jul 19;190(2):241-51. doi: 10.1084/jem.190.2.241.

Llull D, García E, López R. Tts, a processive beta-glucosyltransferase of *Streptococcus pneumoniae*, directs the synthesis of the branched type 37 capsular polysaccharide in Pneumococcus and other Gram-positive species. *J Biol Chem* 2001 Jun 15;276(24):21053-61. doi: 10.1074/jbc.M010287200.

Lougheed KE, Osborne SA, Saxty B et al. Effective inhibitors of the essential kinase PknB and their potential as anti-mycobacterial agents. *Tuberculosis (Edinb)* 2011 Jul;91(4):277-86. doi: 10.1016/j.tube.2011.03.005

Loughran AJ, Orihuela CJ, Tuomanen EI. *Streptococcus pneumoniae*: invasion and inflammation. *Microbiol Spectr* 2019; Mar;7(2), doi:10.1128/microbiolspec.GPP3-0004-2018.

Lutkenhaus J. The ParA/MinD family puts things in their place. *Trends Microbiol* 2012 Sep;20(9):411-8. doi: 10.1016/j.tim.2012.05.002.

Magee AD, Yother J. Requirement for capsule in colonization by *Streptococcus pneumoniae*. *Infect Immun* 2001 Jun;69(6):3755-61. doi: 10.1128/IAI.69.6.3755-3761.2001.

Majcherczyk PA, Langen H, Heumann D et al. Digestion of *Streptococcus pneumoniae* cell walls with its major peptidoglycan hydrolase releases branched stem peptides carrying proinflammatory activity. *J Biol Chem* 1999 Apr 30;274(18):12537-43. doi: 10.1074/jbc.274.18.12537.

Malishev R, Salinas N, Gibson J et al. Inhibition of *Staphylococcus aureus* biofilm-forming functional amyloid by molecular tweezers. *Cell Chem Biol* 2021 Sep 16;28(9):1310-1320.e5. doi: 10.1016/j.chembiol.2021.03.013.

Marangu D, Zar HJ. Childhood pneumonia in low-and-middle-income countries: An update. *Paediatr Respir Rev* 2019 Nov;32:3-9. doi: 10.1016/j.prrv.2019.06.001.

Maréchal M, Amoroso A, Morlot C et al. *Enterococcus hirae* LcpA (Psr), a new peptidoglycan-binding protein localized at the division site. *BMC Microbiol* 2016 Oct 12;16(1):239. doi: 10.1186/s12866-016-0844-y.

Marks LR, Reddinger RM, Hakansson AP. Biofilm formation enhances fomite survival of *Streptococcus pneumoniae* and *Streptococcus pyogenes*. *Infect Immun* 2014;82(3):1141-6, doi: 10.1128/IAI.01310-13.

Marra A, Lawson S, Asundi JS et al. In vivo characterization of the *psa* genes from *Streptococcus pneumoniae* in multiple models of infection. *Microbiology (Reading)* 2002 May;148(Pt 5):1483-91. doi: 10.1099/00221287-148-5-1483.

Marshall JE, Faraj BHA, Gingras AR et al. The crystal structure of pneumolysin at 2.0Å resolution reveals the molecular packing of the pre-pore complex. *Sci Rep* 2015 Sep 3;5:13293. doi: 10.1038/srep13293.

Martin B, García P, Castanié MP et al. The *recA* gene of *Streptococcus pneumoniae* is part of a competence-induced operon and controls lysogenic induction. *Mol Microbiol* 1995 Jan;15(2):367-79. doi: 10.1111/j.1365-2958.1995.tb02250.x.

Martin B, Soulet AL, Mirouze N et al. ComE/ComE~P interplay dictates activation or extinction status of pneumococcal X-state (competence). *Mol Microbiol* 2013 Jan;87(2):394-411. doi: 10.1111/mmi.12104.

Martner A, Skovbjerg S, Paton JC et al. *Streptococcus pneumoniae* autolysis prevents phagocytosis and production of phagocyte-activating cytokines. *Infect Immun* 2009 Sep;77(9):3826-37. doi: 10.1128/IAI.00290-09.

Mavroidi A, Aanensen DM, Godoy D et al. Genetic relatedness of the *Streptococcus pneumoniae* capsular biosynthetic loci. *J Bacteriol* 2007 Nov;189(21):7841-55. doi: 10.1128/JB.00836-07.

Melin M, Trzciński K, Antonio M, et al. Serotype-related variation in susceptibility to complement deposition and opsonophagocytosis among clinical isolates of *Streptococcus pneumoniae*. *Infect Immun* 2010 Dec;78(12):5252-61. doi: 10.1128/IAI.00739-10.

Mella-Herrera RA, Ramona Neunuebel M, Golden JW. *Anabaena* sp. strain PCC 7120 conR contains a LytR-CpsA-Psr domain, is developmentally regulated, and is essential for diazotrophic growth and heterocyst morphogenesis. *Microbiology (Reading)* 2011 Mar;157(Pt 3):617-626. doi: 10.1099/mic.0.046128-0.

Mellroth P, Daniels R, Eberhardt A et al. LytA, major autolysin of *Streptococcus pneumoniae*, requires access to nascent peptidoglycan. *J Biol Chem* 2012 Mar 30;287(14):11018-29. doi: 10.1074/jbc.M111.318584.

Mercy C, Ducret A, Slager J et al. RocS drives chromosome segregation and nucleoid protection in *Streptococcus pneumoniae*. *Nat Microbiol* 2019 Oct;4(10):1661-1670. doi: 10.1038/s41564-019-0472-z.

Mesquita FS, Brito C, Mazon Moya MJ et al. Endoplasmic reticulum chaperone Gp96 controls actomyosin dynamics and protects against pore-forming toxins. *EMBO Rep* 2017 Feb;18(2):303-318. doi: 10.15252/embr.201642833.

Międzybrodzki R, Hoyle N, Zhvaniya F et al. Current updates from the long-standing phage research centers in Georgia, Poland, and Russia. *Bacteriophages* 2018. 1–31. doi:10.1007/978-3-319-40598-8_31-1

Miller JD, Neely MN. Zebrafish as a model host for streptococcal pathogenesis. *Acta Trop* 2004

Jun;91(1):53-68. doi: 10.1016/j.actatropica.2003.10.020.
Minic Z, Marie C, Delorme C et al. Control of EpsE, the phosphoglycosyltransferase initiating exopolysaccharide synthesis in *Streptococcus thermophilus*, by EpsD tyrosine kinase. *J Bacteriol* 2007 Feb;189(4):1351-7. doi: 10.1128/JB.01122-06.
Mintz, G. R. Technical note: an irreversible serine protease inhibitor. *BioPharm International* 1993; 6 34-38.
Mitchell TJ, Alexander JE, Morgan PJ et al. Molecular analysis of virulence factors of *Streptococcus pneumoniae*. *J Appl Microbiol* 1997;26:62S-71S. PMID: 9436318.
Mitchell AM, Mitchell TJ. *Streptococcus pneumoniae*: Virulence factors and variation. *Clin Microbiol Infect* 2010 May;16(5):411-8. doi: 10.1111/j.1469-0691.2010.03183.x.
Mollerach M, López R, García E. Characterization of the *galU* gene of *Streptococcus pneumoniae* encoding a uridine diphosphoglucose pyrophosphorylase: A gene essential for capsular polysaccharide biosynthesis. *J Exp Med* 1998 Dec 7;188(11):2047-56. doi: 10.1084/jem.188.11.2047.
Monteiro JM, Fernandes PB, Vaz F et al. Cell shape dynamics during the staphylococcal cell cycle. *Nat Commun* 2015 Aug 17;6:8055. doi: 10.1038/ncomms9055.
Morona JK, Morona R, Paton JC. Characterization of the locus encoding the *Streptococcus pneumoniae* type 19F capsular polysaccharide biosynthetic pathway. *Mol Microbiol* 1997 Feb;23(4):751-63. doi: 10.1046/j.1365-2958.1997.2551624.x.
Morona JK, Morona R, Paton JC et al. Analysis of the 5' portion of the type 19A capsule locus identifies two classes of *cpsC*, *cpsD*, and *cpsE* genes in *Streptococcus pneumoniae*. *J Bacteriol* 1999 Jun;181(11):3599-605. doi: 10.1128/JB.181.11.3599-3605.1999.
Morona JK, Paton JC, Miller DC et al. Tyrosine phosphorylation of CpsD negatively regulates capsular polysaccharide biosynthesis in *Streptococcus pneumoniae*. *Mol Microbiol* 2000a Mar;35(6):1431-42. doi: 10.1046/j.1365-2958.2000.01808.x.
Morona R, van den Bosch L, Daniels C. Evaluation of Wzz/MPA1/MPA2 proteins based on the presence of coiled-coil regions. *Microbiology (Reading)* 2000b Jan;146 (Pt 1):1-4. doi: 10.1099/00221287-146-1-1.
Morona JK, Morona R, Miller DC et al. *Streptococcus pneumoniae* capsule biosynthesis protein CpsB is a novel manganese-dependent phosphotyrosine-protein phosphatase. *J Bacteriol* 2002 Jan;184(2):577-83. doi: 10.1128/JB.184.2.577-583.2002.
Morona JK, Morona R, Miller DC et al. Mutational analysis of the carboxy-terminal (YGX)4 repeat domain of CpsD, an autophosphorylating tyrosine kinase required for capsule biosynthesis in *Streptococcus pneumoniae*. *J Bacteriol* 2003 May;185(10):3009-19. doi: 10.1128/JB.185.10.3009-3019.2003.
Morona JK, Miller DC, Morona R et al. The effect that mutations in the conserved capsular polysaccharide biosynthesis genes *cpsA, cpsB,* and *cpsD* have on virulence of *Streptococcus pneumoniae*. *J Infect Dis* 2004 May 15;189(10):1905-13. doi: 10.1086/383352.
Morona JK, Morona R, Paton JC. Attachment of capsular polysaccharide to the cell wall of *Streptococcus pneumoniae* type 2 is required for invasive disease. *Proc Natl Acad Sci USA* 2006 May 30;103(22):8505-10. doi: 10.1073/pnas.0602148103.
Mortier-Barrière I, De Saizieu A, Claverys JP et al. Competence-specific induction of recA is required for full recombination proficiency during transformation in *Streptococcus pneumoniae*. *Mol Microbiol* 1998 Jan;27(1):159-70. doi: 10.1046/j.1365-2958.1998.00668.x.
Mostowy S, Boucontet L, Mazon Moya MJ et al. The zebrafish as a new model for the in vivo

study of *Shigella flexneri* interaction with phagocytes and bacterial autophagy. *PLoS Pathog* 2013;9(9):e1003588. doi: 10.1371/journal.ppat.1003588. Epub 2013 Sep 5.

Mostowy RJ, Croucher NJ, De Maio N et al. Pneumococcal capsule synthesis locus *cps* as evolutionary hotspot with potential to generate novel serotypes by recombination. *Mol Biol Evol* 2017 Oct 1;34(10):2537-2554. doi: 10.1093/molbev/msx173.

Mousavi SM, Babakhani S, Moradi L et al. Bacteriophage as a novel therapeutic weapon for killing colistin-resistant multi-drug-resistant and extensively drug-resistant Gram-negative bacteria. *Curr Microbiol* 2021 Dec;78(12):4023-4036. doi: 10.1007/s00284-021-02662-y.

Muñoz R, Mollerach M, López R et al. Molecular organization of the genes required for the synthesis of type 1 capsular polysaccharide of *Streptococcus pneumoniae*: formation of binary encapsulated pneumococci and identification of cryptic dTDP-rhamnose biosynthesis genes. *Mol Microbiol* 1997Jul;25(1):79-92. doi: 10.1046/j.1365-2958.1997.4341801.x.

Musher DM. Infections caused by *Streptococcus pneumoniae*: clinical spectrum, pathogenesis, immunity, and treatment. *Clin Infect Dis* 1992 Apr;14(4):801-7. doi: 10.1093/clinids/14.4.801.

Navarre WW, Schneewind O. Proteolytic cleavage and cell wall anchoring at the LPXTG motif of surface proteins in Gram-positive bacteria. *Mol Microbiol* 1994 Oct;14(1):115-21. doi: 10.1111/j.1365-2958.1994.tb01271.x.

Neely MN, Pfeifer JD, Caparon M. Streptococcus-zebrafish model of bacterial pathogenesis. *Infect Immun* 2002 Jul;70(7):3904-14. doi: 10.1128/IAI.70.7.3904-3914.2002.

Nelson AL, Roche AM, Gould JM et al. Capsule enhances pneumococcal colonization by limiting mucus-mediated clearance. *Infect Immun*. 2007 Jan;75(1):83-90. doi: 10.1128/IAI.01475-06.

Nourikyan J, Kjos M, Mercy C et al. Autophosphorylation of the bacterial tyrosine-kinase CpsD connects capsule synthesis with the cell cycle in *Streptococcus pneumoniae*. *PLoS Genet* 2015 Sep 17;11(9):e1005518. doi: 10.1371/journal.pgen.1005518.

Ogunniyi AD, Giammarinaro P, Paton JC. The genes encoding virulence-associated proteins and the capsule of *Streptococcus pneumoniae* are upregulated and differentially expressed in vivo. *Microbiology (Reading)*. 2002 Jul;148(Pt 7):2045-2053. doi: 10.1099/00221287-148-7-2045.

Olivares-Illana V, Meyer P, Bechet E et al. Structural basis for the regulation mechanism of the tyrosine kinase CapB from *Staphylococcus aureus*. *PLoS Biol* 2008 Jun 10;6(6):e143. doi: 10.1371/journal.pbio.0060143.

Orio AGA, Piñas GE, Cortes PR et al. Compensatory evolution of pbp mutations restores the fitness cost imposed by β-lactam resistance in *Streptococcus pneumoniae*. *PLoS Pathog* 2011 Feb;7(2):e1002000. doi: 10.1371/journal.ppat.1002000.

Over B, Heusser R, Mccallum N et al. LytR-CpsA-Psr proteins in *Staphylococcus aureus* display partial functional redundancy and the deletion of all three severely impairs septum placement and cell separation. *FEMS Microbiol Lett* 2011 Jul;320(2):142-51. doi: 10.1111/j.1574-6968.2011.02303.x.

Park IH, Geno KA, Sherwood LK et al. Population-based analysis of invasive nontypeable pneumococci reveals that most have defective capsule synthesis genes. *PLoS One* 2014 May 15;9(5):e97825. doi: 10.1371/journal.pone.0097825.

Pasteur L. Note sur la maladie nouvelle provoquée par la salive d'un enfant mort de la rage. *Bull Acad Med* 1881;10:94-103.

Pathak A, Bergstrand J, Sender V et al. Factor H binding proteins protect division septa on encapsulated *Streptococcus pneumoniae* against complement C3b deposition and amplification. *Nat Commun* 2018 Aug 23;9(1):3398. doi: 10.1038/s41467-018-05494-w.

Paton JC, Rowan KB, Ferrante A. Activation of human complement by the pneumococcal toxin pneumolysin. *Infect Immun* 1984 Mar;43(3):1085-7. doi: 10.1128/iai.43.3.1085-1087.1984.

Paton JC, Trappetti C. *Streptococcus pneumoniae* capsular polysaccharide. *Microbiol Spectr* 2019 Mar;7(2). doi: 10.1128/microbiolspec.GPP3-0019-2018.

Pereira PM, Filipe SR, Tomasz A et al. Fluorescence ratio imaging microscopy shows decreased access of vancomycin to cell wall synthetic sites in vancomycin-resistant *Staphylococcus aureus*. *Antimicrob Agents Chemother* 2007 Oct;51(10):3627-33. doi: 10.1128/AAC.00431-07.

Pérez-Dorado I, Galan-Bartual S, Hermoso JA. Pneumococcal surface proteins: when the whole is greater than the sum of its parts. *Mol Oral Microbiol* 2012 Aug;27(4):221-45. doi: 10.1111/j.2041-1014.2012.00655.x.

Pestova E V, Håvarstein LS, Morrison DA. Regulation of competence for genetic transformation in *Streptococcus pneumoniae* by an auto-induced peptide pheromone and a two-component regulatory system. *Mol Microbiol* 1996 Aug;21(4):853-62. doi: 10.1046/j.1365-2958.1996.501417.x.

Petranovic D, Michelsen O, Zahradka K et al . *Bacillus subtilis* strain deficient for the protein-tyrosine kinase PtkA exhibits impaired DNA replication. *Mol Microbiol* 2007 Mar;63(6):1797-805. doi: 10.1111/j.1365-2958.2007.05625.x.

Philips BJ, Meguer JX, Redman J et al. Factors determining the appearance of glucose in upper and lower respiratory tract secretions. *Intensive Care Med* 2003 Dec;29(12):2204-2210. doi: 10.1007/s00134-003-1961-2.

Pinho MG, Kjos M, Veening JW. How to get (a)round: Mechanisms controlling growth and division of coccoid bacteria. *Nat Rev Microbiol* 2013 Sep;11(9):601-14. doi: 10.1038/nrmicro3088.

Pletz MW, Maus U, Krug N et al. Pneumococcal vaccines: mechanism of action, impact on epidemiology and adaption of the species. *Int J Antimicrob Agents* 2008 Sep;32(3):199-206. doi: 10.1016/j.ijantimicag.2008.01.021.

Pollard AJ, Perrett KP, Beverley PC. Maintaining protection against invasive bacteria with protein-polysaccharide conjugate vaccines. *Nat Rev Immunol*. 2009 Mar;9(3):213-20. doi: 10.1038/nri2494.

Pozzi G, Oggioni MR, Tomasz A. DNA probe for identification of *Streptococcus pneumoniae*. *J Clin Microbiol* 1989 Feb;27(2):370-2. doi: 10.1128/jcm.27.2.370-372.1989.

Price KE, Camilli A. Pneumolysin localizes to the cell wall of *Streptococcus pneumoniae*. *J Bacteriol* 2009 Apr;191(7):2163-8. doi: 10.1128/JB.01489-08.

Rayner CFJ, Jackson AD, Rutman A et al. Interaction of pneumolysin-sufficient and -deficient isogenic variants of *Streptococcus pneumoniae* with human respiratory mucosa. *Infect Immun* 1995 Feb;63(2):442-7. doi: 10.1128/iai.63.2.442-447.1995.

Reid BG, Flynn GC. Chromophore formation in green fluorescent protein. *Biochemistry* 1997 Jun 3;36(22):6786-91. doi: 10.1021/bi970281w.

Romero-Steiner S, Pilishvili T, Sampson JS et al. Inhibition of pneumococcal adherence to human nasopharyngeal epithelial cells by anti-PsaA antibodies. *Clin Diagn Lab Immunol* 2003 Mar;10(2):246-51. doi: 10.1128/cdli.10.2.246-251.2003.

Rosenow C, Ryan P, Weiser JN et al. Contribution of novel choline-binding proteins to adherence, colonization and immunogenicity of *Streptococcus pneumoniae*. *Mol*

Microbiol 1997 Sep;25(5):819-29. doi: 10.1111/j.1365-2958.1997.mmi494.x.

Rounioja S, Saralahti A, Rantala L et al. Defense of zebrafish embryos against *Streptococcus pneumoniae* infection is dependent on the phagocytic activity of leukocytes. *Dev Comp Immunol* 2012 Feb;36(2):342-8. doi: 10.1016/j.dci.2011.05.008.

Rowe HM, Hanson BR, Runft DL et al. Modification of the CpsA protein reveals a role in alteration of the *Streptococcus agalactiae* cell envelope. *Infect Immun* 2015 Apr;83(4):1497-506. doi: 10.1128/IAI.02656-14.

Sabelnikov AG, Greenberg B, Lacks SA. An extended -10 promoter alone directs transcription of the *DpnII* operon of *Streptococcus pneumoniae*. *J Mol Biol* 1995 Jul 7;250(2):144-55. doi: 10.1006/jmbi.1995.0366.

Sambrook J., Fritsch E. F., Maniatis T. Molecular cloning : a laboratory manual. *Cold Spring Harbor Laboratory Press* 1989.

Sanchez CJ, Hinojosa CA, Shivshankar P et al. Changes in capsular serotype alter the surface exposure of pneumococcal adhesins and impact virulence. *PLoS One* 2011;6(10):e26587. doi: 10.1371/journal.pone.0026587.

van der Sar AM, Stockhammer OW, van der Laan C et al. MyD88 innate immune function in a zebrafish embryo infection model. *Infect Immun* 2006 Apr;74(4):2436-41. doi: 10.1128/IAI.74.4.2436-2441.2006.

Saraiva B, Krippahl L, Filipe S et al. EHooke: a tool for automated image analysis of spherical bacteria based on cell cycle progression. *Biological Imaging* 2021; 1-25. doi:10.1017/S2633903X21000027.

Schnell U, Dijk F, Sjollema KA et al. Immunolabeling artifacts and the need for live-cell imaging. *Nat Methods* 2012 Jan 30;9(2):152-8. doi: 10.1038/nmeth.1855.

Shainheit MG, Mulé M, Camilli A. The core promoter of the capsule operon of *Streptococcus pneumoniae* is necessary for colonization and invasive disease. *Infect Immun* 2014 Feb;82(2):694-705. doi: 10.1128/IAI.01289-13.

Schindelin J, Arganda-Carreras I, Frise E et al. Fiji: an open-source platform for biological-image analysis. *Nat Methods* 2012 Jun 28;9(7):676-82. doi: 10.1038/nmeth.2019.

Sørensen UBS, Blom J, Birch-andersen A et al. Ultrastructural localization of capsules, cell wall polysaccharide, cell wall proteins, and F antigen in pneumococci. *Infect Immun*. 1988 Aug;56(8):1890-6. doi: 10.1128/iai.56.8.1890-1896.1988.

Sørensen UB, Henrichsen J, Chen HC et al. Covalent linkage between the capsular polysaccharide and the cell wall peptidoglycan of *Streptococcus pneumoniae* revealed by immunochemical methods. *Microb Pathog* 1990 May;8(5):325-34. doi: 10.1016/0882-4010(90)90091-4.

Sørensen UBS, Yao K, Yang Y et al. Capsular polysaccharide expression in commensal streptococcus species: genetic and antigenic similarities to *Streptococcus pneumoniae*. *mBio.* 2016 Nov 15;7(6):e01844-16. doi: 10.1128/mBio.01844-16.

Standish AJ, Whittall JJ, Morona R. Tyrosine phosphorylation enhances activity of pneumococcal autolysin LytA. *Microbiology (Reading)* 2014 Dec;160(Pt12):2745-2754. doi: 10.1099/mic.0.080747-0.

Steinmoen H, Knutsen E, Håvarstein LS. Induction of natural competence in *Streptococcus pneumoniae* triggers lysis and DNA release from a subfraction of the cell population. *Proc Natl Acad Sci USA* 2002 May 28;99(11):7681-6. doi: 10.1073/pnas.112464599.

Sternberg G. A fatal form of septicaemia in the rabbit, produced by the subcutaneous injection of human saliva. *Natl Board Heal Bull* 1881;2:781-783.

Sun X, Ge F, Xiao CL et al. Phosphoproteomic analysis reveals the multiple roles of

phosphorylation in pathogenic bacterium *Streptococcus pneumoniae*. *J Proteome Res* 2010 Jan;9(1):275-82. doi: 10.1021/pr900612v.

Syed S, Hakala P, Singh AK et al. Role of pneumococcal NanA neuraminidase activity in peripheral blood. *Front Cell Infect Microbiol* 2019 Jun 26;9:218. doi: 10.3389/fcimb.2019.00218.

Talbot UM, Paton AW, Paton JC. Uptake of *Streptococcus pneumoniae* by respiratory epithelial cells. *Infect Immun* 1996 Sep;64(9):3772-7. doi: 10.1128/iai.64.9.3772-3777.1996.

Toniolo C, Balducci E, Romano MR et al. *Streptococcus agalactiae* capsule polymer length and attachment is determined by the proteins CpsABCD. *J Biol Chem*. 2015 Apr 10;290(15):9521-32. doi: 10.1074/jbc.M114.631499.

Troeger C, Blacker B, Khalil IA et al. Estimates of the global, regional, and national morbidity, mortality, and aetiologies of lower respiratory infections in 195 countries, 1990–2016: a systematic analysis for the Global Burden of Disease Study 2016. *Lancet Infect Dis*. 2018 Nov;18(11):1191-1210. doi: 10.1016/S1473-3099(18)30310-4.

Tseng H-J, Mcewan AG, Paton JC et al . Virulence of *Streptococcus pneumoniae*: PsaA mutants are hypersensitive to oxidative stress. *Infect Immun* 2002 Mar;70(3):1635-9. doi: 10.1128/IAI.70.3.1635-1639.2002.

Urban CF, Reichard U, Brinkmann V et al . Neutrophil extracellular traps capture and kill *Candida albicans* yeast and hyphal forms. *Cell Microbiol* 2006 Apr;8(4):668-76. doi: 10.1111/j.1462-5822.2005.00659.x.

Utaida S, Dunman PM, Macapagal D et al. Genome-wide transcriptional profiling of the response of *Staphylococcus aureus* to cell-wall-active antibiotics reveals a cell-wall-stress stimulon. *Microbiology (Reading)* 2003 Oct;149(Pt 10):2719-2732. doi: 10.1099/mic.0.26426-0.

Valentino MD, Mcguire AM, Rosch JW et al. Unencapsulated *Streptococcus pneumoniae* from conjunctivitis encode variant traits and belong to a distinct phylogenetic cluster. *Nat Commun* 2014 Nov 12;5:5411. doi: 10.1038/ncomms6411.

Valvano MA. Export of O-specific lipopolysaccharide. *Front Biosci* 2003 May 1;8:s452-71. doi: 10.2741/1079.

Varvio S, Auranen K, Arjas E et al . Evolution of the Capsular Regulatory Genes in *Streptococcus pneumoniae*. *J Infect Dis* 2009 Oct 1;200(7):1144-51. doi: 10.1086/605651.

Veening JW, Smits WK, Hamoen LW, Jongbloed JD, Kuipers OP. Visualization of differential gene expression by improved cyan fluorescent protein and yellow fluorescent protein production in *Bacillus subtilis*. *Appl Environ Microbiol* 2004 Nov;70(11):6809-15. doi: 10.1128/AEM.70.11.6809-6815.2004.

Venkateswaran PS, Stanton N, Austrian R. Type variation of strains of *Streptococcus pneumoniae* in capsular serogroup 15. *J Infect Dis* 1983 Jun;147(6):1041-54. doi: 10.1093/infdis/147.6.1041.

Ventura CL, Cartee RT, Forsee WT et al. Control of capsular polysaccharide chain length by UDP-sugar substrate concentrations in *Streptococcus pneumoniae*. *Mol Microbiol* 2006 Aug;61(3):723-33. doi: 10.1111/j.1365-2958.2006.05259.x.

Vermassen A, Leroy S, Talon R et al. Cell wall hydrolases in bacteria: Insight on the diversity of cell wall amidases, glycosidases and peptidases toward peptidoglycan. *Front Microbiol* 2019 Feb 28;10:331. doi: 10.3389/fmicb.2019.00331.

Vincent C, Doublet P, Grangeasse C et al. Cells of *Escherichia coli* contain a protein-tyrosine kinase, Wzc, and a phosphotyrosine-protein phosphatase, Wzb. *J Bacteriol* 1999 Jun;181(11):3472-7. doi: 10.1128/JB.181.11.3472-3477.1999.

Vollmer W, Tomasz A. The *pgdA* gene encodes for a peptidoglycan N-acetylglucosamine deacetylase in *Streptococcus pneumoniae*. *J Biol Chem* 2000 Jul 7;275(27):20496-501. doi: 10.1074/jbc.M910189199.

Vollmer W, Blanot D, de Pedro MA. Peptidoglycan structure and architecture. *FEMS Microbiol Rev* 2008 May;7(3). doi: 10.1128/microbiolspec.GPP3-0018-2018.

Vollmer W, Massidda O, Tomasz A. The cell wall of *Streptococcus pneumoniae*. *Microbiol Spectr* 2019 May;7(3). doi: 10.1128/microbiolspec.GPP3-0018-2018.

Voss S, Gámez G, Hammerschmidt S. Impact of pneumococcal microbial surface components recognizing adhesive matrix molecules on colonization. *Mol Oral Microbiol* 2012 Aug;27(4):246-56. doi: 10.1111/j.2041-1014.2012.00654.x.

de Vuyst L, Degeest B. Heteropolysaccharides from lactic acid bacteria. *FEMS Microbiol Rev* 1999 Apr;23(2):153-77. doi: 10.1111/j.1574-6976.1999.tb00395.x.

Walker JA, Allen RL, Falmagne P et al. Molecular cloning, characterization, and complete nucleotide sequence of the gene for pneumolysin, the sulfhydryl-activated toxin of *Streptococcus pneumoniae*. *Infect Immun* 1987 May;55(5):1184-9. doi: 10.1128/iai.55.5.1184-1189.1987.

Wartha F, Beiter K, Albiger B et al. Capsule and D-alanylated lipoteichoic acids protect *Streptococcus pneumoniae* against neutrophil extracellular traps. *Cell Microbiol* 2007 May;9(5):1162-71. doi: 10.1111/j.1462-5822.2006.00857.x. Epub 2007 Jan 9.

Weiser JN, Austrian R, Sreenivasan PK et al. Phase variation in pneumococcal opacity: relationship between colonial morphology and nasopharyngeal colonization. *Infect Immun* 1994 Jun;62(6):2582-9. doi: 10.1128/iai.62.6.2582-2589.1994.

Weiser JN, Kapoor M. Effect of intrastrain variation in the amount of capsular polysaccharide on genetic transformation of *Streptococcus pneumoniae*: implications for virulence studies of encapsulated strains. *Infect Immun* 1999 Jul;67(7):3690-2. doi: 10.1128/IAI.67.7.3690-3692.1999.

Weiser JN, Bae D, Epino H et al. Changes in availability of oxygen accentuate differences in capsular polysaccharide expression by phenotypic variants and clinical isolates of *Streptococcus pneumoniae*. *Infect Immun* 2001 Sep;69(9):5430-9. doi: 10.1128/IAI.69.9.5430-5439.2001.

Weiser JN. The pneumococcus: why a commensal misbehaves. *J Mol Med* 2010;88:97–102. doi: 10.1007/s00109-009-0557-x.

Welte T, Köhnlein T. Global and local epidemiology of community-acquired pneumonia: the experience of the CAPNETZ Network. *Semin Respir Crit Care Med* 2009 Apr;30(2):127-35. doi: 10.1055/s-0029-1202941.

Wen Z, Sertil O, Cheng Y et al. Sequence elements upstream of the core promoter are necessary for full transcription of the capsule gene operon in *Streptococcus pneumoniae* strain D39. *Infect Immun* 2015 May;83(5):1957-72. doi: 10.1128/IAI.02944-14.

Whitfield C, Paiment A. Biosynthesis and assembly of Group 1 capsular polysaccharides in *Escherichia coli* and related extracellular polysaccharides in other bacteria. *Carbohydr Res* 2003 Nov 14;338(23):2491-502. doi: 10.1016/j.carres.2003.08.010.

World Health Organization. Immunization surveillance, assessment and monitoring: estimated Hib and pneumococcal deaths for children under 5 Years of age - estimated pneumococcal deaths and cases. February 2011 [cited 28 August 2012].

World Health Organization. Global priority list of antibiotic-resistant bacteria to guide research, discovery, and development of new antibiotics. 2017.

Wiley W, Schneewind O. Surface proteins of Gram-positive bacteria and mechanisms of their

targeting to the cell wall envelope. *Microbiol Mol Biol Rev* 1999 Mar;63(1):174-229. doi: 10.1128/MMBR.63.1.174-229.1999.

Winkelstein JA. The role of complement in the host's defense against *Streptococcus pneumoniae*, *Reviews of Infectious Diseases*, 1981 Mar-Apr;3(2):289-98. doi: 10.1093/clinids/3.2.289.

Wu K, Xu H, Zheng Y et al. CpsR, a GntR family regulator, transcriptionally regulates capsular polysaccharide biosynthesis and governs bacterial virulence in *Streptococcus pneumoniae*. *Sci Rep* 2016 Jul 8;6:29255. doi: 10.1038/srep29255.

Wu ZC, Cameron MD, Boger DL. Vancomycin C-terminus guanidine modifications and further insights into an added mechanism of action imparted by a peripheral structural modification. *ACS Infect Dis* 2020 Aug 14;6(8):2169-2180. doi: 10.1021/acsinfecdis.0c00258.

Wyres KL, Lambertsen LM, Croucher NJ et al. Pneumococcal capsular switching: a historical perspective. *J Infect Dis*. 2013 Feb 1;207(3):439-49. doi: 10.1093/infdis/jis703.

Xayarath B, Yother J. Mutations blocking side chain assembly, polymerization, or transport of a Wzy-dependent *Streptococcus pneumoniae* capsule are lethal in the absence of suppressor mutations and can affect polymer transfer to the cell wall. *J Bacteriol* 2007 May;189(9):3369-81. doi: 10.1128/JB.01938-06.

Xu Q, Kaur R, Casey JR et al. Nontypeable *Streptococcus pneumoniae* as an otopathogen. *Diagn Microbiol Infect Dis* 2011 Feb;69(2):200-4. doi: 10.1016/j.diagmicrobio.2010.09.019.

Yahiaoui RY, den Heijer CD, van Bijnen EM et al. Prevalence and antibiotic resistance of commensal *Streptococcus pneumoniae* in nine European countries. *Future Microbiol* 2016 Jun;11:737-44. doi: 10.2217/fmb-2015-0011.

Yahiaoui RY, Bootsma HJ, Den Heijer CDJ et al. Distribution of serotypes and patterns of antimicrobial resistance among commensal *Streptococcus pneumoniae* in nine European countries. *BMC Infect Dis*. 2018 Aug 29;18(1):440. doi: 10.1186/s12879-018-3341-0.

Ye W, Zhang J, Shu Z, Yin Y, Zhang X, Wu K. Pneumococcal LytR protein is required for the surface attachment of both capsular polysaccharide and teichoic acids: essential for pneumococcal virulence. *Front Microbiol* 2018 Jun 13;9:1199. doi: 10.3389/fmicb.2018.01199.

Yother J, McDaniel LS, Briles DE. Transformation of encapsulated *Streptococcus pneumoniae*. *J Bacteriol* 1986 Dec;168(3):1463-5. doi: 10.1128/jb.168.3.1463-1465.1986.

Yother J. Capsules of *Streptococcus pneumoniae* and other bacteria: paradigms for polysaccharide biosynthesis and regulation. *Annu Rev Microbiol* 2011;65:563-81. doi: 10.1146/annurev.micro.62.081307.162944.

Zafar MA, Wang Y, Hamaguchi S et al. Host-to-host transmission of *Streptococcus pneumoniae* is driven by its inflammatory toxin, pneumolysin. *Cell Host Microbe* 2017 Jan 11;21(1):73-83. doi: 10.1016/j.chom.2016.12.005.

Zhu W, Lomsadze A, Borodovsky M. Ab initio gene identification in metagenomic sequences. *Nucleic Acids Res* 2010 Jul;38(12):e132. doi: 10.1093/nar/gkq275.

Zhang J-R, Mostov KE, Lamm ME et al. The polymeric immunoglobulin receptor translocates pneumococci across human nasopharyngeal epithelial cells. *Cell* 2000 Sep 15;102(6):827-37. doi: 10.1016/s0092-8674(00)00071-4.

2021

JOANA BAPTISTA DA SILVA FIGUEIREDO

STRATEGIES TO PREVENT THE TIMELY SUB-CELLULAR LOCALIZATION OF THE CAPSULE SYNTHETIC MACHINERY IN *STREPTOCOCCUS PNEUMONIAE*